Universidade de Aveiro Departamento de Química
2011

PEDRO JORGE MARQUES CARVALHO

TRATAMENTO DE CORRENTES DE GÁS NATURAL COM LÍQUIDOS IÓNICOS

TREATMENT OF NATURAL GAS STREAMS WITH IONIC LIQUIDS

Universidade de Aveiro Departamento de Química
2011

PEDRO JORGE MARQUES CARVALHO

TRATAMENTO DE CORRENTES DE GÁS NATURAL COM LÍQUIDOS IÓNICOS

TREATMENT OF NATURAL GAS STREAMS WITH IONIC LIQUIDS

Dissertação apresentada à Universidade de Aveiro para cumprimento dos requisitos necessários à obtenção do grau de Doutor em Engenharia Química, realizada sob a orientação científica do Doutor João Manuel da Costa E Araújo Pereira Coutinho, Professor Associado com Agregação do Departamento de Química da Universidade de Aveiro e da Doutora Isabel Maria Delgado Jana Marrucho Ferreira, Investigadora Auxiliar do Instituto de Tecnologia Química e Biológica da Universidade Nova de Lisboa e Professora Auxiliar do Departamento de Química da Universidade de Aveiro

Apoio financeiro do POCTI no âmbito do III Quadro Comunitário de Apoio.

Ciência.Inovação 2010
Programa Operacional Ciência e Inovação 2010
MINISTÉRIO DA CIÊNCIA, TECNOLOGIA E ENSINO SUPERIOR

O doutorando agradece o apoio financeiro da FCT no âmbito do III Quadro Comunitário de Apoio (SFRH/BD/41562/2007) .

o júri

presidente

Prof. Doutor Paulo Jorge dos Santos Gonçalves Ferreira
professor catedrático do Departamento de Electrónica, Telecomunicações e Informática da Universidade de Aveiro

Prof. Doutor João Paulo Serejo Goulão Crespo
professor catedrático no Departamento de Química da Faculdade de Ciências e Tecnologia da Universidade Nova de Lisboa

Prof. Doutor João Manuel da Costa E Araújo Pereira Coutinho
professor associado com agregação no Departamento de Química da Universidade de Aveiro

Prof. Doutor Luís Manuel das Neves Belchior Faia dos Santos
professor associado da Faculdade de Ciências da Universidade do Porto

Prof. Doutor Jean-Luc Daridon
professor do Departamento de Fisica da Université de Pau et des Pays de L'Adour

Profª. Doutora Isabel Maria Delgado Jana Marrucho Ferreira
investigadora auxiliar do Instituto de Tecnologia Química e Biológica da Universidade Nova de Lisboa e professora auxiliar no Departamento de Química da Universidade de Aveiro

agradecimentos

"*Everything has been said before, but since nobody listens we have to keep going back and beginning all over again.*" Andre Gide

Não posso deixar de começar por agradecer ao Prof. João Coutinho por este fascinante, enriquecedor e atrativo "*PATh*^{minho}". Por acreditar, investir, incentivar, desafiar diariamente e por ter trilhado comigo este sedutor mundo da ciência, um muito obrigado.

"*Creation requires influence.*"

A todos os membros do grupo PATh que além de colegas se tornaram amigos o meu mais profundo agradecimento pelos momentos passados e por tornarem este grupo um excelente e divertido local de trabalho. Ao Prof. Avelino um especial obrigado pela confiança e pelos divertidos momentos perfumados pelo doce aroma do café.

"*Be careful the environment you choose for it will shape you; be careful the friends you choose for you will become like them.*" W. Clement Stone

A todas as pessoas e grupos com quem tive o privilégio de colaborar. Pela colaboração, pela amizade e pelo trabalho desenvolvido um especial obrigado ao Prof. Luís Belchior, Prof. Jean Luc Daridon e Prof. Jérôme Pauly, Profª. Josefa Fernandez e Teresa Regueira, Profª. Silvana Mattedi e Prof. Víctor Álvarez, Prof. Abel Ferreira, Prof. João Paulo Crespo e Drª. Luisa Neves.

"Alone we can do so little; together we can do so much." Helen Keller

Estou agradecido a todos os amigos que fiz, por todas as pessoas que conheci, por todas as oportunidades que tive para viajar e alargar os horizontes. Mas nada disto teria possível sem o apoio dos meus pais e da Fatolas. Obrigado por estarem sempre por perto, mesmo quando a distância é grande, pelo apoio, pelo amor... por serem vocês mesmos.

"In every conceivable manner, the family is link to our past, bridge to our future." ***Alex Haley***

palavras-chave

Líquidos iónicos, equilíbrio de fase, metano, dióxido de carbono, alta pressão, equação de estado, lei de Henry, solventes não voláteis.

resumo

Apresentando uma elevada relevância em várias aplicações tecnológicas, a solubilidade de gases ácidos em solventes com baixa volatilidade é ainda mal descrita e compreendida. Este trabalho, visando a purificação de gás natural, contribui para uma melhor compreensão e para o desenvolvimento de uma descrição da solubilidade de gases ácidos neste tipo de compostos, em particular em líquidos iónicos. Um equipamento, desenvolvido e validado especialmente para estudar o equilíbrio de fases deste tipo de sistemas, permitiu o estudo detalhado da influência da basicidade, peso molecular e polaridade do líquido iónico na absorção de dióxido de carbono e metano. A não idealidade de soluções de dióxido de carbono tanto em líquidos iónicos como noutros solventes com baixa volatilidade, com os quais o dióxido de carbono forma complexos aceitadores-dadores de electrões, é investigado, permitindo o desenvolvimento de uma correlação capaz de descrever a solubilidade do dióxido de carbono em solventes com baixa volatilidade. Por sua vez, a não idealidade de soluções de compostos leves, como o SO_2, NH_3 e H_2S em líquidos iónicos é também abordada, mostrando-se que os desvios negativos à idealidade na fase líquida observados podem ser descritos pelo modelo de Flory-Huggins. Por fim, o efeito da polaridade do líquido iónico, descrito através dos parâmetros Kamlet-Taft, nas selectividades de CO_2/CH_4 e H_2S/CH_4 é investigado, revelando-se uma ferramenta viável para a selecção de líquidos iónicos com elevada selectividade.

keywords

Ionic Liquids, phase equilibria, methane, carbon dioxide, high pressure, equation of state, Henry's law, nonvolatile solvents.

abstract

Being of high relevance for many technological applications, the solubility of sour gases in solvents of low volatility is still poorly described and understood. Aiming at purifying natural gas streams, the present work contributes for a more detailed knowledge and better understanding of the solubility of sour gases in these fluids, in particularly on ionic liquids. A new apparatus, developed and validated specially for phase equilibria studies of this type of systems, allowed the study of the solvent basicity, molecular weight and polarity influence on the absorption of carbon dioxide and methane. The non ideality of carbon dioxide solutions in ionic liquids and other low volatile solvents, with which carbon dioxide is known to form electron donor-acceptor complexes, is discussed, allowing the development of a correlation able to describe the carbon dioxide solubility in low volatile solvents. Furthermore, the non ideality of solutions of light compounds, such as SO_2, NH_3 and H_2S, in ionic liquids is also investigated and shown to present negative deviations to the ideality in the liquid phase, that can be predicted by the Flory-Huggins model. For last, the effect of the ionic liquid polarity, described through the Kamlet-Taft parameters, on the CO_2/CH_4 and H_2S/CH_4 selectivities is also evaluated and shown to stand as a viable tool for the selection of ionic liquids with enhanced selectivities.

Table of Contents

CONTENTS

CONTENTS

List of Abbreviations

$[C_2mim][NTf_2]$	1-ethyl-3-methyl-imidazolium Bis(trifluoromethylsulfonyl)imide
$[C_4mim][Ac]$	1-butyl-3-methyl-imidazolium Acetate
$[C_4mim][CH_3SO_3]$	1-butyl-3-methylimidazolium Methanesulphonate
$[C_4mim][DCA]$	1-butyl-3-methyl-imidazolium Dicyanamide
$[C_4mim][NTf_2]$	1-butyl-3-methyl-imidazolium Bis(trifluoromethylsulfonyl)imide
$[C_4mim][TFA]$	1-butyl-3-methyl-imidazolium Trifluoroacetate
$[C_5mim][NTf_2]$	1-Methyl-3-pentyl-imidazolium Bis(trifluoromethylsulfonyl)imide
[THTDP][Cl]	Trihexyltetradecylphosphonium Chloride
$[THTDP][NTf_2]$	Trihexyltetradecylphosphonium Bis(trifluoromethylsulfonyl)imide
$[C_nmim]$	1-Alkyl-3-methyl-imidazolium
$\lvert\Delta H_{12}\rvert$	Henry's constant average absolute deviations
H_{12}	Henry's constant
m-2-HEAPr	2-methyhydroxyethylammonium Propinate
$a_i^{(m)}$	Activity of gas i
BSSE	Basic Set Superposition Errors
CCl_4	Carbon Tetrachloride
CH_4	Methane
CO_2	Carbon Dioxide
COS	Carbon Sulfide
CPA EoS	Cubic plus Association Equation of State
CS_2	Carbon Disulphide
DEA	Diethanolamine
EDA	Electron Donor-acceptor
EOR	Enhanced Oil Recovery
EoS	Equation of State

ϕ_{gas}	Fugacity Coefficient
GC-EoS	Group Contribution Equation of State
G^E	Gibbs Energy
G^E_{comb}	Gibbs Energy Combinatorial contribution
$G^E_{residual}$	Gibbs Energy Residual contribution
H_2S	Hydrogen Sulphide
HRMAS NMR	High Resolution and Magic Angle Spinning NMR
ILs	Ionic Liquids
m-2-HEAA	N-methyl-2-hydroxy ethylammonium Acetate
m-2-HEAF	N-methyl-2-hydroxy ethylammonium Formate
m-2-HEAPr	N-methyl-2-hydroxy ethylammonium Propinate
MEA	Monoethanolamine
M_w	Molecular Weight
N_2	Nitrogen
NFC	Not Full Consistent
NH_3	Ammonia
NMR	Nuclear Magnetic Resonance
NRTL EoS	Non-Random Two-Liquid Equation of State
NTf_2	Bis(trifluoromethylsulfonyl)imide
OF	Objective Function
p	Pressure
PEG	Polyethylene Glycol
pFAP	Bis(pentafluoroethyl)trifluorophosphate
PR EoS	Peng-Robinson Equation of State
p^{σ}_{gas}	Vapor Pressure of the Gas

SAFT	Statistical Association Fluid Theory
SO_2	Sulfur Dioxide
SRK EoS	Soave-Redlich-Kwong Equation of State
T	Temperature
T_c	Critical Temperature
TC	Thermodynamic Consistent
TI	Thermodynamic Inconsistent
TMSP	Trimethylsilyl Propanoic Acid
TOC	Total Organic Carbon Content
T_r	Reduced Temperature
UNIQUAC	UNIversal QUAsiChemical Equation of State
VLE	Vapor Liquid Equilibrium
V_m^{gas}	Molar Volume of the Gas
V_m^{IL}	Molar Volume of the Ionic Liquid
VOCS	Volatile Organic Compounds
WS/NRTL	Wong-Sandler mixing rule using the NRTL model for the activity coefficient
WS/UNIQUAC	Wong-Sandler mixing rule using the UNIQUAC model for the activity coefficient
ZPEs	Zero-point Energies
$\gamma_i^{(m)}$	Activity Coefficient of Gas i
φ_{gas}	Volume Fraction of the Gas

List of Tables

List of Figures

1. General Introduction

"*The most exciting phrase to hear in science, the one that heralds new discoveries, is not 'Eureka!' ('I found it!') but rather 'hmm....that's funny...*"

Isaac Asimov

1.1. General Context

Natural gas occurs in subsurface rock formations in two distinct forms, associated with oil or, on higher percentage (60%), non-associated.[1] Natural gas is mostly composed by methane, being the remainder a mixture of variable quantities of hydrocarbons, like ethane, propane, C_4+, and other gases like CO_2, H_2S, mercaptans, helium and argon, and, in some cases, important quantities of mercury.[1] Natural gas resides in reservoirs in contact with connate water, thus, it is common to find methane combined with other low molecular weight natural gases, forming a solid hydrate even at temperatures above the water freezing point.

Able to block transmission lines, plug blowout preventers, jeopardize the foundation of deepwater platforms and pipelines, causing the collapse of tubes, heat exchangers, valves and expanders, hydrates are considered an inconvenient. On the other hand, while acid gases are responsible for the pipelines corrosion, while the mercury, besides its high toxicity, damages the heat exchangers aluminum components.

Upon the extraction impurities must be removed, from the gas stream, in order to convert the stream essentially into methane with small percentage of light hydrocarbons.

There are several techniques available to remove the aforementioned impurities and recover the natural gas high-value compounds. Polymeric membranes, from cellulose acetate or hollow polyamide fibers, are been used to remove CO_2 and H_2S.[2, 3] Molecular sieves, containing silver or sulfur, are used to remove mercury.[4] The gas dehydration can be made by using molecular sieves.[5] Nonetheless, the absorption continues to be the most used and reliable method for the natural gas stream treatment. Ethylene glycol is normally used for the gas dehydration;[1] Acid gas removal can be carried by using methanol at low temperatures (Rectisol process[6]), polyethylene glycol dimethylic esters (Selexol process[7]) or solutions potassium carbonate under high temperatures (Benfield process[8]), or alcanol amines like MEA and DEA.[3, 9, 10]

Despite their low capital and operational costs, high operational simplicity and

feasibility,[2] this technologies present also several disadvantages like solvent loss and release, gas stream moisture saturation, hydrocarbon loss and the presence of acid gases on the gas streams.[3] Chemical solvents like amines present high gas removal capability but, at the same time, hard regeneration due to the formation of complexes between the species carrying high energetic costs.[9, 10] Nonetheless, these absorbents advantages at low pressures disappear rapidly for higher pressures where physical absorbents present notorious advantages.[3]

Aiming at sweetening sour gases from natural gas streams under high pressures, specially carbon dioxide, this thesis will focus on pursuing a suitable solvent able to replace those currently used. For that purpose, a new class of solvents, ionic liquids (ILs), will be investigated .

Ionic liquids, a class of *neoteric* solvents composed of large organic cations and organic or inorganic anions, that cannot form an ordered crystal and thus remain liquid at or near room temperature, are becoming one of the fastest growing "green" media for chemists and engineers, bridging academia and industrial interests and standing as a viable alternative for natural gas streams treatment. The tunable properties of ILs through an endless combination of cations and anions, allow the design of solvents for the development of more efficient processes and products. Among the several applications foreseeable for ionic liquids such as solvents in organic synthesis,[11, 12] homogeneous and biphasic transfer catalysts,[13-15] separation processes,[16-19] their use in processes with supercritical gases is one of the most exciting.

The high solubility of CO_2 in ionic liquids has been the object of extensive research during the last few years. Aiming at enhancing sour gases solubility and ultimately replace the hazard volatile organic compounds (VOCs), many researchers have judiciously tailored ionic liquids to accomplish such task either through the introduction of fluorinated groups on the IL ions, or by adding basic groups such as amines or acetates.[16, 20-33] With the exception of this last type of ILs, where chemical interactions dominate the sorption mechanism, in most ionic liquids the gas solubility is simply driven by a physical

absorption mechanism.[30, 34, 35] Among the ILs previously reported in the literature the imidazolium-based, specially those with fluorinated anions such as the bis(trifluoromethylsulfonyl)imide, NTf_2, and bis(pentafluoroethyl)trifluorophosphate, pFAP, anions, are the ones with the highest CO_2 solubilities reported.[28, 33, 36]

A large amount of work concerning the development of ionic liquids with special affinity towards CO_2 has been carried. Bates et al.[16] reported amine functionalized ILs, while Yuan et al.[31] and Sun et al.[32] used hydroxyl-functionalized ILs as a novel efficient catalyst for chemical fixation of CO_2. Yu et al.[37] and Huang et al.[26] proposed guanidinium based ILs, where the electron-donating groups increased the strength of the donor-acceptor interactions on $-NH_2$ and consequently enhanced the interactions between $-NH_2$ and CO_2. Muldoon et al.[28] and Lopez-Castillo[38] reported that CO_2 can be used to enhance the solubility of other gases that typically present low solubilities in ILs. Solinas et al.[39] showed that inducing CO_2 pressure on a system improves the activation, tuning and immobilization of chiral iridium catalysts in IL/CO_2 for the enantioselective hydrogenation reaction of imines.

1.2. Scope and Objectives

The solubility of CO_2 in solvents of low volatility or non volatile is highly relevant for many technological applications. Enhanced Oil Recovery (EOR) requires the knowledge of the CO_2 solubility in heavy hydrocarbons;[40] purification of vegetable or animal oils or the extraction of value added compounds from them using supercritical technologies is related with the CO_2 solubility in these oils, and their fatty acids and esters; [41-44] and the Selexol process uses a mixture of dimethyl ethers of polyethylene glycol for the removal of acid gases from feed gas streams.[45] Recently a great deal of works address the use of ionic liquids for CO_2 capture and gas separation purposes.[20, 27, 29, 30, 33, 36, 46-64] In all these cases the understanding and description of the absorption of CO_2 in solvents of low volatility is of importance for the design and operation of processes or the design of new and enhanced sorbents for CO_2.

Sulfur-compounds, including hydrogen sulfide (H_2S) and sulfur dioxide (SO_2), frequently appear as contaminants in process streams in the production, processing and refining of fossil fuels.[65, 66] Gasification of heavy residual oil, petroleum coke, coal feedstocks and hydrocarbons is increasing in importance and the key gas separation is the selective removal of contaminants, like H_2S, COS, NH_3 and SO_2, from the synthesis gas. In addition, the presence of acid gases (COS, H_2S, CO_2) and other impurities require the syngas to undergo a gas treatment process to make it suitable for downstream use. The solubility of gases like SO_2, NH_3, and H_2S in solvents of low volatility or non volatile is thus highly relevant for many technological applications and, therefore, will be addressed along this work.

Twelve ionic liquids, described and listed on **C**hapter 3 "Materials", were selected in order to further contribute for a more detailed knowledge and thus a better understanding of the solubility of supercritical CO_2 and CH_4 in these fluids aiming at identify ionic liquids suitable for their separation. The selected ILs allowed to test and validate the apparatus, described on **C**hapter 2 "Experimental Equipment", and to study the influence of the solvent basicity, molecular weight and polarity on the absorption of carbon dioxide and methane. Moreover, due to the difficulties normally found when measuring this type of mixtures, Valderrama and Álvarez[67] developed a thermodynamic consistency test for systems with incomplete *pTxy* data and proposed a methodology, described on **C**hapter 4 "Thermodynamic Modeling and Consistency Theory", to analyze the experimental data measured.

For a question of simplicity this document is divided in chapters according to the work published along the development of this thesis. Therefore, **C**hapter 5 "Carbon Dioxide Interactions" focus on study the interactions between CO_2 and different compounds. In this chapter the CCl_4 and CS_2 were chosen due to their similar structure to CH_4 and CO_2, respectively, allowing to anticipate the interactions between like and unlike molecules that can be found at binary and multicomponent systems constituted by CO_2

and/or CH_4. **C**hapter 6 "High Pressure Phase Behavior of Carbon Dioxide in 1-alkyl-3-methylimidazolium bis(trifluoromethylsulfonyl)imide Ionic Liquids" stands as the beginning of our high pressure phase behavior of gas + ionic liquids study; two NTf_2-based ionic liquids were selected to validate the high pressure cell, developed to investigate these systems, and to further contribute for a more detailed knowledge and thus a better understanding of the solubility of CO_2 in ionic liquids. On **C**hapter 7 "Specific Solvation Interactions of CO2 on Acetate and Trifluoroacetate Imidazolium Based Ionic Liquids at High Pressures" and **C**hapter 8 "High Pressure Phase Behavior of Carbon Dioxide in 1-Butyl-3-methylimidazolium Bis(trifluoromethylsulfonyl)imide and 1-Butyl-3-methylimidazolium Dicyanamide Ionic Liquids" the basicity of the anion as means to enhance the absorption of sour gases by ionic liquids, along with another strategy to foster the gas solubility in an IL by the fluorination of its alkyl chains, were compared and evaluated aiming at a better understanding of the mechanisms of solvation of CO_2 on ILs with these characteristics.

From the knowledge amassed to this point, the solubility mechanism of CO_2 in ionic liquids based on the CO_2 formation of electron donor-acceptor (EDA) complexes with the solvent seemed questionable. In fact, on **C**hapter 9 "On the Nonideality of CO2 Solutions in Ionic Liquids and Other Low Volatile Solvents" the deviations from the ideality were observed not to be related with the stability of the EDA complexes formed. Actually, these deviations are in most cases small and dominated by entropic effects. Furthermore, it will be shown that when the CO_2 concentration is expressed in molality, the pressure *versus* concentration phase diagrams of CO_2 in non volatile solvents are, within the uncertainty of the experimental data, solvent independent. Following this approach a correlation for the solubility of CO_2 in non volatile solvents, valid for pressures up to 8 MPa and temperatures ranging from room temperature up to 363

K, was developed and proposed.

In the wake of the previous chapters, **C**hapter 10 "High Carbon Dioxide Solubilities in Trihexyltetradecylphosphonium-based Ionic Liquids" continues the effort to identify ILs with large CO_2 solubilities and to further explore the mechanism behind the absorption of carbon dioxide by the ionic liquids. For that purpose phosphonium-based ILs with cations and anions that minimize any specific interactions between the IL and the carbon dioxide were chosen. This approach allowed also to evaluate the applicability and validity of the correlation developed and described on **C**hapter 9.

Until now, studies concerning ionic liquids have been based on the imidazolium cation and, to a lesser extent, on the phosphonium, alkyl pyridiniums and trialkylamines. Protic ionic liquids (PILs), investigated on **C**hapter 11 "High pressure CO2 solubility in N-methyl-2-hydroxyethylammonium protic ionic liquids", have, however, received limited attention. The presence of an anion with a strong basic character was shown before on **C**hapter 7 to enhance the gas solubility, thus PILs could be an interesting alternative to be applied for the capture of acid gases.

In the following of the work developed so far, the mechanism behind the solubility of light compounds such as NH_3, SO_2 and H_2S, in ionic liquids, is investigated on **C**hapter 12 "Non-ideality of Solutions of NH3, SO2, and H2S in Ionic Liquids and the Prediction of their Solubilities using the Flory-Huggins Model" by analyzing their deviations to ideality in the liquid phase. This approach allows not only to achieve a deeper understanding of the mechanism behind the solvation of these gases in ionic liquids but also to establish models that can be used to predict the solubility of these gases in ionic liquids.

Having understand the mechanisms behind the solvation of gases in ionic liquids

and aiming at designing ILs for the purification of natural gas, the solubility of methane in ionic liquids is investigated on **C**hapter 13 "The Polarity Effect upon the Methane Solubility in Ionic Liquids: A Contribution for the Design of Ionic Liquids for Enhanced CO2/CH4 and H2S/CH4 Selectivities" through the measurement of the solubilities of methane in four ionic liquids, in a wide range of molar fractions, temperature and pressures. Furthermore, the effect of the ionic liquid polarity, described through the Kamlet-Taft parameters, on the CO_2/CH_4 and H_2S/CH_4 selectivities is also evaluated and shown to be a viable key to the selection of ionic liquids with enhanced selectivities.

As described before and despite the exponential interest on ionic liquids, the availability of thermophysical properties data is still limited and often of questionable quality, making difficult the development of correlations or predictive models for these properties and the design of ionic liquids for new products and process applications. Several studies, addressing this issue, have been carried during the thesis. Surface tensions (*J. Chem. Eng. Data 53, 2008, 1346-1350; J. Chem. Eng. Data 55, 2010, 3807-3812*), densities (*J. Chem. Eng. Data 52, 2007, 1881-1888; J. Chem. Eng. Data 53, 2008, 805-811; J. Chem. Eng. Data 53, 2008, 1914-1921*) and viscosities (*J. Chem. Eng. Data 55, 2010, 645-652; J. Chem. Eng. Data 55, 2010, 4514–4520; Fluid Phase Equilib. 301, 2011, 22-32*) and ILs – water mutual solubilities (*J. Phys. Chem. B 111, 2007, 13082-13089; J. Phys. Chem. B 112, 2008, 1604-1610; J. Chem. Eng. Data 53, 2008, 2378-2382; J. Phys. Chem. B 113, 2009, 202-211; J. Chem. Thermodyn. 43, 2011, 948-957*) were measured but, for the sake of conciseness, they were not included in this manuscript, keeping its focus on the gas solubilities.

Our group has proposed a number of predictive methods, including the correlation developed on **C**hapter 9, for the thermophysical properties of ionic liquids. ThermophIL, described on **C**hapter 14 "THERMOPHIL – An Application for Ionic Liquids Property Estimation" was developed as a way of disclosing the correlation developed for the CO_2 solubility on non-volatile solvents for users worldwide and free-of-use.

Furthermore, since our group has developed several other models (density, isobaric expansivity and isothermal compressibility, viscosity, surface tension, speed of sound, ionic conductivity, heat capacity and water solubility) those models were also made available through the same interface, providing a platform for the quick estimation of the thermophysical properties of ILs by an interested user, and making publicity to the work developed in the group.

2. Experimental Equipment

“Inanimate objects can be classified scientifically into three major categories; those that don't work, those that break down and those that get lost.”

Russell Baker

2.1. The High Pressure Equilibrium Cell

The high pressure equilibrium cell developed in this work uses the synthetic method and is sketched in Figure 2.1 and pictured in Figure 2.2. The cell, based on the design of Daridon et al.[68-72], consists of a horizontal hollow stainless-steel cylinder, closed at one end by a movable piston and at the other end by a sapphire window.

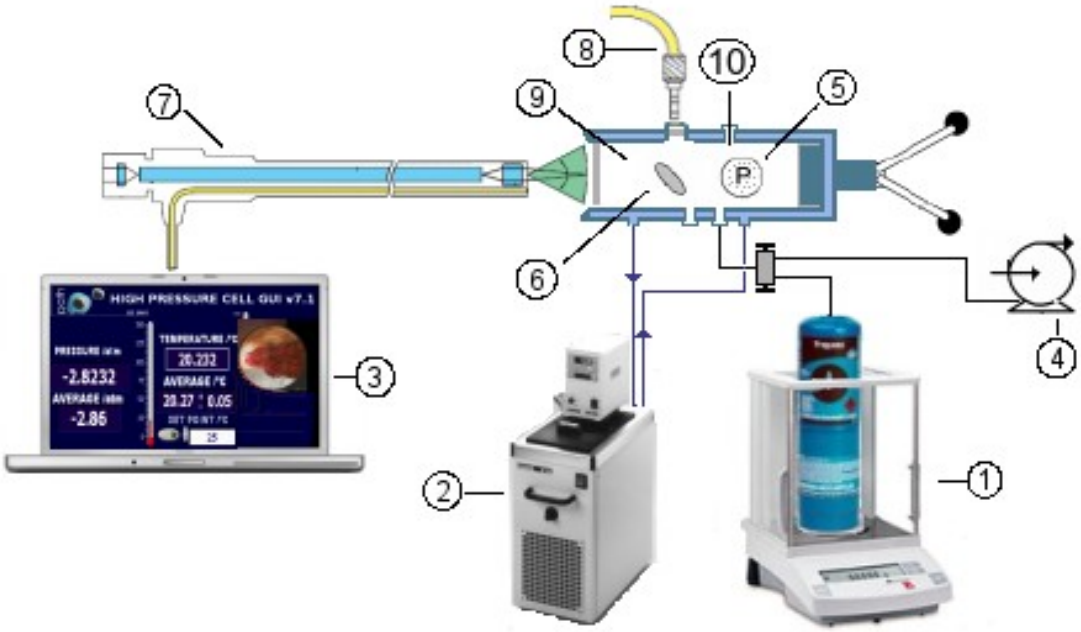

Figure 2.1. Schematic apparatus: 1 – Analytical balance (Sartorius LA200P); 2 – Thermostatized bath circulator (Julabo MC); 3 – Computer to data and video acquisition; 4 – Vacuum pump (Edwards RV3); 5 – Piezoresistive pressure transducer (Kulite HEM 375); 6 – Magnetic bar; 7 – Endoscope plus a video camera; 8 – Light source with optical fiber cable; 9 – High-pressure variable-volume cell; 10 – Temperature probe (K type thermocouple).

This window, along with a second window on the cell wall, through which an optical fiber lights the cell chamber, allows the operator to follow the behavior of the sample with pressure and temperature. The orthogonal positioning of both sapphire windows minimizes the parasitic reflections and improves the observation in comparison to axial lighting.

A small magnetic bar placed inside the cell allows the homogenization of the mixture by means of an external magnetic stirrer. The sapphire window on the cell wall

limits the minimum internal volume of the cell to 8 cm^3, while the maximum value is set to 30 cm^3. The presence of the magnetic stirrer, as well as the cell reduced volume, help to minimize the inertia and temperature gradients within the sample.

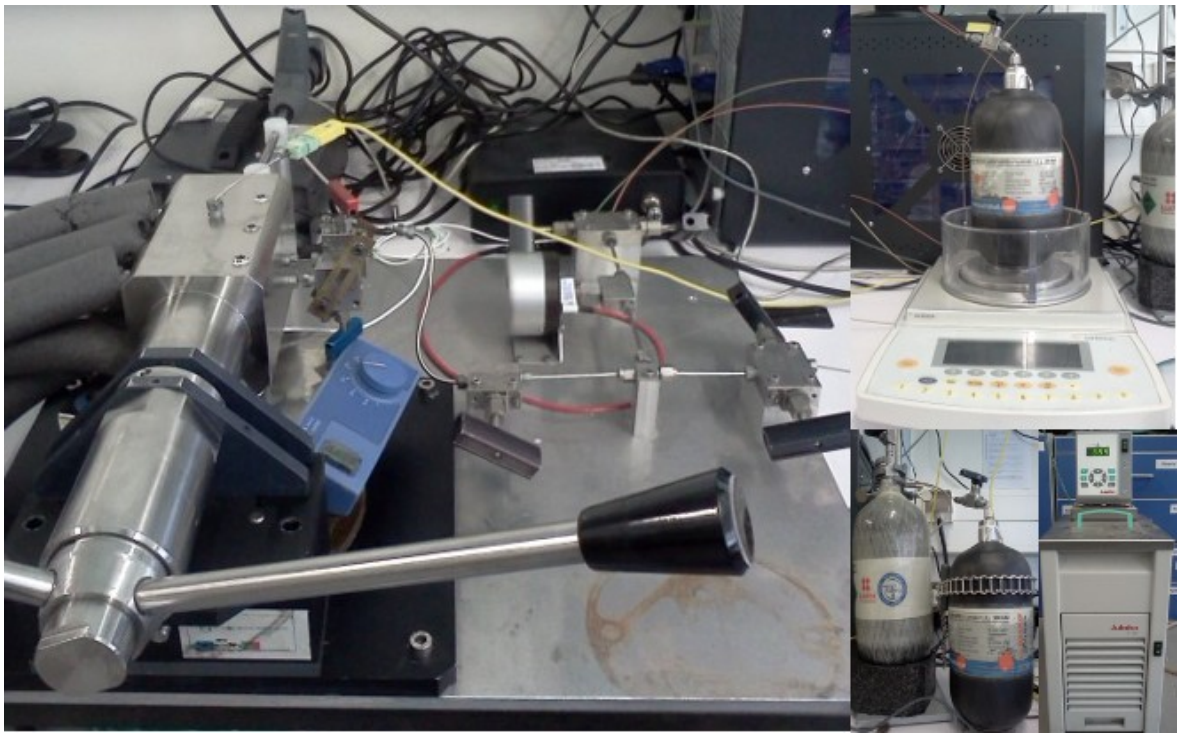

Figure 2.2. High Pressure Equilibrium Cell and Gas line (left), thermostat bath circulator (bottom right), high weight/high precision balance (top right) and ultralight-weight composite cylinders (top and bottom right).

The cell is thermostatized by circulating a heat-carrier fluid through three flow lines directly managed into the cell. The heat-carrier fluid is thermo-regulated with a temperature stability of ±0.01 K by means of a thermostat bath circulator (Julabo MC). The temperature is measured with a high precision K type thermocouple, with an accuracy of 0.01 K, inserted inside the cell close to the sample. The pressure is measured by a piezoresistive silicon pressure transducer (Kulite HEM 375) fixed directly inside the cell to reduce dead volumes, that was previously calibrated and certified by an independent laboratory with IPAC accreditation, following the EN 837-1 standard and with accuracy better than 0.2%.

2.2. Equilibrium Pressure Determination

A fixed amount of IL was introduced inside the cell, its exact mass was determined by weighting, using a high weight/high precision balance with an accuracy of 1 mg (Sartorius LA200P). In order to avoid any interference of atmospheric gases during the manipulation, after placing the IL inside the cell, it was kept under vacuum overnight, while stirring and heating at 353 K.

The gas is introduced under pressure from an ultralight-weight composite cylinder, Figure 2.3. Its mass was measured with the precision balance and introduced into the measuring cell by means of a flexible high pressure capillary.

Technical Data

Design pressure at 15 °C:	450 bar (6527 psi)
Working pressure at 15 °C:	300 bar (4351 psi)
In conformity with:	EN 12245:2002
Directive:	1999/36/WE (Moduł B)
Thread:	UNF 5/8 18/1"
Liner:	Thermoplastic
Colour:	natural fiber colour

Figure 2.3. Ultralight-weight composite cylinder image and specifications.

After preparation of a mixture of known composition and the desired temperature at low pressure was reached, the pressure was then slowly increased at constant temperature until the system becomes monophasic. The pressure at which the last bubble disappears represents the equilibrium pressure for the fixed temperature.

3. Materials

“Anybody who has been seriously engaged is scientific work of any kind realizes that over the entrance to the gates of the temple of science are written the words: 'We must have faith'.”

Max Planck

3.1. Ionic Liquids and Gases

Twelve ionic liquids were selected and used on this study. The ILs' name, abbreviations, supplier and water content is listed in Table 3.1. The compounds were either acquired from IoLiTec, offered by Cytec or synthesized in our laboratory or by Profs. Mattedi and Iglesias from UFBA, Brazil. All the ILs presented mass fraction purities > 99% and bromide impurity mass fraction < 10^{-4}, after the purification procedures.

The phosphonium-based ILs offered by Cytec were received with mass fraction purity higher than 97% and chloride impurity inferior to 0.1% and were further purified, as described on section 3.2, in order to achieve the above mentioned higher purity.

The protic ionic liquids, N-methyl-2-hydroxy ethylammonium acetate, m-2-HEAA, N-methyl-2-hydroxy ethylammonium formate, m-2-HEAF, and 2-methyhydroxyethylammonium propinate, m-2-HEAPr supplied by Profs. Mattedi and Iglesias were synthesized by reacting equimolar amounts of amine and organic acid. The amine was placed in a three necked glass flask, mounted in a thermal bath at 283.15 K, equipped with a reflux condenser, a PT-100 temperature probe for controlling temperature and a dropping funnel. Strong agitation (ca. 450 rpm) was applied in order to improve the contact between the reactants allowing the reaction to be completed. The organic acid was added drop wise to the flask under stirring with a magnetic bar. Stirring was continued for 24 h at laboratory temperature, in order to obtain a final viscous liquid. Then, agitation, slight heating (temperature up to 293.15 K for m-2-HEAF and up to 323.15 K for m-2-HEAA and m-2-HEAPr) and moderate vacuum (20 KPa) for the vaporization of residual non reactants were applied for at least 48 h. During the purification step and storage the m-2-HEAF was light protected in order to prevent any degradation. More details about the synthesis can be found in Alvarez et al.[73].

The 1-butyl-3-methylimidazolium Acetate, [C_4mim][Ac], was synthesized by means of Carbonate based ionic liquid synthesis (CBILS©) of proionic / Sigma – Aldrich. [74] 1-Butyl-3-methylimidazolium hydrogencarbonate (the CBIL precursor as a 50.0 %

solution in H_2O) was treated with an exact stoichiometric amount of acetic acid (FIXANAL / Riedel-de Haën). After the evolution of CO_2 ceased, water and solvents were removed under vacuum. The purities stated by the supplier and those of the [C_4mim][Ac] IL, were checked by ^{1}H NMR, ^{13}C NMR and ^{19}F NMR. For the [C_4mim][Ac] the ^{1}H-NMR obtained presents (chloroform-d, δ/ ppm relative to TMS): 10.56 (s, 1H), 7.47 (d, 2H), 4.08 (s, 6H).

All the ILs were dried under high vacuum (10^{-4} Pa), stirring and moderate temperature (353 K), for a period of at least 48 hours prior to the measurements, as described in section 3.2. The final ILs water content was determined with a Metrohm 831 Karl Fischer coulometer and the purity of each ionic liquid was checked by ^{1}H NMR, ^{13}C NMR and ^{19}F NMR.

The carbon disulphide was acquired from Panreac with mass fraction purities 99.9% and the carbon tetrachloride was acquired from SDS with mass fraction purities 99.9%, as stated by the supplier.

The carbon dioxide (CO_2) was acquired from Air Liquide with a purity of ≥ 99.998% and H_2O, O_2, C_nH_m, N_2 and H_2 impurities volume fractions lower than (3, 2, 2, 8 and 0.5)•10^{-6}, respectively.

The methane (CH_4) was acquired from Air Liquide with a purity ≥ 99.9% and H_2O, O_2, CO_2, C_nH_m, N_2, H_2 and C_2H_6 impurities volume fractions lower than (20, 50, 10, 80, 500, 40 and 400)•10^{-6}, respectively.

Table 3.1. List of Ionic liquids, abbreviations and structures.

Ionic Liquid	Abbreviation	Supplier	Water Content[1] $10^{-6}w_{H2O}$
1-ethyl-3-methylimidazolium bis(trifluoromethylsulfonyl)imide	$[C_2mim][NTf_2]$	io·li·tec	42
1-butyl-3-methylimidazolium bis(trifluoromethylsulfonyl)imide	$[C_4mim][NTf_2]$	io·li·tec	50
1-methyl-3-pentylimidazolium bis(trifluoromethylsulfonyl)imide	$[C_5mim][NTf_2]$	io·li·tec	20
1-butyl-3-methylimidazolium methanesulphonate	$[C_4mim][CH_3SO_3]$	io·li·tec	97
1-butyl-3-methylimidazolium dicyanamide	$[C_4mim][DCA]$	io·li·tec	28
1-butyl-3-methylimidazolium Trifluoroacetate	$[C_4mim][TFA]$	io·li·tec	495
1-butyl-3-methylimidazolium Acetate	$[C_4mim][Ac]$	Synthesized	554
trihexyltetradecylphosphonium bis(trifluoromethylsulfonyl)imide	$[THTDP][NTf_2]$	CYTEC Technology ahead of its time™ www.cytec.com	68
trihexyltetradecylphosphonium chloride	[THTDP][Cl]		97
N-methyl-2-hydroxy ethylammonium acetate	m-2-HEAA	Synthesized[2]	184
N-methyl-2-hydroxy ethylammonium formate	m-2-HEAF	Synthesized[2]	60
2-methyhydroxyethylammonium propinate	m-2-HEAPr	Synthesized[2]	250

1 *after purification*

2 *supplied by Profs. Mattedi and Iglesias from UFBA, Brazil, and the details about the synthesis can be found in Alvarez et al.*[73]

3.2. Ionic Liquids Purification

It is well established that ILs physical properties are influenced by their water content.[75-78] Blanchard et al.[79] reported that even minor amounts of water, dissolved in 1-butyl-3-methylimidazolium hexafluorophosphate ([C_4mim][PF_6]), lead to a reduction of 77% on the CO_2 solubility. More recently, in a systematically study on the influence of water on the solubility of CO_2 for the same compound, Fu et al.[80] reported a less pronounced, < 15%, yet non negligible influence. Furthermore, being an active proton acceptor, water can dramatically increase the degree of dissociation of an acid in a neutral ionic liquid. Similarly, in a neutral IL the state of a base will be altered by the presence of water and in a basic IL, water will be at least partly dissociated producing OH^-.[81] These reports made researchers aware of the importance of implementing purifying procedures prior to the measurements. Thus, in order to reduce the content of water and volatile compounds to negligible values high vacuum (10^{-4} Pa), stirring and moderate temperature (353 K), were applied for a period of at least 48 hours prior to the measurements to the ILs. The final water content was determined with a Metrohm 831 Karl Fischer coulometer.

The ionic liquids [THTDP][NTf_2] and m-2-HEAPr were further purified. The [THTDP][NTf_2] was washed with ultra pure water followed by drying under high vacuum (1×10^{-4} Pa) and moderate temperature (353K), for a period of 48 h. The purification process was repeated until no impurities were observed in the IL by NMR analysis. The water used was double-distilled, passed through a reverse osmosis system, and further treated with a MilliQ plus 185 water purification apparatus. It has a resistivity of 18.2 MΩ cm, a TOC smaller than 5 μg L^{-1}, and it is free of particles greater than 0.22 μm. The m-2-HEAPr was double distilled. Initially, a low vacuum (1 Pa) distillation was carried and a small fraction of IL, ≈ 5 mL, rich in water and other volatile compounds was discarded, while the remaining sample was distilled in high vacuum (1×10^{-4} Pa). The final IL was colorless in contrast with its dark yellow initial color.

All the ILs were dried under high vacuum (10^{-4} Pa), stirring and moderate temperature (353 K), for a period of at least 48 hours prior to the measurements.

4. Thermodynamic Modeling and Consistency Theory

“In all science, error precedes the truth, and it is better it should go first than last.”

Hugh Walpole

4.1. Thermodynamic Modeling and Consistency

Valderrama and Álvarez[67] developed a thermodynamic consistency test for systems with incomplete *pTxy* data, cataloging them as thermodynamic consistent (TC), thermodynamic inconsistent (TI) or not full consistent (NFC). The authors analyzed the difficulties normally found when modeling this type of mixtures and proposed a methodology to analyze the experimental data, concluding about their thermodynamic consistency or inconsistency. Recently, Álvarez and Aznar[82, 83] applied an extension of this approach to several supercritical fluid + IL systems using a method based on the Gibbs-Duhem equation, on the fundamental phase equilibrium equation, and on the the Peng-Robinson equation of state,[84]

$$p = \frac{RT}{V - b_m} + \frac{a_m}{V(V + b_m) + b_m(V - b_m)} \tag{4.1}$$

with the Wong-Sandler mixing rule[85] using the UNIQUAC model[86] for the activity coefficient

$$b_m = \frac{\Sigma\Sigma x_i x_j (b - a/RT)_{ij}}{1 - \Sigma x_i \, a_i / b_i RT - A^E_\infty(x)/\Omega RT} \qquad \left(b - \frac{a}{RT}\right)_{ij} = \frac{1}{2}\left[b_i + b_j\right] - \frac{\sqrt{a_i a_j}}{RT}(1 - k_{ij}) \tag{4.2}$$

$$a_m = b_m \left(\sum x_i \left[\frac{a_i}{a_j} \right] + \frac{A^E_\infty(x)}{\Omega} \right) \tag{4.3}$$

where a_m and b_m are the equation of state constants, Ω = 0.34657 for the Peng-Robinson equation, and $A^E_\infty(x)$ is calculated using the UNIQUAC model and assuming that $A^E_\infty(x) \approx A^E_0(x) \approx G^E_0(x)$, being $G^E_0(x)$ the excess Gibbs free energy at low pressure described as

$$\frac{G^E}{RT} = \sum_{i=1}^{n} x_i \ln\left(\frac{\Phi_i}{x_i}\right) + \frac{Z}{2}\sum_{i=1}^{n} q_i x_i \ln\frac{\theta_i}{\Phi_i} - \sum_{i=1}^{n} x_i q_i \ln\left[\sum_{j=1}^{n} \theta_j \exp\left(-\frac{\lambda_{ij} - \lambda_{ii}}{q_i RT}\right)\right] \tag{4.4}$$

with

$$\Phi_i = \frac{x_i r_i}{\sum_j x_j r_j} \quad \text{and} \quad \theta_i = \frac{x_i q_i}{\sum_j x_j q_j} \tag{4.5}$$

The test uses the Gibbs-Duhem equation expressed in the integral form, where the left-hand side is denoted as A_P and the right-hand side as A_ϕ, as it follows:

$$A_P = \int \frac{1}{p y_2} dp \tag{4.6}$$

$$A_\varphi = \int \frac{(1-y_2)}{y_2(Z-1)} \frac{d\varphi_1}{\varphi_1} + \int \frac{1}{(Z-1)} \frac{d\varphi_2}{\varphi_2} \tag{4.7}$$

The values for A_P are obtained with experimental Py_2 data, and the values for A_ϕ are obtained with calculated values of Z, ϕ_i and y_2. The subscripts 1 and 2 denote CO_2 and ionic liquid compounds, respectively. The individual percent area deviation, ΔA_i, is given as:

$$\Delta A_i = 100\left[(A_\varphi - A_P)/A_P\right]_i \tag{4.8}$$

where the subscript i refers to the i^{th} data point. The quality of the correlation was analyzed through the relative deviations in the calculated pressure and solute concentration in the gas phase for each point i, defined as:

$$\Delta p_i = 100\,(p_i^{cal} - p_i^{\exp})/p_i^{\exp} \tag{4.9}$$

$$\Delta y_{2_i} = 100\left[(y_2^{cal} - y_2^{\exp})/y_2^{\exp}\right]_i \tag{4.10}$$

The method implies the minimization of the deviations of Eqs. 4.8, 4.9 and 4.10, setting as the objective function, OF, for the consistency test the minimization of the deviations in VLE data and the individual percent area deviation.

$$OF = \sum_{i=1}^{N-1}\left[\frac{A_P - A_\varphi}{\sigma_A}\right]_i^2 + \sum_{i=1}^{N}\left[\frac{p^{cal} - p^{\exp}}{\sigma_p}\right]_i^2 + \sum_{i=1}^{N}\left[\frac{y_{fluid}^{cal} - 1}{\sigma_y}\right]_i^2 \tag{4.11}$$

where N is the number of data points, p is the pressure, y_{fluid} is the vapor mole fraction of the supercritical fluid for data point i, the superscripts "*exp*" and "*cal*" refers to the

experimental and calculated values respectively, and σ_A, σ_p and σ_y are the standard deviations of those quantities. The experimental uncertainties in the pressure data were used for σ_P, the value 10^{-5} for σ_y and the value of A_P for σ_A. The minimization method was performed using a genetic algorithm code, implemented and fully explained in Alvarez et al.[87]. The difference between experimental and calculated values was calculated as the average percent deviation, expressed in absolute form, as follows:

$$|\Delta p| = \frac{100}{N} \sum_{i=1}^{N} \left[\left| p_i^{cal} - p_i^{\exp} \right| / p_i^{\exp} \right] \tag{4.12}$$

Furthermore the proposed model was applied, in the diluted region limit, to determine the Henry's constant for the studied systems.

4.2. The Henry's Law

The Henry's law relates the amount of a given gas dissolved in a given type and volume of liquid, at a constant temperature, to the fugacity of that gas in equilibrium with that liquid and can be described as

$$H_{12}(T, p) = \lim_{x_1 \to 0} \frac{f_i^L}{x_1} \tag{4.13}$$

where $H_{12}(T, p)$ is the Henry's constant, x_1 is the mole fraction of gas dissolved in the liquid phase, and f_1^L is the fugacity of gas in the liquid phase. As shown, Eq. 4.13 is only rigorously valid in the diluted region limit. The Henry constants for the CO_2 in the ILs investigated, were estimated by fitting the PR-WS/UNIQUAC model to the data and calculating the limiting slope as the solubility approaches zero.

This approach introduces some uncertainty on the estimated Henry's constants but the values of these constants for the two studied systems are different enough to allow a discussion of the interactions between the gas and the ionic liquids based on these values.

4.3. Gibbs Energy: Partial Molar Entropy and Enthalpy

The results for the Henry's constant of CO_2 in the ionic liquids, on the studied

pressure, temperature and composition range, can be correlated as a function of temperature by an empirical equation of the type

$$\ln(H_{12}) = A\left(\frac{1}{T}\right) + B \tag{4.14}$$

The effect of temperature on CO_2 solubility can be related to the Gibbs energy, the partial molar entropy and partial molar enthalpy of solvation[88] and can be calculated from an appropriate correlation of Henry's constant:

$$\Delta_{solv} G^0 = R.T\left(\ln\left(H_{12}\right)\right)_p \tag{4.15}$$

$$\Delta_{solv} H^0 = -T^2\left(\frac{\partial \Delta_{solv} G^0}{\partial T}\right)_T = -R.T^2\left(\frac{\partial \ln H_{12}}{\partial T}\right)_p \tag{4.16}$$

$$\Delta_{solv} S^0 = \frac{\Delta_{solv} H^0 - \Delta_{solv} G^0}{T} = -R.T\left(\frac{\partial \ln H_{12}}{\partial T}\right)_p - R.ln(H_{12})_p \tag{4.17}$$

The partial molar enthalpy of solvation gives an indication of the strength of interactions between the gas and the IL, while the partial molar entropy illustrates the amount of ordering present in the gas/IL mixture.

5. Carbon Dioxide Interactions

"No one wants to learn from mistakes, but we cannot learn enough from successes to go beyond the state of the art."

Henry Petroski

5.1. Abstract

The knowledge about the nature of the interactions between carbon dioxide and different organic molecules is of relevance for designing, operating and optimizing many industrial processes. In fact, numerous studies concerning the interactions of CO_2 with other compounds have been presented, using both experimental and theoretical approaches. Thus, to fully understand the interactions between CO_2 and different compounds, the high pressure phase equilibria of CO_2 binary systems containing carbon disulphide (CS_2) and carbon tetrachloride (CCl_4) were investigated, involving experimental measurements of high pressure phase equilibria and modeling with the Cubic plus Association (CPA) Equation of State (EoS). The CCl_4 and CS_2 were chosen due to their similar structure to CH_4 and CO_2, respectively, allowing to anticipate the interactions between like and unlike molecules that can be found at binary and multicomponent systems constituted by CO_2 and/or CH_4.

5.2. Introduction

Numerous studies concerning the interactions of CO_2 with other compounds have been presented, using both experimental and theoretical approaches.[89-99] It is well established that CO_2 can be, depending on the nature of the other organic molecule, an electron acceptor or donor or a proton acceptor forming hydrogen bonds.[100] In the presence of Lewis bases such as water, alcohols, ketones, amines, amides and aromatics, CO_2 acts as a Lewis acid favoring the formation of electron donor-acceptor complexes.[101-103] For instance, experimental spectroscopic observations put in evidence the presence of strongly attractive alcohol (OH group)-CO_2 interactions, due to highly stable complexes formed through the sp^3 O-donating atoms,[100, 101, 104, 105] and the existence of weaker specific Lewis acid-base interactions between CO_2 and the carboxyl oxygen of esters.[106]

Raman scattering and *ab initio* calculations have also shown that CO_2, a linear simple molecule with a large quadruple moment (-15×10^{-40} C m^2)[107] forms dimers with a slipped-parallel (offset face to face) geometry.[98, 108-110]

Recently,[89, 111] it was shown that the non ideality of CO_2 solutions on low volatile compounds (heavy alcohols, alkanes, fatty acids and fatty acid esters) and its impact on the CO_2 solubility is a result of a complex and delicate balance between the solute-solute, solute-solvent, and solvent-solvent interactions and cannot be inferred from the strength of solute-solvent interactions alone. These multiple interactions that can be found in different CO_2 systems make the description of the phase equilibria of CO_2 containing systems challenging.

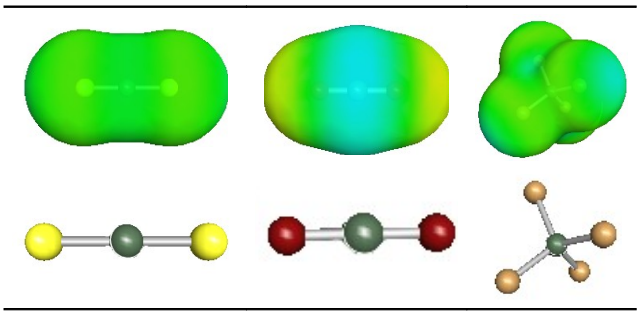

Figure 5.1. Carbon disulphide, CS_2, (left), carbon dioxide, CO_2, (middle) and carbon tetrachloride, CCl_4, right structures and sigma surface.

The breakthrough in the modeling of polar and highly non ideal systems in large temperature and pressure ranges came with the development of association equations of state that explicitly take into account the specific interactions between like (self-association) molecules and unlike molecules (cross-association). Molecular-based equation of state, like the statistical associating fluid theory (SAFT)[95, 112-114] and its framework derivatives, group contribution equation of state (GC-EoS)[115] and group contribution-associating-equation of state (GCA-EoS)[115], just to mention some, have been successfully use to describe the phase equilibria of a wide set of systems as well as to gain deeper insights on these systems molecular interaction. Nonetheless, one of the most successful models of that kind is the Cubic-Plus-Association (CPA) equation of state considering its quality, reliability and wide range of applicability.[113, 114, 116]

The CPA EoS was previously used for an adequate description of the VLE of an extensive series of CO_2 binary systems containing several non-self associating, associating and cross-associating components. A detailed investigation regarding the differing behavior

of CO_2 depending on the nature of the second component and how the CPA EoS can best describe them was presented.[111, 117]

Aiming at fully understand the interactions between CO_2 and different compounds, the high pressure phase equilibria of CO_2 binary systems containing CS_2 and CCl_4 were here investigated, involving experimental measurements of high pressure phase equilibria and modeling with the CPA EoS. The CCl_4 and CS_2 were chosen due to their similar structure to CH_4 and CO_2, respectively, allowing to anticipate the interactions between like and unlike molecules that can be found at binary and multicomponent systems constituted by CO_2 and/or CH_4.

5.3. Results and Discussion

The solubility of carbon dioxide in carbon disulphide and carbon tetrachloride was measured for mole fractions ranging from (0.05 to 0.7) at 293 K, 313 K and 333 K in the pressure range of (1 to 9) MPa, as reported in Tables A.1 and A.2 and depicted in Figures 5.2 and 5.3.

Apart from Reiff et al.[118] work, that reported a systematic study around the CO_2 + CS_2 system, there isn't, to our knowledge, more data available in literature. As depicted in Figure 5.4 the data reported by Reiff et al.[118] presents the same phase behavior but with slightly lower CO_2 solubilities than those reported in this work.

The CO_2 solubility on these solvents decreases with temperature and increases with pressure as commonly observed for the solubility of light gases in liquids.[30, 36, 50, 119] In the CO_2 molar fraction region investigated, the CO_2 + CCl_4 system presents a near linear dependency of the solubility with the CO_2 concentration as shown in Figure 5.2. For the CO_2 + CS_2 system this linear dependency is observed only at the lowest concentrations of carbon dioxide. For CO_2 concentrations above 0.5 in molar fraction the system seems to reach a plateau in pressure, as depicted in Figure 5.3.

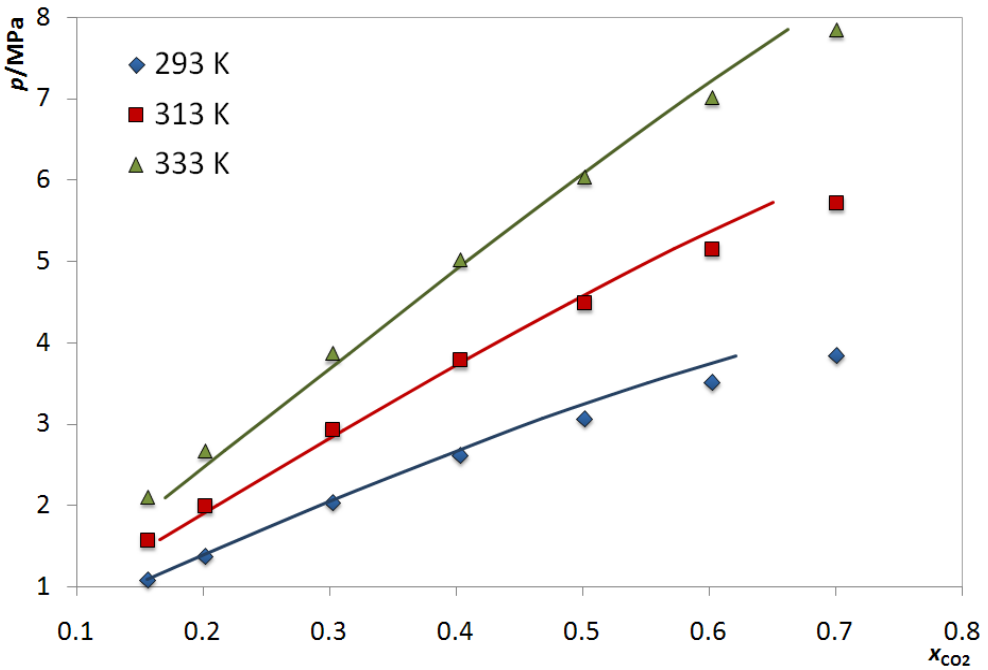

Figure 5.2. Pressure – composition diagram of the binary systems CO_2 + CCl_4. The solid lines represent the CPA EoS predictions with non-association.

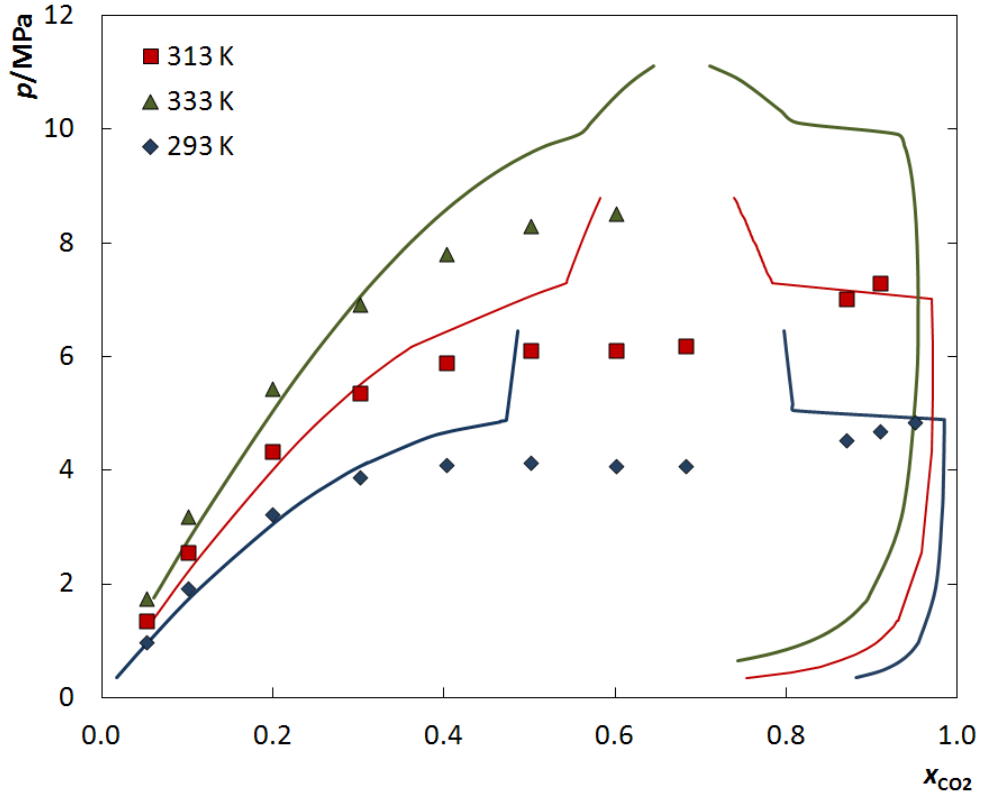

Figure 5.3. Pressure – composition diagram of the binary systems CO_2 + CS_2. The solid lines represent the CPA EoS predictions with non-association.

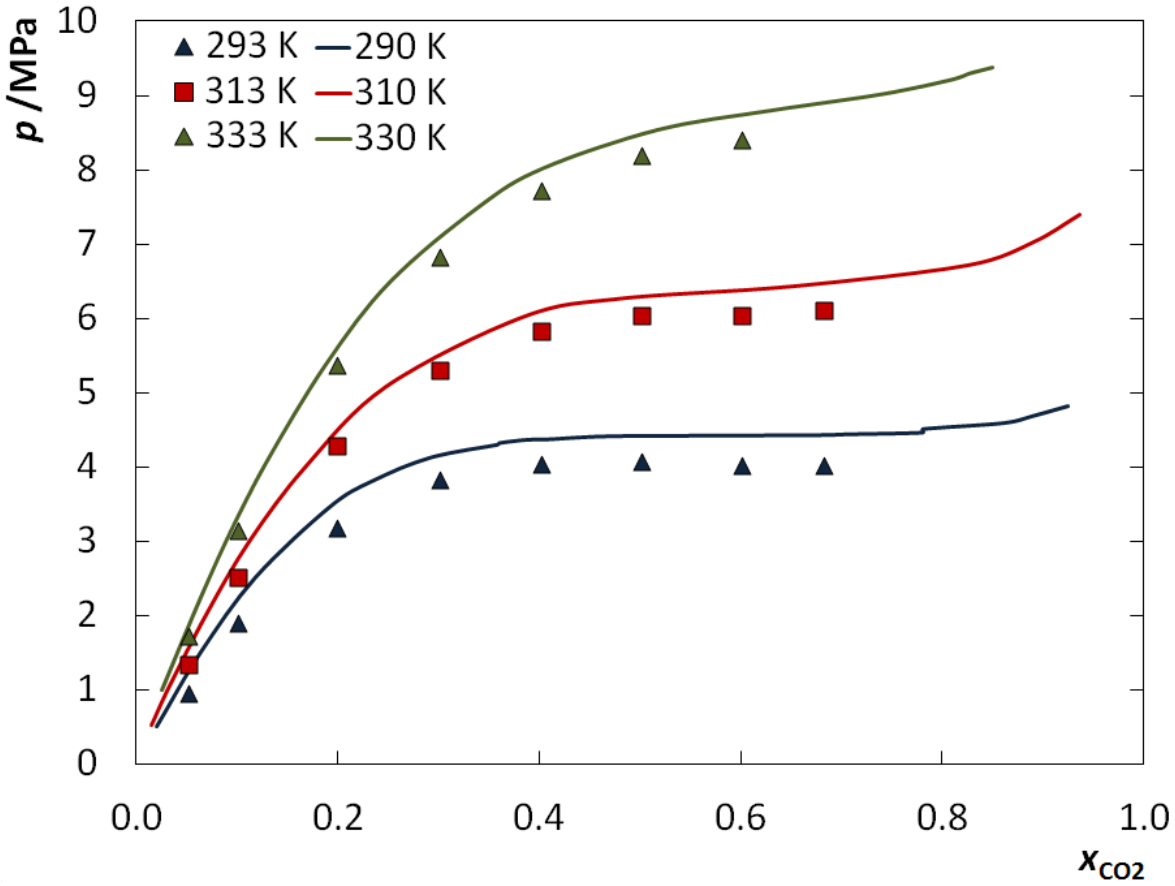

Figure 5.4. Pressure – composition diagram of the binary systems CO_2 + CS_2. The solid lines represent the data reported by Reiff et al.[118].

5.3.1. Cubic plus Association Equation of State Modeling.

The CPA EoS is composed by two terms: a physical term described by the Soave-Redlich-Kwong equation of state (SRK EoS), that takes into account the physical interactions between the components, and an associating term described by the Wertheim's theory, which accounts for the specific site-site interactions due to hydrogen bonding and solvation effects.[113]

In terms of the compressibility factor, the CPA EoS is expressed by

$$Z = Z^{phys.} + Z^{assoc.} \quad (5.1)$$

$$Z^{phys.} = \frac{1}{1-b\rho} - \frac{a\rho}{RT(1+b\rho)} \tag{5.2}$$

$$Z^{assoc.} = \frac{-1}{2}\left(1+\rho\frac{\partial \ln g}{\partial \rho}\right)\sum_i x_i \sum_{A_i}\left(1-X_{A_i}\right) \tag{5.3}$$

where a is an energy parameter, b the co-volume, ρ the density of the liquid, x_i the mole fraction of the component i, X_{Ai} the mole fraction of pure component i not bonded at site A and g the simplified radial distribution function[120]

$$g(\rho) = \frac{1}{1-1.9\eta} \tag{5.4}$$

$$\eta = \frac{1}{4} b\rho \tag{5.5}$$

The energy parameter for pure components is given by a Soave-type temperature dependency

$$a = a_0\left[1+c_1\left(1-\sqrt{T_r}\right)\right]^2 \tag{5.6}$$

where T_r is the reduced temperature ($T_r = T/T_c$, being T_c the critical temperature). The a_0 and c_1 constants are estimated by fitting experimental vapor pressure and liquid density data of the pure component.

X_{Ai} is the central point of the association term and is related to the association strength between two sites belonging to two different molecules

$$X_{A_i} = \frac{1}{1+\rho\sum_j x_j \sum_{B_j} X_{B_j}\Delta^{A_i B_j}} \tag{5.7}$$

where B_j represents the summation over all sites and depends on the class of the association scheme and the $\Delta^{Ai\,Bj}$ is the association strength that can be determined by

$$\Delta^{A_i B_j} = g(\rho)\left[\exp\left(\frac{\varepsilon^{A_i B_j}}{RT}\right)-1\right] b_{ij}\beta^{A_i B_j} \tag{5.8}$$

CPA requires the knowledge of three pure component parameters for the physical part, a_0, c_1 and b, and two more for the association term, ε and β. These last two are only present in associating compounds. These parameters are estimated through a simultaneous regression of the liquid density and vapor pressure data, carried by the minimization of the objective function, *OF*,

$$OF = \sum_{i}^{NP} \left(\frac{p_i^{\exp} - p_i^{calc}}{p_i^{\exp}} \right)^2 + \sum_{i}^{NP} \left(\frac{\rho_i^{\exp} - \rho_i^{calc}}{\rho_i^{\exp}} \right)^2 \tag{5.9}$$

In order to determine the pure compound parameters it is necessary to assign an association scheme, that is, the number and type of association sites for the associating compound. The nomenclature proposed by Huang and Radosz[121] is adopted here.

When dealing with mixtures, the energy and co-volume parameters of the physical term are calculated employing the conventional van der Waals one-fluid mixing rules. As will be explained, the compounds here in consideration will be taken as non-associating and for mixtures composed of that kind of compounds, no combining rules are required for the association term and thus, the binary interaction parameter, k_{ij}, is the only adjustable parameter

$$a = \sum_i \sum_j x_i x_j a_{ij} = \sum_i \sum_j x_i x_j \sqrt{a_i a_j (1 - k_{ij})} \tag{5.10}$$

$$b = \sum_i x_i b_i \tag{5.11}$$

The k_{ij} parameter was estimated by the minimization of the following objective function

$$OF = \sum_{i}^{NP} \left(\frac{x_i^{calc} - x_i^{\exp}}{x_i^{\exp}} \right)^2 \tag{5.12}$$

where x_i is the mole fraction of component *i* in the phases selected for the optimization.

Considering the CO_2 as a self-associating molecule, applying association equations

of state that explicitly take into account hydrogen bonding interactions, is a debatable issue, as discussed by Oliveira et al.[111]. Nonetheless, from the evaluation of the CPA EoS capability to model the phase equilibria of CO_2 systems with alkanes, alcohols, esters and acids, it is feasible to conclude that CO_2 can be considered both as an inert or as an associating compound, explicitly accounting or not for the polar interactions, depending on the nature of the other component of the binary system.

With that in mind, phase equilibria of the CO_2 + CCl_4 and CO_2 + CS_2 systems were evaluated with the CPA EoS. For both systems, the components were treated as inert compounds without explicitly accounting for their polarity. The CPA pure compound parameters were determined from a simultaneous regression of their vapor pressure and liquid density data, taken from DIPPR[122]. A very good description for the vapor pressures and liquid densities was achieved, as seen in Table A.3, with global average deviations inferior to 1%.

Knowing the pure compound parameters it was then possible to compute the phase equilibria of the systems. For the CO_2 + CCl_4 system, very good results were obtained using single and positive binary interaction parameters, with a global average deviation of 3.9% in composition, as reported in Table A.4 and depicted in Figure 5.2. Using a temperature independent binary interaction parameter would lead to a significant increase on the average deviations.

Similarly, very good results were also obtained using a single, positive and temperature independent binary interaction parameter of 0.1598 for the CO_2 + CS_2 system, as depicted in Figure 5.3, with a global average deviation of 9.6% in composition, for CO_2 molar fractions up to 0.4. Furthermore, the plateau in pressure observed for this system suggests the presence of a liquid-liquid equilibrium region for CO_2 molar fractions between 0.5 and 0.8 that decreases with increasing temperature. This hypothesis is supported by the CPA EoS prediction of a liquid-liquid phase split at this regions, by the drastic increase and change on the equilibrium pressure behavior, as depicted in Figure 5.3.

5.3.2. *Henry's Constants.*

As described on section 4.2. the estimated Henry's constants were determined and the results, reported in Table A.4, indicate that Henry's constant increase (i.e., CO_2 solubility decreases) with the temperature.

The results for the Henry's constant of CO_2 in CCl_4 and in CS_2 were correlated as a function of temperature by equation 4.14 where, the coefficients *A* and *B* are listed in Table A.5, together with the Henry's constant average absolute deviations, $|\Delta H_{12}|$, obtained for each solvent.

The effect of temperature on CO_2 solubility can be related to the Gibbs energy, the partial molar entropy and partial molar enthalpy of solvation[88], as described in section 4.3. The results presented in Table A.5 show that the partial entropies of solvation are almost identical for both systems, indicating similar structural solvation interactions. Furthermore, the higher absolute value for the partial molar enthalpy of solvation of the CO_2 + CCl_4 system, indicates a more favorable interaction between the CO_2 and the CCl_4 when compared with the CS_2. The enthalpies and entropies of solvation contribution make the solubility of CO_2 in both systems non-spontaneous.

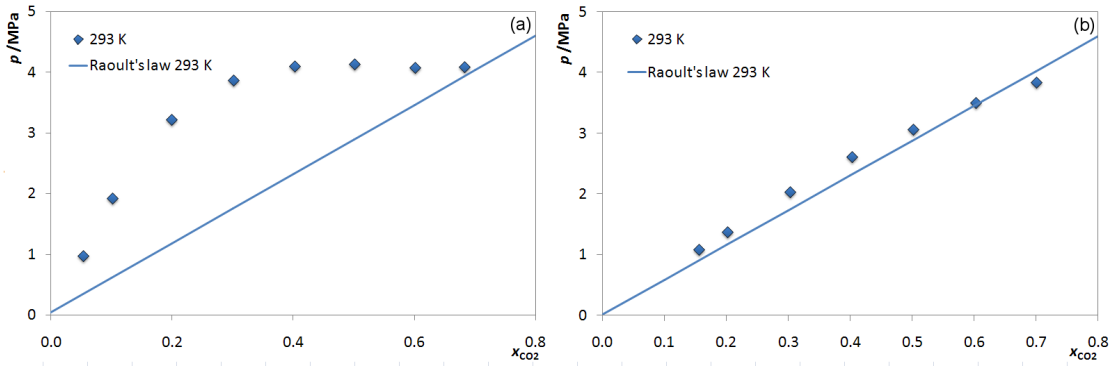

Figure 5.5. Pressure – composition diagram of the binary systems (a) CO_2 + CS_2, and (b) CO_2 + CCl_4. The solid lines represent the ideal behavior predicted by the Raoult's law.

Taking into consideration the similarity between the CO_2 and the CS_2 molecules, one would expect similar interactions and a near ideal behavior. However what is

experimentally observed is that this system presents strong positive deviations to ideality, as shown by the deviations to the Raoult's law, presented in Figure 5.5a. Nonetheless, these results can be explained if the atoms electronegativities and the molecules atomic charges, dipoles and quadrupoles are taken into account. Hajime Torii[123] results picture a CS_2 as being an essentially non polar molecule due to the electronegativity of the S atom being similar to the C. On the opposite, Torii[123] reported that the electric field around CCl_4 goes out of the chloride atom on the line extended from the C-Cl bond towards the chlorine atom on the side of the bond, due to the existence of atomic quadrupoles on the chloride atoms. The absence of charges on CS_2 leads to poor CO_2 – CS_2 interactions and consequently to a strong non-ideal system while on the CO_2 – CCl_4 the dipole-dipole interactions between the two molecules produce an almost ideal behavior, as shown in Figure 5.5b.

5.4. Conclusions

New Gas–Liquid equilibrium data of two binary systems, namely, Carbon Disulphide + CO_2 and Carbon Tetrachloride + CO_2 have been investigated for mole fractions ranging from (0.05 to 0.7) at 293 K, 313 K and 333 K in the pressure range of (1 to 9) MPa, aiming at understanding the interactions between the CO_2 + CS_2 and CO_2 + CCl_4 molecules.

The Cubic plus Association Equation of State was used in description of the measured data. The model allows a good description of the experimental data and the estimation of the Henry's constants for these systems, using only one, small and positive binary interaction parameter.

The partial Gibbs energy, enthalpies and entropies of solvation estimated from Henry's constants show that the solubility of CO_2 in both is non spontaneous at standard pressure (0.1 MPa). The entropy of solvation and the partial molar enthalpy are slightly lower for the CO_2 + CCl_4 system indicating better interactions between the CO_2 and the CCl_4 than between the CO_2 and the CS_2.

6. High Pressure Phase Behavior of Carbon Dioxide in 1-alkyl-3-methylimidazolium bis(trifluoromethylsulfonyl)imide Ionic Liquids

"*No amount of experimentation can ever prove me right; a single experiment can prove me wrong.*"

Albert Einstein

6.1. Abstract

New standards concerning environmental and safety issues are creating an increasing interest on Ionic Liquids as alternative solvents for a wide range of industrial applications. In this work, a new apparatus developed to measure vapor – liquid phase equilibrium in a wide range of pressures and temperatures was used to measure the phase behavior of the binary systems of carbon dioxide (CO_2) + 1-ethyl-3-methyl-imidazolium bis(trifluoromethylsulfonyl)imide ([C_2mim][NTf_2]) and CO_2 + 1-methyl-3-pentyl-imidazolium bis(trifluoromethylsulfonyl)imide ([C_5mim][NTf_2]) at temperatures up to 363 K and pressures up to 50 MPa. A thermodynamic consistency test, developed for systems with incomplete *PTxy* data and based on the Gibbs-Duhem equation, was applied to the experimental data measured in this work and the Peng-Robing EoS using the Wong Sandler mixing rule was used to describe the experimental data with excellent results.

6.2. Introduction

The successful development of IL based processes using supercritical fluids depends on the adequate knowledge of the phase behavior of the systems. Several authors, such as Brennecke,[47, 48, 79] Peters,[60, 61, 124] Noble,[125] Lim,[126] Baltus,[127] Outcalt,[55] Yokozeki,[64] and Majer,[128] have been reporting supercritical carbon dioxide solubility in common ILs, but few have focused their studies on the NTf_2 anion based ionic liquids.[55, 60, 124-127]

Apart task specific ILs, the NTf_2 anion based ILs are the ones presenting the highest CO_2 solubility. Although both anion and cation influence the CO_2 solubility, the anion has the strongest influence.[47-49, 129] The presence of fluoroalkyl groups, known to be "*CO_2-philic*", make the NTf_2 anion based ILs in compounds with great CO_2 solubilities. However, this behavior is yet poorly understood and while some authors emphasize the role of the interactions between the CO_2 and the NTf_2 anion,[47, 48, 130] others identify the large free volume of the ionic liquid as the main factor responsible for the large solubility. [28]. On the other hand, the alkyl chain length of the cations, also influences the CO_2

solubility, indicating an entropic, rather than enthalpic, effect is present.[47] For a given cation, the data available seems to indicate that the longer the alkyl chain, the higher the free volume, and consequently the larger the solubility.[46, 47, 60-62, 79, 130, 131]

In this work, a new apparatus was developed to investigate the high pressure phase behavior of gas + ionic liquid systems. Two NTf_2 based ionic liquids were selected in order to further contribute for a more detailed knowledge and thus a better understanding of the solubility of supercritical CO_2 in these fluids. The system of CO_2 + 1-ethyl-3-methyl-imidazolium bis(trifluoromethylsulfonyl)imide ($[C_2mim][NTf_2]$) was chosen because it allows the evaluation of the quality of the measurements by direct comparison with literature data,[124] and the CO_2 + 1-methyl-3-pentyl-imidazolium bis(trifluoromethylsulfonyl)imide ($[C_5mim][NTf_2]$) system was studied to investigate the effect of the alkyl chain length on the CO_2 solubility in ionic liquids. Both systems were measured at temperatures up to 363 K and pressures of 50 MPa.

A thermodynamic consistency test,[67, 82] developed for systems with incomplete *PTxy* data and based on the Gibbs-Duhem equation, and the the Peng-Robinson equation of state[84] with the Wong-Sandler mixing rule[85] using the UNIQUAC model[86] for the activity coefficients, was applied to describe the experimental data measured in this work. It will be shown that the model provides an excellent representation of the experimental data and the consistency test shows that the data here reported, unlike many other systems available in the literature, is thermodynamically consistent [67, 82, 83].

6.3. Results and Discussion

Although measurements were previously carried by us and others in similar apparatuses,[68-72] $[C_2mim][NTf_2]$ was selected to validate the methodology and experimental procedure adopted in this work and the measurements were compared against data by Schilderman et al.[124]. High pressure binary vapor-liquid mixtures data of CO_2 in ILs are scarce and significant discrepancies among data from different authors[55, 124, 126] are common in literature. The identification of the data with the highest quality available in the literature was carried using the thermodynamic consistency test described in section 4.1.

[83] The most reliable data identified by Àlvarez and Aznar[82, 83] were those by Schilderman et al.[124] for the system CO_2 + [C_2mim][NTf_2], where the isotherms at 313 K, 323 K e 363 K were found to be thermodynamically consistent. A comparison between our data and the data reported by Schilderman et al.[124] showed a good agreement. Moreover, as will be shown below, the data here measured was found to be essentially thermodynamic consistent.

The solubility of carbon dioxide in the studied ILs was measured for mole fractions from (0.2 to 0.8), in the temperature range (293 to 363) K and pressures from (0.6 to 50) MPa, as reported in Tables B.1 and B.2 and depicted in Figures 6.1a and b. The temperature increase leads to an increase on the equilibrium pressure and by increasing CO_2 concentration, the equilibrium pressures increase gradually, at first, and rapidly for higher CO_2 contents.

Due to the presence of fluoroalkyl groups, NTf_2 anion based ILs, are "*CO_2-philic*", meaning that they present higher CO_2 solubilities than other ILs resulting in low equilibrium pressures for high CO_2 mole fractions, as can be seen in Figure 6.1. This behavior, yet poorly understood, is reported to be related to the interaction between the negative fluorine atoms and the positive charge on the carbon of the CO_2 molecule.[47, 48]

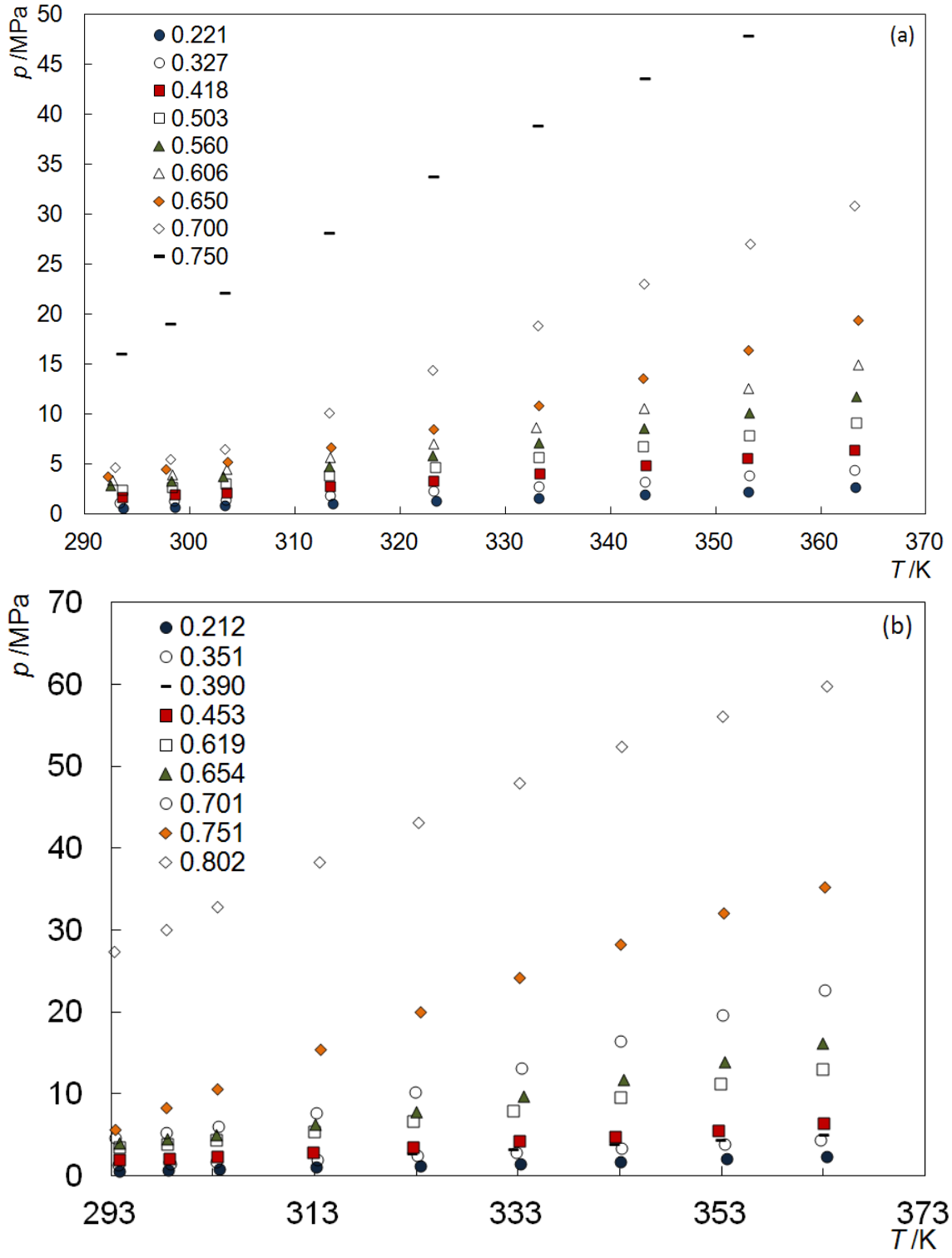

Figure 6.1. Pressure – temperature diagram of the binary systems (a) CO_2 + $[C_2mim][NTf_2]$ and (b) CO_2 + $[C_5mim][NTf_2]$.

It is known that the substituents on the imidazolium ring can affect the ILs properties[60, 61, 75, 78, 132-135]. For CO_2, a slight increase on solubility can be observed with the alkyl chain length at all pressures as shown in Figure 6.2.[47, 60, 79, 124] Nonetheless, in the NTf_2 based ILs, the alkyl chain length on the imidazolium ring seem to have a lower influence on the solubility than other IL families, even for higher CO_2 concentrations.[47, 124] Kazarian et al.[136], using ATR–IR spectroscopy, suggested that the increase in solubility is not related to any specific interactions between the CO_2 and the cation. Shariati et al.[60] and Aki et al.[47] explained this phenomenon based on entropic rather enthalpic considerations, due to the decrease of the compounds densities with the increase of the alkyl chain length leading to a greater free volume.

For the thermodynamic consistency test, the isopleths were interpolated with the method proposed by Álvarez and Aznar[83] (section 4.1.) and the results are shown in Table B.4, for the CO_2 + $[C_2mim][NTf_2]$ system and for the CO_2+ $[C_5mim][NTf_2]$ system, respectively. The physical properties used in the model for all substances are reported in Table B.3.

The results of the application of the thermodynamic consistency test to the binary systems containing ionic liquid is presented in Table B.5. In this Table, *NP* is the number of data points, *T* is the temperature, k_{12}, A_{12} and A_{21} are the interaction parameters of the model, where *1* stands for the CO_2 and *2* for the ionic liquid. This Table is divided in sections for each system studied. The consistency analyses for the CO_2 + $[C_2mim][NTf_2]$ system measured by Schilderman et al.[124] at 363.15 K are also reported here.

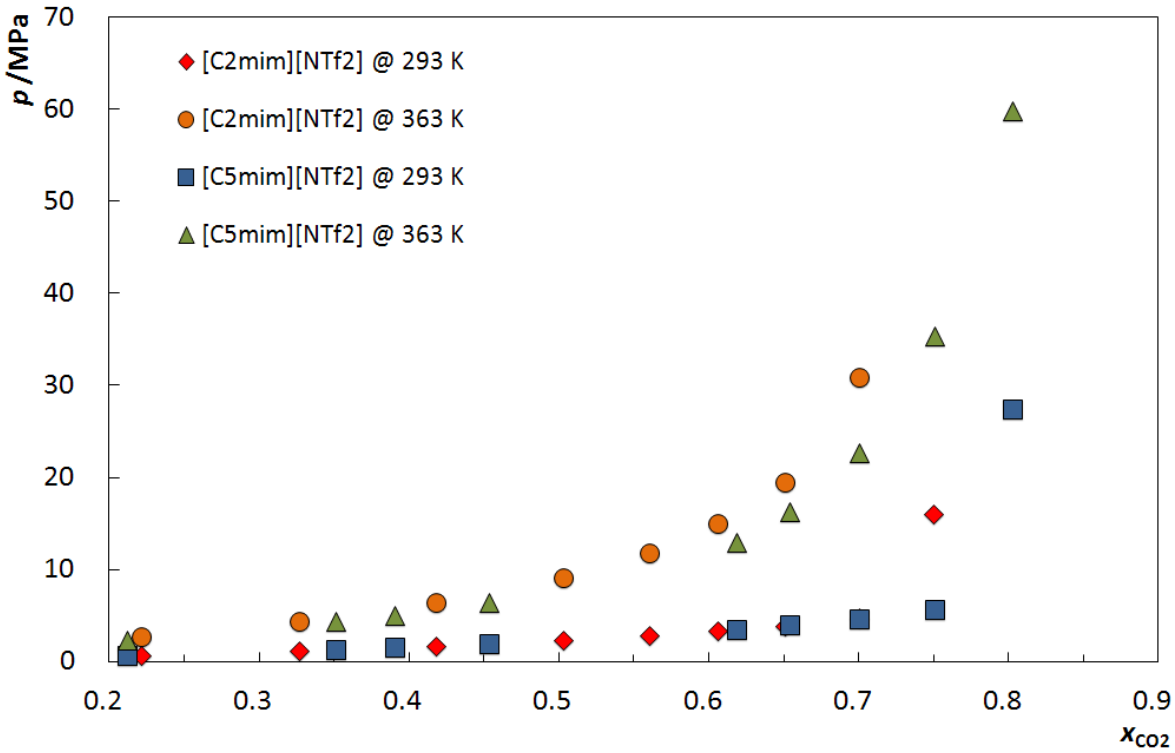

Figure 6.2. Pressure – composition diagram of CO_2 in [$C_n$mim][NTf_2].

Some detailed results are shown in Tables B.6, B.7 and B.8. These tables are divided in two parts, the upper part shows the original data set, while the lower part shows the remaining data after removing some experimental points that have been found to be thermodynamically inconsistent. Table B.6 also includes the detailed results for the system CO_2 + [C_2mim][NTf_2] at 363.15 K by Schilderman et al.[124]. These data have deviations within the established limit values of ΔA_i, being thermodynamically consistent. In Table B.7, where detailed results at 298.15 K for the system CO_2 + [C_2mim][NTf_2] are presented, the upper part shows that these data have deviations in the final values of ΔA_i (bold and italic type) outside the established limits; the lower part shows that when the highest area deviation is eliminated, the deviations for the remaining eight points are within the defined limits of ±20% . Therefore, although the original data set with nine data points is not fully thermodynamically consistent, the new set with the remaining eight points is thermodynamically consistent; however, the x_{CO2}=0.606 point has a good probability to be

inconsistent, because two $\Delta P_i < 5$ yields $\Delta A_i > 10$.

The same procedure is applied for the data of the system CO_2 + $[C_5mim][NTf_2]$, at 298.15, reported in Table B.8. Again, although the original data are not fully consistent, the remaining eight points, after removing one data point, are within the defined limits of −20% to +20%, which are thermodynamically consistent.

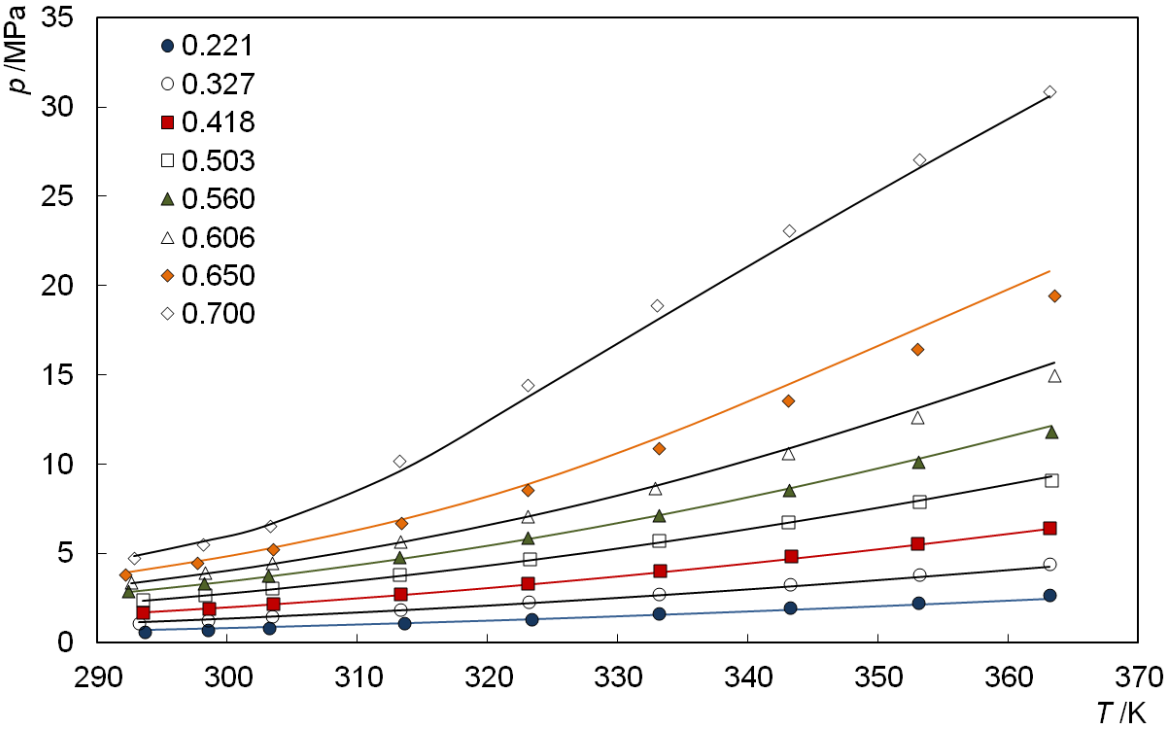

Figure 6.3. PT diagram and modeling for the system CO_2 + $[C_2mim][NTf_2]$.

These results show that the CO_2 + $[C_2mim][NTf_2]$ system has greater deviations in the isopleths at x_1=0.75, while the CO_2 + $[C_5mim][NTf_2]$ system has greater deviations in the isopleths at x_1=0.751 and x_1=0.802. Therefore, the isotherms with these compositions are not fully consistent.

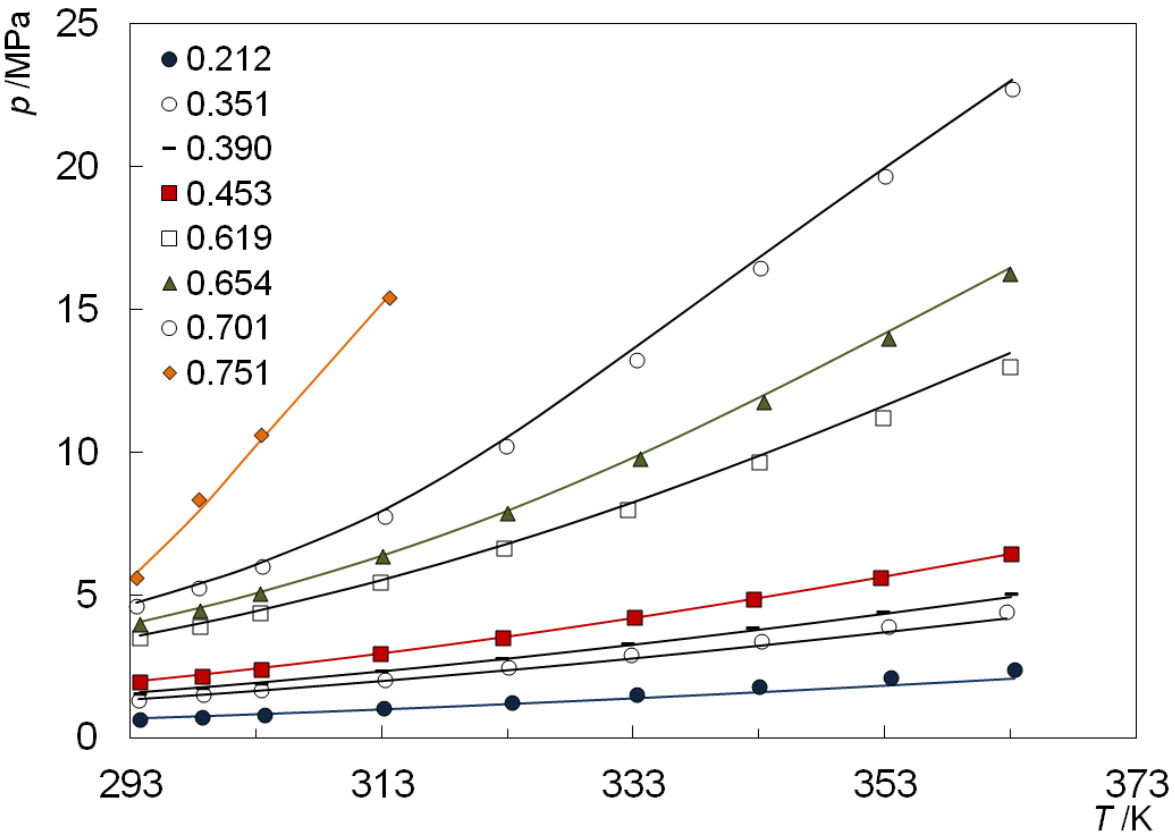

Figure 6.4. PT diagram and modeling for the system CO_2 + [C_5mim][NTf_2].

In Figures 6.3 and 6.4 the description of the experimental data using the model detailed above and the parameters reported in Tables B.3 and B.9 for the CO_2 + [C_2mim][NTf_2] and CO_2 + [C_5mim][NTf_2] systems is presented. As can be seen, using the proposed approach it is possible to obtain a very good description of the experimental data measured in this work.

The Henry's constants were determined, as described in section 4.2. , and the results are shown in Table B.10, where, $|\Delta p|$ is average absolute deviations for pressure and H_{12} is the Henry's constant calculated. For one additional validation of the calculated Henry's constant for the CO_2 + [C_2mim][NTf_2] binary system, Henry's constant at 298.15 K and 3.56 MPa, taken from Schilderman et al.[124], was included showing good agreement with linear tendency obtained in this work. The results indicate that Henry's constant

decreases slightly (i.e., CO_2 solubility increases) as the length of the carbon chain on the imidazolium ring increases.

The results for the Henry's constant of CO_2 in $[C_2mim][NTf_2]$ (where the calculated value 3.56 MPa at 298.15 K was included[124]) and CO_2 in $[C_5mim][NTf_2]$ were correlated as a function of temperature by the empirical equation 4.14 where, the coefficients *A*, *B* and *C* obtained are listed in Table B.11, together with the Henry's constant average absolute deviations, $|\Delta H_{12}|$, obtained for each ionic liquid. The average deviation of 0.1% and a maximum deviation of 0.1% for $[C_2mim][NTf_2]$ and an average deviation of 0.04% and a maximum deviation of 0.04% for $[C_5mim][NTf_2]$ were obtained.

The effect of temperature on CO_2 solubility can be related to the partial molar entropy and partial molar enthalpy of solution[137] and can be calculated from an appropriate correlation of Henry's constant, as described in section 4.3. .

The partial molar enthalpy values obtained are similar to those reported by Brennecke's group[47, 49] and the magnitude consistent with physical absorption. The results in Table B.12 show that although the partial molar enthalpy is slightly higher than the partial molar entropy they are of similar magnitude indicating that the solubility of CO_2 in ILs is not entropically driven, as suggested by some authors,[48, 127, 138] neither essentially an enthalpic phenomena, as suggested by others,[28, 128] but both phenomena control the solubility of CO_2 in ILs.

6.4. Conclusions

A high pressure cell to measure supercritical fluid + liquid phase behavior was validated for studying gas-Ionic Liquid systems with new experimental data for CO_2 solubility in 1-ethyl-1-methyl-imidazolium bis(trifluoromethylsulfonyl)imide and 3-methyl-1-pentyl-imidazolium bis(trifluoromethylsulfonyl)imide in a wide range of temperature, pressure and carbon dioxide mole fractions are reported.

A thermodynamic consistency test based on the Peng-Robinson EoS with the Wong-Sandler/UNIQUAC mixing rule was applied to the measured data showing that they

are thermodynamically consistent. The model allows a good description of the experimental data and the estimation of the Henry constants for these systems. The partial molar enthalpies and entropies of solution for these systems are of similar magnitude what allows to conclude that this solubility is not driven predominantly by entropic or enthalpic phenomena, as previously admitted by various authors.

7. Specific Solvation Interactions of CO_2 on Acetate and Trifluoroacetate Imidazolium Based Ionic Liquids at High Pressures

"The great tragedy of science - the slaying of a beautiful hypothesis by an ugly fact."

Thomas Huxley

7.1. Abstract

New classes of acidic or basic ionic liquids are gaining special attention, since the efficiency of many processes can be enhanced by the judicious manipulation of these properties. The absorption of sour gases can be enhanced by the basic character of the IL. The fluorination of the cation or the anion can also contribute to enhance the gas solubility. In this work these two characteristics are evaluated through the study of the gas – liquid equilibrium of two ionic liquids based on similar anions, 1-butyl-3-methylimidazolium acetate ([C_4mim][Ac]) and 1-butyl-3-methylimidazolium trifluoroacetate ([C_4mim][TFA]), with carbon dioxide (CO_2) at temperatures up to 363 K and pressures up to 76 MPa. The data reported are shown to be thermodynamically consistent. Henry's constants estimated from the experimental data show the solubility of CO_2 on the [C_4mim][Ac] to be spontaneous unlike in [C_4mim][TFA] due to the differences in solvation enthalpies in these systems.

Ab initio calculations were performed on simple intermolecular complexes of CO_2 with acetate and trifluoroacetate using MP2/6-31G(d), and the G3 and G3MP2 theoretical procedures to understand the interactions between CO_2 and the anions. The theoretical study indicates that although both anions exhibit a simultaneous interaction of the two oxygen of the carboxylate group with the CO_2, the acetate acts as a stronger Lewis base than the trifluoroacetate. ^{13}C high resolution and magic angle spinning (HRMAS) NMR spectra provide further evidence for the acid/base solvation mechanism and the stability of the acetate ion on these systems. Further similarities and differences observed between the two anions in what concerns the solvation of CO_2 are discussed.

7.2. Introduction

A considerable amount of work, concerning the development of task specific ionic liquids, has been carried, addressing essentially the IL cation. Bates el al.[16] reported amino functionalized ILs, while Yuan et al.[31] and Sun et al.[32] used hydroxyl-functionalized ILs as novel efficient catalyst for chemical fixation of CO_2. Yu et al.[37] and

Huang et al.[26] proposed guanidinium based ILs, where the electron-donating groups increased the strength of the donor-acceptor interactions on -NH_2 and consequently enhanced the interactions between -NH_2 and CO_2. Li et al.[139] investigated the ability of switching the ILs basicity by repeatedly bubbling CO_2 and N_2, improving processes efficiency. Bara et al.[21] synthesized imidazolium based ILs with one, two or three oligo(ethylene glycol) substituents that, in spite of presenting similar CO_2 solubilities to that in [$C_n$mim][NTf2] analogues, present lower solubilities towards N_2 and CH_4 and therefore enhanced selectivities.

Acidic or basic ILs represent new classes of acids or bases. The study of the acidity/basicity of the ILs is of great importance, since the efficiency of many processes depends on the basicity of the media or can be controlled by it. Crowhurst et al.[140] reported that the hydrogen bond basicities of ILs are controlled by the anion, and the hydrogen bond donating behavior is also dominated by the hydrogen bond basicity of the anions, with a smaller contribution from the hydrogen bond acidity of the cation. Furthermore, for the imide ionic liquids an increase of the hydrogen bond acidity with the cation change was found.[140] Nonetheless, changing to more basic anions leads to a dramatic drop in the acidity. Pennline et al.[141] screened quaternary ammonium polyethers ILs as potential solvents for CO_2 capture based in the Pearson's “hard and soft acid-base” principles, where the solvent should possess a Pearson “hard base” allowing a strong affinity towards CO_2. Maginn et al. [142] and Shiflett et al.[29, 33, 34] reported on imidazolium based ionic liquid with the acetate and other carboxylate anions that seem to present an uncharacteristic behavior. The systems with the acetate based IL present a low vapor pressure for mixtures up to about 20 mol%, indicating that CO_2 could have formed a non-volatile or very low vapor pressure molecular complex with the ionic liquid. The solvation of CO_2 by these anions is, however, yet poorly understood.

The present study will explore the basicity of the anion as a means to enhance the absorption of sour gases by ionic liquids, along with another strategy to foster the gas solubility in a IL by the fluorination of its alkyl chains.[28, 47] On this work the two effects

will be compared and evaluated in a wide range of pressures and temperatures aiming at a better understanding of the mechanisms of solvation of CO_2 on ILs with these characteristics. For that purpose the Gas-Liquid Equilibrium (GLE) of the atypical and challenging binary systems, CO_2 + 1-butyl-3-methylimidazolium acetate ([C_4mim][Ac]), and CO_2 + 1-butyl-3-methylimidazolium trifluoroacetate ([C_4mim][TFA]) previously approached only by Shiflett et al.[29, 33, 34], will be here extended to higher pressures, temperatures and concentrations. The comparison between these two systems will provide not only a better understanding of the anion acid – base interactions with the CO_2 but also the influence of the fluoroalkyl groups in the molecule behavior and consequently, in the CO_2 solubility. A thermodynamic consistency test developed for systems with incomplete *pTxy* data[67, 82, 83, 143], is here used to evaluate the quality of the data reported through its thermodynamic consistency.

There is plenty of evidence in the literature for Lewis Acid (A)/Lewis Base (B) interaction between CO_2 and the carbonyl group[105, 144, 145]. Raveendran and Wallen[146] have studied the role of a cooperative C-H···O interaction as an additional stabilizing interaction between the CO_2 and the carbonyl group and their implications for the solvation of CO_2 on these compounds. The CO_2 acts as a LA where the acidic central carbon interacts with charged or uncharged Lewis bases.

To understand the interactions between CO_2 and the [Ac] and [TFA] anions, ab initio calculations were performed on simple intermolecular complexes using MP2/6-31G(d), and the G3 and G3MP2 theoretical procedures. A simultaneously interaction, of the two oxygen of the carboxylate group with the CO_2 is found in both anions, [Ac] and [TFA].

^{13}C high resolution and magic angle spinning (HRMAS) NMR spectra of the CO_2 + [C_4mim][Ac] are shown to further support the acid/base interaction mechanism behind the solvation of CO_2 at low pressures. They also provide further evidence to the stability of the acetate on these systems.

7.3. Results and Discussion

7.3.1. Experimental Data

High pressure gas – liquid data for mixtures of CO_2 and ILs are scarce and important discrepancies among data from different authors[47, 49, 126] can be found in the literature.

The solubility of carbon dioxide in the ILs studied in this work was measured for mole fractions from (0.2 to 0.8), in the temperature range (293 to 363) K and pressures from (0.2 to 76) MPa, as reported in Tables C.1 and C.2 and depicted in Figure 7.1. The shape of the phase diagrams obtained for these systems is analogous to what was previously reported to binary mixtures of CO_2 and ionic liquids. At low CO_2 concentrations the pressure increase with the CO_2 content is almost linear while for CO_2 mole fractions higher than 0.4 for [C_4mim][Ac] and 0.55 for [C_4mim][TFA] a dramatic increase in pressure with concentration is observed. At temperatures below the CO_2 critical temperature a two phase region is observed above these concentrations. The most surprising feature observed on these systems is the very large solubility of CO_2 in [C_4mim][Ac] up to a mole fraction of 0.3. This IL seems to be able to dissolve a very large amount of carbon dioxide at low pressure. This was also observed by Shifflet et al.[29, 33, 34] In spite of this larger solubility at low pressures, as the CO_2 concentration increases its solubility in [C_4mim][Ac] becomes inferior to the solubility in [C_4mim][TFA] as observed in Figure 7.2.

The results of the application of the thermodynamic consistency test to the binary systems containing ionic liquids is presented in Table C.3 for the thermodynamically consistent data, and in supporting information, for all the experimental data .

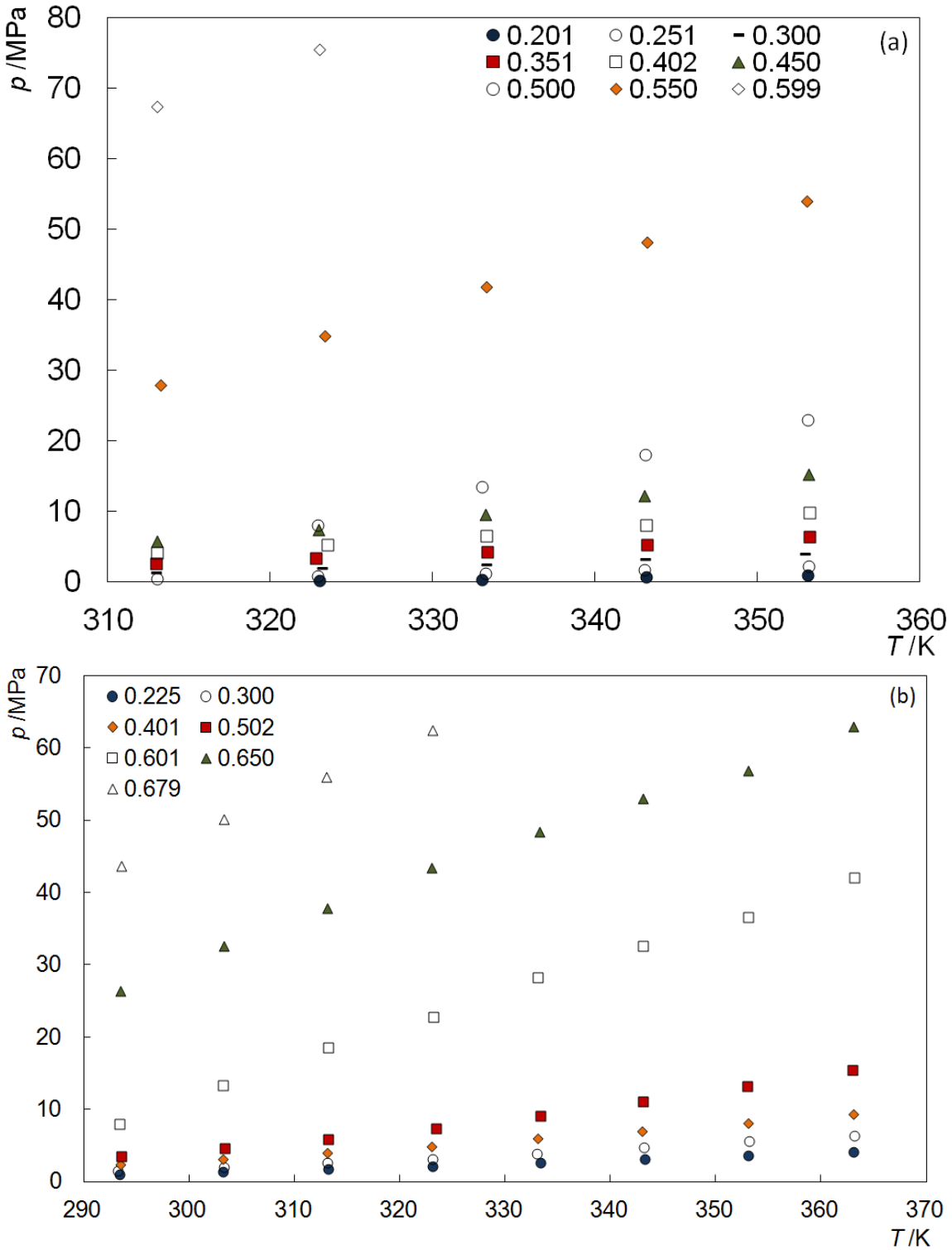

Figure 7.1. Pressure – temperature diagram of the binary systems (a) CO_2 + [C_4mim][Ac] and (b) CO_2 + [C_4mim][TFA].

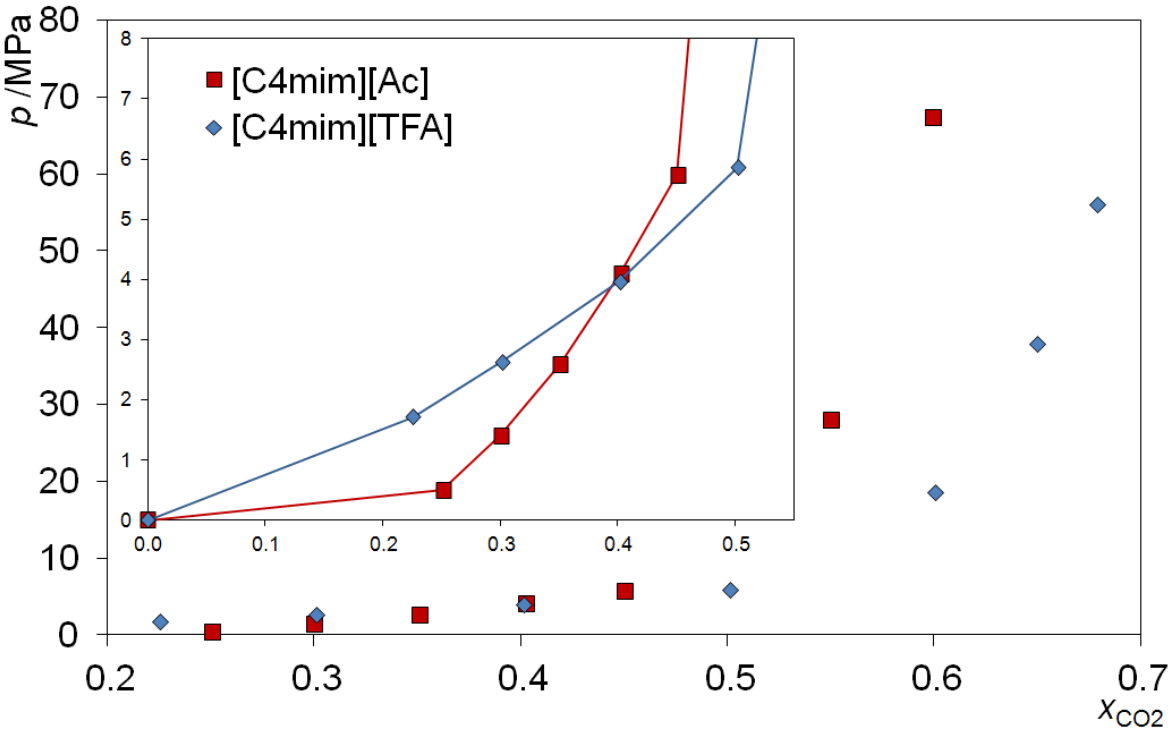

Figure 7.2. Pressure – composition diagram of the binary systems CO_2 + [C_4mim][Ac] and CO_2 + [C_4mim][TFA] at 313 K.

In this Table, *NP* is the number of data points, *T* is the temperature, k_{12}, α_{12}, g_{12}-g_{22} and g_{21}-g_{11} are the interaction parameters of the model, where *1* stands for the CO_2 and *2* for the ionic liquid. This Table is divided in sections for each system studied. The CO_2 + [C_4mim][Ac] system determined by Shifflet et al.[29] was also investigated. The parameters used in the thermodynamic model are reported in Table C.4. The consistency test shows that, in general, the data measured in this work are thermodynamically consistent with the exception, in a few cases, of the mixtures richer in CO_2. The results obtained denote larger deviations in individual areas for the CO_2 + [C_4mim][Ac] system for x_1>0.5 isopleths, and for the CO_2 + [C_4mim][TFA] system for the x_1>0.65 isopleths leading to not fully consistent isotherms. However these data points at higher CO_2 concentrations must be considered with care, since they present a more complex phase behavior which could be the cause for the apparent inconsistencies. The data for the CO_2 + [C_4mim][Ac] system here reported present a thermodynamic coherence superior to the data previously reported by Shifflet et al.[29], in particular at lower and higher temperatures for which the data

presents deviations larger than the established limit for the values of $\%\Delta p_i$ and thereafter, the test could not be applied, denoting inaccuracies in the experimental data measurements.

As depicted in Figure 7.3 the equation of state used provides a good description of the experimental data.

Given the good description of the experimental data provided by the equation of state used, the Henry constants for the CO_2 in the ILs studied in this work were estimated extrapolating the equation of state description of the experimental data to the dilute region. [34] The estimated Henry's constants are reported in Table C.3. The results indicate that the Henry's constant decreases slightly (i.e., CO_2 solubility increases) as the temperature decreases. Nonetheless, Henry's constant for the [C_4mim][TFA] presents a larger temperature dependence than the one of [C_4mim][Ac].

The results for the Henry's constant of CO_2 in [C_4mim][Ac] and CO_2 in [C_4mim][TFA] were correlated as a function of temperature by the empirical equation 4.14 where, the coefficients A and B obtained are listed in Table C.5, together with the Henry's constant average absolute deviations, $|\Delta H_{12}|$, obtained for each ionic liquid.

The effect of temperature on the CO_2 solubility was related to the Gibbs energy of solvation, the partial molar entropy and partial molar enthalpy of solvation[88] through the appropriate correlation of Henry's constant.

The results in Table C.5 show that the partial molar entropies in both fluids are essentially identical, what is expectable since that they are structurally very similar. The partial molar enthalpy of solvation of the CO_2 in [C_4mim][Ac] is lower than in [C_4mim][TFA], indicating a stronger interaction between the CO_2 and the [C_4mim][Ac] when compared with the [C_4mim][TFA]. The differences between the enthalpies and entropies of solvation observed make the solubility of CO_2 in [C_4mim][Ac] spontaneous, unlike for [C_4mim][TFA], which explain the large solubility observed at low pressures.

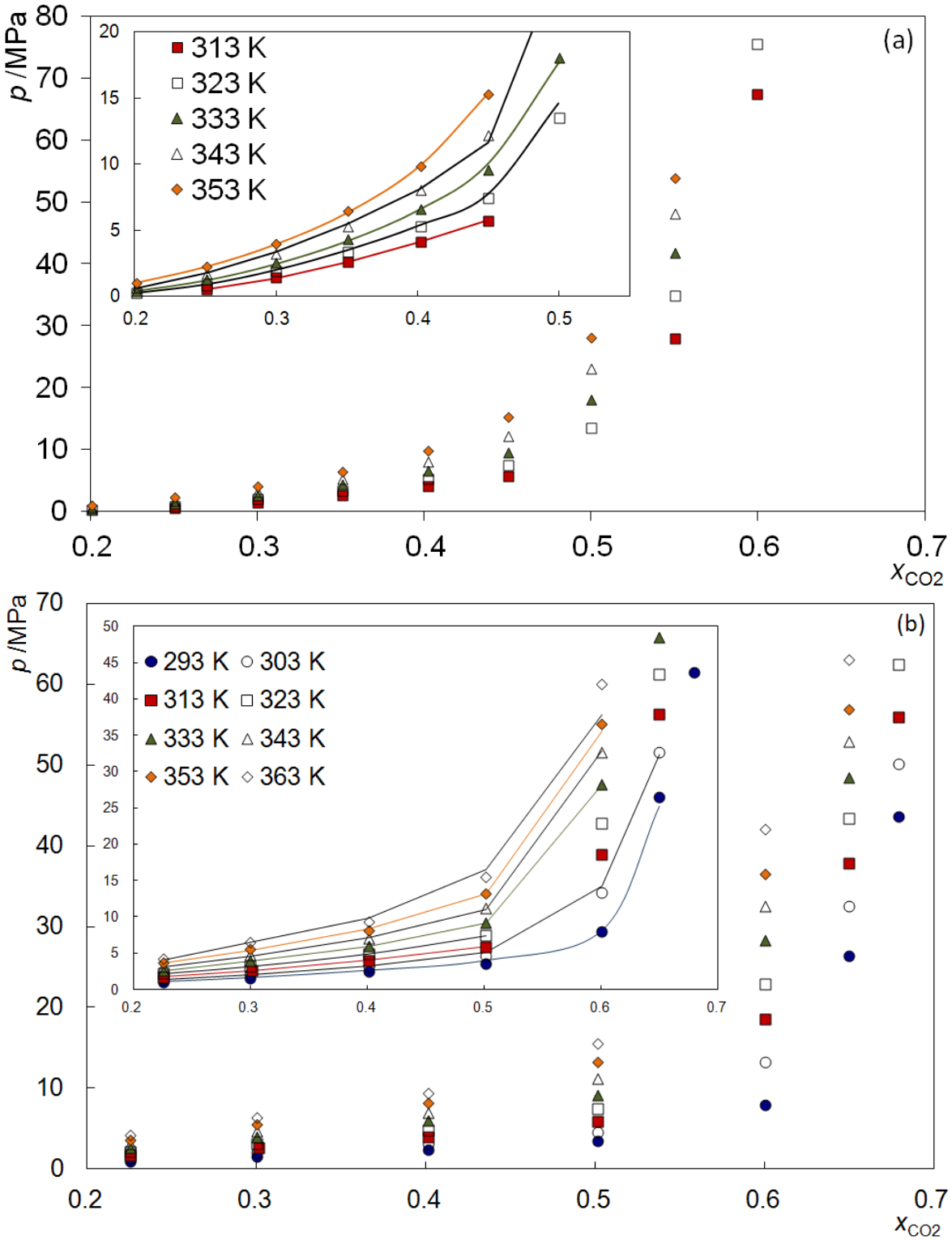

Figure 7.3. *PTx* diagram and modeling for the systems CO_2 + [C_4mim][Ac] (a) and CO_2 + [C_4mim][TFA] (b). The solid lines represents the calculations from PR-WS/NRTL EoS.

In order to obtain further information about the interaction CO_2 – [C_4mim][Ac], that seems to be responsible for the enhanced solubility of CO_2 in this IL at low pressures, ^{13}C HRMAS NMR spectra of the pure and CO_2 saturated IL at atmospheric pressure were acquired and reported in Figure 7.4. The comparison between the two spectra shows an important downfield shift of the carboxylate carbon (11) (from 179 to 183 ppm) due to the presence of CO_2 and indicating the Lewis acid/base interaction to be responsible for the enhanced solubility of CO_2 in this solvent. The other major difference observed on these spectra is related with the cation carbon (2), that is connected to an acid hydrogen. In the absence of CO_2 (Figure 7.4a), this resonance is significantly broadened and so are, to a lesser extent, ring resonances C(4) and C(5). This is expected due the proximity to the quadrupolar nuclei of the neighboring ^{14}N atoms, in case molecular motion is relatively slow and unable to average out ^{13}C-^{14}N interactions. The introduction of CO_2 in the system will shift the interaction of the acetate from the imidazolium ring, and particularly C(2), towards the gas increasing the mobility of the imidazolium ring with a noticeable effect on the peaks of the carbon at the imidazolium ring, most spectacularly C(2). Interestingly, in both systems resonances C(6), C(7) and C(10) are also broadened due to nitrogen proximity. This shift in the interaction of the acetate from the imidazolium towards the gas may also explain the upfield shift observed in C(7). These spectra also confirm that, even in presence of CO_2, there is no formation of acetic acid in the system as suggested by some authors.[29, 142] The fact a CO_2 peak is not observed (possibly at about 120-130 ppm) can only be attributed to the high mobility of this molecule in solution. Its strong interaction with the acetate does not bind it to the carboxylate group but instead the CO_2 must be quickly changing among neighbor carboxylates.

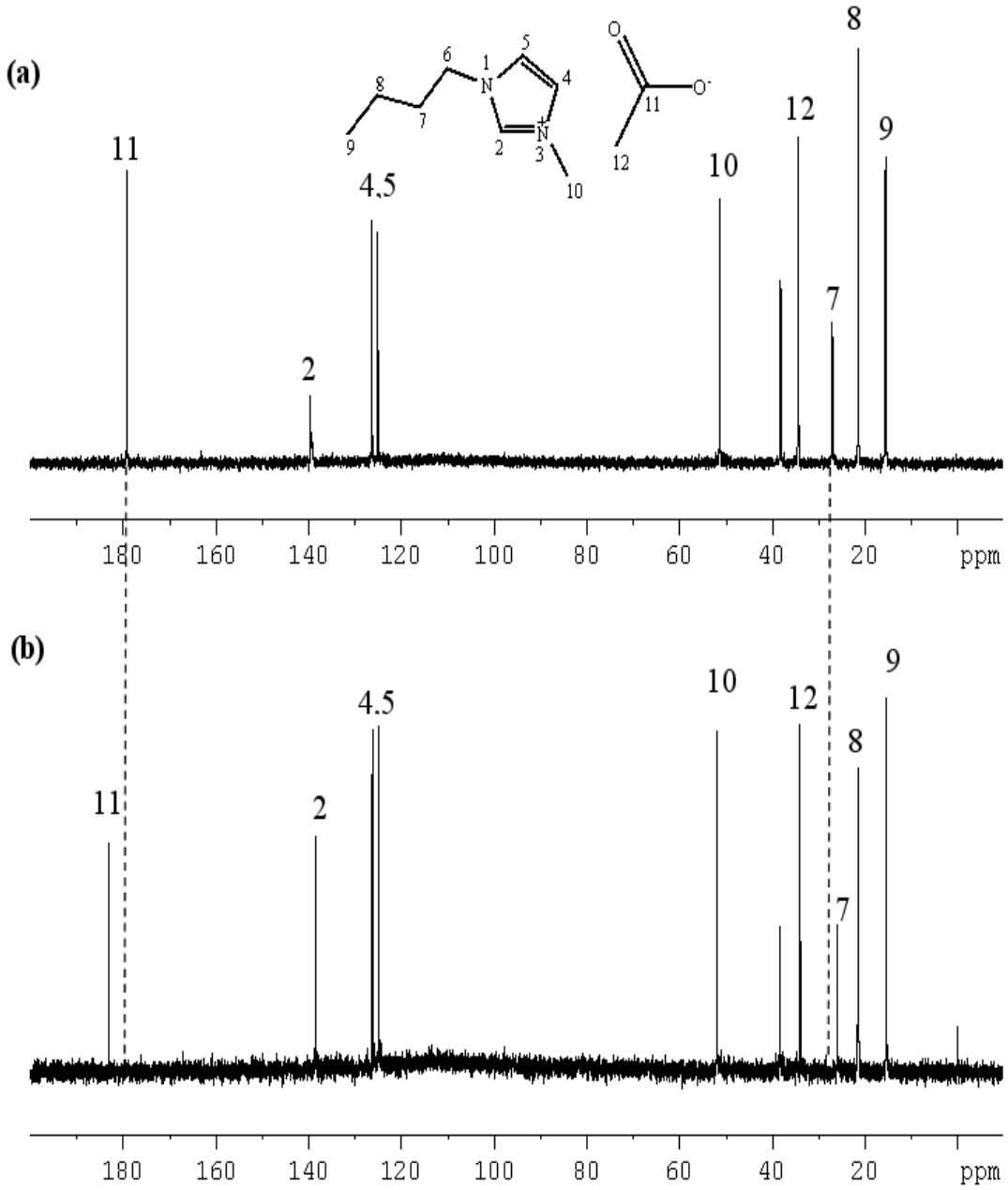

Figure 7.4. ^{13}C HRMAS NMR spectra for pure [C_4mim][Ac], 128 scans (a) and [C_4mim][Ac] saturated with CO_2 , 256 scans (b).

Solubility measurements[49, 130], spectroscopic studies[136] and molecular simulations[130] indicated that CO_2 solubility in ILs depends primarily on the strength of interaction of the CO_2 with the anion. Furthermore, Crowhurst et al.[140] reported that in terms of solvation the ionic liquid hydrogen bond donor behavior was dominated by the

hydrogen bond basicity of the anions, with a low contribution from the hydrogen bond acidity of the cation. Thus, the presence of fluoroalkyl groups in the basic trifluoroacetate anion based ILs[147] makes them "CO_2-philic", meaning that they present higher CO_2 solubilities than other ILs resulting in lower equilibrium pressures. This behavior, not yet fully understood, seems to be related to the interaction between the negative fluorine atoms and the positive charge on the carbon of the CO_2 molecule[47, 48, 92, 148, 149]. Anderson et al.[150] suggests that the NTf_2 anion is the anion displaying the most significant influence in the hydrogen bond donor ability of the IL. In fact, Anderson's statement reflects well the behavior off the [C_4mim][NTf_2] and [C_4mim][TFA] ILs, since both presents higher solubility, than other ILs, for a wider range of CO_2 mole fractions[36, 50].

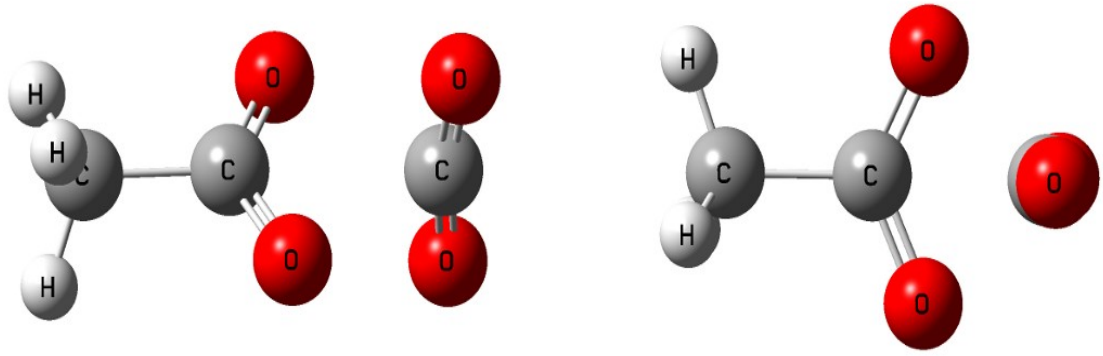

Figure 7.5. Geometry optimizations of CO_2 - acetate complex (conformation A) at MP2/6-31+G(d) level of theory. Carbon to carbon distance C (carboxylate) - C (CO_2) distance 2.963 Å. CO_2 , O-C-O angle 169.0 degrees.

The comparison between the solubilities of CO_2 in [C_4mim][Ac] and [C_4mim][TFA] reveals a curious behavior. For low CO_2 molar fractions (< 30 %) the [C_4mim][Ac] presents higher CO_2 solubility than any IL previously studied[29] but, as the CO_2 molar fraction increases, the solubility in [C_4mim][Ac] quickly drops below the solubility in [C_4mim][TFA] as shown in Figure 7.2. This behavior could be explained by a chemisorption taking place in [C_4mim][Ac] at low CO_2 pressure but, as the chemical solvation sites become saturated and the physisorption dominates, the solvation capacity of the fluorinated acetate becomes dominant. The fluorination of the acetate seems however to reduce its chemical solvation capacity. For a deeper understanding of these interactions we resorted to ab initio calculations to analyze the interactions between the fluorinated and

non fluorinated acetate and the CO_2.

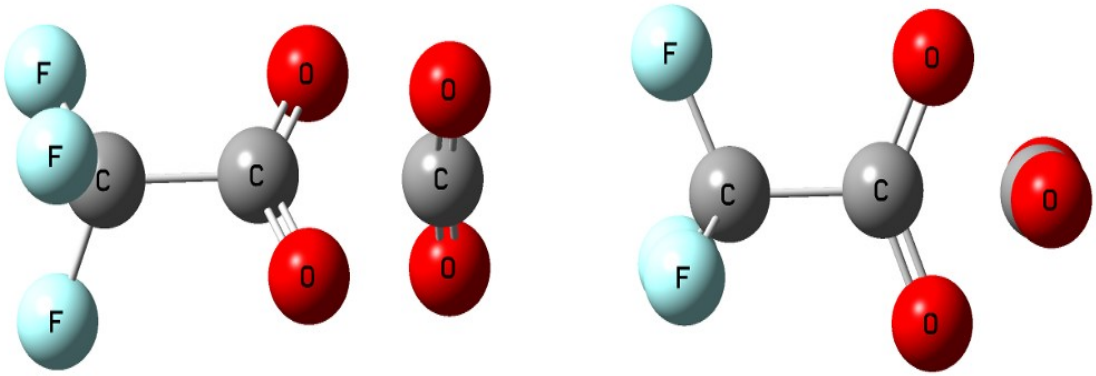

Figure 7.6. Geometry optimization of CO_2 - trifluoroacetate complex at MP2/6-31+G(d) level of theory. Carbon to carbon distance C (carboxylate) - C (CO_2) distance 3.059 Å. CO_2, O-C-O angle 172.9 degrees.

7.3.2. *Ab initio* calculations

Ab initio calculations on the CO_2-[Ac] and CO_2-[TFA] interactions were performed using the Gaussian 03 program.[151] Geometry optimizations were performed at the second-order Møller-Plesset (MP2) level using 6-31+G(d) basis set to include the effects of electron correlation. The vibrational frequencies were also calculated to confirm that the structures were at the real potential energy minimum. The optimized geometries are shown in Figures 7.5 and 7.6 for the CO_2 complex with the acetate and trifluoroacetate respectively. I. The CO_2 is interacting as Lewis acid with the acetate group which acts as Lewis base. The CO_2 molecule is significantly distorted from linearity. The shorter C(carboxylate) to C(CO_2) distance and the larger CO_2 distortion angle in the CO_2 complex with the acetate is a structural indication that the CO_2 -[Ac] interaction is stronger than CO_2 -[TFA]

The conformation "B", depicted in Figure 7.7, represents the complex formation of the CO_2 with the oxygen of the carboxylate that was found to have a local energy minimum with a MP2/6-31+G(d).

The Gaussian-3 (G3)[152] and (G3MP2)[153] theoretical procedures were used to evaluate the interaction enthalpies of the complexes between the acetate Lewis base (B) and the CO_2 Lewis acid (A) according the following equation:

$$\Delta H = H_{AB} - \left(H_A + H_B\right) \quad (7.1)$$

where H_{AB} is the G3 or G3MP2 enthalpy of the CO_2 complex with acetate or trifluoroacetate and the H_A and H_B represent the G3 or G3MP2 enthalpies of the monomers. Gaussian-3 (G3) theory is based on the 6-31G(d,p) basis set and several basis extensions, including the G3 large basis set. Geometries are calculated at MP2(full)/6-31G(d) level and scaled (0.8929) HF/6-31G(d) zero-point energies are included in the final energies. Treatment of electron correlation is done by Møller-Plesset (MP) perturbation theory and quadratic configuration interaction and the final energies are effectively performed at the QCISD(T)/G3large level. Gaussian-3 (G3MP2) theory represents a simplification of the (G3) theory with a reduced Møller-Plesset (MP) order, thus eliminating the MP4 calculation.

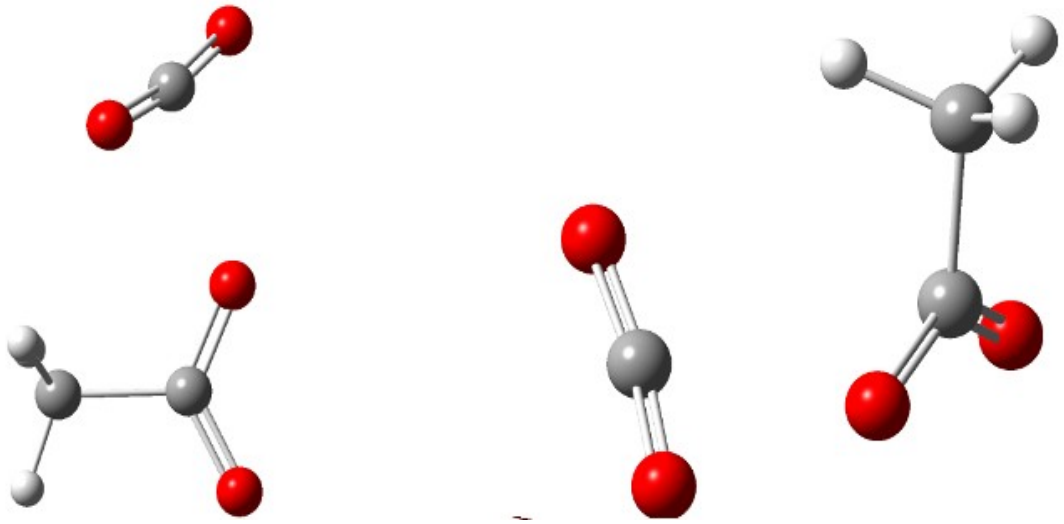

Figure 7.7. Geometry optimization of CO_2 - acetate complex (conformation B) at MP2/6-31+G(d) level of theory. Carbon to carbon distance O (carboxylate) - C (CO_2) distance 2.466 Å. CO_2 , O-C-O angle 169.5 degrees.

The enthalpic interactions were also evaluated directly using the MP2/6-31+G(d) energies. zero-point energies (ZPEs) and the enthalpic correction to 298 K were included in the interaction using the MP2 frequencies scaled by (0.95) for the calculation of ZPEs and the enthalpies correction to 298 K. The basis set superposition errors (BSSE) for the MP2/6-31+G(d) interaction was also evaluated and found to be negligible, taking into

account the large energy interaction. The binding enthalpies at the different levels of theory are listed in Table C.6. It is interesting to observe that the difference between the enthalpic interactions (acetate and trifluoroacetate) obtained by ab initio in gas phase (7 to 10 kJ.mol^{-1}), present a good agreement with the experimental difference between the enthalpy of solvation of the CO_2 in the [C_4mim][Ac] and in [C_4mim][TFA] (13 ± 3.9 kJ.mol^{-1}).

The calculated interactions support the idea of a chemisorption of CO_2 in [C_4mim][Ac] but seem to fail in explaining the low, and non spontaneous nature, of CO_2 solubility in [C_4mim][TFA] as both interactions seem to be similar with a difference of just 10 kJ mol^{-1} between the two. Yet this small difference does make all the difference and is indeed enough to explain the differences observed between the two ILs. Since, as shown before, the entropies of solvation are identical in the two ionic liquids, the differences in the Gibbs energy of solvation arises essentially from the differences in the enthalpies of solvation. If Equation 4.17 is used to estimate the differences in the Gibbs energies of solvation between the two fluids in the temperature range [313-353] K these values range between 11.6 and 12.1 kJ.mol^{-1}. The differences in solubility between the two fluids result essentially from their the solvation enthalpy differences and a value of 11-12 kJ.mol^{-1} is enough to explain the observed solubility difference. The “chemisorption” observed is nothing more than the expression of the spontaneous solubility of CO_2 on the ionic liquid due to an enthalpy of solvation larger than the corresponding entropy of solvation. We postulate that all ionic liquids with an enthalpy of solvation contribution superior to their entropy of solvation contribution to the Gibbs free energy of solvation, and thus to the solubility, will present a behavior similar to what is presented by [C_4mim][Ac] while the others will behave as [C_4mim][TFA]. This could explain the differences observed between ionic liquids with carboxylate anions studied by Yokozeki et al.[34] where some do have a “chemisorption-like” behavior while others do not. More studies are however required to provide support for this hypothesis.

7.4. Conclusions

Gas solubility of CO_2 in two ionic liquids, namely, 1-butyl-3-methylimidazolium acetate and 1-butyl-3-methylimidazolium trifluoroacetate have been investigated in a wide range of temperatures, pressures and CO_2 mole fractions aiming at understanding the effect of the basicity and the fluorination of the anion on the gas solubility in the ionic liquids.

The two systems studied present interesting contrasting behaviors. The binary system 1-butyl-3-methylimidazolium acetate + CO_2 at low pressures presents a high CO_2 solubility, larger than those observed for the other ILs at this pressures, but as the CO_2 molar fraction increases the solubility decreases exponentially and the solubilities become more important on [C_4mim][TFA] at high pressures.

The data is shown to be thermodynamically consistency, and the Peng-Robinson EoS with the Wong-Sandler/NRTL mixing rule allows a good description of the experimental data and the estimation of the Henry constants for these systems. The partial Gibbs energy, enthalpies and entropies of solvation estimated from the Henry's constants show the solubility of CO_2 in [C_4mim][Ac] to be spontaneous at the standard pressure (0.1 MPa) while the entropies of solvation in the two systems to be essentially identical, making the solubility on these systems controlled by the solvation enthalpies.

^{13}C HRMAS NMR spectra and ab initio calculations indicate that the preferential interaction of the CO_2 with [C_4mim][Ac] results from an acid/base interaction between the carboxylate and the acid carbon in the CO_2 molecule. A good agreement between the measured and calculated differences in the interactions between the CO_2 and the anion in the two systems were obtained and it is shown that a difference of in the order of 10 kJ.mol^{-1} in the interaction energy is enough to explain the solubility differences observed between the two systems.

8. High Pressure Phase Behavior of Carbon Dioxide in 1-Butyl-3-methylimidazolium Bis(trifluoromethylsulfonyl)imide and 1-Butyl-3-methylimidazolium Dicyanamide Ionic Liquids

"Nothing has such power to broaden the mind as the ability to investigate systematically and truly all that comes under thy observation in life."

Marcus Aurelius

8.1. Abstract

The acidity/basicity of the reaction media has a substantial influence on the efficiency of many reactive processes; therefore, a new class of acidic or basic ionic liquids is gaining special attention due to the possibility of increasing the efficiency of many processes by a wise manipulation of their properties. The absorption of sour gases is one of the processes that can be enhanced by the basic character of the ionic liquid. The fluorination of the cation or anion can also contribute to the gas solubility enhancement. In this work, these two characteristics are evaluated and compared through the study of gas–liquid equilibrium of two ionic liquids, 1-butyl-3-methylimidazolium dicyanamide ([C_4mim][DCA]) and 1-butyl-3-methylimidazolium bis(trifluoromethylsulfonyl)imide ([C_4mim][NTf_2]), with carbon dioxide (CO_2) at temperatures up to 363 K and pressures up to 74 MPa.

A thermodynamic model based on the Peng–Robinson equation of state with the Wong–Sandler mixing rule, using the UNIQUAC model for the activity coefficients, was used to describe the experimental data and for the estimation of the Henry's constants.

The solubility of CO_2 in 1-butyl-3-methylimidazolium dicyanamide is much lower than anticipated on the basis of the reported pKa of the anion when compared with the acetate anion. No chemisorption is observed and the solvation enthalpy is quite low, ruling out any Lewis acid/base interaction between the anion and the CO_2. The 1-butyl-3-methylimidazolium bis(trifluoromethylsulfonyl)imide ionic liquid, known to present one of the highest solubilities towards CO_2 due to the presence of fluoroalkyl groups, showed a much larger solubility for CO_2 than 1-butyl-3-methylimidazolium dicyanamide.

8.2. Introduction

Acidic or basic ionic liquids (ILs) represent new classes of acids or bases. The study of the acidity/basicity of these task-specific ionic liquids is of great importance since the efficiency of many processes depends on the acidity/basicity of the media or can be controlled by it. These compounds aptness for the fine tuning of their properties through an

endless combination of cations and anions, cataloging them as *designer* solvents, allow the design of solvents for the development of more efficient and sustainable processes and products.

Crowhurst et al.[140] reported that the hydrogen bond basicities of ILs are controlled by the anion, while the hydrogen bond donation behavior is dominated by the hydrogen bond basicity of the anions with a smaller contribution from the hydrogen bond acidity of the cation. Therefore, changing to more basic anions leads to a dramatic drop in the acidity. Based in the Pearson's "hard and soft acid-base" principles, allowing a strong affinity towards CO_2, Pennline et al.[141] screened quaternary ammonium polyethers ILs as potential solvents for CO_2 capture. In a previous work,[30] following the works by Shiflett et al.[29] and Yokozeki et al.[34], imidazolium–based IL with the acetate and trifluoroacetate anions were studied by our group. The acetate ion is shown to present a chemical absorption behavior for low CO_2 mole fractions (<30 %) and ab initio calculations and ^{13}C HRMAS NMR spectroscopy provided a deeper understanding of the CO_2-acetate interactions.[30]

The purpose of the present study is to further explore the basicity of the anion as a mean to enhance the absorption of carbon dioxide by the ionic liquids. For that purpose, following the suggestion of MacFarlane et al.[81] that dicyanamide would be a basic anion (the pKa for dicyanoamine reported by MacFarlane is higher than the pKa for the acetic acid), a dicyanamide anion based ionic liquid was here chosen to further investigate the effect of the anion basicity on the solvation of CO_2. The 1-butyl-3-methylimidazolium dicyanamide was thus selected for that purpose and the solubility of the CO_2 in this IL is compared to that in the 1-butyl-3-methylimidazolium bis(trifluoromethylsulfonyl)imide ionic liquid, here also studied and known to present one of the highest solubility towards CO_2 due to the presence of fluoroalkyl groups. Both systems were measured at temperatures up to 363 K and pressures up to 74 MPa.

The Peng–Robinson equation of state[84] with the Wong–Sandler/UNIQUAC mixing rule[85] using the UNIQUAC model[86] for the activity coefficients, was used to model the experimental data measured in this work. It will be shown that the model provides an

excellent representation of the experimental data.

The solubility of CO_2 in 1-butyl-3-methylimidazolium dicyanamide is much lower than anticipated on the basis of the reported pKa of the anion when compared with the acetate anion. No chemisorption is observed and the solvation enthalpy is quite low ruling out any acid/base interaction between the anion and the CO_2.

8.3. Results and Discussion

The solubility of carbon dioxide in the studied ILs was measured for mole fractions ranging from (0.2 to 0.8), in the temperature range (293 to 363) K and pressures from (0.6 to 74) MPa, as reported in Tables E.1 and E.2 and depicted in Figure 8.1. The temperature increase leads to an increase on the equilibrium pressures and by increasing CO_2 concentration, the equilibrium pressures increase gradually, at first, and rapidly for higher CO_2 contents as also observed previously for other ILs.[30, 36]

The experimental data here reported is generally in agreement with those available in literature, covering however a wider range of carbon dioxide concentrations, pressures and temperatures. For the system CO_2 + [C_4mim][NTf_2] a good agreement is observed with the data by Shin et al.[126] for mole fractions below 0.7. Above these concentrations, their data is scarce and ours provide a mode detailed view of the phase diagram. The data by Anthony et al.[49] for this system is available only in the low pressure region and seems to present some deviations from both the data here reported and by Shin et al.[126]. For the system CO_2 + [C_4mim][DCA] only three isotherms below 10 MPa were reported by Aki et al.[47]. A good agreement is obtained with this data in the lower pressure region while again the data here reported provide a more complete description of the phase diagram for high pressures.

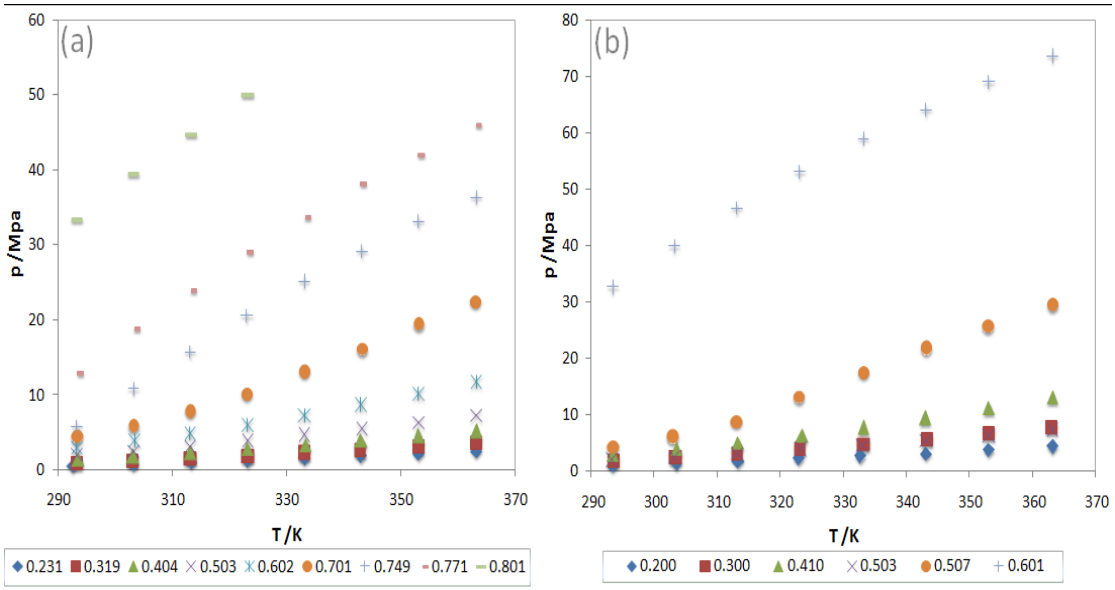

Figure 8.1. Pressure – temperature diagram of the binary systems (a) CO_2 + [C_4mim][NTf_2] and (b) CO_2 + [C_4mim][DCA].

Contrary to what was expected, the higher basicity character of the dicyanamide anion, compared to the bis(trifluoromethylsulfonyl)imide, as expressed in their pKa values, does not enhance the CO_2 solubility as was previously observed with the acetate anion. The explanation for this fact seems to be that, as shown previously,[30] the solubility of CO_2 on an IL is enhanced by a Lewis acid/base interaction between the gas and the anion. The dicyanamide, in spite of its large pKa value, seems however to be a much weaker Lewis base than the acetate anion.

8.4. Thermodynamic Modeling and Henry's Constants

The results of the application of the thermodynamic modeling to the binary systems containing ionic liquids studied in this work are presented in Table E.3 for all the experimental data. In this Table, *NP* is the number of data points, *T* is the temperature, k_{12}, A_{12} and A_{21} are the interaction parameters of the model, where *1* stands for the CO_2 and *2* for the ionic liquid. This Table is divided in sections for each system studied. The parameters used in the thermodynamic model are reported in Table E.4. As depicted in Figure 8.2 the model describes well the experimental data. The proposed methodology was applied to determine the Henry's constant for the studied systems.

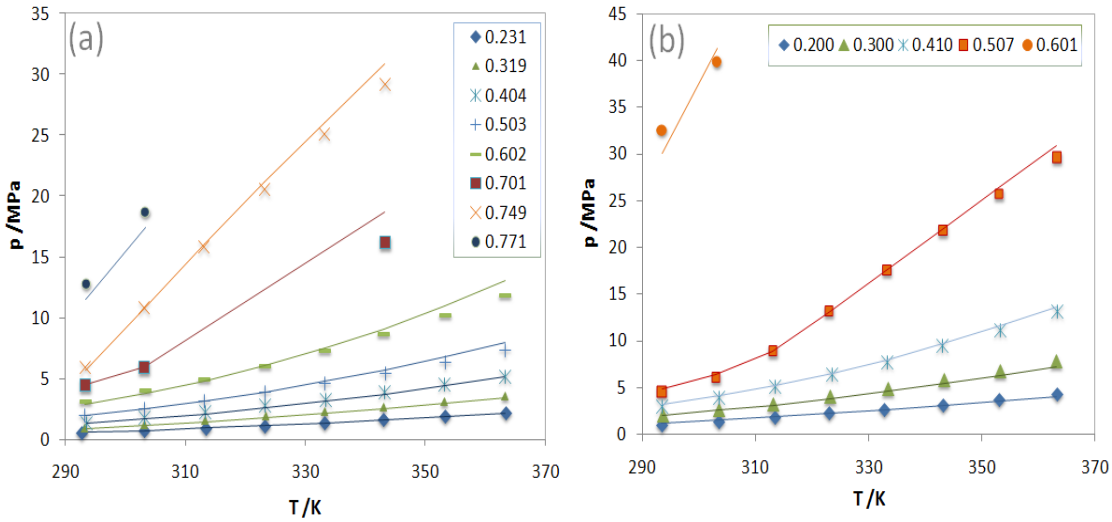

Figure 8.2. *PTx* diagram and modeling for the systems CO_2 + [C_4mim][NTf_2] (a) and CO_2 + [C_4mim][DCA] (b). The solid lines represents the calculations with PR-WS/NRTL EoS.

The Henry's constants for the CO_2 in the investigated ILs were estimated by fitting the PR-WS/UNIQUAC model to the data and calculating the limiting slope as the solubility approaches zero. The estimated Henry's constants results, reported in Table E.3, indicate that Henry's constant decreases slightly (i.e., CO_2 solubility increases) with the temperature .

The results for the Henry's constant of CO_2 in [C_4mim][DCA] and in [C_4mim][NTf_2] were correlated as a function of temperature by the empirical equation 4.14 where, the coefficients *A* and *B* are listed in Table E.5, together with the Henry's constant average absolute deviations, $|\Delta H_{12}|$, obtained for each ionic liquid.

The effect of temperature on CO_2 solubility was related to the Gibbs energy, the partial molar entropy and partial molar enthalpy of solvation[88] and calculated from an appropriate correlation of Henry's constant, as described on section 4.3. . The results presented in Table E.5 show that the partial entropies in both fluids are essentially identical, indicating a similar structural solvation interaction. The partial molar enthalpy of solvation of the CO_2 in [C_4mim][NTf_2] is lower than in [C_4mim][DCA], indicating a slightly stronger interaction between the CO_2 and the [C_4mim][NTf_2] when compared with the [C_4mim][DCA]. The enthalpies and entropies of solvation contribution make the

solubility of both systems non-spontaneous and moreover, controlled by physical absorption. The partial molar enthalpies of solvation observed for these ILs are also much lower than those previously reported for [C_4mim][Acetate] and [C_4mim][TFA][30] showing that, as discussed previously, in spite of the pKa of dycianamide no acid/base interaction is observed for the ILs studied in this work.

8.5. Conclusions

New Gas–Liquid equilibrium data of two binary systems, namely, 1-butyl-3-methylimidazolium dicyanamide + CO_2 and 1-butyl-3-methylimidazolium bis(trifluoromethylsulfonyl)imide + CO_2 have been investigated in a wide range of temperatures, pressures and CO_2 mole fractions aiming at the understanding the effect of the basicity of the anion in the gas solubility in the ionic liquids.

Contrary to what the dicyanamide anion basicity would suggest the [C_4mim][DCA] ionic liquid do not show a significant enhancement on the CO_2 solubility. In fact, the interaction between the negative fluorine atoms and the positive charge on the carbon of the CO_2 molecule seems to be stronger in the NTf_2 anion based IL.

A thermodynamic model based on the Peng-Robinson EoS with the Wong-Sandler/UNIQUAC mixing rule was used in description of the measured data. The model allows a good description of the experimental data and the estimation of the Henry's constants for these systems.

The partial Gibbs energy, enthalpies and entropies of solvation estimated from Henry's constants show that the solubility of CO_2 in both systems is non spontaneous at standard pressure (0.1 MPa). The entropies of solvation in the two systems are essentially identical and the partial molar enthalpy of solvation of CO_2 in [C_4mim][NTf_2], when compared to the one of [C_4mim][DCA], indicate similar interactions between the CO_2 and the two ionic liquids.

9. On the Nonideality of CO_2 Solutions in Ionic Liquids and Other Low Volatile Solvents

"If an elderly but distinguished scientist says that something is possible, he is almost certainly right; but if he says that it is impossible, he is very probably wrong."

Arthur C. Clarke

"There is no adequate defense, except stupidity, against the impact of a new idea."

Percy Williams Bridgman

9.1. Abstract

The non ideality of CO_2 solutions in ionic liquids and other low volatile solvents, with which CO_2 is known to form electron donor-acceptor (EDA) complexes, is here investigated. It is shown that the deviations from the ideality observed are not related with the stability of the EDA complex formed and in most cases these deviations are small and dominated by entropic effects. For this reason when the CO_2 concentration is expressed in molality, the pressure *versus* concentration phase diagrams of CO_2 in non volatile solvents are, within the uncertainty of the experimental data, solvent independent. Following this approach a correlation for the solubility of CO_2 in non volatile solvents, valid for pressures up to 8 MPa and temperatures ranging from room temperature up to 363 K, is here proposed. These results are tested with success by measuring the solubility of CO_2 in [THTDP][Cl] to show that in such heavy ionic liquid the solubility, although identical in molality units, if expressed in mol fractions is larger than in [C_4mim][NTf_2].

9.2. Introduction

The solubility of CO_2 in solvents of low volatility or non volatile is highly relevant for many technological applications. Enhanced Oil Recovery (EOR) requires the knowledge of the CO_2 solubility in heavy hydrocarbons;[40] purification of vegetable or animal oils or the extraction of value added compounds from them using supercritical technologies is related with the CO_2 solubility in these oils, and their fatty acids and esters; [41-44] and the Selexol process uses a mixture of dimethyl ethers of polyethylene glycol for the removal of acid gases from feed gas streams.[45] Recently a great deal of works address the use of ionic liquids for CO_2 capture and gas separation purposes.[20, 27, 29, 30, 33, 36, 46-64] In all these cases the understanding and description of the absorption of CO_2 in solvents of low volatility is of importance for the design and operation of processes or the design of new and enhanced sorbents for CO_2.

Equations of state (EoSs) are useful to correlate the experimental data available and extrapolate the data into conditions for which no experimental data is available. A

number of EoSs have been used to describe the experimental data for the systems mentioned above.[58, 71, 82, 90, 97, 154-166] The EoSs available have however a number of shortcomings. They have a very limited predictive ability for systems not previously studied. Moreover, given that empirical binary parameters are required to fit the experimental data for the most complex systems, the understanding of the solubility at a molecular level is quickly lost.

The best approach to obtain direct molecular level interaction information for CO_2 containing systems is through spectroscopic techniques. It is well known that the CO_2 molecule can act both as proton acceptor or electron donor according to the nature of the solvent, forming electron donor-acceptor (EDA) complexes.[99-102, 144-146, 148, 167-176] A number of authors have been investigating the interactions between CO_2 and carbonyl groups,[99, 144, 148, 167-169] ester groups,[102, 146, 170] hydroxyl groups,[101, 171-175] ether groups[100, 145, 176] and with ionic liquids.[136, 177-180, 180] While these interactions observed by spectroscopic techniques are of high relevance for an understanding of the solvation of CO_2 in non volatile solvents, they are not enough to fully explain its solubility nor the deviations to the ideal behavior on these systems. Though the CO_2 EDA complexes with sp^3 O-donating atoms (such as H_2O and alcohols) are more stable than complexes involving sp^2 O-donating atoms (such as aldehydes and ketones) the solubility on the former is inferior to that observed on the latter.[100] Kazarian et al.[136] based on the solubility and spectroscopic evidence for the interactions of CO_2 with BF_4 and PF_6 anions were the first to recognize that "the strength of the interactions cannot be solely responsible for the solubility of CO_2 in ionic liquids" [136]. Seki et al.[180] on a recent work show that although the interactions of CO_2 with BF_4 and PF_6 anion-based ILs are stronger than those with the NTf_2, the solubility of CO_2 on these ionic liquids is larger than in the former and thus the interactions alone are not enough to provide an explanation for the CO_2 sorption. They recognize that "the strong Lewis acid-base interactions between the ionic liquids and the dissolved CO_2 has no promotional effect on the solubility of CO_2".[180]

These observations shouldn't come entirely as a surprise since the non ideality of a

solution and its impact on the solubility of a given solute depends not only on the solute-solvent interactions, observed and discussed by these authors, but on a delicate balance between the solute-solute; solute-solvent, and solvent-solvent interactions. Moreover, in systems of non volatile solvents, these solvents present in general a large molar volume and the solute-solvent size and shape asymmetries will generate important entropic and free volume contributions to the non ideality of the system with significant impact on the CO_2 solubility on these systems.

The aim of this work is to study the deviations to non ideality of solutions of CO_2 in non volatile solvents. Non volatile solvents are here defined as those with a vapor pressure at room temperature inferior to 100 Pa. This value was chosen because in the systems with CO_2 here studied this leads to a vapor phase composed essentially by CO_2, i.e. the concentration of solvent in the vapor phase is typically inferior to 0.01 mol%. In this group of solvents are the alkanes above C_{12}, fatty acids heavier than C_5, fatty acid esters larger than octanoate, polyethylene glycol (PEG) with molecular weight above 400, alcohols larger than *n*-heptanol and ionic liquids in general. These systems will be here studied to develop a deeper understanding of the molecular mechanisms that dominate the CO_2 sorption on these liquids and, through it, develop a model to describe the CO_2 solubility in non volatile solvents.

9.3. The non ideality of CO_2 solutions in non volatile solvents

To analyze the non ideality of CO_2 solutions in non volatile solvents, experimental VLE data at subcritical and near critical conditions for a wide range of systems, comprising alcohols, fatty acids, fatty acid esters, PEGs, and ionic liquids, was compared with the solubilities predicted by the Raoult's law described as

$$P = x_{CO_2} \gamma_{CO_2} p^{\sigma}_{CO_2} \qquad (9.1)$$

where $\gamma_{CO2}=1$ is the CO_2 activity coefficient and p^{σ}_{CO2} the vapor pressure of CO_2, estimated using the correlation of the DIPPR database.[122] Since at high CO_2 concentrations most systems will exhibit a liquid-liquid region with strong positive deviations to ideality, the

analysis will be restricted to the low concentration region before the deviations related to this region appear.

In spite of the strong CO_2-OH interactions observed spectroscopically[101, 103, 105, 171-175] the alcohol systems are the only with positive deviations to ideality as sketched in Figure 9.1 (actual data is reported on Appendix D). This is a striking example showing that strong solute-solvent interactions are not enough to guarantee enhanced solubility if the solvent-solvent interactions destroyed during the solvation of the solute are not energetically compensated by that process.

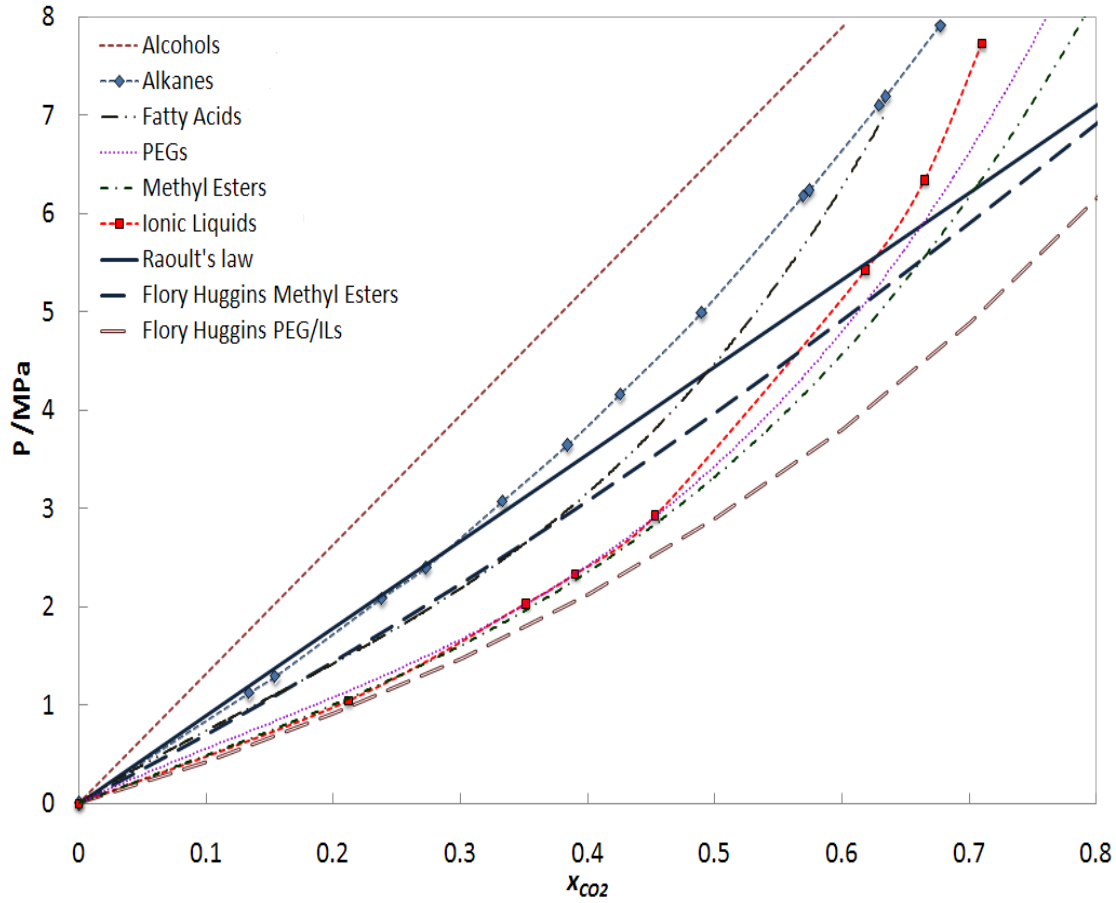

Figure *9.1.* Sketch of the pressure - CO_2 molar composition diagram for the systems CO_2 + Alcohols, CO_2 + Alkanes, CO_2 + Fatty acids, CO_2 + PEGs, CO_2 + Fatty acid esters, and , CO_2 + Ionic liquids at 313 K.

In the analysis of the other systems it must be recalled that the non-ideality results not only from differences in the energetic interactions between the molecules, as described

by the residual contribution to the Gibbs free energy, but also from entropic effects due to their size and shape differences, the combinatorial contribution, as summarized by

$$G^E = G^E_{comb} + G^E_{residual} \tag{9.2}$$

The entropic effects will always have a negative contribution to the non-ideality that in terms of activity coefficients can be described by the Flory-Huggins equation[181, 182]

$$\ln\left(\gamma^{comb}_{CO_2}\right) = \ln\frac{\varphi_{CO_2}}{x_{CO_2}} + \left(1 - \frac{\varphi_{CO_2}}{x_{CO_2}}\right) \tag{9.3}$$

If the combinatorial contributions to the non-ideality alone are taken into account the Eq. (9.1) will become

$$P = x_{CO_2} \exp\left(\ln\frac{\varphi_{CO_2}}{x_{CO_2}} + \left(1 - \frac{\varphi_{CO_2}}{x_{CO_2}}\right)\right) P^{\sigma}_{CO_2} \tag{9.4}$$

The pressure *vs*. mol fraction plot of the CO_2 solubility in alkanes sketched in Figure 1 shows a behavior very close to the ideal behavior described by Raoult's law (actual data is reported on Appendix D). Given the negative deviations to ideality predicted by the Flory-Huggins model for these systems the near ideal behavior must result from positive deviations in the residual (enthalpic) term. These arise from CO_2-alkane interactions that must be weaker than the CO_2-CO_2 or alkane-alkane interactions.

All the other systems studied present negative deviations to ideality. The deviations observed in ionic liquids are intermediate between an ideal behavior and what would be predicted by the Flory-Huggins model as shown in Figure 9.1. This indicates that while on the IL systems the combinatorial term is larger than the residual, thus the solubility is controlled by entropic effects, the two contributions to the Gibbs free energy still have opposite signs. This implies that there is a misfit in the solute-solvent interactions relatively to the solute-solute and solvent-solvent interactions that, like in the alcohol and alkane systems, are not enough to energetically compensate for the interactions that are destroyed upon mixing.

Both fatty acids and PEGs show a non-ideal behavior than can be well described by the Flory-Huggins equation while the esters display the largest deviations to the ideal behavior observed for all the systems studied, as shown in Figure 9.1 (see also the actual data reported on Appendix D). This suggests that the residual contribution for the non ideality is negligible or even negative. It results from the fact that on these systems the Electron Donor-Acceptor complexes formed between CO_2 and the carbonyl group, though not more stable than those formed with the hydroxyl groups of alcohols are favored as the CO_2-carbonyl interactions seem to be energetically favorable when compared with the CO_2-CO_2 interactions and the carbonyl-carbonyl interactions established between the ester molecules. This is in agreement with the results of Besnard et al.[102] that indicate that the stabilization energy of the CO_2-acetone heterodimer is larger by at least a factor of two when compared with the CO_2 homodimer.

A special and extreme case of the formation of EDA complexes is the solubility of CO_2 in ionic liquids with anions such as acetates and other conjugated bases of organic acids reported and discussed by Shiflett and Yokozeki[29, 33, 34] and us[30]. Unlike the other systems here discussed, in the low concentration range the solubility on these systems is completely dominated by the formation of the complex and thus will not be considered in this work.

The most striking result from this analysis, is that, in spite of the major differences in the chemical nature of the solvents here studied and of the interactions of their molecules in pure state, the non ideality of the CO_2 in solution on the composition range studied is remarkably lower than could be anticipated and, in most cases, is essentially driven by entropic effects. Moreover, as has been noticed before by other authors[136, 180] this analysis on the non ideality of these systems also stresses that there is no direct relationship between the stability of the EDA complex formed between the CO_2 and a given solvent and the non ideality of CO_2 on this solvent. These two observations combined suggest that by increasing the size difference between the CO_2 and the solvent, the solubility must increase as the entropic contribution to the solution non-ideality

increases.

Since, with the exception of the alcohols, all the systems here reported present relatively small negative deviations to ideality, there should be possible to derive a comprehensive framework for the description of the solubility of CO_2 in non volatile solvents. The approach here proposed is detailed below.

9.4. Model development

Adopting the approach suggested by the IUPAC for CO_2 solubilities in ionic liquids[183] and followed in the works of Maurer and co workers[51, 54, 184] the solubility of a gas *i* in a liquid can be described by the extended Henry's law[182, 184]

$$k_{H,i}^{(m)}[T,p]a_i^{(m)}[T,p,m_i] = f_i^V[T,p,y_i] \tag{9.5}$$

where $k_{H,i}^{(m)}[T,p]$ is the Henry's constant of gas *i* (on the molality scale), at temperature *T* and pressure *p*, in a particular solvent. The reference state for the chemical potential of gas *i* in the liquid phase is an one molal solution of gas in the solvent, which experiences interactions as at infinite dilution in that solvent. The $a_i^{(m)}$ is the activity of gas *i* in the liquid phase and it is described as[182, 184]

$$a_i^{(m)}[T,p,m_i] = \frac{m_i}{m^o}\gamma_i^{(m)} = m_i^o\gamma_i^{(m)} \tag{9.6}$$

where m^o=1 mol·kg^{-1} and the activity coefficient $\gamma_i^{(m)} \rightarrow 1$ as $m_i \rightarrow 0$.

For non volatile solvents, the gas phase is a pure gas, in this case pure CO_2. For pressures up to 10 MPa the fugacity of CO_2 is proportional to the pressure and Eqs. (9.5) and (9.6) can thus be combined as

$$p = H_i m_i^o \tag{9.7}$$

where H_i combines the Henry's constant, $k_{H,i}^{(m)}$, with the gas phase non ideality, proportional to pressure, and the liquid phase non ideality, proportional to concentration.

Since, as discussed above, the deviation to Raoult's law for the systems investigated is not large, Equation (9.7) suggests the possibility of obtaining a general correlation for the solubility of CO_2 in solvents of low volatility or non volatile. This hypothesis is tested in Figure 9.2 where it is plotted the solubility of CO_2 in a large number of ionic liquids, alkanes (pentadecane, hexadecane and nonadecane), alcohols (undecan-2-ol), and methyl esters (methyl oleate and methyl and ethyl myristate) on a *p-m* diagram at 313 K. With exception of the data represented inside the ellipse for [BMIM] Acetate, due to the reasons discussed above, and the fatty acid esters that show a larger CO_2 solubility than observed for the other systems, the agreement observed between the solubilities in the other solvents studied is remarkable, suggesting that a common behavior is followed by the solubility of CO_2 on these solvents.

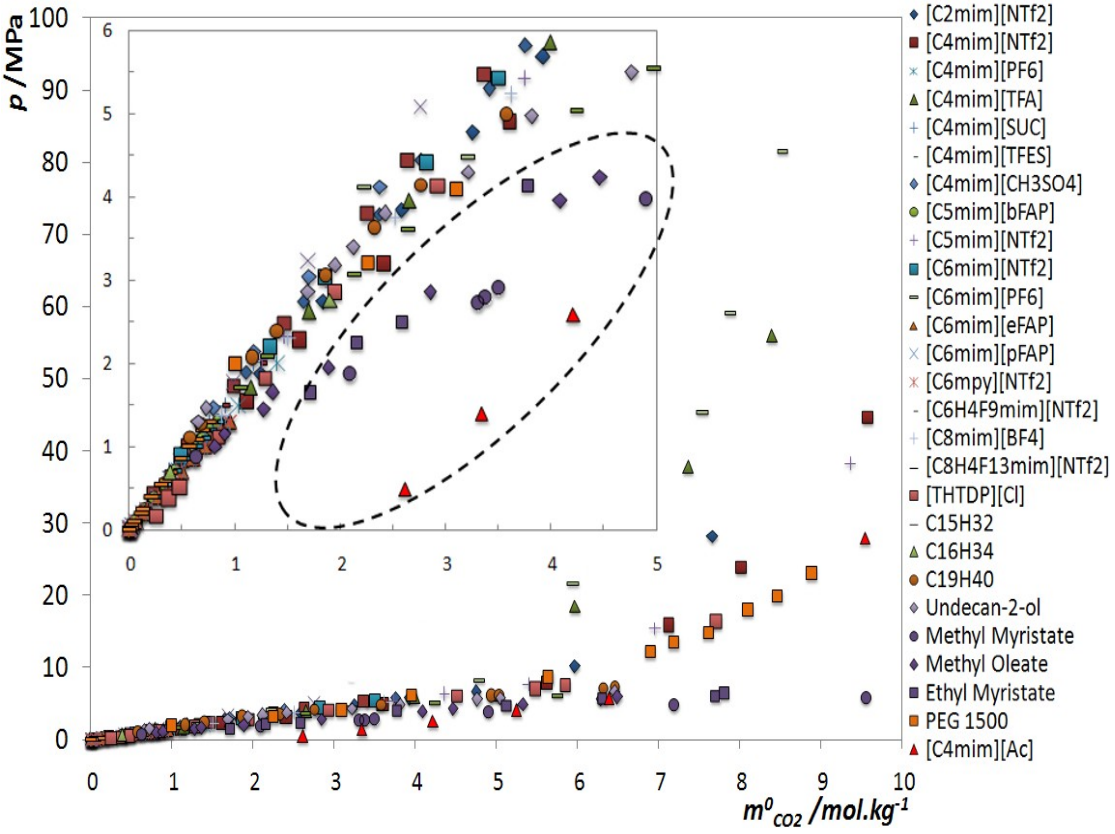

Figure *9.2.* Pressure - molality diagram of CO_2 + non volatile solvents at 313 K. Data from Ref.[28, 30, 30, 34, 36, 50, 52, 53, 59, 62, 131, 166, 185-188].

To extend the Eq. (9.7) to a larger temperature range the temperature dependency

of the Henry's constant proposed by Benson and Krause[182] was adopted. Within a temperature range of up to 100 K it can be expressed as

$$\ln H_i = \alpha + \frac{\beta}{T} \tag{9.8}$$

Combining Eqs. (9.7) and (9.8) it is possible to develop a general description for the solubility of CO_2 in non volatile solvents. For this purpose experimental data from various authors and in various types of non volatile solvents was used.[30, 36, 50, 52, 59, 131] The result is shown in Figure 9.3 (complete data is reported as Supp Info) where the value of H_i at each temperature is reported. A general correlation for the solubility of CO_2 in non volatile solvents, including ILs, expressed in molality, as function of pressure and temperature, can thus be proposed as

$$p = m_i^0 e^{\left(6.8591 - \frac{2004.3}{T}\right)} \tag{9.9}$$

This correlation is valid for pressures up to 5 MPa, for temperatures ranging from room temperature up to 363 K and molalities up to 3 $mol.kg^{-1}$. Note that the IUPAC reference data for CO_2 solubilities in ionic liquids is expressed in molalities using an approach similar to what is here proposed.[183]

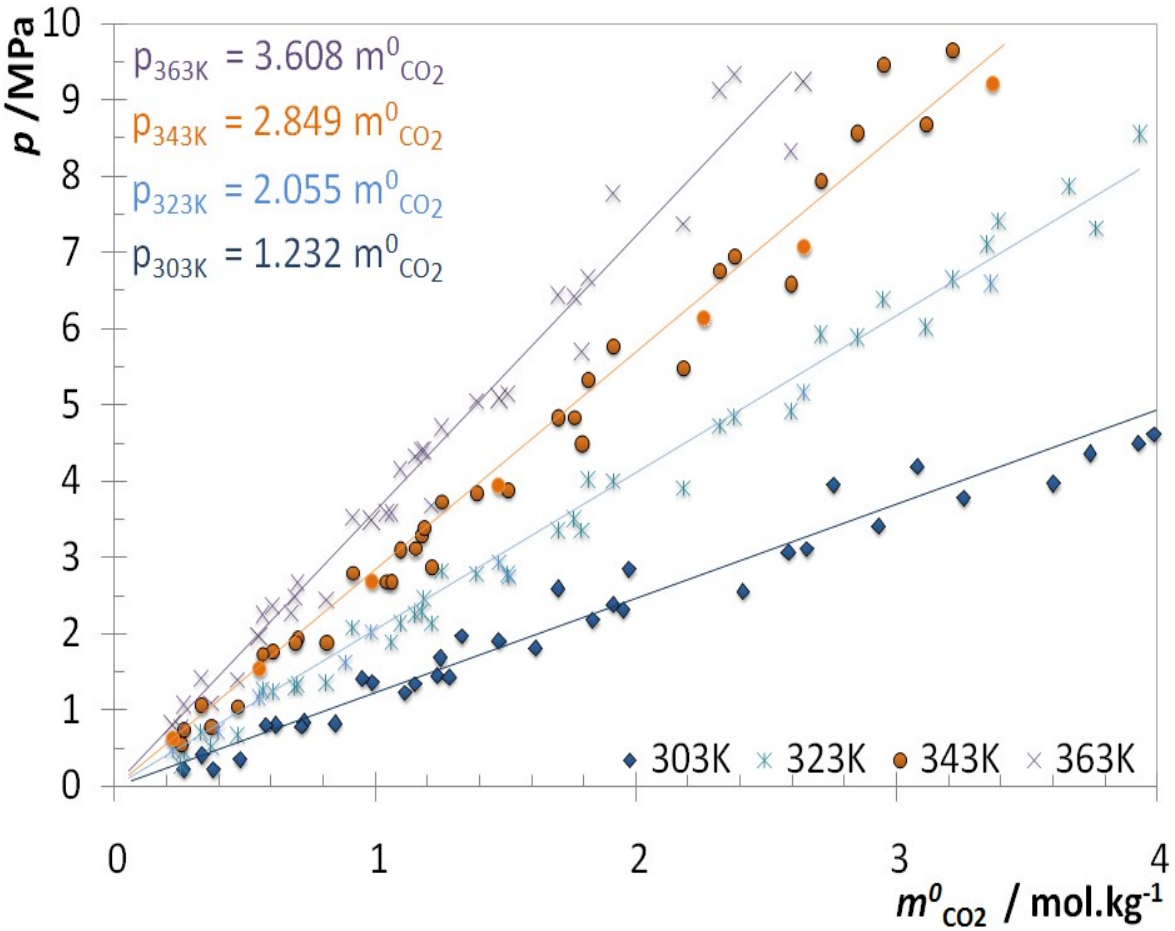

Figure *9.3.* Pressure - molality diagram of CO_2 + non volatile solvents.[30, 36, 50, 52, 59, 131]

Equation (9.7) and the results presented in Figures 9.2 and 9.3 indicate that the solubility of CO_2 in non volatile solvents, expressed in molality, is, within the experimental uncertainty of the data available,[183] and with the few exceptions discussed above, solvent independent. Solubilities in the literature are however generally reported in molar fractions and not molalities. For a dilute solution the relationship between the solubility expressed in molar fraction and molality can be obtained as

$$x_{solute} \approx m_{solute} Mw_{solvent} \qquad (9.10)$$

This means that, if at a given pressure two solvents present similar solubilities when expressed in molalities, their solubilities will differ when expressed in molar fractions.

Moreover, it shows that the solubility value, expressed in molar fraction, will increase with the solvent molecular weight, *Mw*. Ionic liquids and PEGs, due to their large molecular weights present larger solubilities, expressed in molar fractions, than other solvents, even when their solubilities are identical when expressed in molalities. This is also a consequence of the non ideality of these solutions being dominated by the entropic effects as discussed above. The larger the solvent the higher the solubility of CO_2 on this solvent due to the entropic contribution to the Gibbs free energy. This is valid, in particular, for two ionic liquids of different molecular weight and provide a good explanation for the fact that ILs based on the bis(trifluoromethylsulfonyl)imide, [NTf_2], anion present one of the largest CO_2 solubilities reported,[30, 36, 50] in spite of the weak interactions observed by spectroscopy, [180] and that the solubility of CO_2 in ILs increases with the alkyl chain length of the cation. [30, 36, 50]

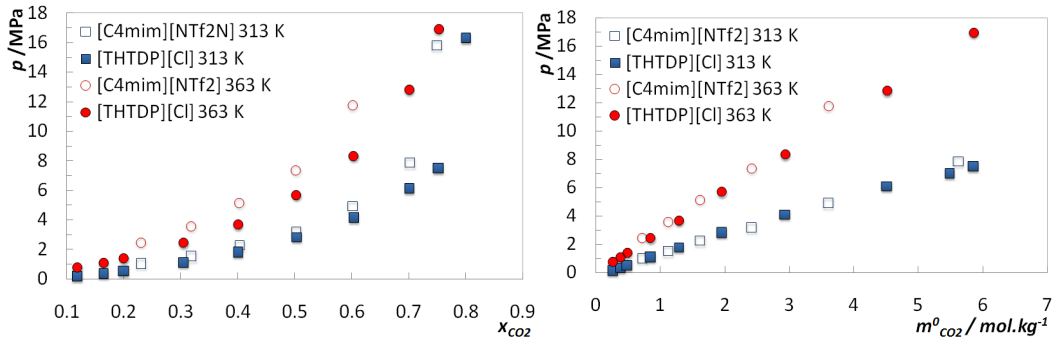

Figure 9.4. Pressure - mole fraction (left) and pressure - molality (right) diagrams of [THTDP][Cl] and [C_4mim][NTf_2] + CO_2 at 313 K and 363 K.[50]

The results here obtained indicate that any IL with a molecular weight large enough, even if it is not based on the [NTf_2] anion, should present a CO_2 solubility larger than an imidazolium with a fluorinated anion.[130] To test this hypothesis a chloride, [Cl], based ionic liquid was chosen, along with a cation that is formed essentially by alkyl chains, to create an IL with a very large molecular weight, while at the same time minimizing the possibility of forming EDA complexes with CO_2 or have any type of significant intermolecular interactions besides London dispersion forces. The IL chosen for this purpose was the trihexyltetradecylphosphonium chloride, [THTDP][Cl] (*Mw*=519.31). The results for the solubility of CO_2 in [THTDP][Cl] measured by us, using a technique

and apparatus detailed elsewhere (cf. Appendix D for experimental details and results), are compared in Figure 9.4 against 1-butyl-3-methylimidazolium bis(trifluoromethyl-sulfonyl)imide, [C_4mim][NTf_2] (*Mw*=419.36), one of the ILs with largest CO_2 solubility reported,[28, 30, 34, 36, 50, 52, 53, 59, 131, 185] at 313 K and 363 K. It is here shown that the solubility of CO_2, expressed in mole fraction, is indeed larger in [THTDP][Cl] than in [C_4mim][NTf_2] as predicted. Nevertheless, when expressed in molality, the solubilities in the two ILs overlap each other as shown in Figure 9.4.

9.5. Conclusions

This work shows that the solubility of CO_2 in non volatile solvents is not driven exclusively or predominantly by the favorable interactions between the gas and the solvent. The CO_2 displays an approximately ideal solubility in alkanes and minor negative deviations to ideality in ionic liquids that are lower than expected from that predicted from entropic factors alone as described by the Flory-Huggins equation. Negative deviations are observed for carbonyl containing systems such as fatty acid esters and, in spite of CO_2-OH being the most stable EDA complex formed on the systems studied, the solubility of CO_2 in alcohols presents actually a positive deviation to ideality. The non ideality of these solutions, and its impact on the CO_2 solubility, is thus the result of a complex and delicate balance between the solute-solute, solute-solvent and solvent-solvent interactions and cannot be inferred from the strength of solute-solvent interactions alone. This study suggests that the use of large molecular weight solvents and the introduction of sp^2 O-donating atoms (such as in ether and carbonyl groups) in the IL alkyl chain may have a favorable impact on the CO_2 solubility on these compounds.

When the molecular weight effect is removed from the analysis by comparing the solubilities in molalities instead of molar fractions the differences in solubilities, among the various systems studied are minimized and the solubility of CO_2 on non volatile solvents seems to be essentially solvent independent within the uncertainty of the experimental data available. Based on these results it was possible to develop a general correlation for the solubility of CO_2 in non-volatile solvents.

10. High Carbon Dioxide Solubilities in Trihexyltetradecylphosphonium-based Ionic Liquids

"Science is simply common sense at its best, that is, rigidly accurate in observation, and merciless to fallacy in logic."

Thomas Huxley

10.1. Abstract

This section studies the solubility of CO_2 on phosphonium based ionic liquids that, unlike imidazolium based ILs, have received little attention in the last few years in spite of their interesting characteristics. This work addresses the study of the gas–liquid equilibrium of two ionic liquids, trihexyltetradecylphosphonium bis(trifluoromethylsulfonyl)imide and trihexyltetradecylphosphonium chloride, in a wide range of temperatures, pressures, showing that phosphonium ionic liquids can dissolve even larger amounts of CO_2 (on a molar fraction basis) than the corresponding imidazolium based ILs. In particular trihexyltetradecylphosphonium bis(trifluoromethylsulfonyl)imide seems to be the IL with the largest CO_2 sorption capacity reported up to present revealing the potential of phosphonium based ILs for CO_2 capture.

A thermodynamic model based on the Peng–Robinson equation of state with the Wong–Sandler mixing rule, using the UNIQUAC model for the activity coefficients, was here adopted to describe the experimental data and for the estimation of the Henry's constants. An universal correlation, for the description of the solubility of CO_2 in ILs previously proposed by us was also applied to the description of the data here measured showing a good agreement with the experimental data.

10.2. Introduction

The high solubility of CO_2 in ionic liquids has been the object of extensive research during the last few years. Aiming at enhancing sour gases solubility and ultimately replace the hazard volatile organic compounds (VOCs), many researchers have judiciously tailored ionic liquids (ILs) to accomplish such task either through the introduction of fluorinated groups on the IL ions, or by adding basic groups such as amines or acetates.[16, 20-33] With the exception of this last type of ILs, where chemical interactions dominate the sorption mechanism, in most ionic liquids the gas solubility is simply driven by a physical absorption mechanism.[30, 34, 35] Among the ILs previously reported in the literature the imidazolium-based, specially those with fluorinated anions such as the

bis(trifluoromethylsulfonyl)imide, NTf_2, and bis(pentafluoroethyl)trifluorophosphate, pFAP, anions, are the ones with the highest CO_2 solubilities reported.[28, 33, 36]

Despite their attractive characteristics, such as negligible vapor pressures, high thermal stability, large liquidus range, nonflammability, high solvation capacity, compatibility with strong alkaline solutes, stabilizing effect on palladium catalysts, effective media for Heck and Suzuki reactions and their low cost, the phosphonium-based ionic liquids have received surprisingly little attention in the last few years from academia.[27, 49, 70, 189-194] Some have focused their study on the solubility of alcohols[195], alkanes and alkenes,[46, 49, 194, 196-199] or even on methane,[198, 199] carbon monoxide[46] or oxygen[198] in phosphonium ILs but few have reported solubilities of carbon dioxide on these ILs.[49, 70, 193, 194, 197] Furthermore, among those only a couple reported CO_2 solubilities under high pressure. [70, 197] Ferguson and Scovazzo[194] have shown that imidazolium and phosphonium based ILs have similar solubilities for several gases, while Anthony and coworkers[49] suggested that the nature of the anion has the most significant influence on the gas solubility. Hutchings and co-workers[27] have reported that, at subcritical temperatures, several phosphonium ionic liquids would completely dissolve as soon as all the CO_2 condensed and that the isopleths for these systems follow the vapor pressure curve of the pure CO_2.

Disregarding academia lack of interest, their properties and low cost have attracted the industry attention.[200] Central Glass Co., Ltd., from Japan, developed pharmaceutical intermediates using phosphonium ionic liquids,[200] while Texaco used a *"ruthenium melt catalyst"* dispersed n phosphonium or quaternary ammonium ILs to convert syngas into acetic acid, esters, alcohols and glycol.[201] Rhone-Poulenc, by other hand, used a tetrabutylphosphonium chloride to estabilize zero-valent palladium catalysts for carbonylation[201] and Eastman Chemical Company used a Lewis basic phosphonium iodide ionic liquid along with a Lewis acid catalyst for the isomeration of 3,4-epoxybut-1-ene to 2,5-dihydrofuran.[200]

In the wake of previous works,[30, 35, 36, 50] the purpose of the present study is to

identify ILs with large CO_2 solubilities and to further explore the mechanism behind the absorption of carbon dioxide by the ionic liquids. For that purpose, the trihexyltetradecylphosphonium chloride, [THTDP][Cl], and the trihexyltetradecylphosphonium bis(trifluoromethylsulfonyl)imide, [THTDP][NTf_2], ionic liquids were chosen. The structure of the phosphonium cation permits to minimize any specific interactions between the IL cation and the carbon dioxide. Furthermore, the chloride anion of the [THTDP][Cl] allows also to minimize any anion interaction with the CO_2.

The Peng–Robinson equation of state[84] with the Wong–Sandler/UNIQUAC mixing rule,[85] using the UNIQUAC model[86] for the activity coefficients, was used to model the experimental data measured in this work and to estimate the Henry's constants from which the enthalpies and entropies of solvation are derived and used to assess the CO_2 IL interactions.

10.3. Results and Discussion

The solubility of carbon dioxide in the studied ILs was measured for mole fractions ranging from (0.2 to 0.9), in the temperature range (293 to 363) K and pressures from (0.1 to 72) MPa, as reported in Tables F.1 and F.2 and depicted in Figure 10.1. The temperature increase leads to an increase on the equilibrium pressures and by increasing CO_2 concentration, the equilibrium pressures increase gradually at first, and then rapidly for higher CO_2 contents as a liquid-liquid like region is reached, as also observed previously for other ILs.[30, 36, 50] A singular phenomenon was observed for the system [THTDP][NTf_2] + CO_2 at CO_2 concentrations higher than 0.8. At these conditions the equilibrium pressure changes its behavior and starts to decrease with the temperature increase, as depicted in Figures 10.1b and Figure 10.2b. This unusual behavior, previously observed for the solubility of CO_2 in aqueous solutions of phosphonium based ILs is related to the liquid-liquid region, as previously noticed,[70] and to a change in the relative densities of the phases. At low pressures the IL phase is denser than the CO_2 and dp/dT is positive. At high pressures the CO_2 phase becomes denser than the IL phase and then, as predicted by the

Clausius-Clapeyron equation, the *dp*/*dT* becomes negative and the solubility increases with temperature.

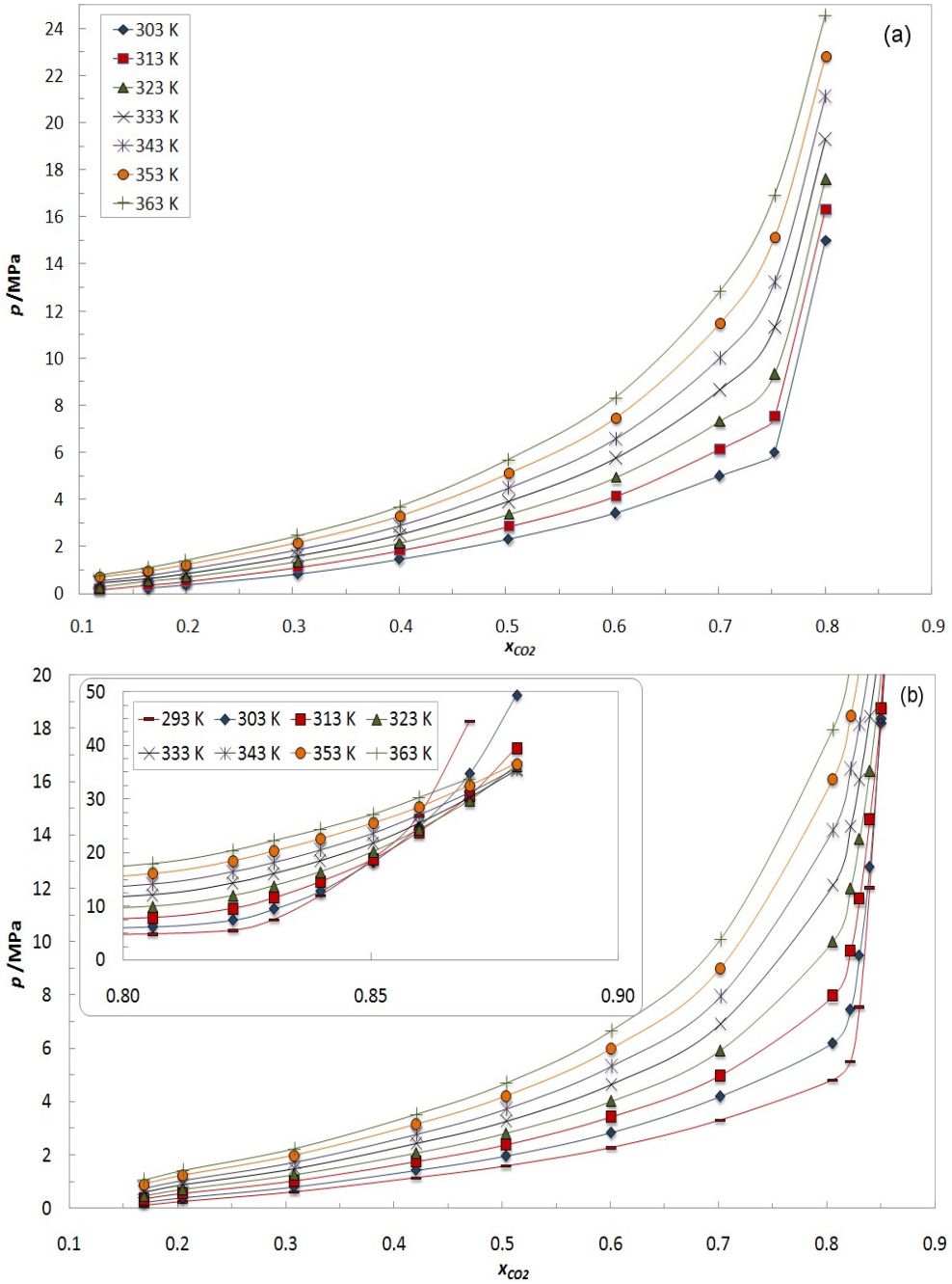

Figure 10.1. Pressure–composition diagram of the binary systems (a) CO_2 + [THTDP][Cl] and (b) CO_2 + [THTDP][NTf_2]. The solid curves are guides for the eye.

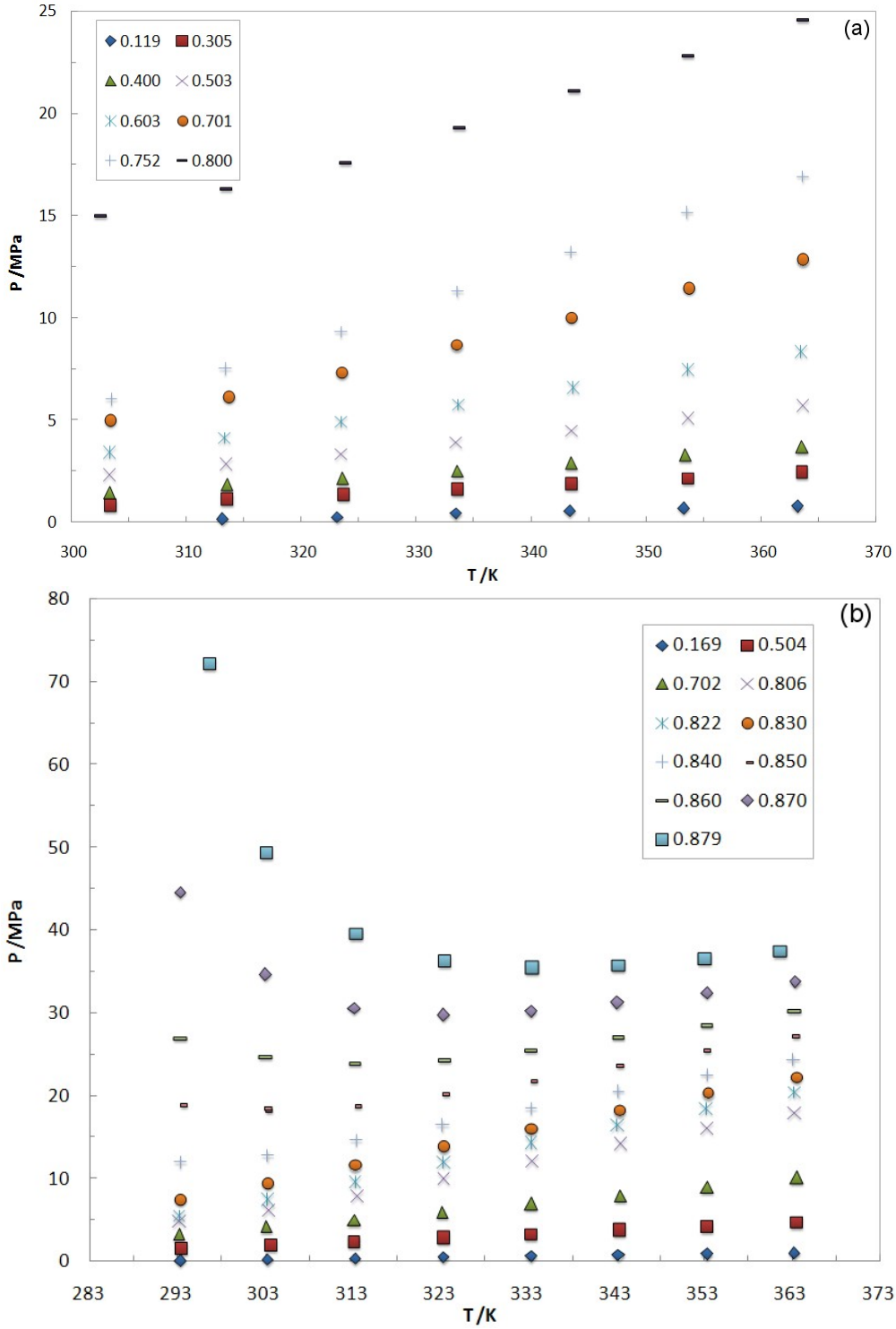

Figure 10.2. Pressure–temperature diagram, as function of CO_2 mole fractions, of the binary systems (a) CO_2 + [THTDP][Cl] and (b) CO_2 + [THTDP][NTf_2].

The solubilities of CO_2 in the ILs studied on this work are among the highest reported up to present. These ILs present higher CO_2 solubilities than those reported for imidazolium-based ILs, with fluorinated anions like the NTf_2[28, 33, 52, 59] or pFAP,[28, 33] for which several authors justify the high solubilities as a result of special interactions between the CO_2 and the IL ions. A comparison of the solubility of CO_2 on these ILs is depicted in Figure 10.4.

Hutchings and co-workers[27] have reported that for subcritical temperatures several phosphonium ionic liquids, including the [THTDP][Cl] here studied, would completely dissolve as soon as all the CO_2 condensed and that the isopleths for these systems follow the vapor pressure curve of the pure CO_2. In this work we have tried to reproduce the results from Hutchings et al.[27] without success. No significant solubility of phosphonium ionic liquids in near or supercritical CO_2 was observed.

The results of the application of the equation of state to the modeling of the binary systems containing ionic liquids studied in this work are presented in Table F.3 for all the experimental data. In the Table, *NP* is the number of data points, *T* is the temperature, k_{12}, A_{12} and A_{21} are the interaction parameters of the model, where *1* stands for the CO_2 and *2* for the ionic liquid. This Table is divided in sections for each system studied. The properties of the compounds used in the modeling are reported in Table F.4. As depicted in Figure 10.3, the model provides a good description of the experimental data. The equation of state was then used to estimate the Henry's constant for the studied systems.

The Henry's constants for the CO_2 in the investigated ILs were estimated by fitting the PR-WS/UNIQUAC model to the experimental data and calculating the limiting slope defined in Eq. (4.13) as the solubility approaches zero. The estimated Henry's constants results, reported in Table F.3, indicate that Henry's constant decreases slightly (i.e., CO_2 solubility increases) with the temperature.

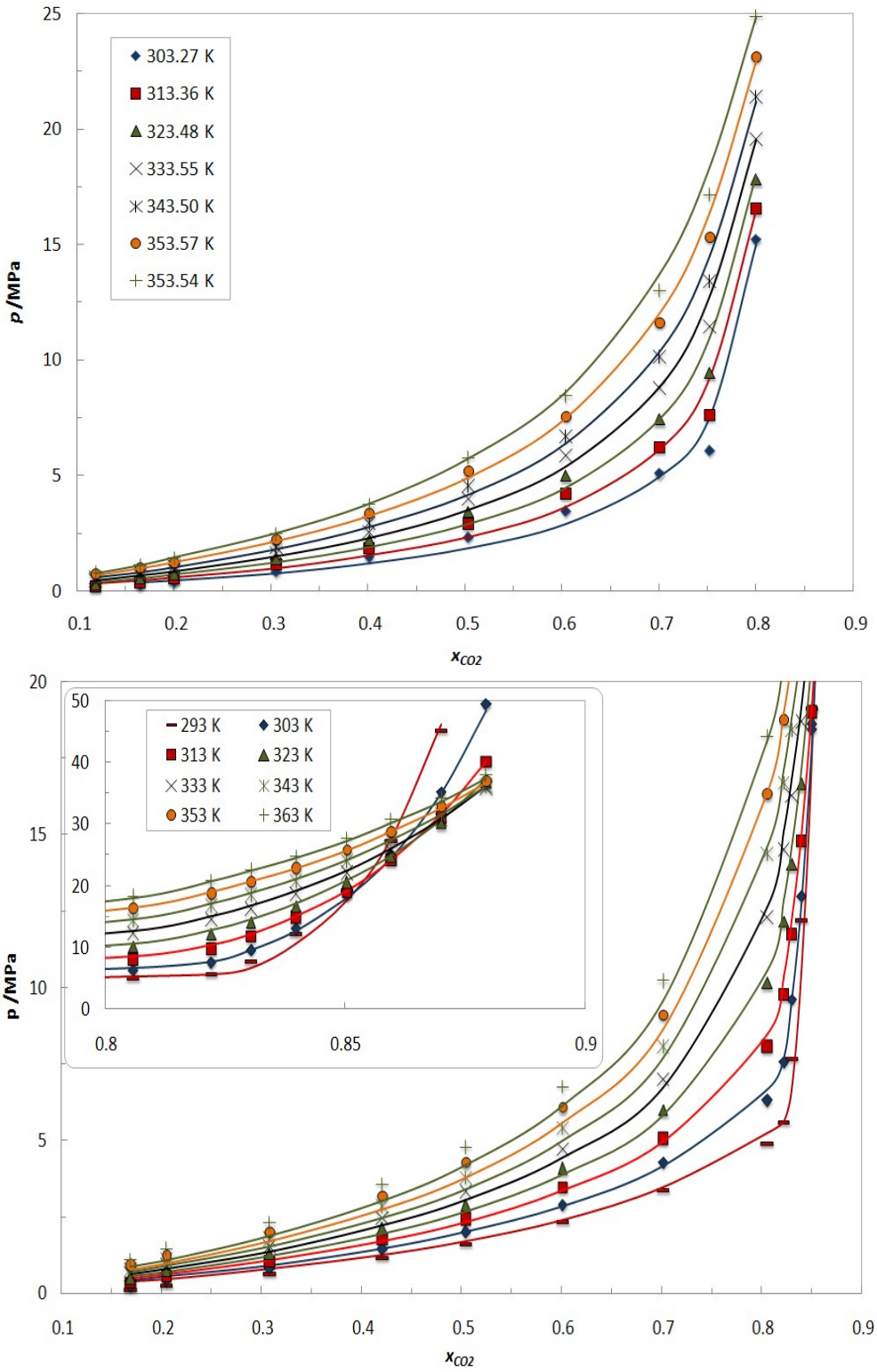

Figure 10.3. PTx diagram and modeling for the systems CO_2 + [THTDP][Cl] (a) and CO_2 + [THTDP][NTf_2] (b). The solid lines represent the calculations with PR-WS/UNIQUAC EoS.

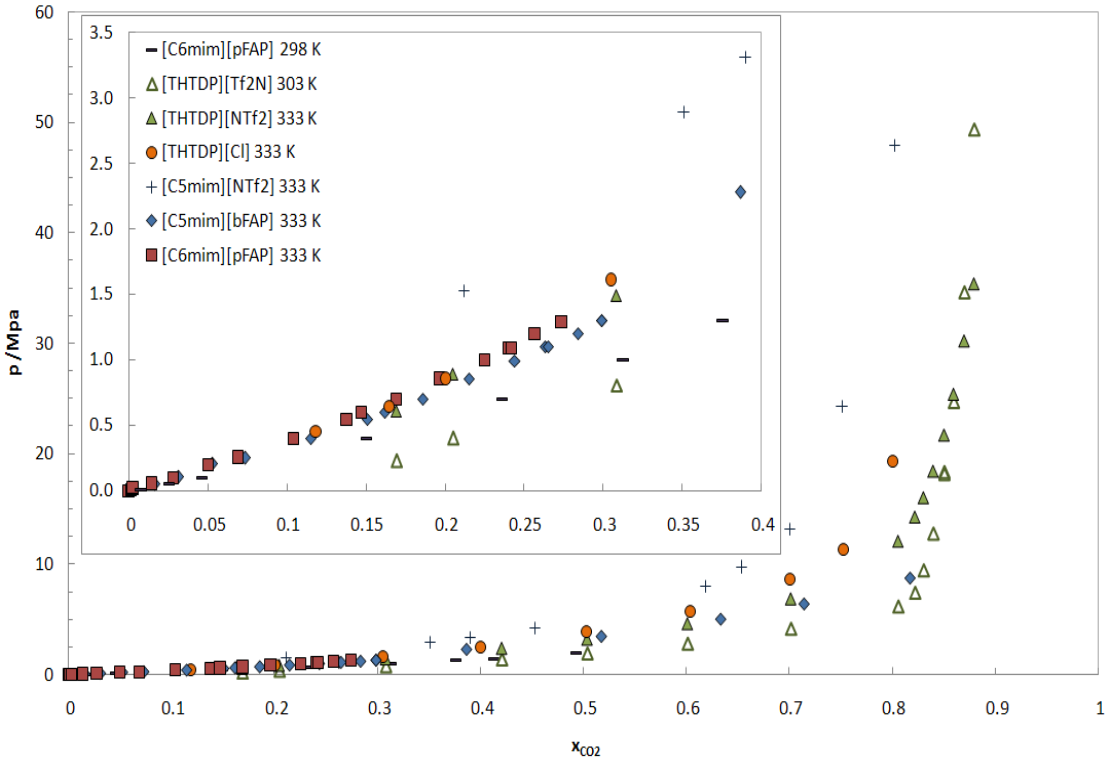

Figure 10.4. Pressure–composition diagram of the binary systems CO_2 + [THTDP][Cl], ●, CO_2 + [THTDP][NTf_2], ▲, CO_2 + [C_6mim][pFAP] [28, 33], (■, ━), CO_2 + [C_5mim][pFAP] [28], ◆, and CO_2 + [C_5mim][NTf_2] [36], ┼. The solid curves are guides for the eye.

The results for the Henry's constant of CO_2 in [THTDP][NTf_2] and in [THTDP][Cl] were correlated as a function of temperature by the empirical equation 4.14 where, the coefficients *A* and *B* are listed in Table F.5, together with the Henry's constant average absolute deviations, $|\Delta H_{12}|$, obtained for each ionic liquid.

As discussed on section 4.3. the effect of temperature on CO_2 solubility can be related to the Gibbs energy, the partial molar entropy and partial molar enthalpy of solvation[88] through an appropriate correlation of Henry's constant.

The results presented in Table F.5 show that the partial entropies in both fluids are essentially identical, indicating a similar structural solvation interaction. The partial molar enthalpy of solvation of the CO_2 in [THTDP][NTf_2] is lower than in [THTDP][Cl], indicating a slightly stronger interaction between the CO_2 and the [THTDP][Cl]. The

partial molar enthalpies of solvation observed for these ILs are lower than those previously reported by us for the imidazolium based ionic liquids [C_4mim][Acetate], [C_4mim][Trifluoroacetate], [C_4mim][Dicyanamide] and [C_4mim][NTf_2][30, 36, 50] showing that the interactions between the CO_2 and the phosphonium are small, and the mechanism of solubility of CO_2 on these fluids is essentially a physisorption, as would be expected for these ionic liquids and discussed in a previous work.[35] In spite of these feeble interactions, the ILs here studied are among those presenting a larger sorption capacity for CO_2, showing that the large CO_2 solubility in ionic liquids is not dependent on special interactions with the solvent. Based on this idea, we have proposed a universal correlation for the solubility of CO_2 in ionic liquids[35] that can be described by

$$p = m_i^0 e^{\left(6.8591 + \frac{-2004.3}{T}\right)} \qquad (10.1)$$

The predictions are compared against the experimental data measured in this work in Figure 10.5. As can be seen a good prediction of the experimental data can be obtained using this approach.

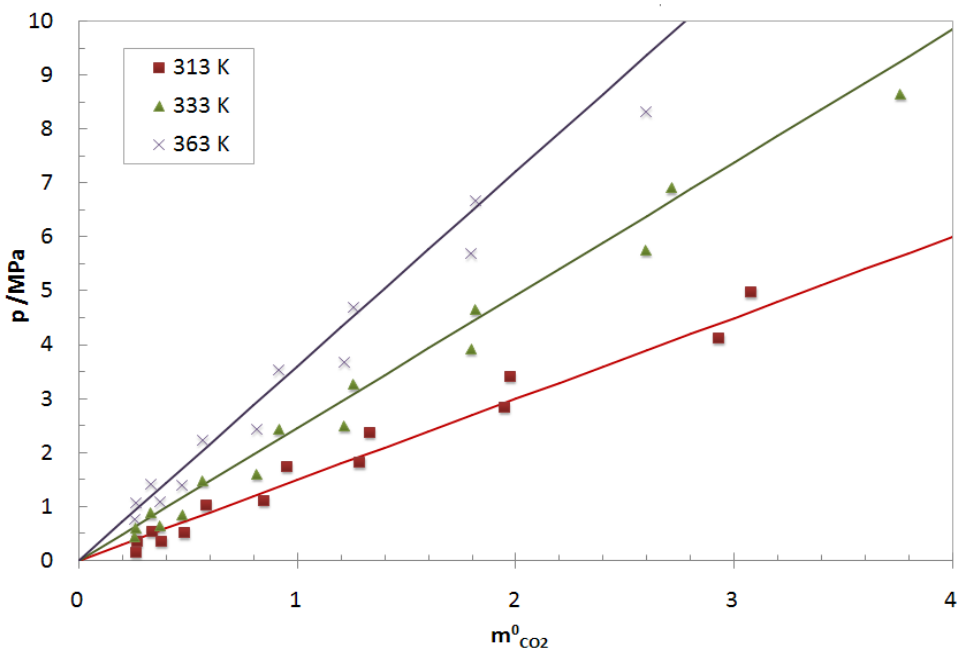

Figure 10.5. pTm^0 diagram for the systems CO_2 + ILs. The solid lines represent the universal correlation previously proposed.[35]

10.4. Conclusions

CO_2 solubility in, trihexyltetradecylphosphonium bis(trifluoromethylsulfonyl)imide and trihexyltetradecylphosphonium chloride was studied in a wide range of temperatures, pressures. It is shown that phosphonium ionic liquids can dissolve even larger amounts of CO_2 (on a molar fraction basis) than the imidazolium based ILs with the same anion. The solubilities here reported are the largest observed for ionic liquids in absence of chemical interactions. Moreover, an interesting increase of the CO_2 solubility with temperature was observed on these ILs at very high pressures.

A thermodynamic model based on the Peng-Robinson EoS with the Wong-Sandler/UNIQUAC mixing rule was used with success in the correlation of the measured data. The model provides a good description of the experimental data and the estimation of the Henry's constants for these systems. The enthalpies of solvation derived from the Henry's constants show a lower interaction between the CO_2 and the ILs than previously observed for the imidazolium ionic liquids. A correlation for the solubility of CO_2 in ILs previously proposed by us was applied to the description of the data here measured showing a good agreement with the experimental data measured.

11. High pressure CO_2 solubility in N-methyl-2-hydroxyethylammonium protic ionic liquids

“The fewer the facts, the stronger the opinion.”

Arnold H. Glasow

11.1. Abstract

Within the enormous group of existing ionic liquids, those based on conjugate bases of carboxylic acids seem to be particularly promising. This work addresses the study of the high pressure CO_2 solubility (up to 80 MPa) in two protic ionic liquids, N-methyl-2-hydroxyethylammonium formate and N-methyl-2-hydroxyethylammonium acetate, in a wide range of temperatures (293 K to 353 K). A thermodynamic model based on the Peng–Robinson equation of state with the Wong–Sandler mixing rule, using the NRTL model for the activity coefficients, was here adopted to describe and evaluate the thermodynamic consistency of the experimental data. Furthermore, the study of a ternary mixture of CO_2 + CH_4 + N-methyl-2-hydroxyethylammonium acetate was investigated showing a high selectivity from the IL towards these solutes.

11.2. Introduction

Until now, studies concerning ionic liquids have been based on the imidazolium cation and, to a lesser extent, on the alkyl pyridiniums and trialkylamines.[190] Protic ionic liquids (PILs) have, however, received limited attention from the academia. The first PIL reported, ethanolammonium nitrate, was reported by Gabriel and Weiner in 1888,[202] followed by ethylammonium nitrate (EAN), in 1914, synthesized by Walden[203]. These PILs were produced by a stoichiometric acid-base Brønsted reaction and their main difference, compared to aprotic ILs (AILs), is the presence of at least a proton, which is/are able to promote extensive hydrogen bonding.[203] These liquids present some characteristics, such as a slightly lower conductivity and stability, which may reduce, at first, their interest for a number of applications. However, their low cost, simple synthesis and purification methods, low toxicity and high biodegradation character, among other set of appealing characteristics, overcomes those limitations for many different purposes.

Recently, some work has been reported on the synthesis, physicochemical and structural characterization of PILs. Bicak[204] synthesized the 2-hydroxyethylammonium formate (2-HEAF), an ionic liquid formed by the neutralization of monoethanolamine with

formic acid. Greaves *et al.*[205] proposed different protic ionic liquids from primary amines and organic and inorganic acids. Cota *et al.*[206], Kurnia *et al.*[207] and Alvarez *et al.*[73] synthesized a family of these ILs by modifying the aliphatic chain of the organic acid and/or using secondary and tertiary hydroxyamines. There were also studies that use PILs in catalytic reactions[206] and on the interaction with hydroxilic solvents (like water and alcohols), showing that 2-HEAF is soluble in water, ethanol and methanol in all the concentration range.[208] Moreover, a relevant aspect, considering the interest in these substances as more environmentally sustainable solvents, is their potential toxicity. This issue has not been sufficiently studied until now, especially taking into account the need of this information to fulfill the REACH (Registration, Evaluation, Authorization and Restriction of Chemical Substances) requirements (UE) and so, allowing the assessment of hygiene and safety issues derived from their manufacture, use, and transport in the industrial sectors in which these substances will be applied. In what is referred to PILs, the first results highlight that total biodegradation and low toxicity are intrinsic characteristics of these kind of ionic liquids.[209, 210]

The presence of an anion with a strong basic character suggests that PILs could be an interesting alternative to be applied to processes with supercritical gases for capture of acid gases, such as CO_2, H_2S and SO_2.[31, 211, 212] In order to study the viability of such alternative, vapor-liquid equilibria data at high and moderate pressures are necessary. Thus, in the wake of previous studies,[30, 36, 50, 119] this work investigates gas-liquid equilibrium of binary CO_2 + N-methyl-2-hydroxy ethylammonium-based ILs systems, in temperatures up to 363.15K and pressures up to 80 MPa. Furthermore, the study of a ternary mixture of CO_2 + CH_4 + N-methyl-2-hydroxyethylammonium acetate was also investigated, showing a high selectivity from the IL towards these solutes.

The Peng–Robinson equation of state with the Wong–Sandler/NRTL mixing rule, using the NRTL model for the activity coefficients, was used to model the experimental data measured in this work.

11.3. Results and Discussion

The solubility of carbon dioxide and methane in the studied ILs was measured for concentrations from (0.2 to 0.9), in the temperature range (293 to 363)K and pressures from (0.1 to 80) Mpa.

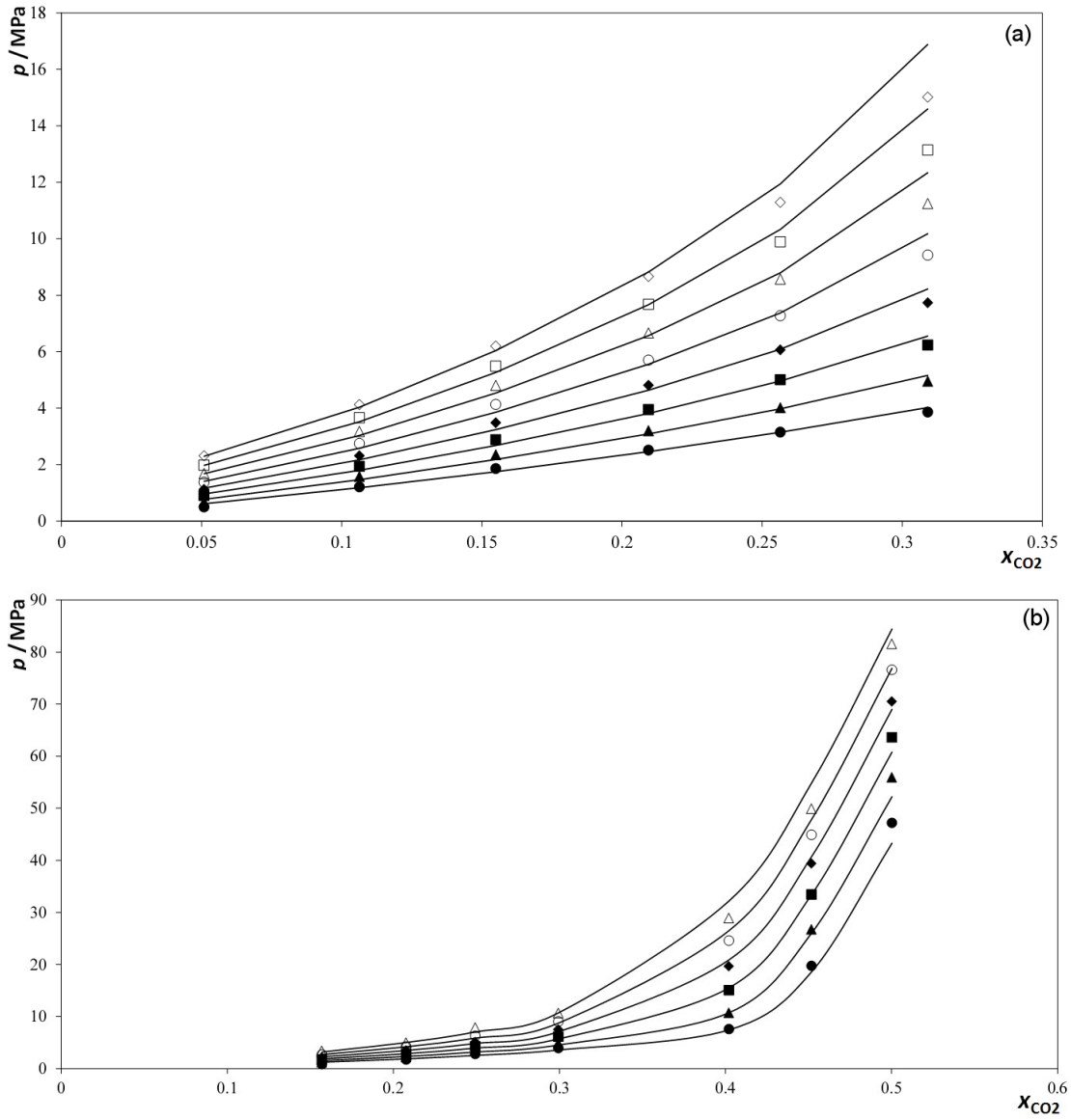

Figure 11.1. PTx diagram and modeling for the systems CO_2 + m-2-HEAF, 293.15 (●), 303.15 (▲), 313.15 (■), 323.15 (♦), 333.15 (○), 343.15 (Δ), 353.15 (□), 363.15 (◊) (a) and CO_2 + m-2-HEAA, 313.15 (●), 323.15 (▲), 333.15 (■), 343.15 (♦), 353.15 (○), 363.15 (Δ), (b). The solid line represents the calculations from PR-WS/NRTL EoS.

The solubility data is reported in Tables G.1 through G.3 and plotted in Figures. 11.1a, b and 11.2. It follows the typical solubility behavior decreasing with temperature and increasing with pressure as observed previously for other ILs.[30, 36, 50, 119]

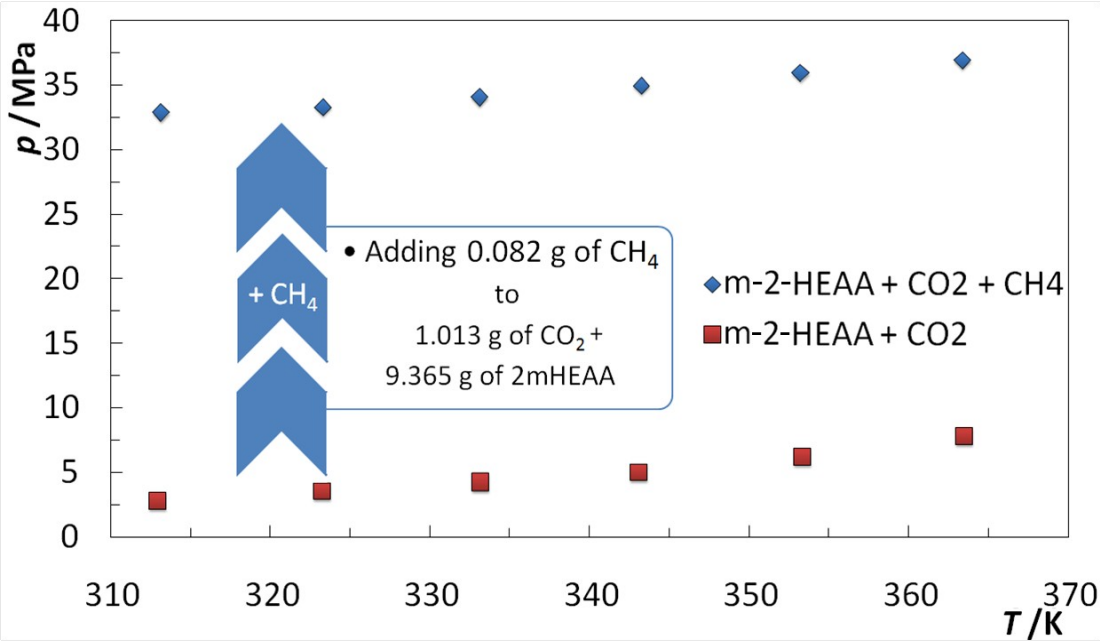

Figure 11.2. Pressure-temperature diagram of the systems CO_2 (x_{CO2} = 0.25) + m-2-HEAA (x_{IL} = 0.75) and CO_2 (x_{CO2} = 0.24) + CH_4 (x_{CH4} = 0.05) + m-2-HEAA (x_{IL}=0.71).

The carbon dioxide solubility in the m-2-HEAF and m-2-HEAA ILs, at 313 K, is compared with the CO_2 solubility in the 2-HEAF and 2-hydroxy ethylammonium acetate (2-HEAA) reported by Yuan et al.[31] as depicted in Figure 11.3. The inclusion of a methyl group on the cation leads to an increase of the CO_2 solubility which is in agreement with the conclusions of our previous work showing that the physical sorption of CO_2 increases with the molecular weight of the compound when the concentration is expressed in mole fractions.[89] Furthermore, while the addition of a methyl group produces a slight increase of the CO_2 solubility in the formate-based ionic liquid (m-2-HEAF and 2-HEAF have similar solubility values at ca. 2MPa) for the acetate-based ILs it leads to a higher increase. The m-2-HEAA phase behavior suggests that, for low CO_2 mole fractions exists chemical interaction between the CO_2 and the IL. The formation of electron donor acceptor (EDA) complexes between CO_2 and acetate anions was previously observed by ^{13}C HRMAS NMR

spectra for the CO_2 + 1-butyl-3-methylimidazolium acetate, [C_4mim][Ac], system.[30] The formation of the EDA complex is here confirmed since, as previously observed[89] for the CO_2 + [C_4mim][Ac] system, the CO_2 + m-2-HEAA system, unlike CO_2 +m-2-HEAF system, does not follow the universal correlation previously proposed,[89] as depicted in Figure 11.4. Moreover, the chemisorption present at low CO_2 mole fractions, leads in the m-2-HEAA system to solubilities higher than those observed for ammonium-based ILs with similar molecular weight[31] for pressures up to ca. 4 MPa. For higher pressures the solubility becomes slightly lower and the equilibrium pressure increases exponentially. This can be explained considering that m-2-HEAA forms the EDA complexes with carbon dioxide in the low pressure region where the chemical absorption is the predominant phenomena. Upon saturation the physical dissolution becomes predominant with small solubility changes induced by large pressure variations. This trend was also observed with another acetate based IL where chemical followed by physical absorption takes place.[30]

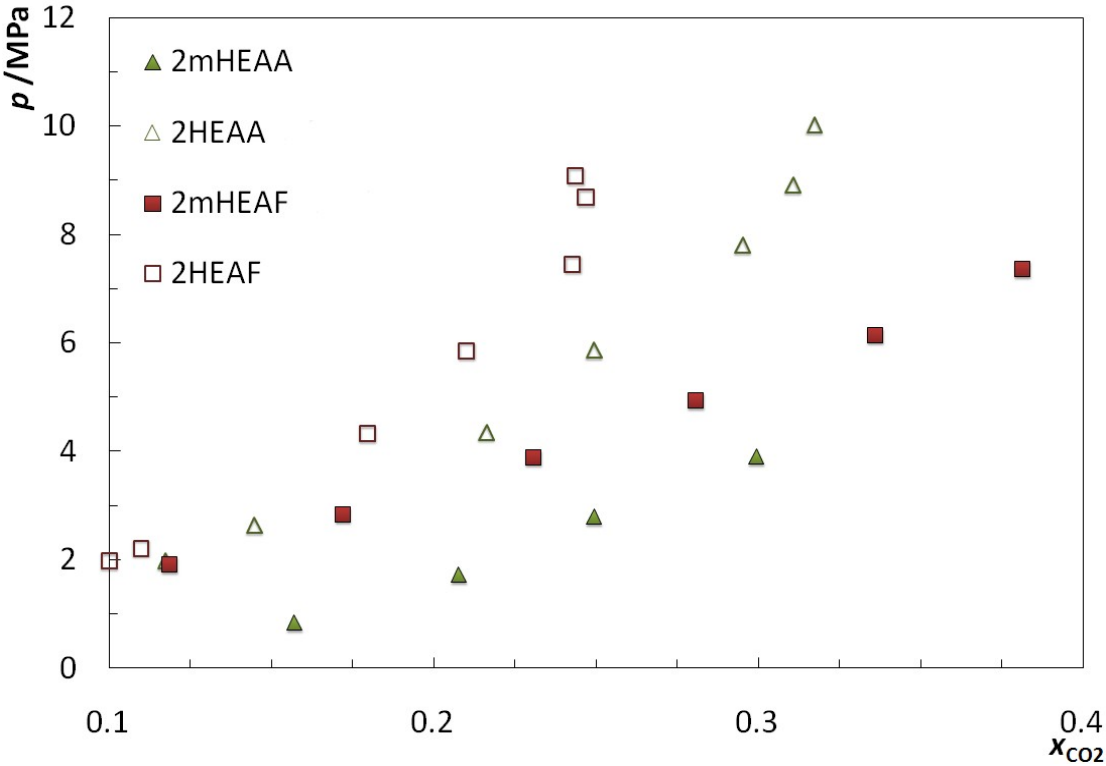

Figure 11.3. Comparison between the CO_2 solubility, at 313 K, in m-2-HEAF and m-2-HEAA and that in 2-HEAF and 2-HEAA previously reported by Yuan et al.[31].

The results of the application of the thermodynamic consistency test to the binary systems are presented in Table G.4, the properties of the substances used in the modeling in Table G.5. They show that the data from CO_2 + m-2-HEAF binary system is thermodynamically consistent (TC), while the CO_2 + m-2-HEAA binary system is not fully consistent (NFC). Nonetheless, the elimination of the data points with individual area deviations greater than 20% leads to consistent data for the remaining points. The CO_2 +m-2-HEAA system presents high deviations for the isopleths at x_1 = 0.5, for temperatures lower than 343 K, and x_1 = 0.157, for temperatures over 343 K. Therefore, the isotherms with these compositions are not fully consistent. Nonetheless, the model provides a very good description of the experimental data, as depicted in Figure 11.1a and b.

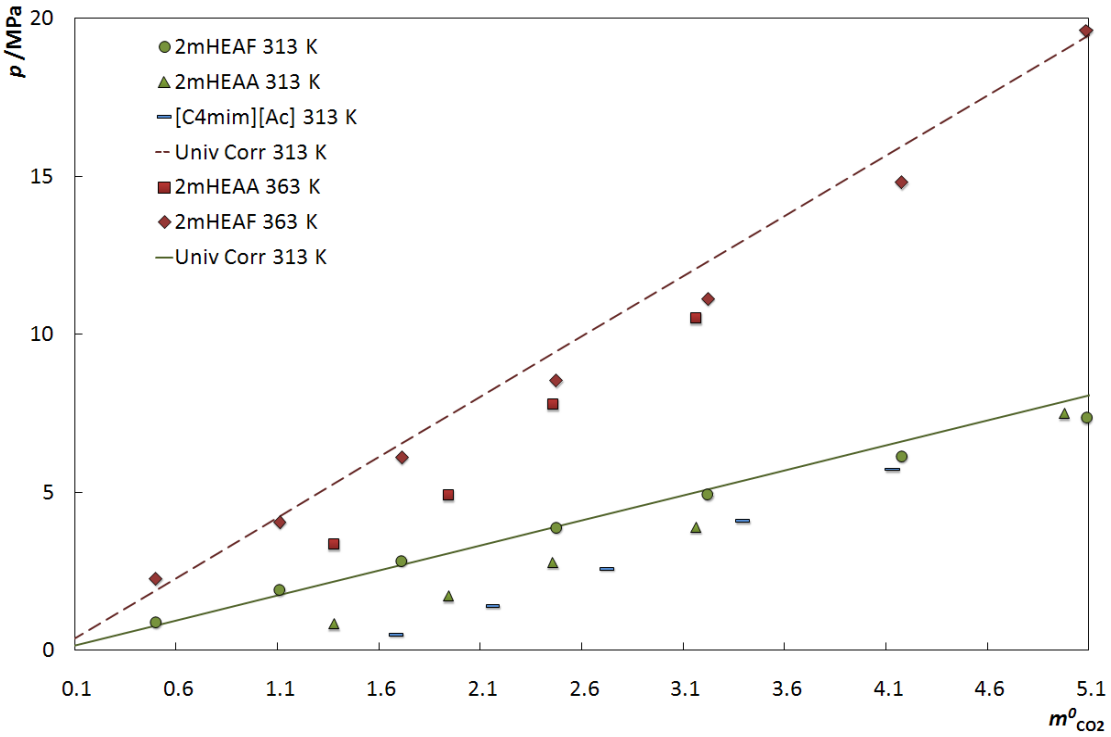

Figure 11.4. Pressure-molality diagram of the systems CO_2 + m-2-HEAF and CO_2 + m-2-HEAA. The solid and dashed line represents the universal correlation for 313 K and 363 K.

The introduction of methane, CH_4 (m_{CH4} = 0.082 g), in the binary system m-2-HEAA + CO_2 (x_{CO2} = 0.249) leads to a strong increase on the equilibrium pressure as shown in Figure 11.2. This indicates that methane, unlike the carbon dioxide, is poorly soluble on this PIL and suggests that the m-2-HEAA could be used to selectively separate

the carbon dioxide from methane.

11.4. Conclusions

Gas solubilities of carbon dioxide in two protic ionic liquids, namely N-methyl-2-hydroxy ethylammonium acetate and N-methyl-2-hydroxy ethylammonium formate, was presented for temperatures from (293 to 353)K and pressures up to 80 Mpa. Comparison with other similar fluids indicates that while the m-2-HEAF presents no specific interaction towards the CO_2 whereas the m-2-HEAA asymmetric and nonideal phase diagram suggests that this ionic liquid interact chemically with the carbon dioxide at low CO_2 molar concentrations.

The data here reported were well correlated by the PR EoS and found to be thermodynamically consistent for the m-2-HEAF + CO_2 system and not fully consistent for the m-2-HEAA + CO_2 system.

The high solubility pressures exhibited by the ternary mixture CO_2 + CH_4 + m-2-HEAA indicate the m-2-HEAA could be used to selectively separate carbon dioxide from methane mixture.

12. Non-ideality of Solutions of NH_3, SO_2, and H_2S in Ionic Liquids and the Prediction of their Solubilities using the Flory-Huggins Model

"You do not really understand something unless you can explain it to your grandmother."

Albert Einstein

12.1. Abstract

The non ideality of solutions of light compounds such as SO_2, NH_3, and H_2S in ionic liquids is here studied using experimental VLE data previously published. The data available for systems of ILs with SO_2, NH_3 and H_2S show these systems to present negative deviations to the ideality in the liquid phase, and that these deviations are dominated by entropic effects. It is here shown that for the solutions of SO_2 and NH_3 in ionic liquids the deviations from ideality, and the gas solubility, can be predicted using the Flory-Huggins model. For the H_2S a positive deviation to the non-ideality that arises from the enthalpic effects decreases somewhat the quality of the description of the experimental data by the Flory-Huggins model predictions.

12.2. Introduction

Sulfur-compounds, including hydrogen sulfide (H_2S) and sulfur dioxide (SO_2), frequently appear as contaminants in process streams in the production, processing and refining of fossil fuels.[65, 66] Gasification of heavy residual oil, petroleum coke, coal feedstocks and hydrocarbons is increasing in importance and the key gas separation is the selective removal of contaminants, like H_2S, COS, NH_3 and SO_2, from the synthesis gas. In addition, the presence of acid gases (COS, H_2S, CO_2) and other impurities require the syngas to undergo a gas treatment process to make it suitable for downstream use. The solubility of gases like SO_2, NH_3, and H_2S in solvents of low volatility or non volatile is thus highly relevant for many technological applications.

Ammonia is widely used in many industrial sectors such as fertilizer, explosives and chemicals production, being one of the most highly produced chemicals in the world. Due to its interesting thermodynamic properties, industrial refrigeration systems are one of the most important industrial applications for NH_3. Moreover, contrary to what is observed for most refrigerants, ammonia is considered to be efficient, economical and environmental friendly, since it does not deplete the ozone layer or contribute to global warming.

Composed by large organic cations and organic or inorganic anions, ionic liquids

(ILs) became one of the fastest growing areas of research for chemists and engineers. The possibility of tuning the ILs properties make these compounds viable candidates for a wide range of processes and products. Among the foreseeable applications in multiple fields, their use in oil and fuel desulphurization processes[213-215] and separation and capture of sour gases[216-218] are some of the most interesting.

The large solubility of gases in ionic liquids has been object, for the past decade, of discussion among the scientific community, concerning the solvation mechanism. Several authors have rationalized that the high gas solubility in ILs was due to specific solute-solvent interactions and some have even evidenced chemical absorption.[26, 30, 46, 93, 129, 177, 179, 216, 219-223] Nonetheless, the information currently available is not enough to support the proposed mechanisms. Ando et al.[219] and Siqueira et al.[220] have shown no evidence of any interaction between the IL and the SO_2 molecule, by Raman spectroscopy and molecular dynamics simulations, apart from the shift to low wave numbers of the Raman band corresponding to S–O symmetric stretching in comparison to pure SO_2. Huang et al.[26] reported weak interactions or no chemical bonding at all between the solvent and the solute SO_2 molecule in the SO_2 – saturated ILs, no significant change of the frequencies of the bands originating from the pure ILs and no significant proton shift in the ^1H NMR spectra of the SO_2 – saturated ILs. Andanson et al.[177], using infrared and Raman spectra, showed that, despite the shift of the PF_6- anion due to stretching, the structure of the ionic liquids does not change significantly. These evidences suggest that, similarly to what was found for the solvation of CO_2 in ILs[89], the mechanism responsible for the solvation of these gases in ionic liquids is essentially physical. Very few cases of chemical complexation of gases with ionic liquids have been reported until now. The most importants are the 1-butyl-3-methylimidazolium acetate[29, 30] and the ionic liquids used for storage of BF_3 and PH_3 reported by Tempel *et* al.[224].

In the following of a previous work,[89] the mechanism behind the solubility of light compounds such as NH_3, SO_2 and H_2S, in ionic liquids, is here investigated by analyzing their deviations to ideality in the liquid phase. This approach allows not only to achieve a

deeper understanding of the mechanism behind the solvation of these gases in ionic liquids but also to establish models that can be used to predict the solubility of gases in ionic liquids.

12.3. *The non ideality of NH_3 and SO_2 solutions in ionic liquids*

Experimental VLE data for systems of ILs with SO_2 and NH_3 are scarce and high discrepancies (up to 35 %) between authors are observed. For IL + NH_3 systems only data by Yokozeki et al.[225] and Li et al.[226] are available for a handful of ionic liquids while for IL + SO_2 only data by Anderson et al.[138], Shiflett et al.[227] and Yuan et al.[211] are available.

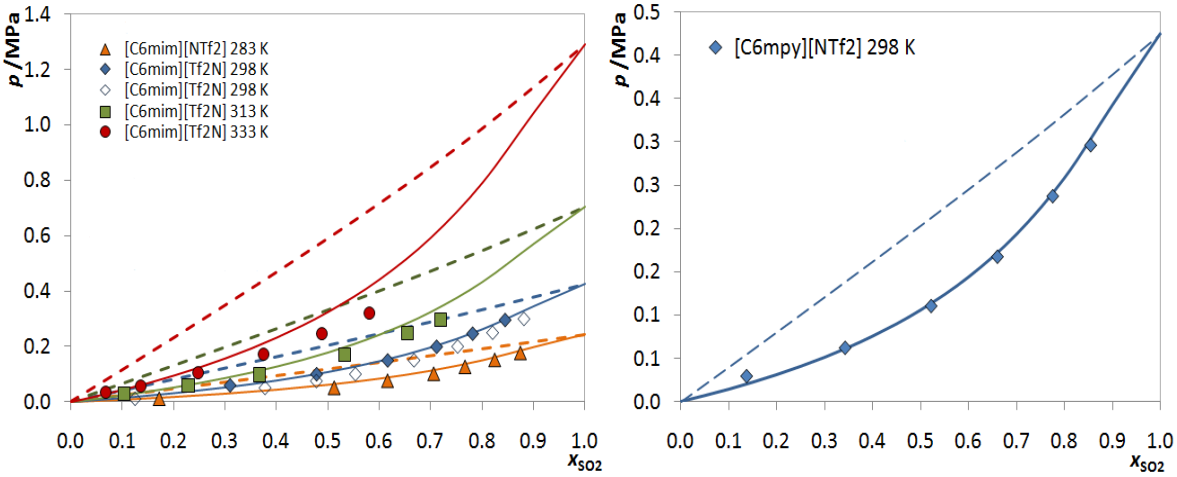

Figure 12.1. Pressure - SO_2 molar composition diagram for the systems SO_2 + ionic liquid.[138, 217, 227] The solid lines represent the Flory-Huggins model and the dashed represent the ideal behavior described by the Raoult's law.

The VLE at low and moderate pressures for these systems can be described by a gamma-phi approach

$$\phi_{gas}\, y_{gas}\, p = x_{gas}\, \gamma_{gas}\, p^{\sigma}_{gas} \qquad (12.1)$$

where in the case of a non volatile solvent such as the ionic liquids y_{gas}=1. The vapor pressure of the gas, p^{σ}_{gas}, was estimated using the correlations reported at the DIPPR database.[122]

On these systems the liquid phase non-ideality results not only from differences in

the energetic interactions between the molecules, as described by the residual contribution to the Gibbs free energy, but also from entropic effects due to their size and shape differences, the combinatorial contribution, as summarized by

$$G^E = G^E_{comb} + G^E_{residual} \tag{12.2}$$

The entropic effects will always have a negative contribution to the non-ideality that, in terms of activity coefficients, can be described by the Flory-Huggins model[181, 182, 228]

$$\ln\left(\gamma^{comb}_{gas}\right) = \ln\frac{\varphi_{gas}}{x_{gas}} + \left(1 - \frac{\varphi_{gas}}{x_{gas}}\right) \tag{12.3}$$

where $\varphi_{gas} = \frac{x_{gas} V_{m_{gas}}}{x_{gas} V_{m_{gas}} x_{IL} V_{m_{IL}}}$ is the volume fraction of the gas. The molar volumes of the ionic liquids were derived from their densities[78, 134, 229-232] and those of the gas obtained from the DIPPR database.[122]

The non ideality of the vapor phase is described by the fugacity coefficient, ϕ_{gas}, that was here estimated using the Peng-Robinson EoS.[84] The critical properties used for the gaseous compounds are listed in Table D.1.

If only the combinatorial contributions to the non-ideality are taken into account the Eq. (12.1) will become

$$p = \frac{x_{gas} \exp\left(\ln\frac{\varphi_{gas}}{x_{gas}} + \left(1 - \frac{\varphi_{gas}}{x_{gas}}\right)\right) p^{\sigma}_{gas}}{\phi_{gas}} \tag{12.4}$$

Figures 12.1 and 12.2 show the VLE phase diagrams for the systems of SO_2 and NH_3 with ionic liquids. The full lines were calculated using Eq. (12.4) while the dashed lines, corresponding to the behavior of an ideal liquid phase, were estimated using Eq. (12.1) with the activity coefficient of the gas in the liquid phase as being γ_{gas}=1. They show that the experimental VLE data for these systems as a non-ideal behavior with strong negative deviations that are well described by the Flory-Huggins model. The average deviations in the equilibrium pressure predicted by the model, presented in Table H.1

(extended pressure deviations as function of SO_2 and NH_3 mole fractions and temperature are available in supporting information), show that the Flory-Huggins equation is able to describe the VLE data within the combined experimental uncertainty of data from different authors. The capacity of the approach here proposed to describe the VLE for these systems suggests that the residual contribution to the excess Gibbs energy is very small, though positive, what implies that there is a small misfit in the solute-solvent interactions relative to the solute-solute and solvent-solvent interactions that are not enough to energetically compensate for the interactions that are destroyed upon mixing.

The most striking result from this analysis, is that, in spite of the major differences in the chemical nature of the solvents here studied and of the interactions of their molecules in pure state, the non-ideality of the SO_2 and NH_3 in solution is remarkably low and essentially driven by entropic effects. Analogous to what was previously reported for CO_2,[89] these observations suggest that by increasing the size difference between the SO_2 or NH_3 and the IL solvent the solubility will increase as the entropic contribution to the solution non-ideality increases. This is in agreement with the results of Huang et al.[26] that have reported weak interactions or no chemical bonding at all between the solvent and the solute SO_2 molecule in the SO_2 – saturated ILs.

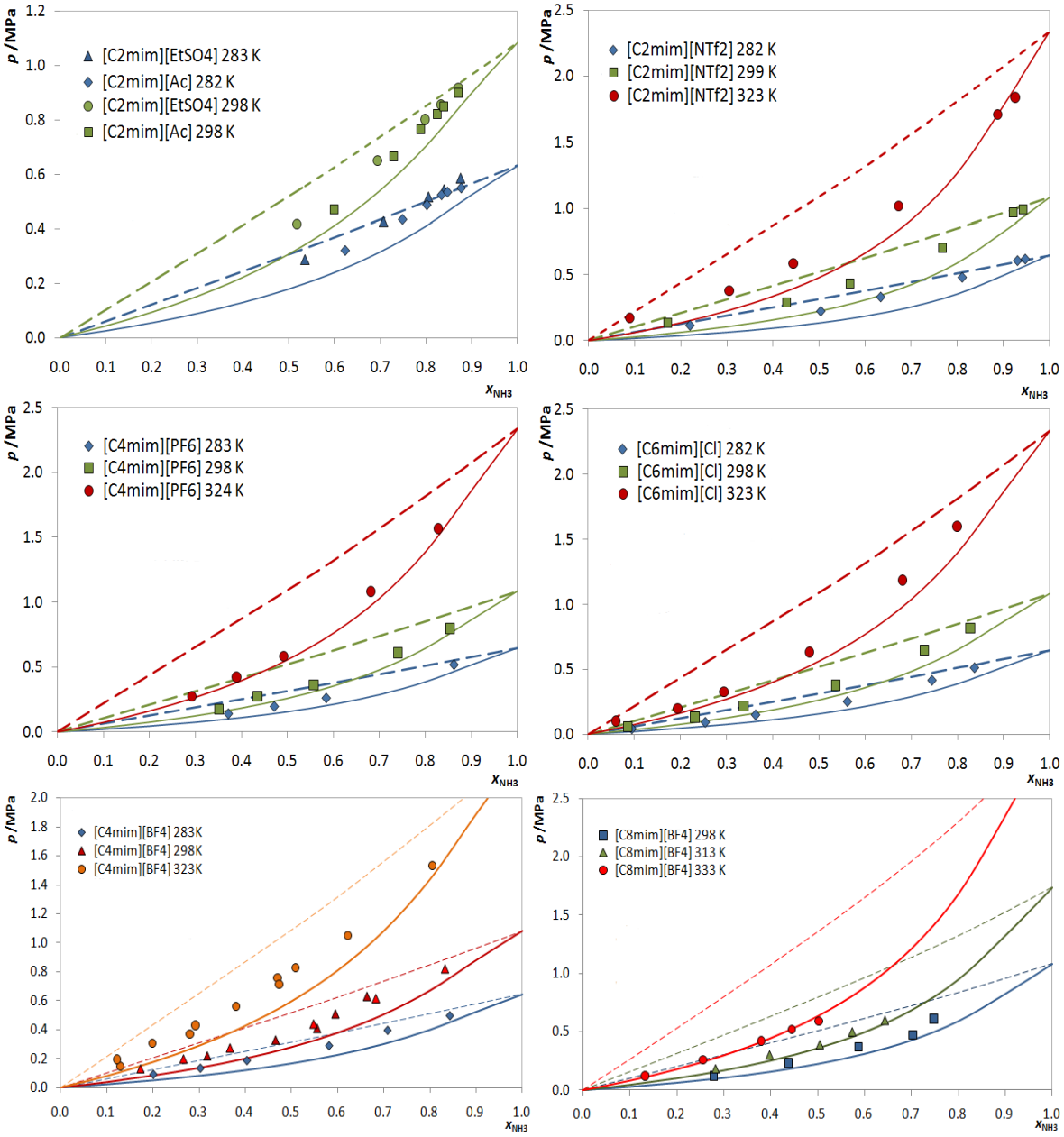

Figure 12.2. Pressure *vs* NH_3 molar composition diagram for the systems NH_3 + ionic liquid.[225, 226] The solid lines represent the Flory-Huggins model and the dashed represent the ideal behavior described by the Raoult's law.

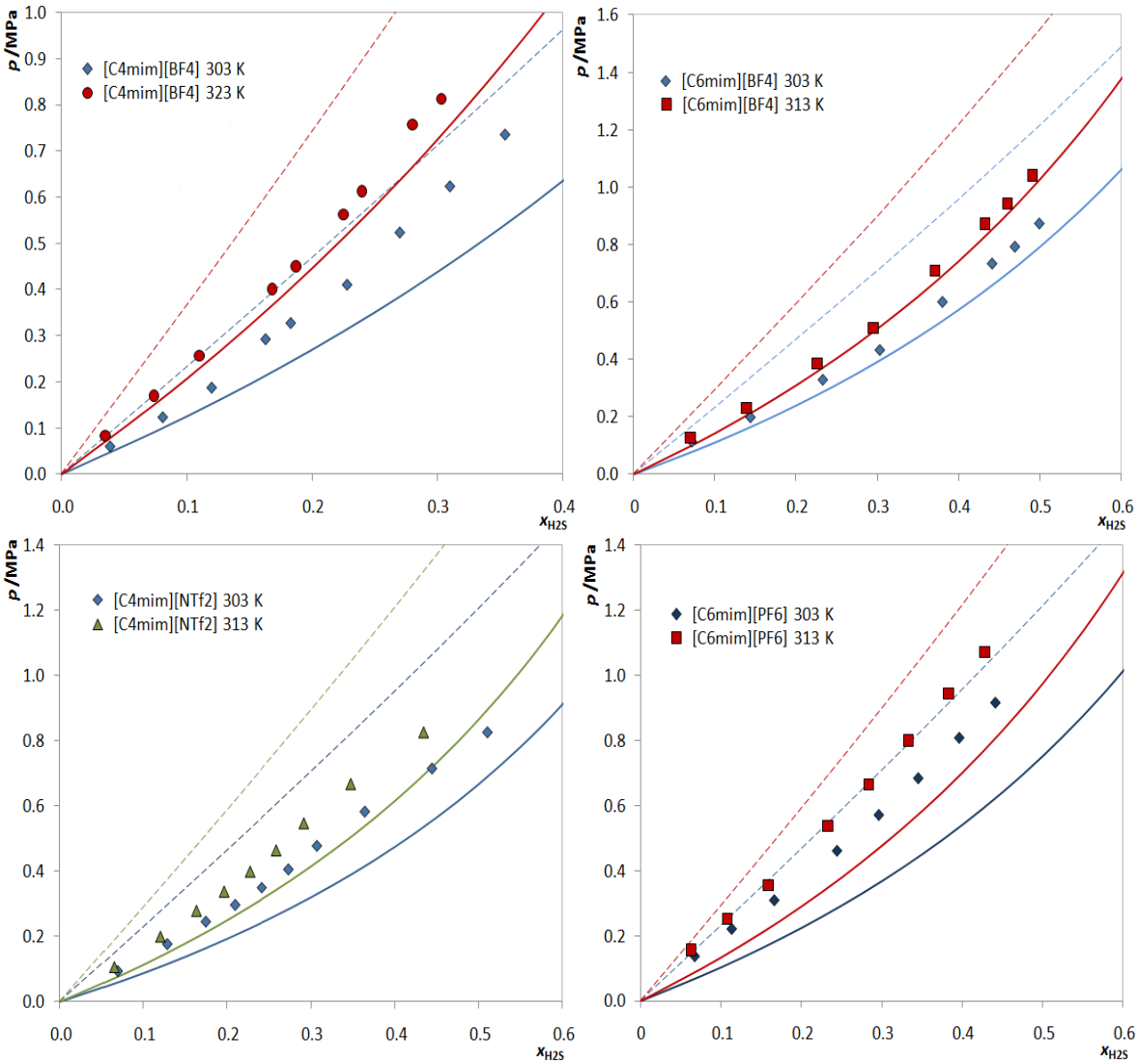

Figure 12.3. Pressure *vs* H_2S molar composition diagram for the systems H_2S + ionic liquid.[233, 234] The solid lines represent the Flory-Huggins model and the dashed represent the ideal behavior described by the Raoult's law.

12.4. The non ideality of H_2S solutions in ionic liquids

The approach described in the previous section was also applied at IL + H_2S systems. With the exception of some data of questionable quality that are not in agreement with results from other authors a fair agreement is observed between the experimental and the predicted Flory-Huggins equilibrium pressure with maximum average pressure deviations of 0.2 MPa as reported in Table H.2 (extended pressure deviations as function of

H_2S mole fractions and temperature are available in supporting information). For the H_2S systems the Flory-Huggins model is no longer able to produce a perfect description of the VLE and the experimental data reported in Figure 12.3 fall between the dashed line of an ideal solution and the full line predicted by the Flory-Huggins model. The only exception within the available data is the $[C_6mim][BF_4]$ system[234] where the model seems to provide a very good description of the system. The results shown in Figure 12.3 suggest that, albeit the solubility of H_2S in ionic liquids is still dominated by entropic factors, the residual contributions for the excess Gibbs energy are positive and more important than those observed for SO_2 and NH_3. It clearly shows that the interactions between the H_2S and the ionic liquids for which data is available are not favorable. An adequate model to describe these systems must take into account the residual contributions to the liquid phase non-ideality.

12.5. Conclusions

This study shows that the solubility of light compounds such as SO_2, NH_3 and H_2S in ionic liquids is driven exclusively or predominantly by entropic effects. For systems where the residual contributions are negligible, such as for NH_3 and SO_2 containing systems, a gamma-phi approach using the Flory-Huggins model to describe the liquid phase non-ideality can provide a very good prediction of the VLE phase diagrams. For acid gases such as H_2S the residual contribution to the excess Gibbs energy presents a non negligible positive contribution that reduces the quality of the predictions by this approach. It is shown that, in spite of its limitations for some systems, the Flory-Huggins model is a powerful tool to predict the solubility of light compounds in ionic liquids.

13. The Polarity Effect upon the Methane Solubility in Ionic Liquids: A Contribution for the Design of Ionic Liquids for Enhanced CO_2/CH_4 and H_2S/CH_4 Selectivities

"Discovery consists of seeing what everybody has seen and thinking what nobody has thought."

Albert Szent-Györgyi

13.1. Abstract

Aiming at designing ionic liquids for the purification of natural gas, the solubility of methane in ionic liquids is here investigated through the measurement of the solubilities of methane in four ionic liquids (ILs), in a wide range of molar fractions, temperature and pressures. With the exception of the phosphonium-based IL, which behaves as an almost ideal solution, the other ionic liquids show strong positive deviations to ideality, resulting from non-favorable interactions between CH_4 and the ILs. The results indicate that the non ideality of the solution increases, and the solubility decreases, with the polarity of the ionic liquid. The effect of the ionic liquid polarity on the CO_2/CH_4 and H_2S/CH_4 selectivities is here evaluated. The ionic liquids here studied present the largest CO_2/CH_4 and H_2S/CH_4 selectivities ever reported. The selectivity models previously proposed in the literature are tested against this new experimental data and shown to fail. Furthermore, it is shown that describing the ILs polarity using the Kamlet-Taft parameters, the CO_2/CH_4 and H_2S/CH_4 selectivities correlate well with the β parameter providing a key to the design of ionic liquids with enhanced selectivities.

13.2. Introduction

Due to energetic and environmental problems, natural gas has been standing out as a clean alternative energy source to coal and oil. Nonetheless, due to natural gas specifications, processing and transportation requirements, the removal of H_2S, CO_2, COS, organic sulfur compounds, mercury and water is required prior to liquefaction. Apart from some alternative processes, natural gas treatment is processed using solvent absorption that, despite being simple, cheap and reliable, presents several technological and environmental inconveniences and limitations.[235] Membrane separation, by other hand, represents the latest approach to methane purification. Polymeric membranes made of silicone rubber,[236] cellulose acetate,[237] polyimide[238, 239] and polyether block amide have been widely tested.[240] Despite, being effective for CO_2/CH_4 separation, the majority of them cannot be used for gas purification because they are damaged by aggressive gases.

Nonetheless, ionic-liquid based liquid membranes, with high fluxes and high selectivities, stand as a promising method for gas separation.[241, 242] "Condensing-liquid membrane"[241] reported enhanced gas separation by removing unwanted and toxic gases through a continuously refreshed surface with condensed water to avoid contamination of the permselective membrane.[241] Furthermore, ionic-liquid membrane gas separation seem controlled by the gas solubility on the ionic liquid rather than on its difusivity.[198, 199]

Ionic liquids, due to their outstanding properties, like negligible vapor pressures, high thermal stability, large liquidus range, nonflammability, and high solvation capacity stand out as a viable alternative to replace the solvents commonly used in natural gas treatment. The ILs' aptness for fine-tuning their properties cataloged them as "*designer solvents*", and this tunable capability, through an endless combination of cations and anions, allows the design of solvents for the development of more efficient and sustainable processes and products. A great deal of work have addressed the use of ionic liquids for CO_2 capture and gas separation purposes,[20, 21, 23, 30, 36, 48, 50, 89, 119, 198, 199, 217, 234-249] or sulfur containing gases[138, 211, 216, 217, 227, 233, 233, 248, 250, 251] but few authors have addressed CH_4 solubility in ionic liquids.[23, 48, 212, 233, 244, 247, 252] The understanding and description of the absorption of sour gases in ionic liquids is of importance for the design and operation of processes or the design of new and enhanced sorbents. However, for gas separation processes, more than just the solubility is the selectivity that dictates the choice of an absorbent. The endless combination of cations and anions limits the feasibility of the experimental characterization of all the ILs. Thus, the development of reliable correlations capable of estimate the solubility of methane and sour gases in the ILs stands as a vital key on the pursuit of alternative solvents.

Having in previous works established the mechanism of solvation and the limits to the physical sorption of the CO_2[89] and other sour gases such as H_2S and SO_2[253] in ionic liquids as being entropicaly driven, it is now clear that the most promising approach to enhance the sour gases/CH_4 selectivities at high pressures is by lowering the methane solubility in ionic liquids and not by increasing the sour gas solubility, that is essentially

dependent of the solvent molar volume.[89, 253]

Aiming at exploring the mechanism behind the absorption of methane by ionic liquids and identify ILs with large sour gases/CH_4 selectivities, the present work investigates the nonideality of CH_4 in ionic liquids through the measurement of solubilities at high pressure. It will here be shown that, unlike for sour gases, the methane solubility is controlled by the interactions between the methane and the ionic liquids, and that the Kamlet-Taft parameter, β, measuring the solvent hydrogen bonding acceptor character, correlates well with the ILs CO_2/CH_4 and H_2S/CH_4 selectivities and could thus be used to guide the choice of the best ionic liquid for natural gas purification.

13.3. Results and Discussion

13.3.1. Methane Solubility

The solubility of methane in the studied ILs, plotted in Figures 13.1 through 13.4 (detailed results are reported in Tables I.1 through I.4 in Appendix I), was measured for concentrations from (0.04 to 0.8), in the temperature range (293 to 363) K and pressures from (0.1 to 100) Mpa.

Initially the solubilities follow the common pattern of gas solubility in ionic liquids decreasing with temperature and increasing with pressure. However, contrary to the CO_2 + ILs systems for which the increase on temperature has a large impact on the solubility, for the CH_4 + ILs systems this influence is very small or, in some cases, even negligible. Another peculiar feature of these systems is that for all the studied systems, with the exception of the $[C_4mim][CH_3SO_3]$ + CH_4, a cross-over is observed above which the temperature dependency of the solubility is reversed and increases with temperature. This type of behavior was previously observed by us, for some high molecular weight ILs (phosphonium-based ILs) + CO_2[70, 119] and CH_4 + heavy alkanes systems.[69, 254]

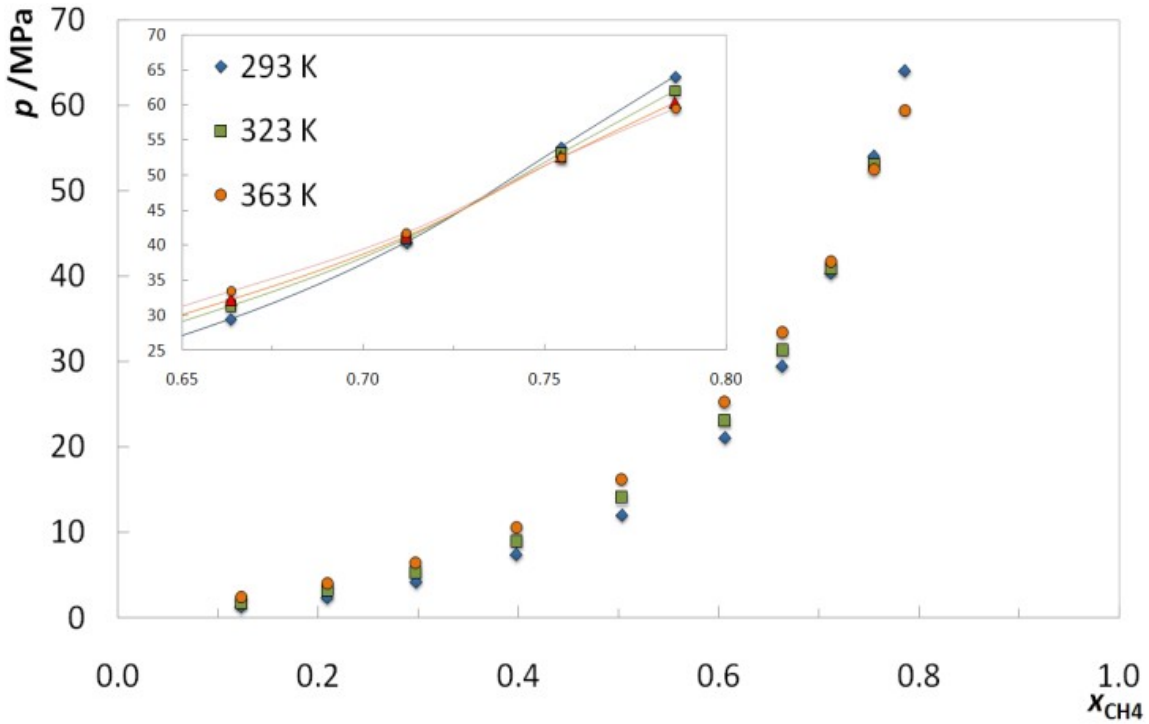

Figure 13.1. Pressure – composition diagram of the binary system [THTDP][NTf_2] + CH_4.

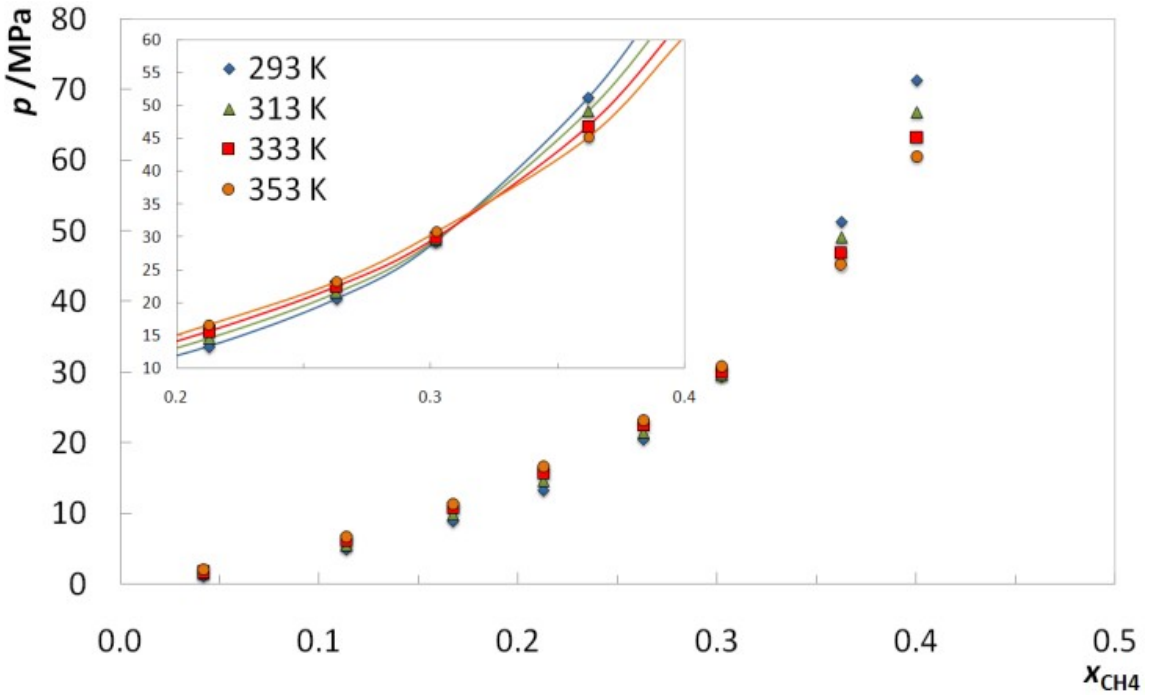

Figure 13.2. Pressure – composition diagram of the binary system [C_4mim][NTf_2] + CH_4.

Nonetheless, to the best of our knowledge, it is here reported for the first time, for ILs + CH_4 systems. Furthermore, while for the ILs + CO_2 system this behavior seems to be associated with a "liquid-liquid like" type behavior where the CO_2 and ionic liquid have similar densities and an inversion of the phase densities is observed,[72, 119] for ILs + CH_4 systems it seems to be more common and not related with the phases density. The change in temperature dependency of the solubility must thus be related with a change from positive to negative of the enthalpy of solution.

13.4. CO_2/CH_4 and H_2S/CH_4 selectivity

Following the approach used in previous works,[89, 255] the mechanism behind the solubility of CH_4 in ionic liquids, is here investigated by analyzing their deviations to ideality in the liquid phase. The system CH_4 + hexane, an athermic, quasi-ideal mixture, with negligible enthalpic interactions and reduced entropic contributions resulting from the differences in size and shape of the species, was adopted to describe the methane ideal behavior. As depicted in Figure 13.5, all the studied ionic liquids, with the exception of the [THTDP][NTf_2] that presents an almost ideal behavior (though with slightly negative deviations), present strong positive deviations to ideality that result from positive deviations in the residual (enthalpic) term, as shown by the deviations to the ideal behavior. These observations do not come as a surprise since the nonideality of a solution and its impact on the solubility of a given solute depends on a delicate balance between the solute-solute, solvent-solvent and solute-solvent interactions.

Thus, the phosphonium-based IL, due to its large cation alkyl chains, would be expected to present similar interactions with the CH_4 and consequently lead to a near ideal behavior, while the other studied ionic liquids would present strong unfavorable solute-solvent interactions. Moreover, the positive deviations to ideality seem related to the IL polarity. The higher the IL polarity the larger are the deviations to ideality.

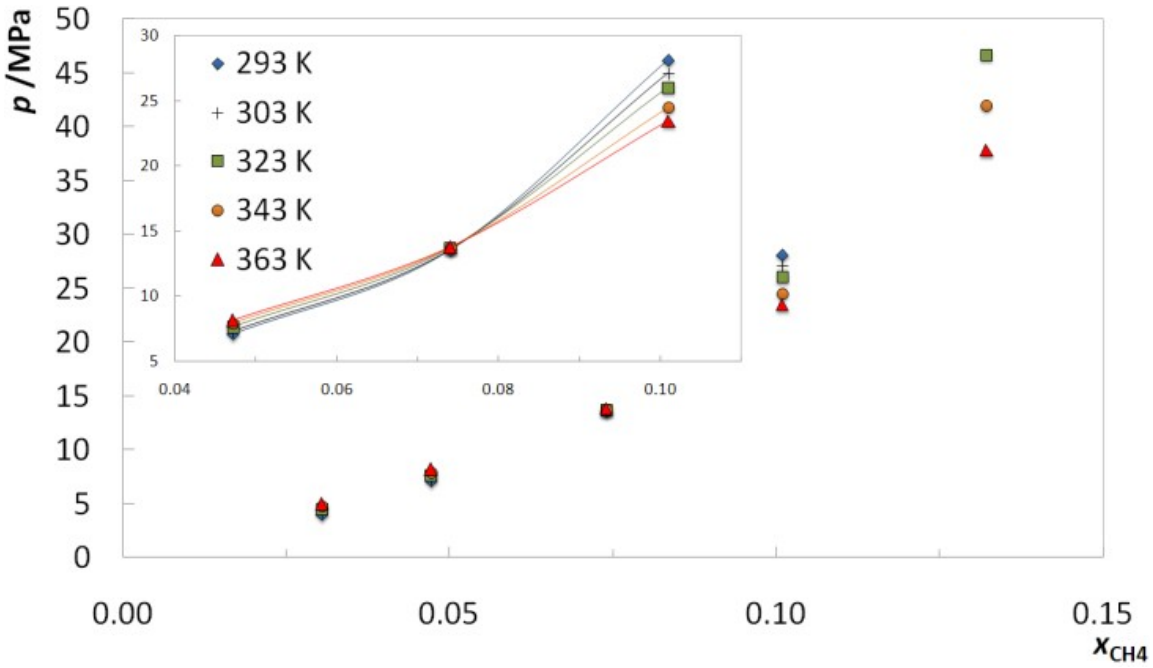

Figure 13.3. Pressure – composition diagram of the binary system [C_4mim][NTf_2] + CH_4.

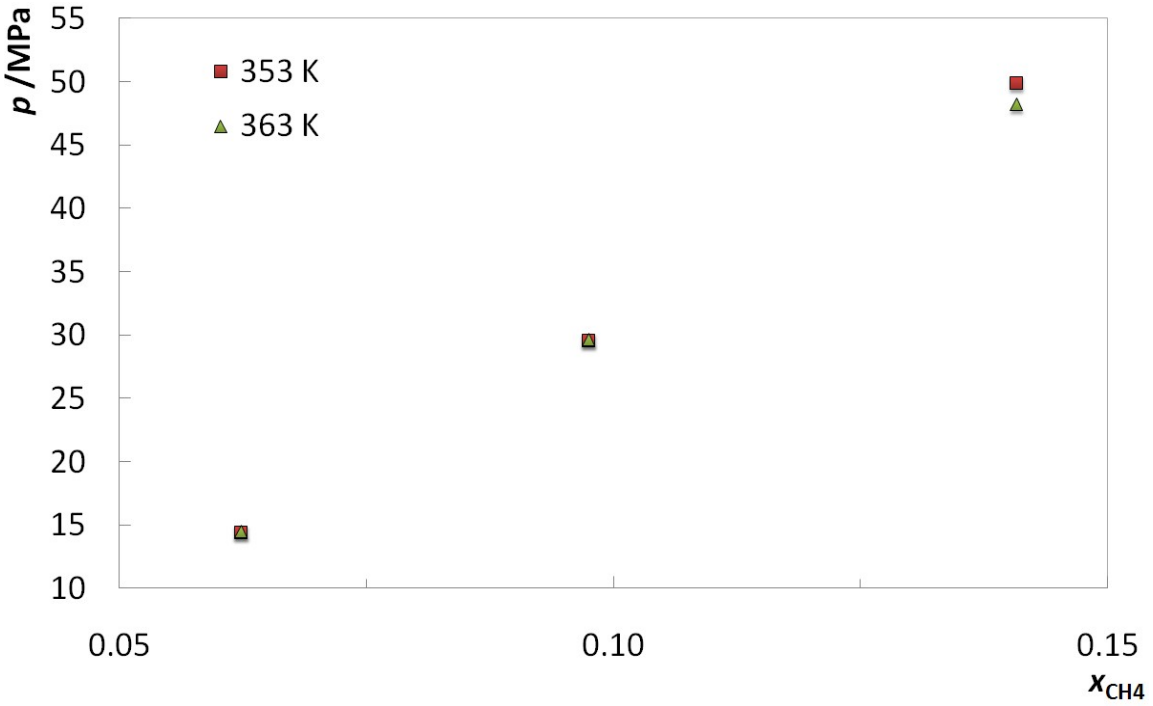

Figure 13.4. Pressure – composition diagram of the binary system [C_4mim][NTf_2] + CH_4.

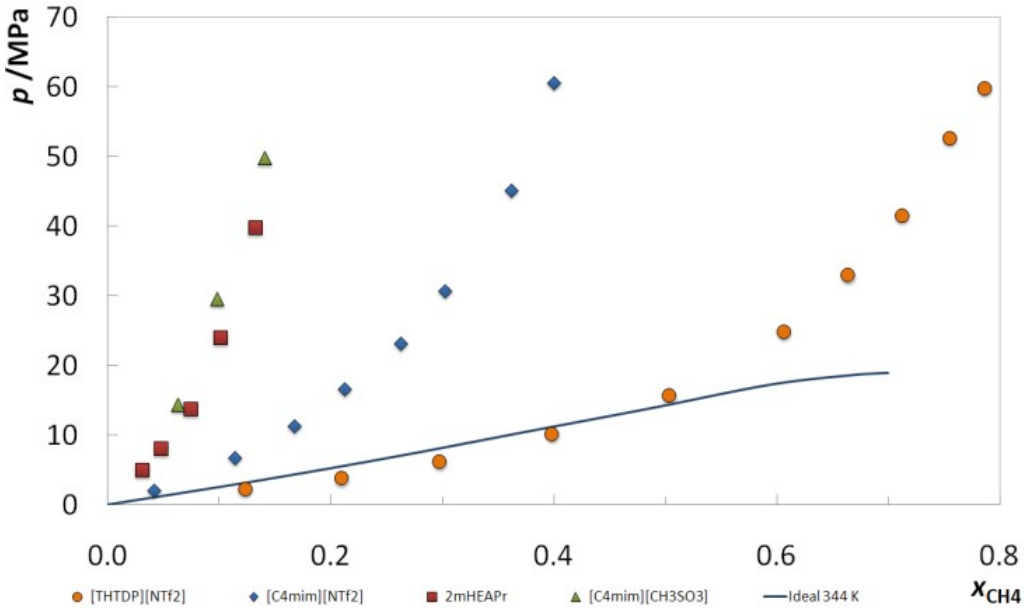

Figure 13.5. Pressure – composition diagram of the binary systems: [THTDP][NTf_2], [C_4mim][NTf_2], 2mHEAPr and [C_4mim][CH_3SO_3] + CH4 at 353 K and the ideal behavior at 344 K.

The selection of a solvent for an efficient CO_2/CH_4 separation must focus on the choice of a highly selective solvent. Since, as shown before,[89] the CO_2 solubility in ionic liquids is controlled by entropic effects and it is to a large extent independent of the ionic liquid, the maximization of the selectivity must address the minimization of the CH_4 solubility on the ionic liquid. According to the results here reported, being the CH_4 solubility controlled by the enthalpic interactions between the gas and the solvent, the ionic liquid that will maximize the non-ideality of the liquid phase will also minimize the gas solubility and thus maximize the selectivity as will be shown below.

To evaluate the CO_2/CH_4 selectivities the carbon dioxide solubilities in these ionic liquids were estimated using the correlation developed, by us, in a previous work.[89] To evaluate the CH_4/H_2S selectivities the hydrogen sulfide solubilities in these ionic liquids were estimated using the γ- ϕ approach based on the Flory-Huggins model described in a recent work.[253] It is shown in Figure 6 that the studied ionic liquids present a wide range of CO_2/CH_4 and H_2S/CH_4 selectivities, following the order: [THTDP][NTf_2] < [C_4mim][NTf_2] < [2mHEAPr] < [C_4mim][CH_3SO_3].

Here the low CH_4 solubilities (and high selectivities) do not seem to be directly related to the solvents molecular weight, as in the case of the carbon dioxide,[89] but instead to the higher or lower polarity of the ionic liquid. To evaluate this relationship the ionic liquids polarity scale adopted was the multidimensional Kamlet-Taft based on three parameters: β, the hydrogen bond accepting ability; α, the hydrogen bond donating ability; and π^*, a measure of non-specific interactions (polarizability, dipole-dipole interactions, and dipole-induce dipole interactions). The α and β parameters are compared with the selectivities on Figure 6. The Kamlet-Taft parameters were obtained from literature.[140, 256-258] Since no data was available for the 2mHEAPr, the Kamlet-Taft parameters for the 2-Hydroxy Ethylammonium Formate were used assuming that they are a good approximation to the protic IL parameters.[258] It can be observed that the ILs CH_4/CO_2 and H_2S/CH_4 selectivities present a similar trend to the Kamlet-Taft β parameter indicating that, as expected from the non-ideality analysis carried above, the solubility of methane in the ILs is related to the ionic liquids polarity, in particular to their hydrogen bond accepting ability. A similar observation has been recently reported for acetylene + ionic liquids systems by Palgunadi et al.[259]. Unfortunately both methane and hydrogen sulfide solubility data and Kamlet-Taft parameters are still scarce and more data is required for a more comprehensive analysis to be carried and a correlation proposed.

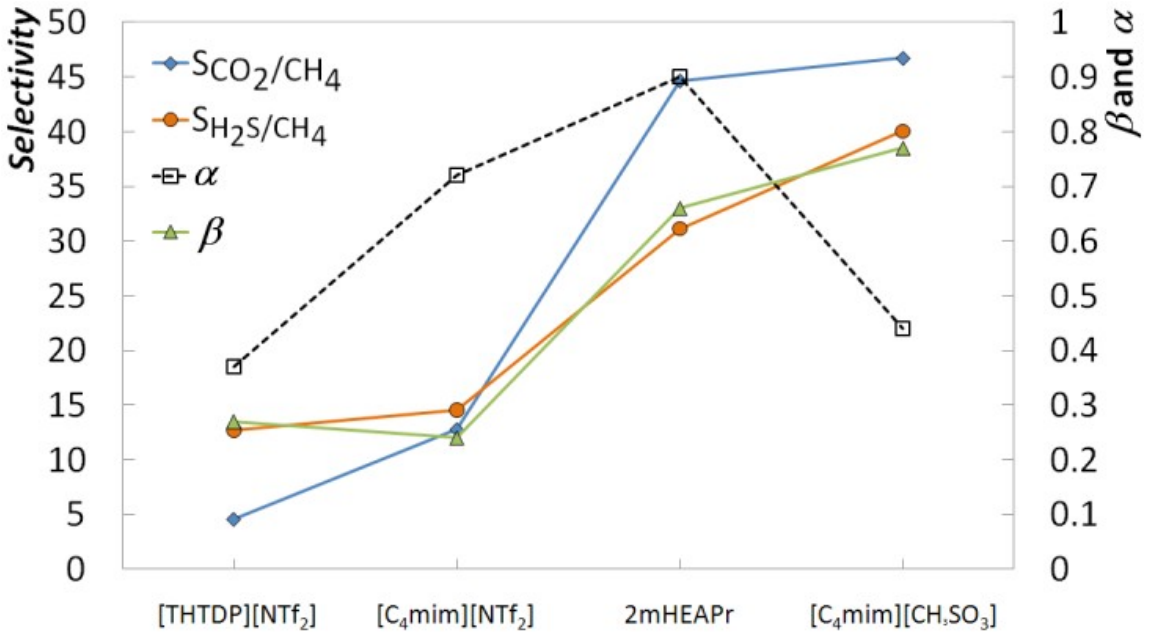

Figure 13.6. Selectivities, Kamlet-Taft α and β parameters for the studied ILs at 353 K.[51-54]

13.5. Ionic Liquids CO_2/CH_4 Selectivity Models

Several authors[260-263] have proposed correlations for gas solubilities in ionic liquids. Camper at al.[260] developed a model for alkyl methyl imidazoliun-based- ionic liquids based on the assumption that single-gas solubility in ILs was primarily a function of molar volume of the IL. Furthermore, Camper's Model stated that the smaller the IL's molar volume the better the selectivity and as the IL molar volume increases the amount of gas absorved per volume of fluid initially increases and then starts to decrease. Kilaru et al. [262, 263] developed a couple of two parameter models, similar to those of Camper's, where the viscosity and surface tension of the IL have an important role on the solubilities. Later, Scovazzo et al.[261], from a multivariable linear regression of a wider set of experimental data, developed a model (so called "Universal Model"), covering an extended set of ILs families, in which the dependence of viscosity on the permeability/selectivity has a minimal influence on the solubility. All the authors, nonetheless, agree that the CO_2-anion interaction is not the dominant factor that determines the relative CO_2 solubility between ILs. This corroborates a recently work[89] where we have developed a model, valid for pressures up to 5 MPa, for temperatures ranging from room temperature up to 363 K and

molalities up to 3 mol.kg^{-1}, showing that when the molecular weight effect is removed from the analysis by comparing the solubilities in molalities, instead of molar fractions, the CO_2 solubilities in various systems (ILs, alkanes, methyl esters, fatty acids, PEGs, etc.) are identical and the solubility of CO_2 on nonvolatile solvents is essentially solvent independent.

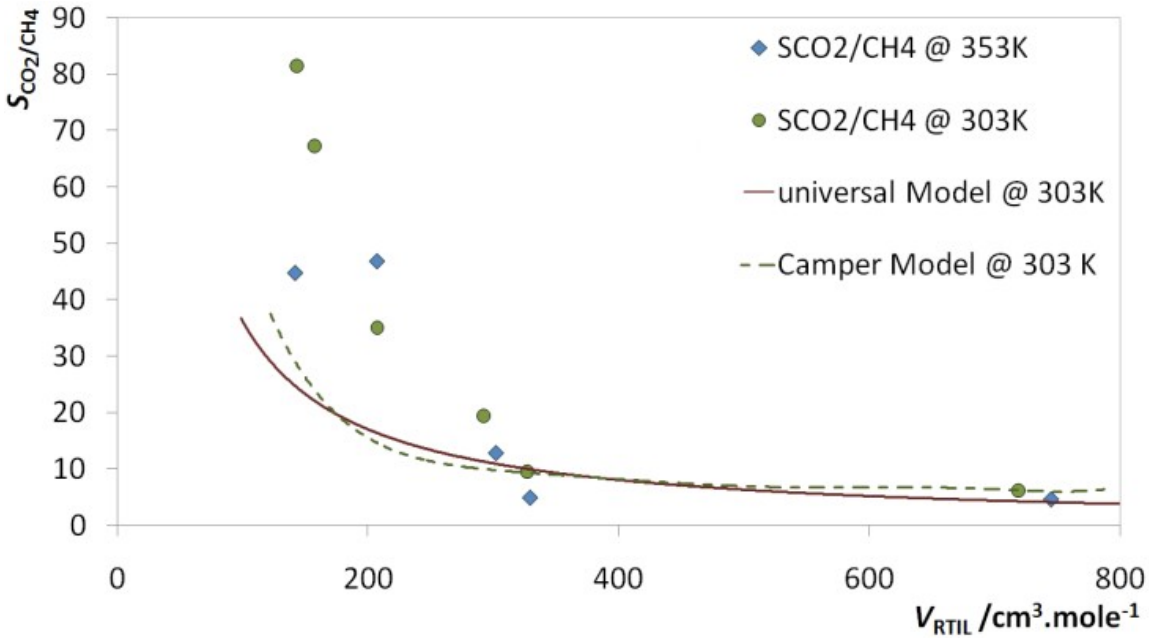

Figure 13.7. Experimental and fitted (Universal57 and Camper's Model56) CO_2/CH_4 selectivity vs ILs molar volume at 303 and 353 K, Table S5.

With the exception of Scovazzo's work[261] none of the other authors extended these models to CH_4 solubilities and selectivities in ionic liquids. Scovazzo's work[261], despite presenting several ILs families like imidazolium, ammonium and phosphonium, focus essentially on ionic liquids based on the bis(trifluoromethylsulfonyl)imide anion. Therefore, given the similar polarities of the ionic liquids, one would expect similar deviations to ideality, and consequently a well-behaved selectivity *vs* IL. In fact, for the set of ionic liquids studied Scovazzo proposed an "*Universal correlation*"[261] that provides a good fit to the experimental data used. However, when new ionic liquids, with different polarities than those used on the model regression, are compared against it, the correlation fails to describe their selectivities, as shown in Figure 13.7. These results show that the

Scovazzo correlation is limited by the nature of the ionic liquids used on its derivation and that a single parameter such as the IL molar volume is not able to describe the CH_4/CO_2 selectivities, as would be expected form their dependency on the CH_4/ionic liquid interactions.

Although we demonstrate in this work that the ionic liquid polarity is an essential feature in the design of ionic liquids with large CH_4/CO_2 selectivities, the limited amount of data available precludes the development of a reliable correlation for CH_4 solubilities of selectivities at present. The development of reliable correlations capable of estimate the solubilities/selectivities of methane in ILs, needs to take into account the high diversity of molecular interactions inherent to the ionic liquids, and they are a vital key for the design of alternative solvents for more sustainable and efficient processes.

13.6. Conclusions

Gas solubilities of methane in four ionic liquids, namely trihexyltetradecylphosphonium bis(trifluoromethylsulfonyl)imide, 1-butyl-3-methylimidazolium bis(trifluoromethylsulfonyl)imide, 1-butyl-3-methylimidazolium methanesulphonate and 2-methyhydroxyethylammonium propinate was presented for molar compositions of 0.04 to 0.8, in the temperature range (293 to 363) K and pressures up to 100 MPa.

With the exception of the [THTDP][NTf_2] that presents slightly negative deviations to ideality, showing that methane solubility on this ionic liquids is dominated by entropic factors, all the remaining ionic liquids present large positive deviations to ideality denoting the strong unfavorable interactions between CH_4 and the ILs.

Adopting the description of the compound's polarity as a multidimensional variable defined by the Kamlet-Taft parameters we have shown that the models available in literature are only able to describe a narrow set of ionic liquids, with similar polarities, but fail to describe the selectivities/solubilities of ionic liquids that fall out of this polarity range.

Furthermore, for the studied systems the Kamlet-Taft β parameter provides a good correlation for the ILs CO_2/CH_4 and H_2S/CH_4 selectivities, indicating that the higher or lower solubility of methane in the ILs is related to the ionic liquids polarity, and not only with the solvent molecular weight as observed for the carbon dioxide or the molar volume as proposed by some authors. The Kamlet-Taft β parameter can thus be used as the basis for the choice of ionic liquids that maximize the selectivities of sour gases/CH_4.

14. THERMOPHIL – An Application for Ionic Liquids Property Estimation

“Whenever anyone says, 'theoretically,' they really mean, 'not really'.”

Dave Parnas

14.1. Introduction

Despite the exponential increase on the interest for ILs, both by academia and industry, the availability of thermophysical properties data is still limited and often of questionable quality, making difficult the development of correlations, predictive models for these properties and the design of ionic liquids for new products and process applications. To overcome this limitation our group has proposed a number of predictive models for the thermophysical properties of ionic liquids.[264-268] These correlations were developed based on a critical analysis of available experimental data along with new data measured at our laboratory.[89, 264-268]

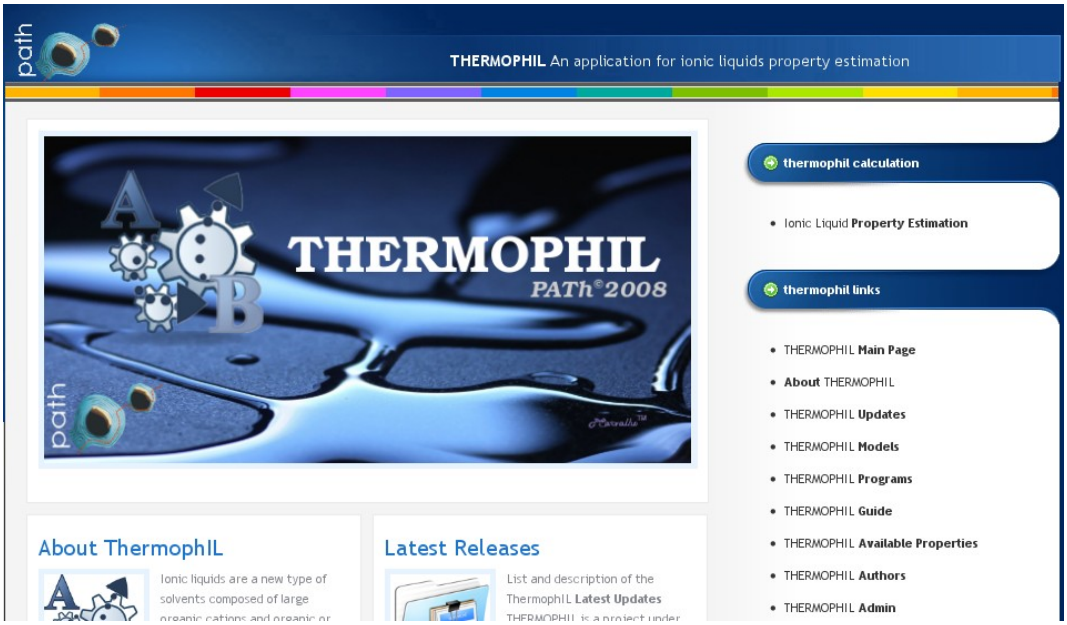

Figure 14.1. ThermophIL main graphical user interface @ http://www.delphil.net/prediction/.

To make the estimation of the thermophysical properties of ionic liquids (density, isobaric expansivity and isothermal compressibility, viscosity, surface tension, speed of sound, ionic conductivity, heat capacity and water solubility, developed by our group, and for the carbon dioxide solubility developed on this thesis) easily available for everybody, an on-line computer application "*THERMOPHIL – An Application for Ionic Liquids Property Estimation*" was developed and made available; first through the PATh web

page http://path.web.ua.pt/thermophil/ and lately through a collaboration with Novionic® and the delph-IL[3] project, on the web link http://www.delphil.net/prediction/.

14.2. ThermophIL Models

Given the huge number of potential ionic liquids, the experimental measurement of the thermophysical and transport properties for all ionic liquids of interest is infeasible. The alternative lies on developing predictive models, based on some experimental data, from which the required properties with the desired accuracy can be obtained. The development of group contribution methods for the properties of ionic liquids is particularly apt for this purpose as (i) from a restricted amount of data, it will be possible to expand the information available to a large number of compounds, and (ii) it will also allow for a critical evaluation of the accuracy of available data. Thus, for each property studied, available data for each individual ionic liquid were fitted to the appropriate predictive equations to obtain parameters.

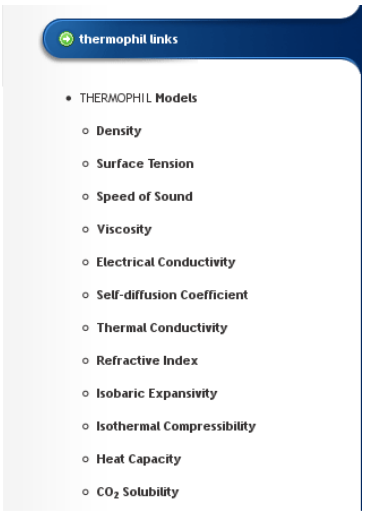

Figure 14.2. ThermophIL – Properties list.

3 delph-IL is a part of Novionic Consulting which provides a full range of consulting services, flexible, adaptive, and responsive to the needs of its clients. It is our aim to provide users worldwide with up-to-date information on publications of experimental investigation on ionic liquids, including numerical values of chemical and physical properties, measurement methods, sample purity, as well as many other significant measurement details.

Then, by comparison of the parameter values of ionic liquids containing similar cations and anions, it was possible to make an initial estimation for the values of parameters for each cation and anion. Then the cation was split into the parent cation (heterocyclic ring, or alkylammonium, or alkylphosphonium), methylene and methyl group. Using these initial estimates, the objective function (square of the difference of experimental and predicted property data) was minimized for all the data points available, to obtain optimum values of the group parameter.

A brief description of the models developed by our group and attainable on the "*THERMOPHIL – An Application for Ionic Liquids Property Estimation tool*" are given on the coming sub-sections:

14.2.1. Density

An extension to Ye and Shreeve model[269] was developed, and calculations for a wide range of temperatures from (273.15 to 393.15) K and pressures from (0.1 to 100) MPa were achieved. The new density correlation was tested against experimental densities available in literature for ionic liquids based on imidazolium, pyridinium, pyrrolidinium and phosphonium-based cations ILs demonstrating a good agreement. For imidazolium-based ILs, the mean percent deviations (MPD) is 0.45% and 1.49% for the phosphonium-based ILs. A low MPD ranging from 0.41% to 1.57% was observed for pyridinium and pyrrolidinium-based ILs.

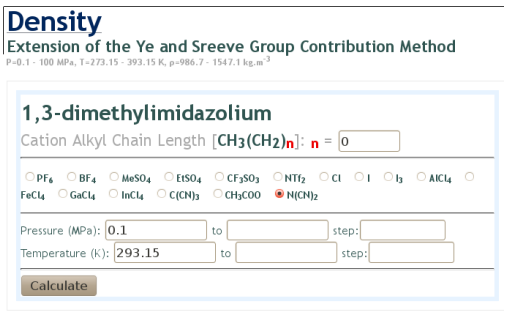

Figure 14.3. ThermophIL – Density method: parameters selection.

14.2.2. Surface Tension

Using estimated densities and Parachors, the prediction of surface tension for imidazolium-based ionic liquids can be accomplished. The parachors were calculated from Knotts et al.[270] parachor QSPR (Quantitative Structure-Property Relationship) correlation using the parameter table, estimated from the second training set, containing experimental surface tension values with an uncertainty lower than 1%. A global number of 361 data points for 38 imidazolium-based ILs were used in the study. For the studied ILs the MPD was 5.75% with a maximum deviation inferior to 16%, which are much lower than the value reported by Knotts et al.[270] for multifunctional compounds in their study.

14.2.3. Heat Capacity

The approach proposed by Ruzicka and Domalski[271, 272] using a second-order group additivity method was adopted. Despite scarce and limited to a few classes of well-studied ILs, based on imidazolium cations with $[PF_6]^-$, $[BF_4]^-$, Br^-, $[EtSO_4]^-$ or $[CF_3SO_3]^-$ as anions, and pyridinium and pyrrolidinium cations with $[Ntf_2]^-$, covers a wide range of temperature (196 – 663) K and liquid heat capacity (264 – 825) $J.mol^{-1}.K^{-1}$. For circa 2396 data points of 19 ILs studied, a MPD of 0.36% with a maximum deviation smaller than 2.5% was observed.

14.2.4. Viscosity

Based on experimental viscosity data collected from literature and using density data obtained by the above mentioned predictive method, a group contribution method, using a Vogel-Tammann-Fulcher equation, was proposed to estimate viscosities of imidazolium-, pyridinium- and pyrrolidinium-based ILs, covering wide ranges of temperature (293 – 393) K and viscosity (4 – 21000) cP. For circa 500 data points of 29 ILs studied, a MPD of 7.5% with a maximum deviation smaller than 23% was observed.

14.2.5. Electrical Conductivity

A database of experimental electrical conductivity available from the open literature

was collected. A global number of 300 data points for 15 ionic liquids based on imidazolium, pyridinium, pyrrolidinium, and tetraalkylammonium cations with $[PF_6]^-$, $[BF_4]^-$, $[NTf_2]^-$, $[EtSO_4]^-$, $[CF_3SO_3]^-$, $[NPf_2]^-$, or $[CF_3COO]^-$ as anions, covering wide ranges of temperature, (258.15 – 433.15) K and electrical conductivity (0.01 – 12.68) $S.m^{-1}$, were used in this study.

A Vogel-Tammann-Fulcher type equation, similar to that used for viscosity, was used to correlate the electrical conductivity of ionic liquids. About 300 experimental electrical conductivity data points for 15 ionic liquids available were then used to estimate the values of the group contribution parameters.

The calculated electrical conductivity for imidazolium-, pyridinium-, pyrrolidinium-, and ammonium-based ionic liquids having $[PF_6]^-$, $[BF_4]^-$, $[NTf_2]^-$, $[EtSO_4]^-$, $[CF_3SO_3]^-$, $[NPf_2]^-$, or $[CF_3COO]^-$ as anions, are in good agreement with the corresponding experimental electrical conductivity. For 307 data points for 15 ionic liquids available in literature, the overall MPD is 4.57% with a maximum deviation of the order of 16%.

14.2.6. Self-diffusion Coefficient

The self-diffusion coefficient is related to viscosity in terms of the fractional form of the Stokes-Einstein relation[273], according to which the self-diffusion coefficient is proportional to the ratio of temperature and viscosity.

Experimental self-diffusion coefficient data of ionic liquids available in the literature were collected to evaluate the relation between the self-diffusion coefficients and the viscosities. For this purpose, the viscosity was calculated using the above mentioned group contribution method. For 45 data points for five ionic liquids based on the imidazolium cation with $[BF_4]^-$ or $[NTf_2]^-$ as anion, covering wide ranges of temperature, (263.15 – 353.15) K and self-diffusion coefficient, $(2.43\times10^{-12} – 3.71\times10^{-10})$ $m^2.s^{-1}$, a very good linear correlation is observed.

It would be interesting to correlate the ionic diffusivity with conductivity through the Nernst-Einstein equation[273], but the limited amount of experimental data available

restricts such a development at this point. We are confident that such correlation for ionic liquids will be possible when an adequate amount of experimental data become available.

14.2.7. Thermal Conductivity

The knowledge of thermal conductivity is important to obtain the heat transfer coefficient of fluids, which is essential for the design of heat transfer fluid and equipments. Among the different transport properties, thermal conductivity is one of the most difficult to estimate using predictive methods.

The data base of experimental thermal conductivity available in the literature contains 107 data points for 16 ionic liquids based on imidazolium, pyrrolidinium, and phosphonium cations with $[PF_6]^-$, $[BF_4]^-$, $[NTf_2]^-$, $[EtSO_4]^-$, $[CF_3SO_3]^-$, or Cl^- as anions, covering a wide range of temperatures, (293 – 390) K, and thermal conductivities, (0.124 – 0.199) $W.m^{-1}.K^{-1}$.

The experimental thermal conductivities suggest that they are weakly dependent on temperature, and could be fitted with a linear correlation. The calculated thermal conductivity, using the group contribution parameters, for imidazolium-, pyrrolidinium-, and phosphonium-based ionic liquids, having $[PF_6]^-$, $[BF_4]^-$, $[NTf_2]^-$, $[EtSO_4]^-$, $[CF_3SO_3]^-$, or Cl^- as anions, are in very good agreement with the corresponding experimental thermal conductivity. For 107 data points for 16 ionic liquids available in literature, the overall MPD is 1.06% with a maximum deviation of 3.5%. The thermal conductivity of the ionic liquids is similar to that observed for organic molecular liquids and much lower than that for pure water. Small amounts of impurities, such as water and chloride, in the ionic liquid sample do not seem to have a significant effect on the thermal conductivity; however, the thermal conductivity seems to increase with the amount of impurities.[274] For ionic liquids having an imidazolium-based cation, the thermal conductivity increases with the anion following the trend: $[NTf_2]^- < [CF_3SO_3]^- \leq [PF_6]^- < [EtSO_4]^- < [BF_4]^-$. The thermal conductivity also increases somewhat with the increase of alkyl chain length on the imidazolium cation.

14.2.8. Refractive Index

Refractive index is a fundamental physical property and it is used to test a material, confirm its purity, or for analytical purposes such as the assessment of the concentration of a mixture. It is also related to other properties such as dielectric constant, density, and surface tension through thermodynamic equations.

Experimental refractive index data available in the open literature, with 245 data points for 24 imidazolium-based ionic liquids having $[PF_6]^-$, $[BF_4]^-$, $[NTf_2]^-$, $[MeSO_4]^-$, $[EtSO_4]^-$, $[CF_3SO_3]^-$, or Cl^- as anions, covering a wide range of temperature, (283.15 – 363.15) K, were used.

For the studied ionic liquids, in the temperature range available, it was observed that the experimental refractive index could be fitted using a linear temperature dependent correlation.

The calculated refractive indexes were in excellent agreement with the corresponding experimental refractive index. For 245 data points of 24 ionic liquids available in the literature, the overall MPD is 0.18% with a maximum deviation of the order of 0.6%. The results indicate that the refractive index of the studied ionic liquids is weakly dependent on temperature and slightly decreases with temperature. For ionic liquids having imidazolium-based cations, the refractive index increases with the anion following the trend: $[PF_6]^- < [BF_4]^- < [NTf_2]^- < [CF_3SO_3]^- < [MeSO_4]^- < [EtSO_4]^- < Cl^-$; and it increases slightly with the increase of alkyl chain length on the imidazolium cation. The low deviations observed in calculated refractive indexes for a wide range of imidazolium-based ionic liquids shows that the group contribution method here developed can predict refractive index of new ionic liquids over wide ranges of temperatures and, as data for new groups of cations and anions become available, can be easily extended to a larger range of ionic liquids.

14.2.9. Isobaric Expansivity

Isobaric expansivity data of ionic liquids are required for their development as heat

transfer fluids or for heat storage applications or, as recently suggested, for ionic liquid based liquid-in-glass thermometers.[275]

A total of 109 data points for experimental isobaric expansivity of 49 ionic liquids (based on imidazolium, pyridinium, pyrrolidinium, piperidinium, phosphonium, and ammonium cations with 19 different anions, at 298.15 K and 0.1 MPa) were collected from the literature or calculated using experimental density data, through the developed group contribution method. In spite of the wide range of ionic liquids investigated, the isobaric expansivities observed fall in a narrow range of values: 4.48×10^{-4} to 7.44×10^{-4} K^{-1} at 298.15 K. As discussed elsewhere,[267] the precision to which this property is currently known precludes any study of its temperature dependency, as this is inferior to the experimental uncertainty. For this reason the isobaric expansivity was correlated at 298.15 K and atmospheric pressure by a group contribution approach.

For the studied ionic liquids, the calculated isobaric expansivity values are in good agreement with the corresponding experimental isobaric expansivity data. For 109 data points of 49 ionic liquids available in literature, the overall MPD is 1.98%, with a maximum deviation of the order of 7%. It was noticed that the isobaric expansivity of the studied ionic liquids is weakly dependent on the anion and increases slightly with the alkyl chain length of the cation.[268]

14.2.10. Isothermal Compressibility

Isothermal compressibility of ionic liquids is relevant for the design of industrial fluids to be used in pumps or compressors.[276]

A total of 26 data points for experimental isothermal compressibility directly available in the literature, or calculated using experimental density data for 22 ionic liquids based on imidazolium, pyridinium, pyrrolidinium, piperidinium, and phosphonium cations with different anions, at 298.15 K and 0.1 MPa, were collected. As discussed elsewhere,[78, 267] the precision to which this property is known precludes any study of its temperature or pressure dependency, as this is inferior to the experimental uncertainty. For this reason, the

isothermal compressibility was correlated at 298.15 K and atmospheric pressure by a group contribution approach in the studied range 0.33 to 0.73 GPa^{-1} of experimental isothermal compressibility data.

For the studied ionic liquids, the isothermal compressibility are in good agreement with the corresponding experimental isothermal compressibility data. For 26 data points of 22 ionic liquids available in literature, the overall MPD is 2.53% with a maximum deviation of the order of 6.7%, and from these about 46.2% of the estimated isothermal compressibility data having less than 1% relative deviation.

However, with the limited amount of experimental data, it is not possible to provide any definitive conclusion on the effect of cation, anion and alkyl chain length on isothermal compressibility of ionic liquids.

14.2.11. Speed of Sound

Experimental data for speed of sound of ILs is scarce and limited to imidazolium-based ILs. The speed of sound in $m.s^{-1}$ units can be estimated using the surface tension in $N.m^{-1}$ units and density in $kg.m^{-3}$ units, through the theoretical Auerbach's relation.[277]

To examine the functional dependence of the speed of sound and the relation of surface tension/density, a double logarithmic plot was drawn using speed of sound data from literature, density and surface tension obtained through the developed group contribution methods.

A correlation for the speed of sound was developed following the approach of Oswal et al.[278, 279]. The experimental speed of sound of imidazolium based ILs obtained displays a good agreement with corresponding calculated speed of sound. For the 133 data points of 14 imidazolium based ILs, the overall MPD is 1.96 % with maximum deviation inferior to 5 %.

14.2.12. CO_2 Solubility

The CO_2 solubility in solvents of low or non volatility was correlated following a

similar approach to that suggested by the IUPAC for CO_2 solubilities in ILs. The gas solubility in a liquid, fully described on section 9. "*On the Nonideality of CO2 Solutions in Ionic Liquids and Other Low Volatile Solvents*", uses the extended Henry's law with the temperature dependency of the Henry's constant described by the Benson and Krause equation[182]. A general correlation (Equation 9.9) for the solubility of CO_2 in non volatile solvents, including ILs, expressed in molality, as function of pressure and temperature, was proposed for pressures up to 5 MPa, temperatures ranging from room temperature up to 363 K and molalities up to 3 $mol.kg^{-1}$.

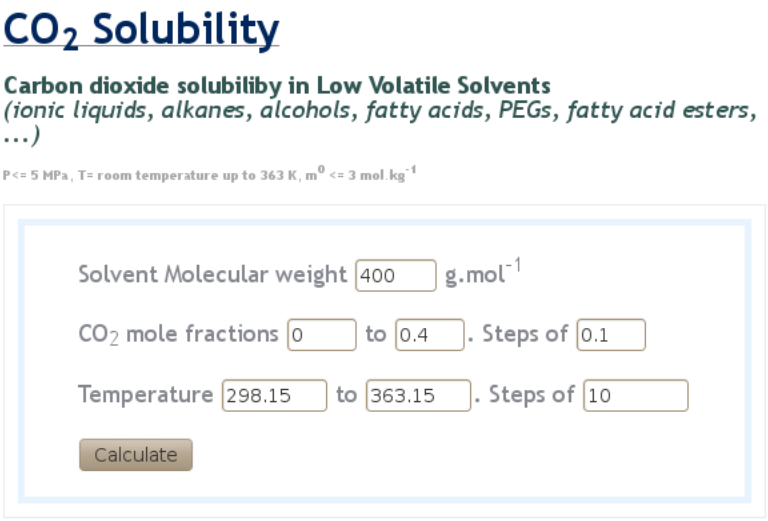

Figure 14.4. ThermophIL – CO_2 Solubility method: parameters selection.

14.3. ThermophIL Graphical User Interface

ThermophIL graphical user interface (GUI) was designed to give users simple and linear control. A level of design sophistication provides for the needs of all the potential users, adapting web technology to their expectations and never requiring readers to conform to an interface that places unnecessary obstacles in their paths.

Users are always able to return easily to ThermophIL home page and to other major navigation points in the website by links presented in consistent locations on every page. Graphic buttons provide basic navigation links and create a graphic identity that tells users

where they are within the site domain.

ThermophIL graphic headers act as navigation aids and are consistently applied across every page. ThermophIL home page provides the user with an interactive menu (right) where background information, features and guided help is available. By initializing the Ionic Liquid Property Estimation the user is able to select the cation family for the desired property estimation. Having selected the cation, among those available for the desired property, the cation alkyl chain length (when applicable), the anion, pressure and

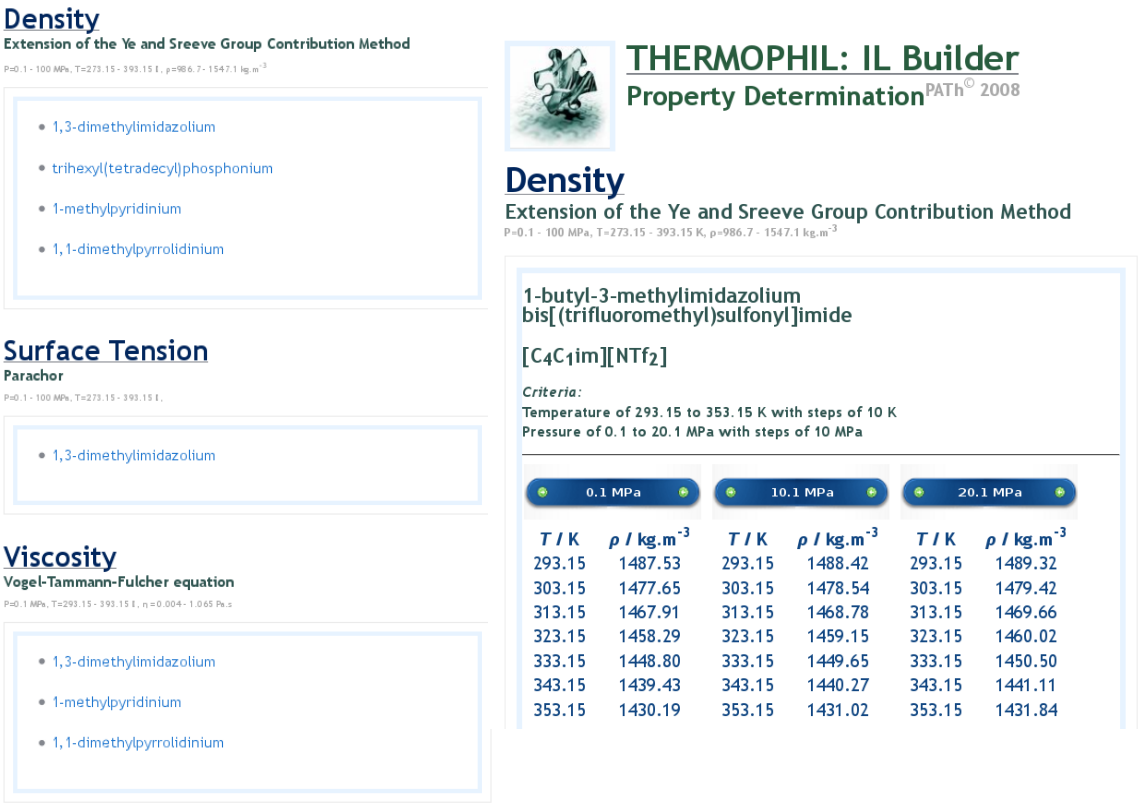

Figure 14.5. ThermophIL – Methods list, cation selection and results screen.

temperature range and step increase are configurable for calculation. The ThermophIL GUI provides a graphical identity reporting the method limitations, cation, anion and substituents selected, as well the calculation criteria on every step of the property calculation. The results GUI provides the calculations through tables, ordered by pressure, with temperature and property results listed.

Furthermore, the option to plot the results is available at the end of the page. The

graphic presents the series, ordered by pressure, for the property results as function of temperature.

14.4. ThermophIL – A Work in Progress

According to Aldrich® Advancing Science "*the combination of a broad variety of cations and anions leads to a theoretically possible number of 10^{18} ionic liquids, although, a realistic number will be magnitudes lower*". Furthermore, since the development of the above mentioned predictive models and its data compilation, a great number of new experimental data has been published. In fact, at the time of closing this thesis ILThermo® - Ionic Liquids Database[4] reports thermodynamic and transport properties for a reduced number (339) of ionic liquids, being among those properties 26, 48 and 36 for pure, binary and ternary ionic liquid systems, respectively. Thus, the revision of the models against more actual experimental data and broader ionic liquids families and cations/anions combinations stand as a major key step on the continuous development of ThermophIL. Moreover, the improvement of the graphical user interface and the ThermophIL content and algorithms will continue to be addressed in order not only to enhance the website structure, effectiveness and content as well as embellish and improve the user interaction.

Additionally new predictive models, developed by the PATh group, will also be included on ThermophIL and made available free-of-use.

4 a free web research tool that allows users worldwide to access an up-to-date data collection from the publications on experimental investigations of thermodynamic, and transport properties of ionic liquids as well as binary and ternary mixtures containing ionic liquids

15. Final Remarks and Future Work

"*The scientist is not a person who gives the right answers, he's one who asks the right questions.*"

Claude Lévi-Strauss

The high solubility and permeability of CO_2 in ionic liquids has been the object of extensive research by us and others during the last few years. Aiming at enhancing sour gases separation and ultimately replace the hazard volatile organic compounds (VOCs), many researchers have judiciously tailored ionic liquids (ILs) to accomplish such task.[16, 21-23, 26, 28, 33] Nonetheless, permeabilities data of CH_4, SO_2, light hydrocarbons or even H_2S are still scarce and focused on a narrow range of ionic liquids families, therefore, determining the sour gases/CH_4 permeabilities is of great interest.

Knowing that the solubility selectivity dominates the permeability selectivity in supported IL membranes,[261] together with the insights acquired during the thesis, that the polarity of the ionic liquids plays a dominant role on the selectivities, a pre-selection of the most adequate ionic liquids will be carried. Having identified the ILs with the highest solubilities/selectivities towards water and acid gases, present on the natural gas streams, the CO_2, CH_4 and SO_2 permeabilities will be measured.

The ILs selection will be made using experimental data available in literature and complemented by additional solubility measurements of the gases of interest (hydrocarbons, water, and CH_4) in highly polar ionic liquids. The solubility measurements of gases in ionic liquids will be investigated on a large range of pressures (1 to 1000 bar) and temperatures (10 to 100 ºC) on the high pressure equilibrium cell described on Chapter 2.

A new permeability cell, will be developed to perform permeability measurements of gases in the ionic liquids previously identified on the (1 to 5 bar) pressure range and on the (0 to 100 ºC) temperature range.

It will be used to study the liquid membranes developed. This permeability cell will be coupled to an online chromatography apparatus, allowing, thus, to investigate the separation efficiency of each component of the mixture as function of time and components compositions.

The ILs with higher selectivities and permeabilities will be identified for the purification of natural gas. Furthermore, through the CO_2/CH_4 selectivities, knowing that the solubility overcomes the diffusivity and dominates the permeability effect,[261] a new correlation, able to describe acid gases permeability in ionic liquids, will be proposed.

16. References

“The science of today is the technology of tomorrow.”

Edward Teller

References

[1] B. Guo, A. Ghalambor, Natural Gas Engineering Handbook, , Gulf Publishing Company (Ed.) (2005)

[2] D. Dortmundt, K. Doshi "**Recent Developments in CO_2 Removal Membrane Tecnology**" *UOP LLC* Des Plaines, Illinois (1999)

[3] W. Echt "**Hybrid Systems: Combinig Tecnologies Leads to More Efficient Gas Conditioning**" *IOP LLC* Laurance Reid Gas Conditioning Conference (2002) 1

[4] G. Corvini, J. Stiltner, K. Clark "**Mercury Removal from Natural Gas and Liquid Streams**" *UOP LLC* Houston, Texas, USA (2002) 1

[5] UOP LLC "**Adsorbents for Dehydration of Petrochemical Streams** " *www.uop.com* (2007)

[6] Linde Engineering, Rectisol Wash, http://www.linde-engineering.com, Linde Group (Ed.) (2007)

[7] W. Breckenridge, A. Holiday, J.O.Y. Ong, C. Sharp "**Use of SELEXOL Process in Coke Gasification to Ammonia Project**" *Laurance Reid Gas Conditioning Conference* (2000)

[8] UOP LLC "**Benfield Process**" *www.uop.com* (2007)

[9] Amines & Plasticizers Limited "**Methyl Diethanolamine (MDEA)**" *www.amines.com* (2007)

[10] H. Herzog "**An Introduction to CO_2 Separation and Capture Technologies**" *MIT Energy Laboratory* (1999)

[11] J.A. Boon, J.A. Levisky, J.L. Pflug, J.S. Wilkes "**Friedel-Crafts Reactions in Ambient-temperature Molten Salts**" *J. Org. Chem.* 51 (1986) 480

[12] S.E. Fry, N.J. Pienta "**Effects of molten salts on reactions. Nucleophilic Aromatic Substitution by Halide Ions in Molten Dodecyltributylphosphonium Salts**" *J. Am. Chem. Soc.* 107 (1985) 6399

[13] H. Zhao "**Innovative Applications of Ionic Liquids as Green Engineering Liquids**" *Chem. Eng. Commun.* 193 (2006) 1660

[14] R. Sheldon "**Catalytic Reactions in Ionic Liquids**" *Chem. Commun.* (2001) 2399

[15] H. Wong, S. Han, A.G. Livingston "**The Effect of Ionic Liquids on Product Yield and Catalyst Stability**" *Chem. Eng. Sci.* 61 (2006) 1338

[16] E. Bates, R. Mayton, I. Ntai, J. Davis "**CO_2 Capture by a Task-Specific Ionic Liquid**" *J. Am. Chem. Soc.* 124 (2002) 926

[17] J.L. Anthony, E.J. Maginn, J.F. Brennecke "**Solution Thermodynamics of Imidazolium-based Ionic Liquids and Water**" *J. Phys. Chem. B* 105 (2001) 10942

[18] J.G. Huddleston, H.D. Willauer, R.P. Swatloski, A.E. Visser, R.D. Rogers "**Room Temperature Ionic Liquids as Novel Media for Clean Liquid-liquid Extraction**" *Chem. Commun.* 16 (1998) 1765

[19] L. Blanchard, J. Brennecke "**Recovery of Organic Products from Ionic Liquids Using Supercritical Carbon Dioxide**" *Ind. Eng. Chem. Res.* 40 (2001) 287

[20] J.L. Anthony, S.N.V.K. Aki, E.J. Maginn, J.F. Brennecke "**Feasibility of using Ionic Liquids for Carbon Dioxide Capture**" *Int. J. Environ. Technol. Manage.* 4 (2004) 105

[21] J.E. Bara, C.J. Gabriel, S. Lessmann, T.K. Carlisle, A. Finotello, D.L. Gin, R.D. Noble "**Enhanced CO_2 Separation Selectivity in Oligo(ethylene glycol) Functionalized Room-Temperature Ionic Liquids**" *Ind. Eng. Chem. Res.* 46 (2007) 5380

[22] U. Domanska, A. Marciniak, M. Krolikowski "**Phase Equilibria and Modeling of Ammonium Ionic Liquid, C_2NTf_2, Solutions**" *J. Phys. Chem. B* 112 (2008) 1218

[23] A. Finotello, J. Bara, D. Camper, R. Noble "**Room-Temperature Ionic Liquids: Temperature Dependence of Gas Solubility Selectivity**" *Ind. Eng. Chem. Res.* 47 (2007) 3453

[24] A. Heintz "**Recent Developments in Thermodynamics and Thermophysics of Non-aqueous Mixtures Containing Ionic Liquids. A Review**" *J. Chem. Thermodyn.* 37 (2005) 525

[25] G. Hong, J. Jacquemin, M. Deetlefs, C. Hardacre, P. Husson, M. Costa Gomes "**Solubility of Carbon Dioxide and Ethane in Three Ionic Liquids Based on the Bis{(trifluoromethyl)sulfonyl}imide Anion**" *Fluid Phase Equilib.* 257 (2007) 27

[26] J. Huang, A. Riisager, R.W. Berg, R. Fehrmann "**Tuning Ionic Liquids for High Gas Solubility and Reversible Gas Sorption**" *J. Mol. Catal. A: Chem.* 279 (2008) 170

[27] J.W. Hutchings, K.L. Fuller, M.P. Heitz, M.M. Hoffmann "**Surprisingly High Solubility of the Ionic Liquid Trihexyltetradecylphosphonium Chloride in Dense Carbon Dioxide**" *Green Chem* 7 (2005) 475

[28] M. Muldoon, S. Aki, J. Anderson, J. Dixon, J. Brennecke "**Improving Carbon Dioxide Solubility in Ionic Liquids**" *J. Phys. Chem. B* 111 (2007) 9001

[29] M.B. Shiflett, D.J. Kasprzak, C.P. Junk, A. Yokozeki "**Phase Behavior of {Carbon Dioxide + [bmim][Ac]} Mixtures**" *J. Chem. Thermodyn.* 40 (2008) 25

[30] P.J. Carvalho, V.H. Álvarez, B. Schröder, A.M. Gil, I.M. Marrucho, M. Aznar, L.M.N.B.F. Santos, J.A.P. Coutinho "**Specific Solvation Interactions of CO_2 on Acetate and Trifluoroacetate Imidazolium Based Ionic Liquids at High Pressures**" *J. Phys. Chem. B* 113 (2009) 6803

[31] X. Yuan, S. Zhang, J. Liu, X. Lu "**Solubilities of CO_2 in Hydroxyl Ammonium Ionic Liquids at Elevated Pressures**" *Fluid Phase Equilib.* 257 (2007) 195

[32] J. Sun, S. Zhang, W. Cheng, J. Ren "**Hydroxyl-functionalized Ionic Liquid: a Novel Efficient Catalyst for Chemical Fixation of CO_2 to Cyclic Carbonate**"

Tetrahedron Lett. 49 (2008) 3588

[33] M.B. Shiflett, A. Yokozeki "**Phase Behavior of Carbon Dioxide in Ionic Liquids: [emim][Acetate], [emim][Trifluoroacetate], and [emim][Acetate] + [emim] [Trifluoroacetate] Mixtures**" *J. Chem. Eng. Data* 54 (2009) 108

[34] A. Yokozeki, M.B. Shiflett, C.P. Junk, L.M. Grieco, T. Foo "**Physical and Chemical Absorptions of Carbon Dioxide in Room-Temperature Ionic Liquids**" *J. Phys. Chem. B* 112 (2008) 16654

[35] P.J. Carvalho, J.A.P. Coutinho "**A Correlation for the High Pressure Solubility of CO2 in Ionic Liquids**" *Ind. Eng. Chem. Res.* (2009) accepted

[36] P.J. Carvalho, V.H. Álvarez, J.J.B. Machado, J. Pauly, J. Daridon, I.M. Marrucho, M. Aznar, J.A.P. Coutinho "**High Pressure Phase Behavior of Carbon Dioxide in 1-Alkyl-3-methylimidazolium Bis(trifluoromethylsulfonyl)imide Ionic Liquids**" *J. Supercrit. Fluids* 48 (2009) 99

[37] G. Yu, S. Zhang, X. Yao, J. Zhang, K. Dong, W. Dai, R. Mori "**Design of Task-Specific Ionic Liquids for Capturing CO_2: A Molecular Orbital Study**" *Ind. Eng. Chem. Res.* 45 (2006) 2875

[38] Z. Lopez-Castillo, S. Aki, M. Stadtherr, J. Brennecke "**Enhanced Solubility of Hydrogen in CO_2-Expanded Liquids**" *Ind. Eng. Chem. Res.* 47 (2008) 570

[39] M. Solinas, A. Pfaltz, P. Cozzi, W. Leitner "**Enantioselective Hydrogenation of Imines in Ionic Liquid/Carbon Dioxide Media**" *J. Am. Chem. Soc.* 126 (2004) 16142

[40] M. Latil, Enhanced Oil Recovery, Institut Français du Pétrole Publications, Technip (Ed.) (1980)

[41] R. Davarnejad, K.M. Kassim, A. Zainal, S.A. Sata "**Extraction of Fish Oil by Fractionation through Supercritical Carbon Dioxide**" *J. Chem. Eng. Data* 53 (2008) 2128

[42] O.J. Catchpole, J. von Kamp, J.B. Grey "**Extraction of Squalene from Shark Liver Oil in a Packed Column Using Supercritical Carbon Dioxide**" *Ind. Eng. Chem. Res.* 36 (1997) 4318

[43] H.J. Passino "**The Solexol Process**" *Ind. Eng. Chem.* 41 (2002) 280

[44] W.B. Nilsson. Supercritical Fluid Extraction and Fractionation of Fish Oils. In *Supercritical Fluid Technology in Oil and Lipid Chemistry*. King JW & List GR (Eds.). 1996. 180.

[45] Y.J. Heintz, L. Sehabiague, B.I. Morsi, K.L. Jones, H.W. Pennline "**Novel Physical Solvents for Selective CO_2 Capture from Fuel Gas Streams at Elevated Pressures and Temperatures**" *Energ. Fuels* 22 (2008) 3824–3837

[46] J. Anthony, E. Maginn, J. Brennecke "**Solubilities and Thermodynamic Properties of Gases in the Ionic Liquid 1-n-Butyl-3-methylimidazolium Hexafluorophosphate**" *J.*

Phys. Chem. B 106 (2002) 7315

[47] S.N.V.K. Aki, B.R. Mellein, E.M. Saurer, J.F. Brennecke "**High-Pressure Phase Behavior of Carbon Dioxide with Imidazolium-Based Ionic Liquids**" *J. Phys. Chem. B* 108 (2004) 20355

[48] J.L. Anderson, J.K. Dixon, J.F. Brennecke "**Solubility of CO_2, CH_4, C_2H_6, C_2H_4, O_2, and N_2 in 1-Hexyl-3-methylpyridinium Bis(trifluoromethylsulfonyl)imide: Comparison to Other Ionic Liquids**" *Acc. Chem. Res.* 40 (2007) 1208

[49] J. Anthony, J. Anderson, E. Maginn, J. Brennecke "**Anion Effects on Gas Solubility in Ionic Liquids**" *J. Phys. Chem. B* 109 (2005) 6366

[50] P.J. Carvalho, V.H. Alvarez, I.M. Marrucho, M. Aznar, J.A.P. Coutinho "**High Pressure Phase Behavior of Carbon Dioxide in 1-Butyl-3-methylimidazolium bis(trifluoromethylsulfonyl)imide and 1-Butyl-3-methylimidazolium Dicyanamide Ionic Liquids**" *J. Supercrit. Fluids* 50 (2009) 105

[51] J. Kumelan, A. Perez-Salado Kamps, D. Tuma, G. Maurer "**Solubility of CO_2 in the Ionic Liquids [bmim][CH_3SO_4] and [bmim][PF_6]**" *J. Chem. Eng. Data* 51 (2006) 1802

[52] J. Kumelan, Á. Pérez-Salado Kamps, D. Tuma, G. Maurer "**Solubility of CO_2 in the Ionic Liquid [hmim][Tf_2N]**" *J. Chem. Thermodyn.* 38 (2006) 1396

[53] J. Kumelan, D. Tuma, G. Maurer "**Solubility of CO_2 in the Ionic Liquids [bmim][CH_3SO_4] and [bmim][PF_6]**" *J. Chem. Eng. Data* 51 (2006) 1802

[54] J. Kumelan, D. Tuma, Á.P. Kamps, G. Maurer "**Solubility of the Single Gases Carbon Dioxide and Hydrogen in the Ionic Liquid [bmpy][Tf_2N]**" *J. Chem. Eng. Data* 55 (2010) 165

[55] B. Lee, S. Outcalt "**Solubilities of Gases in the Ionic Liquid 1-n-Butyl-3-methylimidazolium Bis(trifluoromethylsulfonyl)imide**" *J. Chem. Eng. Data* 51 (2006) 892

[56] K.B. Lee, M.G. Beaver, H.S. Caram, S. Sircar "**Chemisorption of Carbon Dioxide on Sodium Oxide Promoted Alumina**" *AIChE J.* 53 (2007) 2824

[57] J. Palgunadi, J.E. Kang, D.Q. Nguyen, J.H. Kim, B.K. Min, S.D. Lee, H. Kim, H.S. Kim "**Solubility of CO_2 in Dialkylimidazolium Dialkylphosphate Ionic Liquids**" *Thermochim. Acta* 494 (2009) 94

[58] A. Perez-Salado Kamps, D. Tuma, J. Xia, G. Maurer "**Solubility of CO_2 in the Ionic Liquid [bmim][PF_6]**" *J. Chem. Eng. Data* 48 (2003) 746

[59] S. Raeissi, C.J. Peters "**Carbon Dioxide Solubility in the Homologous 1-Alkyl-3-methylimidazolium Bis(trifluoromethylsulfonyl)imide Family**" *J. Chem. Eng. Data* 54 (2009) 382

[60] A. Shariati, C.J. Peters "**High-pressure Phase Behavior of Systems with Ionic Liquids: II. The Binary System Carbon Dioxide+1-ethyl-3-methylimidazolium Hexafluorophosphate**" *J. Supercrit. Fluids* 29 (2004) 43

[61] A. Shariati, C.J. Peters "**High-pressure Phase Behavior of Systems with Ionic Liquids: Part III. The Binary System Carbon Dioxide + 1-hexyl-3-methylimidazolium hexafluorophosphate**" *J. Supercrit. Fluids* 30 (2004) 139

[62] A. Shariati, C.J. Peters "**High-pressure Phase Equilibria of Systems with Ionic Liquids**" *J. Supercrit. Fluids* 34 (2005) 171

[63] M. Shiflett, A. Yokozeki "**Solubilities and Diffusivities of Carbon Dioxide in Ionic Liquids: [bmim][PF_6] and [bmim][BF_4]**" *Ind. Eng. Chem. Res.* 44 (2005) 4453

[64] M. Shiflett, A. Yokozeki "**Solubility of CO_2 in Room Temperature Ionic Liquid [hmim][Tf_2N]**" *J. Phys. Chem. B* 111 (2007) 2070

[65] S. Bashkova, F.S. Baker, X. Wu, T.R. Armstrong, V. Schwartz "**Activated Carbon Catalyst for Selective Oxidation of Hydrogen Sulphide: On the Influence of Pore Structure, Surface Characteristics, and Catalytically-active Nitrogen**" *Carbon* 45 (2007) 1354

[66] I. Mochida, K. Choi "**An Overview of Hydrodesulfurization and Hydrodenitrogenation**" *J. Jpn. Petrol. Inst.* 47 (2004) 145

[67] J.O. Valderrama, V.H. Àlvarez "**A Versatile Thermodynamic Consistency Test for Incomplete Phase Equilibrium Data of High-pressure Gas-liquid Mixtures**" *Fluid Phase Equilib.* 226 (2004) 149

[68] S. Vitu, J.N. Jaubert, J. Pauly, J.L. Daridon, D. Barth "**Phase Equilibria Measurements of CO_2 + Methyl Cyclopentane and CO_2 + Isopropyl Cyclohexane Binary Mixtures at Elevated Pressures**" *J. Supercrit. Fluids* 44 (2008) 155

[69] J. Pauly, J. Coutinho, J.L. Daridon "**High Pressure Phase Equilibria in Methane + Waxy Systems: 1. Methane + Heptadecane**" *Fluid Phase Equilib.* 255 (2007) 193

[70] S.P.M. Ventura, J. Pauly, J.L. Daridon, J.A.L. da Silva, I.M. Marrucho, A.M.A. Dias, J.A.P. Coutinho "**High Pressure Solubility Data of Carbon Dioxide in Tri-iso-butyl(methyl)phosphonium Tosylate - Water Systems**" *J. Chem. Thermodyn.* 40 (2008) 1187

[71] A.M.A. Dias, H. Carrier, J.L. Daridon, J.C. Pamies, L.F. Vega, J.A.P. Coutinho, I.M. Marrucho "**Vapor-Liquid Equilibrium of Carbon Dioxide-Perfluoroalkane Mixtures: Experimental Data and SAFT Modeling**" *Ind. Eng. Chem. Res.* 45 (2006) 2341

[72] S.P.M. Ventura, J. Pauly, J.L. Daridon, I.M. Marrucho, A.M.A. Dias, J.A.P. Coutinho "**High-Pressure Solubility Data of Methane in Aniline and Aqueous Aniline Systems**" *J. Chem. Eng. Data* 52 (2007) 1100

[73] V.H. Alvarez, N. Dosil, R. Gonzalez-Cabaleiro, S. Mattedi, M. Martin-Pastor, M. Iglesias, J.M. Navaza "**Brønsted Ionic Liquids for Sustainable Processes: Synthesis and Physical Properties**" *J. Chem. Eng. Data* 55 (2010) 625

[74] Sigma-Aldrich CBILS© Chemical Synthesis; http://www.sigmaaldrich.com/Area_of_Interest/Chemistry/Chemical_Synthesis/Product_H

ighlights/CBILS.html

[75] M.G. Freire, P.J. Carvalho, A.M. Fernandes, I.M. Marrucho, A.J. Queimada, J.A.P. Coutinho "**Surface Tensions of Imidazolium Based Ionic Liquids: Anion, Cation, Temperature and Water Effect**" *J. Colloid Interface Sci.* 314 (2007) 621

[76] K.R. Seddon, A. Stark, M. Torres "**Influence of Chloride, Water, and Organic Solvents on the Physical Properties of Ionic Liquids**" *Pure Appl. Chem.* 72 (2000) 2275

[77] J.G. Huddleston, A.E. Visser, W.M. Reichert, H.D. Willauer, G.A. Broker, R.D. Rogers "**Characterization and Comparison of Hydrophilic and Hydrophobic Room Temperature Ionic Liquids Incorporating the Imidazolium Cation**" *Green Chem.* 3 (2001) 156

[78] R.L. Gardas, M.G. Freire, P.J. Carvalho, I.M. Marrucho, I.M.A. Fonseca, A.G.M. Ferreira, J.A.P. Coutinho "**High Pressure Densities and Derived Thermodynamic Properties of Imidazolium Based Ionic Liquids**" *J. Chem. Eng. Data* 52 (2007) 80

[79] L. Blanchard, Z. Gu, J. Brennecke "**High-Pressure Phase Behavior of Ionic Liquid/CO_2 Systems**" *J. Phys. Chem. B* 105 (2001) 2437

[80] D. Fu, X. Sun, J. Pu, S. Zhao "**Effect of Water Content on the Solubility of CO_2 in the Ionic Liquid [bmim][PF_6]**" *J. Chem. Eng. Data* 51 (2006) 371

[81] D.R. MacFarlane, J.M. Pringle, K.M. Johansson, S.A. Forsyth, M. Forsyth "**Lewis base ionic liquids**" *Chem. Commun.* 18 (2006) 1905

[82] V.H. Alvarez, M. Aznar "**Thermodynamic Modeling of Vapor-liquid Equilibrium of Binary Systems Ionic Liquid + Supercritical {CO_2 or CHF_3} and Ionic Liquid + Hydrocarbons using Peng-Robinson Equation of State**" *J. Chin. Inst. Chem. Eng.* 39 (2008) 353

[83] V.H. Alvarez, M. Aznar "**Application of a Thermodynamic Consistency Test to Binary Mixtures Containing an Ionic Liquid**" *Open Thermodyn. J.* 2 (2008) 25

[84] D. Peng, D.B. Robinson "**A New Two-Constant Equation of State**" *Ind. Eng. Chem. Fund.* 15 (1976) 59

[85] D.S.H. Wong, S.I. Sandler "**A Theoretically Correct Mixing Rule for Cubic Equations of State**" *AIChE J.* 38 (1992) 671

[86] D.S. Abrams, J.M. Prausnitz "**Statistical Thermodynamics of Liquid Mixtures: A New Expression for the Excess Gibbs Energy of Partly or Completely Miscible Systems**" *AIChE J.* 21 (1975) 116

[87] V.H. Alvarez, R. Larico, Y. Ianos, M. Aznar "**Parameter Estimation for VLE Calculation by Global Minimization: Genetic Algorithm**" *Braz. J. Chem. Eng.* 25 (2008) 409

[88] T.M. Letcher, Developments and Applications in Solubility, Royal Society of Chemistry, (2007)

[89] P.J. Carvalho, J.A.P. Coutinho "**On the Nonideality of CO_2 Solutions in Ionic Liquids and Other Low Volatile Solvents**" *J. Phys. Chem. Lett.* 1 (2010) 774

[90] E. Aionicesei, M. Å kerget, Z. Knez "**Measurement and Modeling of the CO_2 Solubility in Poly(ethylene glycol) of Different Molecular Weights**" *J. Chem. Eng. Data* 53 (2007) 185

[91] J. Andreu, L. Vega "**Capturing the Solubility Behavior of CO_2 in Ionic Liquids by a Simple Model**" *J. Phys. Chem. C* 111(43) (2007) 16028

[92] M.F. Costa Gomes, A.A.H. Padua "**Interactions of Carbon Dioxide with Liquid Fluorocarbons**" *J. Phys. Chem. B* 107 (2003) 14020

[93] J. Deschamps, M.F. Costa Gomes, A.A.H. Padua "**Molecular Simulation Study of Interactions of Carbon Dioxide and Water with Ionic Liquids**" *ChemPhysChem* 5 (2004) 1049

[94] Z. Duan, R. Sun "**An Improved Model Calculating CO_2 Solubility in Pure Water and Aqueous NaCl Solutions from 273 to 533 K and from 0 to 2000 bar**" *Chemical Geology* 193 (2003) 257

[95] A. Galindo, F.J. Blas "**Theoretical Examination of the Global Fluid Phase Behavior and Critical Phenomena in Carbon Dioxide + *n*-Alkane Binary Mixtures**" *J. Phys. Chem. B* 106 (2002) 4503

[96] W. Hayduk, E.B. Walter, P. Simpson "**Solubility of Propane and Carbon Dioxide in Heptane, Dodecane and Hexadecane**" *J. Chem. Eng. Data* 17 (1972) 59

[97] F.H. Huang, M.H. Li, L.L. Lee, K.E. Starling "**An Accurate Equation of State for Carbon Dioxide**" *J. Chem. Eng. Jpn.* 18 (1985) 490

[98] A.J. Illies, M.L. McKee, H.B. Schlegel "**Ab initio Study of the Carbon Dioxide Dimer and the Carbon Dioxide Ion Complexes [$(CO_2)_2$+ and $(CO_2)_3$+]**" *J. Phys. Chem.* 91 (1987) 3489

[99] J. Sadlej, J. Makarewicz, G. Chalasinski "**Ab initio Study of Energy, Structure and Dynamics of the Water-carbon Dioxide Complex**" *J. Chem. Phys.* 109 (1998) 3919

[100] Y. Danten, T. Tassaing, M. Besnard "**Vibrational Spectra of CO_2-Electron Donor-Acceptor Complexes from *ab Initio***" *J. Phys. Chem. A* 106 (2002) 11831

[101] B. Renault, E. Cloutet, H. Cramail, T. Tassaing, M. Besnard "**On the Perturbation of the Intramolecular H-Bond in Diols by Supercritical CO_2: A Theoretical and Spectroscopic Study**" *J. Phys. Chem. A* 111 (2007) 4181

[102] M. Besnard, M.I. Cabaco, S. Longelin, T. Tassaing, Y. Danten "**Raman Investigation of the CO_2 Complex Formation in CO_2-Acetone Mixtures**" *J. Phys. Chem. A* 111 (2007) 13371

[103] M. Besnard, M.I. Cabaco, D. Talaga, Y. Danten "**Raman Spectroscopy and Ab initio Investigations of Transient Complex Formation in CO_2-benzene Mixtures**" *J.*

Chem. Phys. 129 (2008) 224511

[104] P. Lalanne, T. Tassaing, Y. Danten, F. Cansell, S.C. Tucker, M. Besnard "**CO_2-Ethanol Interaction Studied by Vibrational Spectroscopy in Supercritical CO_2**" *J. Phys. Chem. A* 108 (2004) 2617

[105] M.I. Cabaço, Y. Danten, T. Tassaing, S. Longelin, M. Besnard "**Raman Spectroscopy of CO_2-acetone and CO_2-ethanol Complexes**" *Chem. Phys. Lett.* 413 (2005) 258

[106] M.R. Nelson, R.F. Borkman "***Ab Initio* Calculations on CO_2 Binding to Carbonyl Groups**" *J. Phys. Chem. A* 102 (1998) 7860

[107] J.H. Williams "**The Molecular Electric Quadrupole Moment and Solid-state Architecture**" *Acc. Chem. Res.* 26 (1993) 593

[108] J. Kolafa, I. Nezbeda, M. Lisal "**Effect of Short- and Long-range Forces on the Properties of Fluids. III. Dipolar and Quadrupolar Fluids**" *Mol. Phys.* 99 (2001) 1751

[109] M.I. Cabaco, S. Longelin, Y. Danten, M. Besnard "**Transient Dimer Formation in Supercritical Carbon Dioxide as Seen from Raman Scattering**" *J. Chem. Phys.* 128 (2008) 074507

[110] M.I. Cabaço, M. Besnard, S. Longelin, Y. Danten "**Evolution with the Density of CO_2 Clustering Studied by Raman Spectroscopy**" *J. Mol. Liq.* 153 (2010) 15

[111] M.B. Oliveira, A.J. Queimada, G.M. Kontogeorgis, J.A.P. Coutinho "**Evaluation of the CO_2 Behavior in Binary Mixtures with Alkanes, Alcohols, Acids and Esters using the Cubic-Plus-Association Equation of State**" *J. Supercrit. Fluids* 55 (2010) 876

[112] P.M. Ndiaye, E. Franceschi, D. Oliveira, C. Dariva, F.W. Tavares, J.V. Oliveira "**Phase Behavior of Soybean Oil, Castor Oil and their Fatty Acid Ethyl Esters in Carbon Dioxide at High Pressures**" *J. Supercrit. Fluids* 37 (2006) 29

[113] G.M. Kontogeorgis, M.L. Michelsen, G.K. Folas, S. Derawi, N. von Solms, E.H. Stenby "**Ten Years with the CPA (Cubic-Plus-Association) Equation of State. Part 1. Pure Compounds and Self-Associating Systems**" *Ind. Eng. Chem. Res.* 45 (2006) 4855

[114] G.M. Kontogeorgis, M.L. Michelsen, G.K. Folas, S. Derawi, N. von Solms, E.H. Stenby "**Ten Years with the CPA (Cubic-Plus-Association) Equation of State. Part 2. Cross-Associating and Multicomponent Systems**" *Ind. Eng. Chem. Res.* 45 (2006) 4869

[115] H.P. Gros, S. Bottini, E.A. Brignole "**A Group Contribution Equation of State for Associating Mixtures**" *Fluid Phase Equilib.* 116 (1996) 537

[116] M.B. Oliveira, J.A.P. Coutinho, A.J. Queimada "**Mutual Solubilities of Hydrocarbons and Water with the CPA EoS**" *Fluid Phase Equilib.* 258 (2007) 58

[117] I. Tsivintzelis, G.M. Kontogeorgis, M.L. Michelsen, E.H. Stenby "**Modeling Phase Equilibria for Acid Gas Mixtures using the CPA Equation of State Part II. Binary Mixtures with CO_2**" *AIChE J.* 56 (2010) 2965

[118] W. Reiff, H. Roth, K. Lucas "**Phase Equilibria in the Binary System Carbon Disulfide-carbon Dioxide**" *Fluid Phase Equilib.* 73 (1992) 323

[119] P.J. Carvalho, V.H. Álvarez, I.M. Marrucho, M. Aznar, J.A.P. Coutinho "**High Carbon Dioxide Solubilities in Trihexyltetradecylphosphonium-based Ionic Liquids**" *J. Supercrit. Fluids* 52 (2010) 258

[120] G.M. Kontogeorgis, I. V Yakoumis, H. Meijer, E. Hendriks, T. Moorwood "**Multicomponent Phase Equilibrium Calculations for Water-methanol-alkane Mixtures**" *Fluid Phase Equilib.* 158-160 (1999) 201

[121] S.H. Huang, M. Radosz "**Equation of State for Small, Large, Polydisperse and Associating Molecules**" *Ind. Eng. Chem. Res.* 29 (1990) 2284

[122] DIPPR Design Institute for Physical Properties: DIPPR 801 database Brigham Young University; 1998

[123] H. Torii "**The Role of Atomic Quadrupoles in Intermolecular Electrostatic Interactions of Polar and Nonpolar Molecules**" *J. Chem. Phys.* 119 (2003) 2192

[124] A.M. Schilderman, S. Raeissi, C.J. Peters "**Solubility of Carbon Dioxide in the Ionic Liquid 1-Ethyl-3-Methylimidazolium Bis(trifluoromethylsulfonyl)imide**" *Fluid Phase Equilib.* 260 (2007) 19

[125] A. Finotello, J. Bara, D. Camper, R. Noble "**Room-Temperature Ionic Liquids: Temperature Dependence of Gas Solubility Selectivity**" *Ind. Eng. Chem. Res.* 47 (2008) 3453

[126] E. Shin, B. Lee, J.S. Lim "**High-pressure Solubilities of Carbon Dioxide in Ionic Liquids: 1-alkyl-3-methylimidazolium Bis(trifluoromethylsulfonyl)imide**" *J. Supercrit. Fluids* 45 (2008) 282

[127] Y. Hou, R. Baltus "**Experimental Measurement of the Solubility and Diffusivity of CO_2 in Room-Temperature Ionic Liquids Using a Transient Thin-Liquid-Film Method**" *Ind. Eng. Chem. Res.* 46 (2007) 8166

[128] J. Jacquemin, M.F. Costa Gomes, P. Husson, V. Majer "**Solubility of Carbon Dioxide, Ethane, Methane, Oxygen, Nitrogen, Hydrogen, Argon, and Carbon Monoxide in 1-butyl-3-methylimidazolium Tetrafluoroborate Between Temperatures 283 K and 343 K and at Pressures Close to Atmospheric**" *J. Chem. Thermodyn.* 38 (2006) 490

[129] M. Kanakubo, T. Umecky, Y. Hiejima, T. Aizawa, H. Nanjo, Y. Kameda "**Solution Structures of 1-Butyl-3-methylimidazolium Hexafluorophosphate Ionic Liquid Saturated with CO_2: Experimental Evidence of Specific Anion-CO_2 Interaction**" *J. Phys. Chem. B* 109 (2005) 13847

[130] C. Cadena, J. Anthony, J. Shah, T. Morrow, J. Brennecke, E. Maginn "**Why Is CO_2 So Soluble in Imidazolium-Based Ionic Liquids?**" *J. Am. Chem. Soc.* 126 (2004) 5300

[131] K. Gutkowski, A. Shariati, C. Peters "**High-pressure Phase Behavior of the Binary**

Ionic Liquid System 1-octyl-3-methylimidazolium Tetrafluoroborate + Carbon Dioxide" *J. Supercrit. Fluids* 39 (2006) 187

[132] M.G. Freire, C.M.S.S. Neves, P.J. Carvalho, R.L. Gardas, A.M. Fernandes, I.M. Marrucho, L.M.N.B.F. Santos, J.A.P. Coutinho "**Mutual Solubilities of Water and Hydrophobic Ionic Liquids**" *J. Phys. Chem. B* 111 (2007) 13082

[133] M.G. Freire, P.J. Carvalho, R.L. Gardas, I.M. Marrucho, L.M.N.B.F. Santos, J.A.P. Coutinho "**Mutual Solubilities of Water and the [$C_n$mim][Tf_2N] Hydrophobic Ionic Liquids**" *J. Phys. Chem. B* 112 (2008) 1604

[134] R.L. Gardas, M.G. Freire, P.J. Carvalho, I.M. Marrucho, I.M.A. Fonseca, A.G.M. Ferreira, J.A.P. Coutinho "***P*, (rho), *T* Measurements of Imidazolium Based Ionic Liquids**" *J. Chem. Eng. Data* 52 (2007) 1881

[135] P.J. Carvalho, M.G. Freire, I.M. Marrucho, A.J. Queimada, J.A.P. Coutinho "**Surface Tensions for the 1-Alkyl-3-methylimidazolium Bis(trifluoromethylsulfonyl)imide Ionic Liquids**" *J. Chem. Eng. Data* 53 (2008) 1346

[136] S.G. Kazarian, B.J. Briscoe, T. Welton "**Combining Ionic Liquids and Supercritical Fluids: *in situ* ATR-IR Study of CO_2 Dissolved in Two Ionic Liquids at High Pressures**" *Chem. Commun.* (2000) 2047

[137] J.H. Hildebrand, R.L. Scott, Regular and Related Solutions, Van Nostrand Reinhold, New York, (1970)

[138] J. Anderson, J. Dixon, E. Maginn, J. Brennecke "**Measurement of SO_2 Solubility in Ionic Liquids**" *J. Phys. Chem. B* 110 (2006) 15059

[139] W. Li, Z. Zhang, B. Han, S. Hu, J. Song, Y. Xie, X. Zhou "**Switching the Basicity of Ionic Liquids by CO_2**" *Green Chem.* 10 (2008) 1142

[140] L. Crowhurst, P.R. Mawdsley, J.M. Perez-Arlandis, P.A. Salter, T. Welton "**Solvent-solute Interactions in Ionic Liquids**" *Phys. Chem. Chem. Phys.* 5 (2003) 2790

[141] H.W. Pennline, D.R. Luebke, K.L. Jones, C.R. Myers, B.I. Morsi, Y.J. Heintz, J.B. Ilconich "**Progress in Carbon Dioxide Capture and Separation Research for Gasification-based Power Generation Point Sources**" *Fuel Process. Technol.* 89 (2008) 897

[142] E.J. Maginn "**Design and Evaluation of Ionic Liquids as Novel CO_2 absorvents**" *Quarterly Technical Report to DOE* DOE Award Number: DE-FG26-04NT42122 (May 31, 2005)

[143] J.O. Valderrama, A. Reategui, W.W. Sanga "**Thermodynamic Consistency Test of Vapor-Liquid Equilibrium Data for Mixtures Containing Ionic Liquids**" *Ind. Eng. Chem. Res.* 47 (2008) 8416

[144] M.R. Nelson, R.F. Borkman "***Ab Initio* Calculations on CO_2 Binding to Carbonyl Groups**" *J. Phys. Chem. A* 102 (1998) 7860

[145] S.G. Kazarian, M.F. Vincent, F.V. Bright, C.L. Liotta, C.A. Eckert "**Specific**

Intermolecular Interaction of Carbon Dioxide with Polymers" *J. Am. Chem. Soc.* 118 (1996) 1729

[146] P. Raveendran, S.L. Wallen "**Cooperative C ... O Hydrogen Bonding in CO_2 Lewis Base Complexes: Implications for Solvation in Supercritical CO_2**" *J. Am. Chem. Soc.* 124 (2002) 12590

[147] M.G. Freire, P.J. Carvalho, A.M.S. Silva, L.M.N.B.F. Santos, L.P.N. Rebelo, I.M. Marrucho, J.A.P. Coutinho "**Ion Specific Effects on the Mutual Solubilities of Water and Hydrophobic Ionic Liquids**" *J. Phys. Chem. B* 113 (2009) 202

[148] P. Diep, K. Jordan, J. Johnson, E. Beckman "**CO2-Fluorocarbon and CO_2-Hydrocarbon Interactions from First-Principles Calculations**" *J. Phys. Chem. A* 102 (1998) 2231

[149] C. Yonker, B. Palmer "**Investigation of CO_2/Fluorine Interactions Through the Intermolecular Effects on the ^1H and ^{19}F Shielding of CH_3F and CHF_3 at Various Temperatures and Pressures**" *J. Phys. Chem. A* 105 (2001) 308

[150] J. Anderson, J. Ding, T. Welton, D. Armstrong "**Characterizing Ionic Liquids On the Basis of Multiple Solvation Interactions**" *J. Am. Chem. Soc.* 124 (2002) 14247

[151] M.J. Frisch, G.W. Trucks, H.B. Schlegel, G.E. Scuseria, M.A. Robb, J.R. Cheeseman, J.A. Montgomery Jr, T. Vreven, K.N. Kudin, J.C. Burant, Gaussian 03, revision C.02, Wallingford CT, Gaussian I (Ed.) (2004)

[152] L.A. Curtiss, K. Raghavachari, P.C. Redfern, V. Rassolov, J.A. Pople "**Gaussian-3 (G3) Theory for Molecules Containing First and Second-row Atoms**" *J. Chem. Phys.* 109 (1998) 7764

[153] L.A. Curtiss, P.C. Redfern, K. Raghavachari, V. Rassolov, J.A. Pople "**Gaussian-3 theory using Reduced Møller-Plesset Order**" *J. Chem. Phys.* 110 (1999) 4703

[154] P. Subra, S. Castellani, H. Ksibi, Y. Garrabos "**Contribution to the Determination of the Solubility of [beta]-carotene in Supercritical Carbon Dioxide and Nitrous Oxide: Experimental Data and Modeling**" *Fluid Phase Equilib.* 131 (1997) 269

[155] M.C. Kroon, E.K. Karakatsani, I.G. Economou, G. Witkamp, C.J. Peters "**Modeling of the Carbon Dioxide Solubility in Imidazolium-Based Ionic Liquids with the tPC-PSAFT Equation of State**" *J. Phys. Chem. B* 110 (2006) 9262

[156] P. Scovazzo, D. Camper, J. Kieft, J. Poshusta, C. Koval, R. Noble "**Regular Solution Theory and CO_2 Gas Solubility in Room-Temperature Ionic Liquids**" *Ind. Eng. Chem. Res.* 43 (2004) 6855

[157] A.N. Soriano, B.T. Doma, M. Li "**Solubility of Carbon Dioxide in 1-Ethyl-3-methylimidazolium Tetrafluoroborate**" *J. Chem. Eng. Data* 53 (2008) 2550

[158] G. Avlonitis, G. Mourikas, S. Stamataki, D. Tassios "**A Generalized Correlation for the Interaction Coefficients of Nitrogen---Hydrocarbon Binary Mixtures**" *Fluid Phase Equilib.* 101 (1994) 53

[159] R. Bharath, H. Inomata, K. Arai, K. Shoji, Y. Noguchi "**Vapor-liquid Equilibria for Binary Mixtures of Carbon Dioxide and Fatty Acid Ethyl Esters**" *Fluid Phase Equilib.* 50 (1989) 315

[160] H. Byun, K. Kim, M.A. McHugh "**Phase Behavior and Modeling of Supercritical Carbon Dioxide-Organic Acid Mixtures**" *Ind. Eng. Chem. Res.* 39 (2000) 4580

[161] C.J. Chang, K. Chiu, C. Day "**A New Apparatus for the Determination of *P-x-y* Diagrams and Henry's Constants in High Pressure Alcohols with Critical Carbon Dioxide**" *J. Supercrit. Fluids* 12 (1998) 223

[162] C.J. Chang, M. Lee, B. Li, P. Chen "**Vapor-liquid Equilibria and Densities of CO_2 with Four Unsaturated Fatty Acid Esters at Elevated Pressures**" *Fluid Phase Equilib.* 233 (2005) 56

[163] T. Fang, M. Goto, Z. Yun, X. Ding, T. Hirose "**Phase Equilibria for Binary Systems of Methyl Oleate-supercritical CO_2 and [alpha]-tocopherol-supercritical CO_2**" *J. Supercrit. Fluids* 30 (2004) 1

[164] J. Heo, H.Y. Shin, J. Park, S.N. Joung, S.Y. Kim, K. Yoo "**Vapor-Liquid Equilibria for Binary Mixtures of CO_2 with 2-Methyl-2-propanol, 2-Methyl-2-butanol, Octanoic Acid, and Decanoic Acid at Temperatures from 313.15 K to 353.15 K and Pressures from 3 MPa to 24 MPa**" *J. Chem. Eng. Data* 46 (2001) 355

[165] H. Inomata, T. Kondo, S. Hirohama, K. Arai, Y. Suzuki, M. Konno "**Vapour--Liquid Equilibria for Binary Mixtures of Carbon Dioxide and Fatty Acid Methyl Esters**" *Fluid Phase Equilib.* 46 (1989) 41

[166] E. Petrova, C. Crampon, E. Ali, E. Neau, E. Badens, G. Charbit, J.N. Jaubert "**Solubility of CO_2 in some Heavy Alcohols and Correlation of Fluid Phase Equilibrium**" *Fluid Phase Equilib.* 213 (2003) 153

[167] N.M.B. Flichy, S.G. Kazarian, C.J. Lawrence, B.J. Briscoe "**An ATR-IR Study of Poly (Dimethylsiloxane) under High-Pressure Carbon Dioxide: Simultaneous Measurement of Sorption and Swelling**" *J. Phys. Chem. B* 106 (2001) 754

[168] M.H. Jamróz, J.C. Dobrowolski, K. Bajdor, M.A. Borowiak "***Ab initio* Study of the $\nu(CO_2)$ mode in EDA complexes**" *J. Mol. Struct.* 349 (1995) 9

[169] M. Görnert, G. Sadowski "**Phase-Equilibrium Measurements of the Polystyrene/Styrene/Carbon Dioxide Ternary System at Elevated Pressures Using ATR-FTIR Spectroscopy**" *Macromolecular Symposia* 259 (2007) 236

[170] E.J. Beckman "**A Challenge for Green Chemistry: Designing Molecules that Readily Dissolve in Carbon Dioxide**" *Chem. Commun.* (2004) 1885

[171] M. Maiwald, H. Li, T. Schnabel, K. Braun, H. Hasse "**On-line ^{1}H NMR Spectroscopic Investigation of Hydrogen Bonding in Supercritical and Near Critical CO_2-Methanol up to 35 MPa and 403 K**" *J. Supercrit. Fluids* 43 (2007) 267

[172] S. Bai, C.R. Yonker "**Pressure and Temperature Effects on the Hydrogen-Bond**

Structures of Liquid and Supercritical Fluid Methanol" *J. Phys. Chem. A* 102 (1998) 8641

[173] D.S. Bulgarevich, T. Sako, T. Sugeta, K. Otake, Y. Takebayashi, C. Kamizawa, Y. Horikawa, M. Kato "**The Role of General and Hydrogen-Bonding Interactions in the Solvation Processes of Organic Compounds by Supercritical CO_2/*n*-Alcohol Mixtures**" *Ind. Eng. Chem. Res.* 41 (2002) 2074

[174] M. Kanakubo, T. Aizawa, T. Kawakami, O. Sato, Y. Ikushima, K. Hatakeda, N. Saito "**Studies on Solute-Solvent Interactions in Gaseous and Supercritical Carbon Dioxide by High-Pressure ^{1}H NMR Spectroscopy**" *J. Phys. Chem. B* 104 (2000) 2749

[175] J.C. Dobrowolski, M.H. Jamróz "**Infrared Evidence for CO, Electron Donor-Acceptor Complexes**" *J. Mol. Struct.* 275 (1992) 211

[176] I. Pasquali, J. Andanson, S.G. Kazarian, R. Bettini "**Measurement of CO_2 Sorption and PEG 1500 Swelling by ATR-IR Spectroscopy**" *J. Supercrit. Fluids* 45 (2008) 384

[177] J. Andanson, F. Jutz, A. Baiker "**Supercritical CO_2/Ionic Liquid Systems: What Can We Extract from Infrared and Raman Spectra?**" *J. Phys. Chem. B* 113 (2009) 10249

[178] B. Bhargava, S. Balasubramanian "**Probing Anion-Carbon Dioxide Interactions in Room Temperature Ionic Liquids: Gas Phase Cluster Calculations**" *Chem. Phys. Lett.* 444 (2007) 242

[179] B.L. Bhargava, S. Balasubramanian "**Insights into the Structure and Dynamics of a Room-Temperature Ionic Liquid: *Ab Initio* Molecular Dynamics Simulation Studies of 1-n-Butyl-3-methylimidazolium Hexafluorophosphate ([bmim][PF_6]) and the [bmim][PF_6]-CO_2 Mixture**" *J. Phys. Chem. B* 111 (2007) 4477

[180] T. Seki, J. Grunwaldt, A. Baiker "**In Situ Attenuated Total Reflection Infrared Spectroscopy of Imidazolium-Based Room-Temperature Ionic Liquids under "Supercritical" CO_2**" *J. Phys. Chem. B* 113 (2009) 114

[181] P.J. Flory "**Thermodynamics of High Polymer Solutions**" *J. Chem. Phys.* 9 (1941) 660

[182] J.M. Prausnitz, R.N. Lichtenthaler, E. Gomes de Azevedo, Molecular Thermodynamics of Fluid-Phase Equilibria, Prentice Hall International Series: New York, (1999)

[183] R.D. Chirico, V. Diky, J.W. Magee, M. Frenkel, K.N. Marsh "**Thermodynamic and Thermophysical Properties of the Reference Ionic Liquid: 1-Hexyl-3-methylimidazolium bis[(trifluoromethyl)sulfonyl]amide (Including Mixtures). Part 2. Critical Evaluation and Recommended Property Values (IUPAC Technical Report)**" *Pure Appl. Chem.* 81 (2009) 791

[184] G. Maurer, A.P. Kamps, Developments and Applications in Solubility, Letcher, T. M.; RSC Publishing, (2007; pp 41-58)

[185] T. Charoensombut-amon, R.J. Martin, R. Kobayashi "**Application of a Generalized Multiproperty Apparatus to Measure Phase Equilibrium and Vapor Phase Densities of Supercritical Carbon Dioxide in *n*-hexadecane Systems up to 26 MPa**" *Fluid Phase Equilib.* 31 (1986) 89

[186] D.J. Fall, J.L. Fall, K.D. Luks "**Liquid-liquid-vapor Immiscibility Limits in Carbon Dioxide + *n*-paraffin Mixtures**" *J. Chem. Eng. Data* 30 (2002) 82

[187] H. Tanaka, Y. Yamaki, M. Kato "**Solubility of Carbon Dioxide in Pentadecane, Hexadecane, and Pentadecane + Hexadecane**" *J. Chem. Eng. Data* 38 (1993) 386

[188] C. Crampon, G. Charbit, E. Neau "**High-pressure Apparatus for Phase Equilibria Studies: Solubility of Fatty Acid Esters in Supercritical CO_2**" *J. Supercrit. Fluids* 16 (1999) 11

[189] R.D. Rogers, K.R. Seddon "**Ionic Liquids--Solvents of the Future?**" *Science* 302 (2003) 792

[190] K.N. Marsh, J.A. Boxall, R. Lichtenthaler "**Room Temperature Ionic Liquids and Their Mixtures-- A Review**" *Fluid Phase Equilib.* 219 (2004) 93

[191] C. Chiappe, D. Pieraccini "**Ionic Liquids: Solvent Properties and Organic Reactivity**" *J. Phys. Org. Chem.* 18 (2005) 275

[192] M.J. Earle, J.M.S.S. Esperanca, M.A. Gilea, J.N. Canongia Lopes, L.P.N. Rebelo, J.W. Magee, K.R. Seddon, J.A. Widegren "**The Distillation and Volatility of Ionic Liquids**" *Nature* 439 (2006) 831

[193] S. Zhang, Y. Chen, R. Ren, Y. Zhang, J. Zhang, X. Zhang "**Solubility of CO_2 in Sulfonate Ionic Liquids at High Pressure**" *J. Chem. Eng. Data* 50 (2005) 230

[194] L. Ferguson, P. Scovazzo "**Solubility, Diffusivity, and Permeability of Gases in Phosphonium-Based Room Temperature Ionic Liquids: Data and Correlations**" *Ind. Eng. Chem. Res.* 46 (2007) 1369

[195] U. Domanska, K. Paduszynski "**Phase Equilibria Study in Binary Systems (Tetra-n-butylphosphonium Tosylate Ionic Liquid + 1-Alcohol, or Benzene, or n-Alkylbenzene)**" *J. Phys. Chem. B* 112 (2008) 11054

[196] F.S. Oliveira, M.G. Freire, M.J. Pratas, J. Pauly, J.L. Daridon, I.M. Marrucho, J.A.P. Coutinho "**Solubility of Adamantane in Phosphonium-based Ionic Liquids**" *J. Chem. Eng. Data* (2009) accepted

[197] T. Wang, C. Peng, H. Liu, Y. Hu "**Description of the *pVT* Behavior of Ionic Liquids and the Solubility of Gases in Ionic Liquids using an Equation of State**" *Fluid Phase Equilib.* 250 (2006) 150

[198] R. Condemarin, P. Scovazzo "**Gas Permeabilities, Solubilities, Diffusivities, and Diffusivity Correlations for Ammonium-based Room Temperature Ionic Liquids with Comparison to Imidazolium and Phosphonium RTIL Data**" *Chem. Eng. J.* 147 (2009) 51

[199] D. Morgan, L. Ferguson, P. Scovazzo "**Diffusivities of Gases in Room-Temperature Ionic Liquids: Data and Correlations Obtained Using a Lag-Time Technique**" *Ind. Eng. Chem. Res.* 44 (2005) 4815

[200] N.V. Plechkova, K.R. Seddon "**Applications of Ionic Liquids in the Chemical Industry**" *Chem. Soc. Rev.* 37 (2008) 123

[201] J.F. Jenck, F. Agterberg, M.J. Droescher "**Products and Processes for a Sustainable Chemical Industry: A Review of Achievements and Prospects**" *Green Chem.* 6 (2004) 544

[202] S. Gabriel, J. Weiner "**Ueber einige Abkömmlinge des Propylamins**" Ber. 21 (1888) 2669–2679

[203] D.F. Kennedy, C.J. Drummond "**Large Aggregated Ions Found in Some Protic Ionic Liquids**" *J. Phys. Chem. B* 113 (2009) 5690

[204] N. Bicak "**A New Ionic Liquid: 2-hydroxy Ethylammonium Formate**" *J. Mol. Liq.* 116 (2005) 15

[205] T.L. Greaves, A. Weerawardena, C. Fong, I. Krodkiewska, C.J. Drummond "**Protic Ionic Liquids: Solvents with Tunable Phase Behavior and Physicochemical Properties**" *J. Phys. Chem. B* 110 (2006) 22479

[206] I. Cota, R. Gonzalez-Olmos, M. Iglesias, F. Medina "**New Short Aliphatic Chain Ionic Liquids: Synthesis, Physical Properties, and Catalytic Activity in Aldol Condensations**" *J. Phys. Chem. B* 111 (2007) 12468

[207] K. Kurnia, C. Wilfred, T. Murugesan "**Thermophysical Properties of Hydroxyl Ammonium Ionic Liquids**" *J. Chem. Thermodyn.* 41 (2009) 517

[208] M. Iglesias, A. Torres, R. Gonzalez-Olmos, D. Salvatierra "**Effect of Temperature on Mixing Thermodynamics of a New Ionic Liquid: {2-Hydroxy Ethylammonium Formate (2-HEAF) + Short Hydroxylic Solvents}**" *J. Chem. Thermodyn.* 40 (2008) 119

[209] D.J. Couling, R.J. Bernot, K.M. Docherty, J.K. Dixon, E.J. Maginn "**Assessing the Factors Responsible for Ionic Liquid Toxicity to Aquatic Organisms Via Quantitative Structure-Property Relationship Modeling**" *Green Chem* 8 (2006) 82

[210] M. Anouti, M. Caillon-Caravanier, C. Le Floch, D. Lemordant "**Alkylammonium-Based Protic Ionic Liquids Part I: Preparation and Physicochemical Characterization**" *J. Phys. Chem. B* 112 (2008) 9406

[211] X. Yuan, S. Zhang, X. Lu "**Hydroxyl Ammonium Ionic Liquids: Synthesis, Properties, and Solubility of SO_2**" *J. Chem. Eng. Data* 52 (2007) 596

[212] X. Yuan, S. Zhang, Y. Chen, X. Lu, W. Dai, R. Mori "**Solubilities of Gases in 1,1,3,3-Tetramethylguanidium Lactate at Elevated Pressures**" *J. Chem. Eng. Data* 51 (2006) 645

[213] D. Zhao, R. Liu, J. Wang, B. Liu "**Photochemical Oxidation-Ionic Liquid**

Extraction Coupling Technique in Deep Desulphurization of Light Oil" *Energ. Fuels* 22 (2008) 1100

[214] J. Wang, D. Zhao, K. Li "**Oxidative Desulfurization of Dibenzothiophene Catalyzed by Brönsted Acid Ionic Liquid**" *Energ. Fuels* 23 (2009) 3831

[215] R. Schmidt "**[bmim]$AlCl_4$ Ionic Liquid for Deep Desulfurization of Real Fuels**" *Energ. Fuels* 22 (2008) 1774

[216] M.B. Shiflett, A. Yokozeki "**Separation of Carbon Dioxide and Sulfur Dioxide Using Room-Temperature Ionic Liquid [bmim][$MeSO_4$]**" *Energ. Fuels* 24 (2010) 1001

[217] A. Yokozeki, M.B. Shiflett "**Separation of Carbon Dioxide and Sulfur Dioxide Gases Using Room-Temperature Ionic Liquid [hmim][Tf_2N]**" *Energ. Fuels* 23 (2009) 4701

[218] Y.J. Heintz, L. Sehabiague, B.I. Morsi, K.L. Jones, D.R. Luebke, H.W. Pennline "**Hydrogen Sulfide and Carbon Dioxide Removal from Dry Fuel Gas Streams Using an Ionic Liquid as a Physical Solvent**" *Energ. Fuels* 23 (2009) 4822

[219] R.A. Ando, L.J.A. Siqueira, F.C. Bazito, R.M. Torresi, P.S. Santos "**The Sulfur Dioxide-1-Butyl-3-Methylimidazolium Bromide Interaction: Drastic Changes in Structural and Physical Properties**" *J. Phys. Chem. B* 111 (2007) 8717

[220] L.J.A. Siqueira, R.A. Ando, F.F.C. Bazito, R.M. Torresi, P.S. Santos, M.C.C. Ribeiro "**Shielding of Ionic Interactions by Sulfur Dioxide in an Ionic Liquid**" *J. Phys. Chem. B* 112 (2008) 6430

[221] L. Pison, J.N. Canongia Lopes, L.P.N. Rebelo, A.A.H. Padua, M.F. Costa Gomes "**Interactions of Fluorinated Gases with Ionic Liquids: Solubility of CF_4, C_2F_6, and C_3F_8 in Trihexyltetradecylphosphonium Bis(trifluoromethylsulfonyl)amide**" *J. Phys. Chem. B* 112 (2008) 12394

[222] C. Pomelli, C. Chiappe, A. Vidis, G. Laurenczy, P. Dyson "**Influence of the Interaction between Hydrogen Sulfide and Ionic Liquids on Solubility: Experimental and Theoretical Investigation**" *J. Phys. Chem. B* 111 (2007) 13014

[223] S. Ren, Y. Hou, W. Wu, Q. Liu, Y. Xiao, X. Chen "**Properties of Ionic Liquids Absorbing SO_2 and the Mechanism of the Absorption**" *J. Phys. Chem. B* 114 (2010) 2175

[224] D. Tempel, P. Henderson, J. Brzozowski, R. Pearlstein, H. Cheng "**High Gas Storage Capacities for Ionic Liquids Through Chemical Complexation**" *J. Am. Chem. Soc.* 130 (2007) 400

[225] A. Yokozeki, M.B. Shiflett "**Ammonia Solubilities in Room-Temperature Ionic Liquids**" *Ind. Eng. Chem. Res.* 46 (2007) 1605

[226] G. Li, Q. Zhou, X. Zhang, LeiWang, S. Zhang, J. Li "**Solubilities of Ammonia in Basic Imidazolium Ionic Liquids**" *Fluid Phase Equilib.* 297 (2010) 34

[227] M.B. Shiflett, A. Yokozeki "**Chemical Absorption of Sulfur Dioxide in Room-**

Temperature Ionic Liquids" *Ind. Eng. Chem. Res.* 49 (2010) 1370

[228] J.A.P. Coutinho, S.I. Andersen, E.H. Stenby "**Evaluation of Activity Coefficient Models in Prediction of Alkane Solid-Liquid Equilibria**" *Fluid Phase Equilib.* 103 (1995) 23

[229] R. Gomes De Azevedo, J.M.S.S. Esperanca, J. Szydlowski, Z.P. Visak, P.F. Pires, H.J.R. Guedes, L.P.N. Rebelo "**Thermophysical and Thermodynamic Properties of Ionic Liquids over an Extended Pressure Range: [bmim][NTf_2] and [hmim][NTf_2]**" *J. Chem. Thermodyn.* 37 (2005) 888

[230] L.I.N. Tomé, P.J. Carvalho, M.G. Freire, I.M. Marrucho, I.M.A. Fonseca, A.G.M. Ferreira, J.A.P. Coutinho, R.L. Gardas "**Measurements and Correlation of High-Pressure Densities of Imidazolium-Based Ionic Liquids**" *J. Chem. Eng. Data* 53 (2008) 1914

[231] E. Gómez, B. González, A. Domínguez, E. Tojo, J. Tojo "**Dynamic Viscosities of a Series of 1-alkylimidazolium Chloride Ionic Liquids and Their Binary Mixtures with Water at Several Temperatures**" *J. Chem. Eng. Data* 51 (2006) 696

[232] A. Muhammad, M. Abdul Mutalib, C. Wilfred, T. Murugesan, A. Shafeeq "**Thermophysical Properties of 1-hexyl-3-methyl imidazolium Based Ionic Liquids with Tetrafluoroborate, Hexafluorophosphate and bis(trifluoromethylsulfonyl)imide Anions**" *J. Chem. Thermodyn.* 40 (2008) 1433

[233] A.H. Jalili, M. Rahmati-Rostami, C. Ghotbi, M. Hosseini-Jenab, A.N. Ahmadi "**Solubility of H2S in Ionic Liquids [bmim][PF_6], [bmim][BF_4], and [bmim][Tf_2N]**" *J. Chem. Eng. Data* 54 (2009) 1844

[234] M. Rahmati-Rostami, C. Ghotbi, M. Hosseini-Jenab, A.N. Ahmadi, A.H. Jalili "**Solubility of H_2S in Ionic Liquids [hmim][PF_6], [hmim][BF_4], and [hmim][Tf_2N]**" *J. Chem. Thermodyn.* 41 (2009) 1052

[235] J.A. Velasco, L. Lopez, M. Velásquez, M. Boutonnet, S. Cabrera, S. Järås "**Gas to Liquids: A Technology for Natural Gas Industrialization in Bolivia**" *J. Nat. Gas Sci. Eng.* 2 (2010) 222

[236] F. Wu, L. Li, Z. Xu, S. Tan, Z. Zhang "**Transport Study of Pure and Mixed Gases Through PDMS Membrane**" *Chem. Eng. J.* 117 (2006) 51

[237] H.M. Ettouney, G. Al-Enezi, S. Hamam, R. Hughes "**Characterization of the Permeation Properties of CO_2---N_2 Gas Mixtures in Silicone Rubber Membranes**" *Gas Sep. Purif.* 8 (1994) 31

[238] J. Zhang, J. Lu, W. Liu, Q. Xue "**Separation of CO_2 and CH_4 Through Two Types of Polyimide Membrane**" *Thin Solid Films* 340 (1999) 106

[239] J.D. Wind, D.R. Paul, W.J. Koros "**Natural Gas Permeation in Polyimide Membranes**" *J. Memb. Sci.* 228 (2004) 227

[240] S. Sridhar, R. Suryamurali, B. Smitha, T. Aminabhavi "**Development of**

Crosslinked Poly(ether-block-amide) Membrane for CO_2/CH_4 Separation" *Colloid Surface A* 297 (2007) 267

[241] M. Poloncarzova, J. Vejrazka, V. Vesely, P. Izak "**Effective Purification of Biogas by a Condensing-Liquid Membrane**" *Angew. Chem. Int. Ed.* 50 (2011) 669

[242] P. Scovazzo, D. Havard, M. McShea, S. Mixon, D. Morgan "**Long-term, Continuous Mixed-gas Dry Fed CO_2/CH_4 and CO_2/N_2 Separation Performance and Selectivities for Room Temperature Ionic Liquid Membranes**" *J. Memb. Sci.* 327 (2009) 41

[243] J.E. Bara, T.K. Carlisle, C.J. Gabriel, D. Camper, A. Finotello, D.L. Gin, R.D. Noble "**Guide to CO_2 Separations in Imidazolium-Based Room-Temperature Ionic Liquids**" *Ind. Eng. Chem. Res.* 48 (2009) 2739–2751

[244] A. Finotello, J. Bara, S. Narayan, D. Camper, R. Noble "**Ideal Gas Solubilities and Solubility Selectivities in a Binary Mixture of Room-Temperature Ionic Liquids**" *J. Phys. Chem. B* 112 (2008) 2335

[245] S. Mattedi, P.J. Carvalho, J.A.P. Coutinho, V.H. Alvarez, M. Iglesias "**High Pressure CO_2 Solubility in N-methyl-2-hydroxyethylammonium Protic Ionic Liquids**" *J. Supercrit. Fluids* 56 (2011) 224

[246] S. Raeissi, C.J. Peters "**A Potential Ionic Liquid for CO_2-Separating Gas Membranes: Selection and Gas Solubility Studies**" *Green Chem.* 11 (2009) 185

[247] A.H. Jalili, A. Mehdizadeh, M. Shokouhi, A.N. Ahmadi, M. Hosseini-Jenab, F. Fateminassab "**Solubility and Diffusion of CO_2 and H_2S in the Ionic Liquid 1-ethyl-3-methylimidazolium Ethylsulfate**" *J. Chem. Thermodyn.* 42 (2010) 1298

[248] H. Sakhaeinia, A.H. Jalili, V. Taghikhani, A.A. Safekordi "**Solubility of H_2S in Ionic Liquids 1-Ethyl-3-methylimidazolium Hexafluorophosphate ([emim][PF_6]) and 1-Ethyl-3-methylimidazolium Bis(trifluoromethyl)sulfonylimide ([emim][Tf_2N])**" *J. Chem. Eng. Data* 55 (2010) 5839

[249] M. Shokouhi, M. Adibi, A.H. Jalili, M. Hosseini-Jenab, A. Mehdizadeh "**Solubility and Diffusion of H_2S and CO_2 in the Ionic Liquid 1-(2-Hydroxyethyl)-3-methylimidazolium Tetrafluoroborate**" *J. Chem. Eng. Data* 55 (2010) 1663

[250] F. Jou, A.E. Mather "**Solubility of Hydrogen Sulfide in [bmim][PF_6]**" *Int. J. Thermophys.* 28(2) (2007) 490

[251] Y. Jiang, Z. Zhou, Z. Jiao, L. Li, Y. Wu, Z. Zhang "**SO_2 Gas Separation Using Supported Ionic Liquid Membranes**" *J. Phys. Chem. B* 111 (2007) 5058

[252] D.G. Hert, J.L. Anderson, S.N.V.K. Aki, J.F. Brennecke "**Enhancement of Oxygen and Methane Solubility in 1-hexyl-3-methylimidazolium bis(trifluoromethylsulfonyl) imide using Carbon Dioxide**" *Chem. Commun.* 20 (2005) 2603

[253] P.J. Carvalho, J.A.P. Coutinho "**Non-ideality of Solutions of NH_3, SO_2, and H_2S in Ionic Liquids and the Prediction of Their Solubilities Using the Flory-Huggins Model**"

Energy & Fuels 24 (2010) 6662

[254] J. Pauly, J.A. Coutinho, J. Daridon "**High Pressure Phase Equilibria in Methane + Waxy Systems. 2. Methane + Waxy Ternary Mixture**" *Fluid Phase Equilib.* 297 (2010) 149

[255] P.J. Carvalho, A.R. Ferreira, M.B. Oliveira, M. Besnard, M.I. Cabaço, J.A.P. Coutinho "**High Pressure Phase Behavior of Carbon Dioxide in Carbon Disulphide and Carbon Tetrachloride**" *J. Chem. Eng. Data* 56 (2011) 2786

[256] R. Lungwitz, S. Spange "**A Hydrogen Bond Accepting (HBA) Scale for Anions, Including Room Temperature Ionic Liquids**" *New J. Chem.* 32 (2008) 392

[257] R. Lungwitz, V. Strehmel, S. Spange "**The Dipolarity/Polarisability of 1-alkyl-3-methylimidazolium Ionic Liquids as Function of Anion Structure and the Alkyl Chain Length**" *New J. Chem.* 34 (2010) 1135

[258] H. Salari, A. Harifi-Mood, M. Elahifard, M. Gholami "**Solvatochromic Probes Absorbance Behavior in Mixtures of 2-Hydroxy Ethylammonium Formate with Methanol, Ethylene Glycol and Glycerol**" *J. Sol. Chem.* 39 (2010) 1509

[259] J. Palgunadi, S.Y. Hong, J.K. Lee, H. Lee, S.D. Lee, M. Cheong, H.S. Kim "**Correlation Between Hydrogen Bond Basicity and Acetylene Solubility in Room Temperature Ionic Liquids**" *J. Phys. Chem. B* 115 (2011) 1067

[260] D. Camper, J. Bara, C. Koval, R. Noble "**Bulk-Fluid Solubility and Membrane Feasibility of Rmim-Based Room-Temperature Ionic Liquids**" *Ind. Eng. Chem. Res.* 45 (2006) 6279

[261] P. Scovazzo "**Determination of the Upper Limits, Benchmarks, and Critical Properties for Gas Separations Using Stabilized Room Temperature Ionic Liquid Membranes (SILMs) for the Purpose of Guiding Future Research**" *J. Memb. Sci.* 343 (2009) 199

[262] P. Kilaru, R. Condemarin, P. Scovazzo "**Correlations of Low-Pressure Carbon Dioxide and Hydrocarbon Solubilities in Imidazolium-, Phosphonium-, and Ammonium-Based Room-Temperature Ionic Liquids. Part 1. Using Surface Tension**" *Ind. Eng. Chem. Res.* 47 (2008) 900

[263] P. Kilaru, P. Scovazzo "**Correlations of Low-Pressure Carbon Dioxide and Hydrocarbon Solubilities in Imidazolium-, Phosphonium-, and Ammonium-Based Room-Temperature Ionic Liquids. Part 2. Using Activation Energy of Viscosity**" *Ind. Eng. Chem. Res.* 47 (2008) 910

[264] R.L. Gardas, J.A.P. Coutinho "**Applying a QSPR Correlation to the Prediction of Surface Tensions of Ionic Liquids**" *Fluid Phase Equilib.* 265 (2008) 57

[265] R.L. Gardas, J.A. Coutinho "**A Group Contribution Method for Viscosity Estimation of Ionic Liquids**" *Fluid Phase Equilib.* 266 (2008) 195

[266] R.L. Gardas, J.A. Coutinho "**Estimation of Speed of Sound of Ionic Liquids Using**

Surface Tensions and Densities: A Volume Based Approach" *Fluid Phase Equilib.* 267 (2008) 188

[267] R.L. Gardas, J.A. Coutinho "**Extension of the Ye and Shreeve Group Contribution Method for Density Estimation of Ionic Liquids in a Wide Range of Temperatures and Pressures**" *Fluid Phase Equilib.* 263 (2008) 26

[268] R.L. Gardas, J.A.P. Coutinho "**Group Contribution Methods for the Prediction of Thermophysical and Transport Properties of Ionic Liquids**" *AIChE J.* 55 (2009) 1274

[269] C. Ye, J.M. Shreeve "**Rapid and Accurate Estimation of Densities of Room-Temperature Ionic Liquids and Salts**" *J. Phys. Chem. A* 111 (2007) 1456

[270] T.A. Knotts, W.V. Wilding, J.L. Oscarson, R.L. Rowley "**Use of the DIPPR Database for Development of QSPR Correlations: Surface Tension**" *J. Chem. Eng. Data* 46 (2001) 1007

[271] V. Růžička, E.S. Domalski "**Estimation of the Heat Capacities of Organic Liquids as a Function of Temperature using Group Additivity. I. Hydrocarbon Compounds**" *J. Phys. Chem. Ref. Data* 22 (1993) 597

[272] V. Růžička, E.S. Domalski "**Estimation of the Heat Capacities of Organic Liquids as a Function of Temperature using Group Additivity. II. Compounds of Carbon, Hydrogen, Halogens, Nitrogen, Oxygen, and Sulfur**" *J. Phys. Chem. Ref. Data* 22 (1993) 619

[273] J.O. Bockris, G.W. Hooper "**Self-diffusion in Molten Alkali Halides**" *Discuss. Faraday Soc.* 32 (1961) 218

[274] R. Ge, C. Hardacre, P. Nancarrow, D.W. Rooney "**Thermal Conductivities of Ionic Liquids over the Temperature Range from 293 K to 353 K**" *J. Chem. Eng. Data* 52 (2007) 1819

[275] H. Rodríguez, M. Williams, J.S. Wilkes, R.D. Rogers "**Ionic liquids for liquid-in-glass thermometers**" *Green Chem.* 10 (2008) 501

[276] T. Predel, E. Schlucker, P. Wasserscheid, D. Gerhard, W. Arlt "**Ionic Liquids as Operating Fluids in High Pressure Applications**" *Chem. Eng. Technol.* 30 (2007) 1475

[277] N. Auerbach "" *Experientia* 4 (1948) 473

[278] S.L. Oswal, P. Oswal, P.S. Modi, J.P. Dave, R.L. Gardas "**Acoustic, Volumetric, Compressibility and Refractivity Properties and Flory's Reduction Parameters of Some Homologous Series of Alkyl Alkanoates from 298.15 to 333.15 K**" *Thermochim. Acta* 410 (2004) 1

[279] S.L. Oswal, P. Oswal, R.L. Gardas, S.G. Patel, R.G. Shinde "**Acoustic, Volumetric, Compressibility and Refractivity Properties and Reduction Parameters for the ERAS and Flory Models of Some Homologous Series of Amines from 298.15 to 328.15 K**" *Fluid Phase Equilib.* 216 (2004) 33

[280] Diadem Public 1.2, The DIPPR Information and Data Evaluation Manager, AIChE:

New York;

[281] J.O. Valderrama, P.A. Robles "**Critical Properties, Normal Boiling Temperatures, and Acentric Factors of Fifty Ionic Liquids**" *Ind. Eng. Chem. Res.* 46 (2007) 1338

[282] Diadem Public 1.2. The DIPPR Information and Data Evaluation Manager; 2000

[283] J.A. López, V.M. Trejos, C.A. Cardona "**Parameters Estimation and VLE Calculation in Asymmetric Binary Mixtures Containing Carbon Dioxide + *n*-Alkanols**" *Fluid Phase Equilib.* 275 (2009) 1

[284] J.L. Fulton, G.G. Yee, R.D. Smith "**Hydrogen Bonding of Methyl Alcohol-d in Supercritical Carbon Dioxide and Supercritical Ethane Solutions**" *J. Am. Chem. Soc.* 113 (1991) 8327

[285] H. Tanaka, Y. Yamaki, M. Kato "**Solubility of Carbon Dioxide in Pentadecane, Hexadecane, and Pentadecane + Hexadecane**" *J. Chem. Eng. Data* 38 (1993) 386

[286] Y. Sato, Y. Tagashira, D. Maruyama, S. Takishima, H. Masuoka "**Solubility of Carbon Dioxide in Eicosane, Docosane, Tetracosane, and Octacosane at Temperatures from 323 to 473 K and Pressures up to 40 MPa**" *Fluid Phase Equilib.* 147 (1998) 181

[287] N.C. Huie, K.D. Luks, J.P. Kohn "**Phase-equilibriums Behavior of Systems Carbon Dioxide-*n*-eicosane and Carbon Dioxide-*n*-decane-*n*-eicosane**" *J. Chem. Eng. Data* 18 (1973) 311

[288] R. D'souza, J.R. Patrick, A.S. Teja "**High Pressure Phase Equilibria in the Carbon Dioxide - *n*-Hexadecane and Carbon Dioxide - Water Systems**" *Can. J. Chem. Eng.* 66 (1988) 319

[289] C.A. Lockemann "**High-pressure Phase Equilibria and Densities of the Binary Mixtures Carbon Dioxide--Oleic Acid, Carbon Dioxide--Methyl Myristate, and Carbon Dioxide--Methyl Palmitate and of the Ternary Mixture Carbon Dioxide--Methyl Myristate--Methyl Palmitate**" *Chem. Eng. Process.* 33 (1994) 171

[290] O. Ferreira, E.A. Macedo, E.A. Brignole "**Application of the GCA-EoS Model to the Supercritical Processing of Fatty Oil Derivatives**" *J. Food Eng.* 70 (2005) 579

[291] J. Jaubert, L. Coniglio "**The Group Contribution Concept: A Useful Tool To Correlate Binary Systems and To Predict the Phase Behavior of Multicomponent Systems Involving Supercritical CO_2 and Fatty Acids**" *Ind. Eng. Chem. Res.* 38 (1999) 5011

[292] E. Weidner, V. Wiesmet, Z. Knez, M. Skerget "**Phase Equilibrium (Solid-liquid-gas) in Polyethyleneglycol-carbon Dioxide Systems**" *J. Supercrit. Fluids* 10 (1997) 139

[293] M. Daneshvar, S. Kim, E. Gulari "**High-pressure Phase Equilibria of Polyethylene Glycol-carbon Dioxide Systems**" *J. Phys. Chem.* 94 (1990) 2124

[294] K.K. Joback, R. Reid "**Estimation of Pure Component Properties from Group Contribution**" *Chem. Eng. Commun.* 57 (1987) 233

[295] A. Yokozeki, M.B. Shiflett "**Vapor-liquid Equilibria of Ammonia + Ionic Liquid Mixtures**" *Applied Energy* 84 (2007) 1258

[296] J. Kumelan, A. Perez-SaladoKamps, D. Tuma, G. Maurer "**Solubility of the Single Gases Methane and Xenon in the Ionic Liquid [bmim][CH_3SO_4]**" *J. Chem. Eng. Data* 52 (2007) 2319

17. Publications List

"The scientist is motivated primarily by curiosity and a desire for truth."

Irving Langmuir

"We are born at a given moment, in a given place and, like vintage years of wine, we have the qualities of the year and of the season of which we are born. Astrology does not lay claim to anything more."

Carl Jung

1	***Surface tension of liquid fluorocompounds*** M.G. Freire, P.J. Carvalho, A.J. Queimada, I.M. Marrucho, J.A.P. Coutinho. *J. Chem. Eng. Data* 51 (2006) 1820
2	***High pressure densities and derived thermodynamic properties of imidazolium based ionic liquids*** R.L. Gardas, M.G. Freire, P.J. Carvalho, I.M. Marrucho, I.M.A. Fonseca, A.G.M. Ferreira, J.A.P. Coutinho. *J. Chem. Eng. Data* 52 (2007) 80
3	***Mutual solubilities of water and hydrophobic ionic liquids*** M.G. Freire, C.M.S.S. Neves, P.J. Carvalho, R.L. Gardas, A.M. Fernandes, I.M. Marrucho, L.M.N.B.F. Santos, J.A.P. Coutinho. *J. Phys. Chem. B* 111 (2007) 13082
4	***Surface tensions of imidazolium based ionic liquids: anion, cation, temperature and water effect*** M.G. Freire, P.J. Carvalho, A.M. Fernandes, I.M. Marrucho, A.J. Queimada, J.A.P. Coutinho. *J. Colloid Interface Sci.* 314 (2007) 621
5	***P, (rho), t measurements of imidazolium based ionic liquids*** R.L. Gardas, M.G. Freire, P.J. Carvalho, I.M. Marrucho, I.M.A. Fonseca, A.G.M. Ferreira, J.A.P. Coutinho. *J. Chem. Eng. Data* 52 (2007) 1881
6	***Mutual solubilities of water and the [Cnmim][Tf_2N] hydrophobic ionic liquids*** M.G. Freire, P.J. Carvalho, R.L. Gardas, I.M. Marrucho, L.M.N.B.F. Santos, J.A.P. Coutinho. *J. Phys. Chem. B* 112 (2008) 1604
7	***Surface tensions for the 1-alkyl-3-methylimidazolium bis(trifluoromethylsulfonyl)imide ionic liquids*** P.J. Carvalho, M.G. Freire, I.M. Marrucho, A.J. Queimada, J.A.P. Coutinho. *J. Chem. Eng. Data* 53 (2008) 1346
8	***Solubility of water in tetradecyltrihexylphosphonium-based ionic liquids*** M.G. Freire, P.J. Carvalho, R.L. Gardas, L.M.N.B.F. Santos, I.M. Marrucho, J.A.P. Coutinho. *J. Chem. Eng. Data* 53 (2008) 2378
9	***Measurements and correlation of high-pressure densities of imidazolium-based ionic liquids*** L.I.N. Tomé, P.J. Carvalho, M.G. Freire, I.M. Marrucho, I.M.A. Fonseca, A.G.M. Ferreira, J.A.P. Coutinho, R.L. Gardas. *J. Chem. Eng. Data* 53 (2008) 1914
10	***Densities and derived thermodynamic properties of imidazolium-, pyridinium-, pyrrolidinium-, and piperidinium-based ionic liquids*** R.L. Gardas, H.F. Costa, M.G. Freire, P.J. Carvalho, I.M. Marrucho, I.M.A. Fonseca, A.G.M. Ferreira, J.A.P. Coutinho. *J. Chem. Eng. Data* 53 (2008) 805

11	***High pressure phase behavior of carbon dioxide in 1-alkyl-3-methylimidazolium bis(trifluoromethylsulfonyl)imide ionic liquids*** P.J. Carvalho, V.H. Álvarez, J.J.B. Machado, J. Pauly, J. Daridon, I.M. Marrucho, M. Aznar, J.A.P. Coutinho. *J. Supercrit. Fluids* 48 (2009) 99
12	***Ion specific effects on the mutual solubilities of water and hydrophobic ionic liquids*** M.G. Freire, P.J. Carvalho, A.M.S. Silva, L.M.N.B.F. Santos, L.P.N. Rebelo, I.M. Marrucho, J.A.P. Coutinho. *J. Chem. Phys. B* 113 (2009) 202
13	***Specific solvation interactions of CO_2 on acetate and trifluoroacetate imidazolium based ionic liquids at high pressures*** P.J. Carvalho, V.H. Álvarez, B. Schröder, A.M. Gil, I.M. Marrucho, M. Aznar, L.M.N.B.F. Santos, J.A.P. Coutinho. *J. Phys. Chem. B* 113 (2009) 6803
14	***High pressure phase behavior of carbon dioxide in 1-butyl-3-methylimidazolium bis(trifluoromethylsulfonyl)imide and 1-butyl-3-methylimidazolium dicyanamide ionic liquids*** P.J. Carvalho, V.H. Alvarez, I.M. Marrucho, M. Aznar, J.A.P. Coutinho. *J. Supercrit. Fluids* 50 (2009) 105
15	***Solubility of water in fluorocarbons: experimental and COSMO-RS prediction results*** M.G. Freire, P.J. Carvalho, L.M.N.B.F. Santos, L.R. Gomes, I.M. Marrucho, J.A.P. Coutinho. *J. Chem. Thermodyn.* 42 (2010) 213
16	***High carbon dioxide solubilities in trihexyltetradecylphosphonium-based ionic liquids*** P.J. Carvalho, V.H. Álvarez, I.M. Marrucho, M. Aznar, J.A.P. Coutinho. *J. Supercrit. Fluids* 52 (2010) 258
17	***Structural and positional isomerism influence through the physical properties of pyridinium NTf_2-based ionic liquids: pure and water-saturated mixtures*** F.S. Oliveira, M.G. Freire, P.J. Carvalho, I.M. Marrucho, J.A.P. Coutinho. *J. Chem. Eng. Data* 55 (2010) 4514
18	***On the nonideality of CO_2 solutions in ionic liquids and other low volatile solvents*** P.J. Carvalho, J.A.P. Coutinho. *J. Phys. Chem. Lett.* 1 (2010) 774
19	***Effect of water on the viscosities and densities of 1-butyl-3-methylimidazolium dicyanamide and 1-butyl-3-methylimidazolium tricyanomethane at atmospheric pressure*** P.J. Carvalho, T. Regueira, L.M.N.B.F. Santos, J. Fernandez, J.A.P. Coutinho. *J. Chem. Eng. Data* 55 (2010) 645

20	***Non-ideality of solutions of NH_3, SO_2, and H_2S in ionic liquids and the prediction of their solubilities using the flory-huggins model*** P.J. Carvalho, J.A.P. Coutinho. *Energy & Fuels* 24 (2010) 6662
21	***Surface tensions of bis(trifluoromethylsulfonyl)imide anion-based ionic liquids*** P.J. Carvalho, C.M.S.S. Neves, J.A.P. Coutinho. *J. Chem. Eng. Data* 55 (2010) 3807
22	***High pressure CO_2 solubility in n-methyl-2-hydroxyethylammonium protic ionic liquids*** S. Mattedi, P.J. Carvalho, J.A.P. Coutinho, V.H. Alvarez, M. Iglesias. *J. Supercrit. Fluids* 56 (2011) 224
23	***Viscosity of (C2-C14) 1-alkyl-3-methylimidazolium bis(trifluoromethylsulfonyl)amide ionic liquids in an extended temperature range*** M. Tariq, P.J. Carvalho, J.A.P. Coutinho, I.M. Marrucho, J.N.C. Lopes, L.P.N. Rebelo. *Fluid Phase Equilib.* 301 (2011) 22
24	***Measurements and correlation of high-pressure densities of phosphonium based ionic liquids*** L.I.N. Tomé, R.L. Gardas, P.J. Carvalho, M.J. Pastoriza-Gallego, M.M. Piñeiro, J.A.P. Coutinho. *J. Chem. Eng. Data* 56 (2011) 2205-2217
25	***High pressure phase behavior of carbon dioxide in carbon disulphide and carbon tetrachloride*** P.J. Carvalho, A.R. Ferreira, M.B. Oliveira, M. Besnard, M.I. Cabaço, J.A.P. Coutinho. *J. Chem. Eng. Data* 56 (2011) 2786-2792
26	***Thermophysical Properties of Pure and Water-saturated Tetradecyltrihexylphosphonium-based Ionic Liquids*** C.M.S.S. Neves, P.J. Carvalho, M.G. Freire, J.A.P. Coutinho. *J. Chem. Thermodynamic* 43 (2011) 948-957
27	***The Polarity Effect Upon the Methane Solubility in Ionic Liquids: A Contribution for the Design of Ionic Liquids for Enhanced CO2/CH4 and H2S/CH4 Selectivities*** P.J. Carvalho and J.A.P. Coutinho. *Energy Environ. Sci.* 4 (2011) 4614-4619
28	***Thermophysical Characterization of Ionic Liquids Able To Dissolve Biomass*** M.G. Freire, A.R.R. Teles, M.A.A. Rocha, B. Schröder, C.M.S.S. Neves, P.J. Carvalho, D.V. Evtuguin, L.M.N.B.F. Santos and J.A.P. Coutinho. *J. Chem. Eng. Data* (2011) doi:10.1021/je200790q
29	***Chameleonic Behavior of Ionic Liquids and Its Impact on the Estimation of Solubility Parameters*** M.L.S. Batista, C.M.S.S. Neves, P.J. Carvalho, R. Gani and J.A.P. Coutinho. *J. Phys. Chem. B* 115 (2011) 12879-12888

A. Appendix A

Supplementary data for the "Carbon Dioxide Interactions" chapter

Table A.1. Experimental Solubility Data of CO_2 (1) + CCl_4 (2).

x_1	T /K	p /MPa	x_1	T /K	p /MPa	x_1	T /K	p /MPa
0.16	293.22	1.09	0.16	313.25	1.57	0.16	333.26	2.10
0.20	293.20	1.38	0.20	313.21	2.00	0.20	333.26	2.67
0.30	293.22	2.04	0.30	313.20	2.93	0.30	333.18	3.87
0.40	293.16	2.61	0.40	313.31	3.79	0.40	333.17	5.02
0.50	293.20	3.07	0.50	313.29	4.49	0.50	333.27	6.04
0.60	293.23	3.51	0.60	313.26	5.15	0.60	333.23	7.02
0.70	293.30	3.84	0.70	313.28	5.73	0.70	333.17	7.85

Table A.2. Experimental Solubility Data of CO_2 (1) + CS_2 (2).

x_1	T /K	p /MPa	x_1	T /K	p /MPa	x_1	T /K	p /MPa
0.05	293.32	0.97	0.05	313.33	1.36	0.05	333.21	1.75
0.10	293.24	1.93	0.10	313.28	2.55	0.10	333.18	3.18
0.20	293.32	3.22	0.20	313.21	4.34	0.20	332.97	5.44
0.30	293.36	3.87	0.30	313.36	5.37	0.30	333.12	6.92
0.40	293.29	4.09	0.40	313.25	5.90	0.40	333.17	7.81
0.50	293.25	4.13	0.50	313.23	6.11	0.50	333.16	8.30
0.60	293.18	4.07	0.60	313.24	6.12	0.60	333.12	8.52
0.68	293.20	4.08	0.68	313.16	6.19			
0.89	293.16	4.59	0.89	313.53	7.11			
0.93	293.19	4.74	0.93	313.39	7.39			
0.96	293.33	4.91						

Table A.3. CPA Pure Compound Parameters for CO_2, CCl_4 and CS_2 and Modeling Results.

						AAD %
	***T* range**	a_0 **(J.m^3·mol^{-2})**	c_1	$b\times10^5$ **(m^3·mol^{-1})**	p	ρ
CO_2	$T_{melt} - 0.9T_c$	0.35	0.76	2.72	0.22	0.83
CCl_4	$0.45T_c$-$0.85T_c$	1.9	0.74	8.10	1.01	0.63
CS_2	$0.45T_c$-$0.85T_c$	1.14	0.60	4.95	0.76	0.74

Table A.4. Predicted Henry's Constant for the CO_2 + CCl_4 and CO_2 + CS_2 Systems.

CO_2 + CS_2		CO_2 + CCl_4		
k_{ij} = 0.1598; x_{CO2} AAD% = 9.6		x_{CO2} AAD% = 3.9		
***T* /K**	H_{12} **/MPa**	***T* /K**	H_{12} **/MPa**	k_{ij}
293.15	18.56	293.15	7.06	0.075
313.15	24.02	313.15	9.62	0.087
333.15	30.51	333.15	12.82	0.093

Table A.5. Coefficients A and B in Equation (4.14) and Partial Molar Enthalpy and Partial Molar Entropy of Solvation Obtained for CO_2 + CCl_4 and CO_2 + CS_2 Systems.

	A	***B***	$\lvert\Delta H_{12}\rvert$ **%**	$\Delta_{solv}H$ **kJ·mol^{-1}**	$\Delta_{solv}S$ **J·mol^{-1}·K^{-1}**	$-T\cdot\Delta_{solv}S\,\lvert_{T=298\ K}$ **kJ·mol^{-1}**
CS_2	-1212.900	9.359	0.29	-10.08	-77.82	23.20
CCl_4	-1455.725	9.220	0.35	-12.10	-76.66	22.86

B. Appendix B

Supplementary data for the "High Pressure Phase Behavior of Carbon Dioxide in 1-alkyl-3-methylimidazolium bis(trifluoromethylsulfonyl)imide Ionic Liquids" chapter

Table B.1. Bubble point data for the system CO_2 (1) + [C_2mim][NTf_2] (2).

x_1	T /K	p /MPa	x_1	T /K	p /MPa	x_1	T /K	p /MPa	x_1	T /K	p /MPa	x_1	T /K	p /MPa
0.221	293.65	0.620	0.327	293.24	1.130	0.418	293.50	1.688	0.503	293.50	2.398	0.560	292.41	2.879
0.221	298.52	0.725	0.327	298.50	1.295	0.418	298.55	1.945	0.503	298.29	2.706	0.560	298.24	3.351
0.221	303.25	0.837	0.327	303.41	1.462	0.418	303.48	2.185	0.503	303.41	3.076	0.560	303.11	3.778
0.221	313.59	1.083	0.327	313.32	1.868	0.418	313.32	2.745	0.503	313.24	3.845	0.560	313.22	4.780
0.221	323.39	1.345	0.327	323.13	2.292	0.418	323.10	3.365	0.503	323.27	4.725	0.560	323.07	5.883
0.221	333.15	1.645	0.327	333.17	2.758	0.418	333.23	4.054	0.503	333.16	5.708	0.560	333.16	7.173
0.221	343.25	1.957	0.327	343.27	3.287	0.418	343.30	4.836	0.503	343.11	6.769	0.560	343.19	8.569
0.221	353.10	2.276	0.327	353.16	3.850	0.418	353.02	5.565	0.503	353.18	7.912	0.560	353.14	10.115
0.221	363.23	2.680	0.327	363.19	4.408	0.418	363.17	6.436	0.503	363.35	9.128	0.560	363.34	11.821

x_1	T /K	p /MPa	x_1	T /K	p /MPa	x_1	T /K	p /MPa	x_1	T /K	p /MPa
0.606	292.60	3.387	0.650	292.16	3.825	0.700	292.82	4.736	0.750	293.44	16.076
0.606	298.29	3.942	0.650	297.70	4.485	0.700	298.15	5.520	0.750	298.09	19.048
0.606	303.46	4.506	0.650	303.54	5.230	0.700	303.30	6.535	0.750	303.26	22.130
0.606	313.30	5.686	0.650	313.35	6.715	0.700	313.24	10.180	0.750	313.19	28.187
0.606	323.11	7.103	0.650	323.10	8.550	0.700	323.09	14.450	0.750	323.14	33.787
0.606	332.88	8.695	0.650	333.16	10.905	0.700	333.04	18.885	0.750	333.08	38.898
0.606	343.13	10.649	0.650	343.08	13.565	0.700	343.15	23.085	0.750	343.29	43.565
0.606	353.07	12.650	0.650	353.05	16.435	0.700	353.22	27.066	0.750	353.08	47.850
0.606	363.55	14.996	0.650	363.22	19.450	0.700	363.22	30.858			

Table B.2. Bubble point data the system CO_2 (1) + [C_5mim][NTf_2] (2).

x_1	T /K	p /MPa	x_1	T /K	p /MPa	x_1	T /K	p /MPa	x_1	T /K	p /MPa	x_1	T /K	p /MPa
0.212	298.65	0.720	0.351	298.77	1.517	0.390	298.65	1.736	0.453	298.70	2.152	0.619	298.55	3.915
0.212	303.61	0.799	0.351	303.34	1.675	0.390	303.39	1.915	0.453	303.38	2.395	0.619	303.33	4.360
0.212	313.15	1.044	0.351	313.21	2.031	0.390	312.99	2.334	0.453	312.85	2.927	0.619	312.90	5.426
0.212	323.35	1.252	0.351	323.05	2.468	0.390	322.52	2.785	0.453	322.62	3.512	0.619	322.72	6.645
0.212	333.25	1.525	0.351	332.85	2.894	0.390	332.54	3.312	0.453	333.07	4.218	0.619	332.50	7.984
0.212	343.00	1.780	0.351	343.19	3.398	0.390	342.47	3.858	0.453	342.53	4.839	0.619	343.04	9.650
0.212	353.49	2.124	0.351	353.26	3.907	0.390	352.85	4.430	0.453	352.65	5.598	0.619	352.86	11.212
0.212	363.29	2.370	0.351	362.68	4.400	0.390	363.05	5.050	0.453	363.05	6.430	0.619	362.95	12.990
0.212	293.75	0.618	0.351	293.65	1.322	0.390	293.73	1.564	0.453	293.75	1.943	0.619	293.75	3.486

x_1	T /K	p /MPa	x_1	T /K	p /MPa	x_1	T /K	p /MPa	x_1	T /K	p /MPa
0.654	298.47	4.460	0.701	298.45	5.245	0.751	298.42	8.365	0.802	298.37	30.098
0.654	303.32	5.030	0.701	303.49	5.990	0.751	303.38	10.625	0.802	303.38	32.881
0.654	313.00	6.344	0.701	313.19	7.732	0.751	313.57	15.435	0.802	293.30	27.460
0.654	322.96	7.870	0.701	322.85	10.198	0.751	323.34	19.995	0.802	313.44	38.299
0.654	333.56	9.778	0.701	333.28	13.225	0.751	333.11	24.280	0.802	323.19	43.225
0.654	343.37	11.776	0.701	343.08	16.438	0.751	343.05	28.266	0.802	333.08	47.960
0.654	353.30	13.980	0.701	353.06	19.692	0.751	353.20	32.086	0.802	343.14	52.431
0.654	362.95	16.246	0.701	363.12	22.730	0.751	363.11	35.340	0.802	353.13	56.146
0.654	293.76	3.974	0.701	293.43	4.617	0.751	293.42	5.609	0.802	363.29	59.805

Table B.3. Properties of the substances used in the modeling

Compound	T_c /K	P_c /MPa	ω	r	q
CO_2	304.21[a]	7.38[a]	0.2236[a]	3.26[c]	2.38[c]
$[C_2mim][NTf_2]$	1214.22[b]	3.37[b]	0.2818[b]	28.77[c]	18.16[c]
$[C_5mim][NTf_2]$	1249.43[b]	2.63[b]	0.4123[b]	34.23[d]	21.84[d]

a[280], b[281], c[82], d[82]

Table B.4. Interpolated VLE data for the system supercritical CO_2 (1) + $[C_2mim][NTf_2]$ (2) and CO_2 (1) + $[C_5mim][NTf_2]$ (2).

CO_2 (1) + $[C_2mim][NTf_2]$ (2)									
x_1 / T /K	0.221	0.327	0.418	0.503	0.56	0.606	0.65	0.7	0.75
293.15	-	-	-	-	2.935	3.437	3.942	4.783	
298.15	0.718	1.284	1.915	2.699	3.342	3.922	4.540	5.520	19.065
303.15	0.830	1.453	2.178	3.049	3.784	4.459	5.178	6.497	22.207
313.15	1.073	1.861	2.746	3.835	4.772	5.687	6.681	10.142	28.178
323.15	1.341	2.293	3.372	4.724	5.899	7.121	8.561	14.477	33.729
333.15	1.634	2.757	4.054	5.706	7.164	8.762	10.902	18.933	38.862
343.15	1.953	3.280	4.792	6.770	8.568	10.608	13.585	23.085	43.575
353.15	2.297	3.849	5.587	7.907	10.110	12.660	16.464	27.039	-
363.15	2.666	4.406	6.439	9.105	11.791	14.919	19.429	30.832	-
CO_2 (1) + $[C_5mim][NTf_2]$ (2)									
X_1 / T /K	0.212	0.351	0.39	0.453	0.619	0.654	0.701	0.751	0.802
298.15	0.702	1.483	1.718	2.143	3.872	4.429	5.205	8.065	29.980
303.15	0.807	1.664	1.905	2.393	4.352	5.005	5.937	10.577	32.753
313.15	1.028	2.050	2.341	2.938	5.445	6.343	7.723	15.399	38.148
323.15	1.266	2.465	2.817	3.540	6.701	7.919	10.281	19.950	43.205
333.15	1.520	2.912	3.345	4.195	8.103	9.717	13.185	24.231	47.993
343.15	1.792	3.388	3.895	4.899	9.635	11.724	16.461	28.241	52.435
353.15	2.080	3.895	4.447	5.647	11.280	13.925	19.720	31.981	56.153

Table B.5. Results of the consistency test.

Reference	NP	T /K	k_{12}	A_{12} (kJ/kmol)	A_{21} (kJ/kmol)	$\|\Delta P\|$ %	Result
CO_2 + $[C_2mim][NTf_2]$							
[17]	8	363.15	-0.1904	3767.474	-1202.621	0.7	TC
	4	293.15	-0.222	49988.291	-1791.751	0.5	TC
	9	298.15	0.0057	20355.366	-2001.440	2.4	NFC/TC
	9	303.15	-0.0090	8795.384	-1923.852	2.0	NFC/TC
	9	313.15	0.0204	5854.406	-1747.716	1.1	NFC/TC
[This work]	9	323.15	0.0108	4879.271	-1604.227	1.0	NFC/TC
	9	333.15	0.0038	4323.089	-1491.756	1.4	NFC/TC
	9	343.15	-0.0077	3830.967	-1359.963	1.6	NFC/TC
	8	353.15	-0.1468	3458.742	-1158.891	0.5	TC
	8	363.15	-0.1317	3048.107	-1016.976	0.8	TC
CO_2 + $[C_5mim][NTf_2]$							
	9	298.15	0.0639	2642.548	-854.215	1.6	NFC/TC
	9	303.15	0.0606	2477.849	-773.810	1.5	NFC/TC
	9	313.15	0.0489	2232.933	-637.261	1.9	NFC/TC
[This work]	9	323.15	0.0364	2057.406	-528.352	2.4	NFC/TC
	9	333.15	0.0247	1907.507	-429.010	2.8	NFC/TC
	9	343.15	0.0195	1805.985	-356.494	2.9	NFC/TC
	9	353.15	0.0172	1728.749	-298.579	3.0	TI

Table B.6. Detailed results for CO_2 (1) + [C_2mim][NTf_2] (2) at 298.15 K.

A_P	A_ϕ	$\%\Delta A_i$	P^{exp}	P^{cal}	$\%\Delta P$	y_1^{cal}	y_2^{cal}	x_1
(8 data points) k_{12} = -0.1904, A_{12} = 3767.474, A_{21} = -1202.621, $\|\Delta P\|(\%)$ = 0.7								
10865327.5	10387930.5	-4.4	1.303	1.317	1.1	1.0000	0.0000	0.1230
5441391.3	5567544.7	2.3	2.543	2.514	-1.1	1.0000	0.0000	0.2120
2379790.2	2291077.1	-3.7	4.036	4.044	0.2	1.0000	0.0000	0.3030
701940.6	703925.0	0.3	6.023	5.988	-0.6	1.0000	0.0000	0.3920
78335.4	73487.2	-6.2	8.569	8.602	0.4	1.0000	0.0000	0.4790
31674.7	32701.5	3.2	10.258	10.213	-0.4	1.0000	0.0000	0.5190
4092.1	3503.8	-14.4	12.832	12.973	1.1	1.0000	0.0000	0.5700
-	-	-	14.770	14.676	-0.6	0.9999	0.0001	0.5930

Table B.7. Detailed results for CO_2 (1) + [C_2mim][NTf2] (2) at 298.15 K.

A_P	A_ϕ	$\%\Delta A_i$	P^{exp}	P^{cal}	$\%\Delta P$	y_1^{cal}	y_2^{cal}	x_1
(9 data points) k_{12} = 0.0057, A_{12} = 20355.366, A_{21} = -2001.440, $\|\Delta P\|(\%)$ = 2.4								
5.81E+09	5.23E+09	-9.9	0.718	0.763	6.3	1.0000	0.0000	0.221
4.34E+09	4.09E+09	-5.7	1.284	1.294	0.8	1.0000	0.0000	0.327
3.48E+09	3.30E+09	-5.2	1.915	1.889	-1.4	1.0000	0.0000	0.418
1.80E+09	1.82E+09	0.6	2.699	2.619	-3.0	1.0000	0.0000	0.503
1.09E+09	1.21E+09	10.3	3.342	3.248	-2.8	1.0000	0.0000	0.560
7.81E+08	9.40E+08	20.3	3.922	3.874	-1.2	1.0000	0.0000	0.606
7.69E+08	8.71E+08	13.4	4.540	4.618	1.7	1.0000	0.0000	0.650
3.56E+14	2.17E+15	511.2	5.520	5.759	4.3	1.0000	0.0000	0.700
-	-	-	19.065	18.939	-0.7	1.0000	0.0000	0.750
(8 data points) k_{12} = 0.2655, A_{12} = 2013.583, A_{21} = -993.493, $\|\Delta P\|(\%)$ = 2.4								
7.39E+09	6.72E+09	-9.2	0.718	0.754	5.0	1.0000	0.0000	0.221
6.19E+09	5.88E+09	-5.0	1.284	1.283	-0.1	1.0000	0.0000	0.327
5.45E+09	5.20E+09	-4.5	1.915	1.877	-1.9	1.0000	0.0000	0.418
2.99E+09	3.01E+09	0.9	2.699	2.609	-3.4	1.0000	0.0000	0.503
1.79E+09	1.97E+09	10.0	3.342	3.237	-3.1	1.0000	0.0000	0.560
1.16E+09	1.38E+09	18.8	3.922	3.859	-1.6	1.0000	0.0000	0.606
8.25E+08	9.02E+08	9.3	4.540	4.589	1.1	1.0000	0.0000	0.650
-	-	-	5.520	5.673	2.8	1.0000	0.0000	0.700

Table B.8. Detailed results for CO_2 (1) + [C_5mim][NTf_2] (2) at 298.15 K.

A_P	A_ϕ	$\%\Delta A_i$	P^{exp}	P^{cal}	$\%\Delta P$	y_1^{cal}	y_2^{cal}	x_1
(9 data points) k_{12} = 0.0639, A_{12} = 2642.548, A_{21} = -854.215, $\|\Delta P\|(\%)$ = 1.6								
1.11E+12	9.85E+11	-11.3	0.702	0.728	3.7	1.0000	0.0000	0.212
1.96E+11	2.12E+11	8.0	1.483	1.431	-3.5	1.0000	0.0000	0.351
2.57E+11	2.82E+11	9.7	1.718	1.677	-2.4	1.0000	0.0000	0.390
4.55E+11	4.62E+11	1.5	2.143	2.137	-0.3	1.0000	0.0000	0.453
2.23E+10	2.14E+10	-3.8	3.872	3.911	1.0	1.0000	0.0000	0.619
1.13E+10	1.30E+10	14.2	4.429	4.452	0.5	1.0000	0.0000	0.654
6.92E+09	7.76E+09	12.2	5.205	5.344	2.7	1.0000	0.0000	0.701
5.54E+04	2.71E+04	-51.0	8.065	8.036	-0.4	1.0000	0.0000	0.751
-	-	-	29.980	29.988	0.0	0.9999	0.0001	0.802
(8 data points) k_{12} = -0.1037, A_{12} = 4558.106, A_{21} = -1265.823, $\|\Delta P\|(\%)$ = 1.5								
8.94E+11	7.86E+11	-12.1	0.702	0.733	4.3	1.0000	0.0000	0.212
1.37E+11	1.47E+11	7.3	1.483	1.435	-3.2	1.0000	0.0000	0.351
1.67E+11	1.82E+11	8.8	1.718	1.680	-2.2	1.0000	0.0000	0.390
2.67E+11	2.67E+11	0.0	2.143	2.136	-0.3	1.0000	0.0000	0.453
8.66E+09	8.21E+09	-5.1	3.872	3.884	0.3	1.0000	0.0000	0.619
3.92E+09	4.42E+09	12.6	4.429	4.415	-0.3	1.0000	0.0000	0.654
2.03E+09	2.37E+09	16.5	5.205	5.286	1.6	1.0000	0.0000	0.701
-	-	-	8.065	8.061	-0.1	1.0000	0.0000	0.751

Table B.9. Estimated independent-temperature interaction parameters for the CO_2 (1) + ILs (2) systems.

System	NP	x_1	k_{12}	A_{12} kJ/kmol	A_{21} kJ/kmol	$\lvert\Delta P\rvert$ %	Max y_2[a]
CO_2 + $[C_2mim][NTf_2]$	72	0.221-0.700	0.1061	4224.889	-1556.505	2.8	5.5
CO_2 + $[C_5mim][NTf_2]$	63	0.212-0.751	0.0113	2613.005	-785.272	3.0	11.8

[a] These values are expressed as $y_2 \times 10^5$

Table B.10. Interaction parameter for the model and Henry's Constant of CO_2 (1) + ionic liquids (2).

T (K)	$\|\Delta P\|$ /%	H_{12} /MPa
CO_2 + $[C_2mim][NTf_2]$		
k_{ij} = 0. 0077, A_{12} = 2284.160, A_{21} = -723.030		
313.15	0.7	4.66
323.15	0.7	5.50
333.15	0.7	6.40
343.15	0.8	7.36
353.15	0.8	8.37
363.15	0.8	9.43
CO_2 + $[C_5mim][NTf_2]$		
k_{ij} = 0.0113,	A_{12} =2613.005,	A_{21} = -785.272
298.15	1.5	2.79
303.15	1.0	3.16
313.15	0.8	3.92
323.15	1.2	4.78
333.15	0.4	6.23
343.15	0.6	7.63

Table B.11. Coefficients A, B and C obtained for CO_2 (1) + ionic liquids (2)

ionic liquid	A	B	C	$\|\Delta H_{12}\|$ (%)
$[C_2mim][NTf2]$	-153854.908	-685.377	5.298	0.1
$[C_5mim][NTf2]$	-189365.718	-488.274	4.827	0.04

Table B.12. Thermodynamic functions of solvation for CO_2 (1) + ionic liquids (2) at several temperatures.

T (K)	$\Delta_{sol}H$ /J/mol	$\Delta_{sol}S$ /J/mol.K
	$[C_2mim][NTf_2]$	
298.15	-14279.3	-47.5
303.15	-14137.8	-46.5
313.15	-13868.3	-44.3
323.15	-13615.5	-42.3
333.15	-13377.8	-40.3
343.15	-13154.0	-38.4
353.15	-12942.9	-36.5
363.15	-12743.4	-34.7
	$[C_5mim][NTf_2]$	
298.15	-14621.1	-48.8
303.15	-14446.9	-47.6
313.15	-14115.2	-45.1
323.15	-13804.0	-42.8
333.15	-13511.5	-40.5
343.15	-13236.1	-38.3

C. Appendix C

Supplementary data for the “Specific Solvation Interactions of CO2 on Acetate and Trifluoroacetate Imidazolium Based Ionic Liquids at High Pressures“ chapter

Table C.1. Bubble point data of the system CO_2 (1) + [C_4mim][Ac].

x_1	T /K	p /MPa	x_1	T /K	p /MPa	x_1	T /K	p /MPa	x_1	T /K	p /MPa	x_1	T /K	p /MPa
0.201	323.05	0.230	0.251	313.09	0.498	0.300	313.04	1.398	0.351	313.04	2.589	0.402	313.07	4.090
0.201	333.07	0.355	0.251	322.96	0.830	0.300	323.22	1.923	0.351	322.83	3.360	0.402	323.57	5.272
0.201	343.18	0.652	0.251	333.30	1.275	0.300	333.33	2.515	0.351	333.42	4.288	0.402	333.35	6.580
0.201	353.10	0.971	0.251	343.05	1.695	0.300	343.10	3.205	0.351	343.22	5.265	0.402	343.16	8.060
			0.251	353.20	2.235	0.300	352.98	3.980	0.351	353.22	6.430	0.402	353.24	9.850
x_1	T /K	p /MPa	x_1	T /K	p /MPa	x_1	T /K	p /MPa	x_1	T /K	p /MPa			
0.450	313.09	5.730	0.500	322.98	13.478	0.550	313.31	27.965	0.599	313.10	67.371			
0.450	323.00	7.394	0.500	333.06	18.051	0.550	323.40	34.865	0.599	323.09	75.526			
0.450	333.27	9.564	0.500	343.10	22.985	0.550	333.37	41.807						
0.450	343.06	12.188	0.500	353.13	28.055	0.550	343.25	48.107						
0.450	353.18	15.281				0.550	353.05	53.904						

Table C.2. Bubble point data of the system CO_2 (1) + [C_4mim][TFA].

x_1	T /K	p /MPa	x_1	T /K	p /MPa	x_1	T /K	p /MPa	x_1	T /K	p /MPa
0.225	293.43	0.979	0.300	293.25	1.540	0.401	293.52	2.419	0.502	293.61	3.513
0.225	303.22	1.338	0.300	303.30	2.056	0.401	303.23	3.108	0.502	303.40	4.611
0.225	313.20	1.706	0.300	313.15	2.619	0.401	313.14	3.959	0.502	313.18	5.860
0.225	323.11	2.146	0.300	323.08	3.160	0.401	323.04	4.84	0.502	323.49	7.413
0.225	333.35	2.587	0.300	333.06	3.912	0.401	333.08	5.996	0.502	333.35	9.135
0.225	343.23	3.105	0.300	343.15	4.726	0.401	343.02	6.957	0.502	343.07	11.151
0.225	353.08	3.612	0.300	353.13	5.559	0.401	353.07	8.144	0.502	353.03	13.225
0.225	363.04	4.165	0.300	363.18	6.416	0.401	363.07	9.337	0.502	363.03	15.498

x_1	T /K	p /MPa	x_1	T /K	p /MPa	x_1	T /K	p /MPa
0.601	293.44	7.936	0.650	293.46	26.422	0.679	293.59	43.625
0.601	303.21	13.268	0.650	303.35	32.581	0.679	303.34	50.189
0.601	313.21	18.548	0.650	313.17	37.835	0.679	313.08	55.966
0.601	323.21	22.835	0.650	323.04	43.392	0.679	323.08	62.473
0.601	333.09	28.263	0.650	333.25	48.458			
0.601	343.14	32.589	0.650	343.06	52.947			
0.601	353.10	36.545	0.650	353.11	56.890			
0.601	363.12	42.075	0.650	363.10	62.989			

Table C.3. Estimated interaction parameters, for the thermodynamically consistent data, and Henry constant predicted for the CO_2 (1) + ILs (2) systems at different temperatures.

Reference	NP	T /K	k_{ij}	α_{12}	g_{12}-g_{22} kJ /kmol	g_{21}-g_{11} kJ/kmol	$\lvert\Delta p\rvert$ %	$\lvert\Delta A\rvert$ %	H MPa
CO_2 + [C_4mim][Ac]									
[29]	8	298.10	-0.6470	0.2166	-32855.6133	5999.5654	2.5	6.1	-
	7	323.10	1.0000	0.3244	-11206.7412	2763.3943	3.4	7.3	-
[This work]	5	313.10	-0.0146	0.2979	-29707.8203	7932.1289	1.3	3.8	0.056
	7	323.09	-0.3497	0.2482	-50410.7500	-1595.7640	1.0	4.6	0.086
	7	333.00	0.2981	0.3177	-40720.8945	-2724.8025	2.6	9.4	0.121
	7	343.00	-0.8572	0.3043	-44254.0312	89950.4766	4.2	10.8	0.137
	6	348.00	0.7969	0.4229	-32920.5625	-3534.8833	1.2	2.7	0.203
	6	352.98	0.9949	0.4392	-33570.1133	-4218.7607	0.8	3.7	0.253
CO_2 + [C_4mim][TFA]									
[This work]	5	294.00	0.2188	0.2045	34112.2930	-2444.4580	5.8	4.3	3.40
	5	298.00	0.2236	0.2059	34037.5859	-2354.5664	6.2	4.7	3.85
	5	303.00	0.2422	0.2027	34804.6875	-2620.2393	3.1	7.1	4.03
	4	313.00	0.0625	0.2132	35599.7812	-1764.0344	0.6	4.2	5.93
	4	323.00	0.2745	0.2497	33887.6523	-1097.2380	0.8	4.4	7.45
	5	333.00	-0.0063	0.2001	42388.7930	-1258.0310	0.7	15.3	8.97
	5	343.00	0.0801	0.2000	45219.8125	-781.5312	1.2	11.7	11.74
	5	348.00	-0.0001	0.2008	46516.1133	-791.0156	1.5	9.3	11.94
	5	353.00	0.1250	0.2006	47268.5469	-702.7494	1.9	12.5	13.50
	4	363.00	0.1601	0.2026	46758.0273	-1230.8120	6.0	4.4	13.57

Table C.4. Properties of the substances used in the modeling.

Compound	T_c /K	p_c /MPa	ω
CO_2	304.21[a]	7.38[a]	0.2236[a]
[C_4mim][TFA]	826.72[b]	2.09[b]	0.6891[b]
[C_4mim][Ac]	847.31[b]	2.44[b]	0.6681[b]

[a] [282]

[b] Calculated with [143]

Table C.5. Coefficients A, B, partial molar enthalpy and partial molar entropy obtained for CO_2 (1) + ILs (2).

Ionic Liquid	***A***	***B***	$\|\Delta H_{12}\|$ **%**	$\Delta_{sol}H^0$ **kJ.mol^{-1}**	$\Delta_{sol}S^0 \pm$ **J.mol^{-1}.K^{-1}**	$-T\cdot\Delta_{sol}S^0 \pm \|_{T=298\ K}$ **kJ.mol^{-1}**
[C_4mim][Ac]	-3891.728 ± 365.437	11.842 ± 1.0921	0.45	-32.4 ± 3.04	-98.5 ± 9.06	29.4 ± 2.71
[C_4mim][TFA]	-2325.298 ± 105.649	11.445 ± 0.3255	0.22	-19.3 ± 0.88	-95.2 ± 2.71	28.4 ± 0.81

[0]Standard (P_0=0.1MPa) molar entropy

Table C.6. Enthalpies of complex formation between the acetate / trifluoroacetate with the CO_2 in gas phase derived by ab initio calculation at different levels of theory (values in $kJ.mol^{-1}$).

	ΔH(Ac:CO_2) Acetate ··· CO_2	ΔH(TFA:CO_2) Trifluoroacetate ··· CO_2	Diff [(b)]
Gaussian-G3 Conformation "A"	– 41.4	– 33.7	+ 7.7
Gaussian-G3(MP2) Conformation "A"	– 39.5	– 32.2	+ 7.3
MP2/6-31+G(d) [(a)] Conformation "A"	– 42.0	– 31.8	+ 10.2
MP2/6-31+G(d) [(a)] Conformation "B"	– 29.7		

[(a)] Zero point energies and enthalpy correction were performed using the values of harmonic frequencies scaled by 0.95.
[(b)] Diff = ΔH(TFA:CO_2) - ΔH(Ac:CO_2)

D. Appendix D

Supplementary data for the "On the Nonideality of CO2 Solutions in Ionic Liquids and Other Low Volatile Solvents" chapter

The non ideality of CO_2 solutions in non volatile solvents:

To analyze the non ideality of CO_2 solutions in non volatile solvents, experimental VLE data at subcritical and near critical conditions for a wide range of systems, comprising alcohols, alkanes fatty acids, fatty acid esters, PEGs, and ionic liquids, was compared with the solubilities predicted by the Raoult's law (eq. (9.1)) described as

$$P = x_{CO_2} \gamma_{CO_2} P^{\sigma}_{CO_2} \tag{D.1}$$

where $\gamma_{CO2}=1$ is the CO_2 activity coefficient and P^{σ}_{CO2} the vapor pressure of CO_2, determined using DIPPR information and data evaluations manager for the vapor pressure of liquid CO_2

$$P^{\sigma}_{CO_2}(Pa) = e^{140.54 - \frac{4735}{T/K} - 21.268 \ln(T/K) + 0.040909\, T/K} \tag{D.2}$$

In the analysis of the other systems it must be recalled that the non-ideality results not only from differences in the energetic interactions between the molecules, as described by the residual contribution to the Gibbs free energy, but also from entropic effects due to their size and shape differences, the combinatorial contribution, as summarized by

$$G^E = G^E_{comb} + G^E_{residual} \tag{D.3}$$

The entropic effects will always have a negative contribution to the non-ideality that in terms of activity coefficients can be described by the Flory-Huggins equation

$$\ln\left(\gamma^{comb}_{CO_2}\right) = \ln\frac{\varphi_{CO_2}}{x_{CO_2}} + \left(1 - \frac{\varphi_{CO_2}}{x_{CO_2}}\right) \tag{D.4}$$

where $\varphi_{CO_2} = x_{CO_2} V_{CO_2} \Big/ \sum_i x_i V_i$ is the volume fraction and V_i are the molar volumes of the various compounds present in the mixture.

If the combinatorial contributions to the non-ideality alone are taken into account the Eq. (D.1) will become

$$P = x_{CO_2} \exp\left(\ln \frac{\varphi_{CO_2}}{x_{CO_2}} + \left(1 - \frac{\varphi_{CO_2}}{x_{CO_2}} \right) \right) P^{\sigma}_{CO_2} \qquad \text{(D.5)}$$

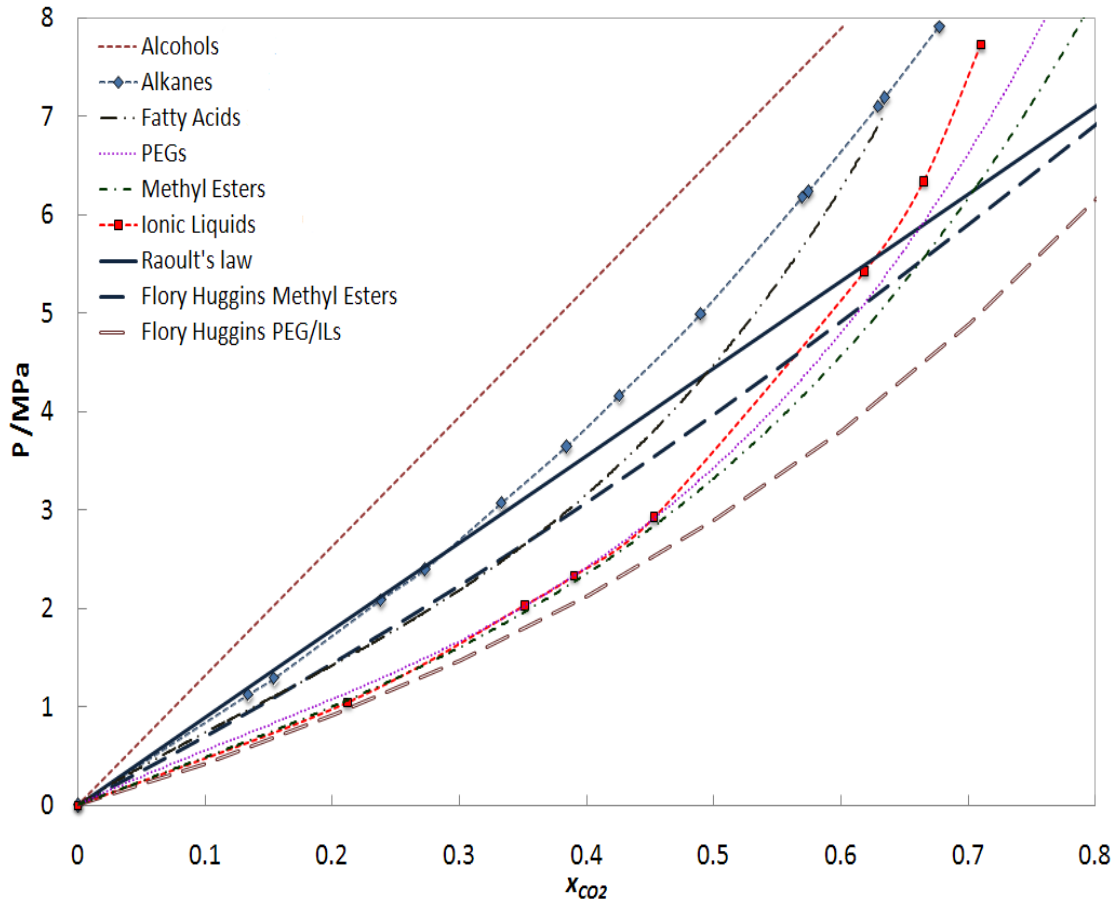

Figure D.1. *(Chapter 9 Figure 9.1)* Sketch of the pressure - CO_2 molar composition diagram for the systems CO_2 + Alcohols, CO_2 + Alkanes, CO_2 + Fatty acids, CO_2 + PEGs, CO_2 + Fatty acid esters, and , CO_2 + Ionic liquids at 313 K.

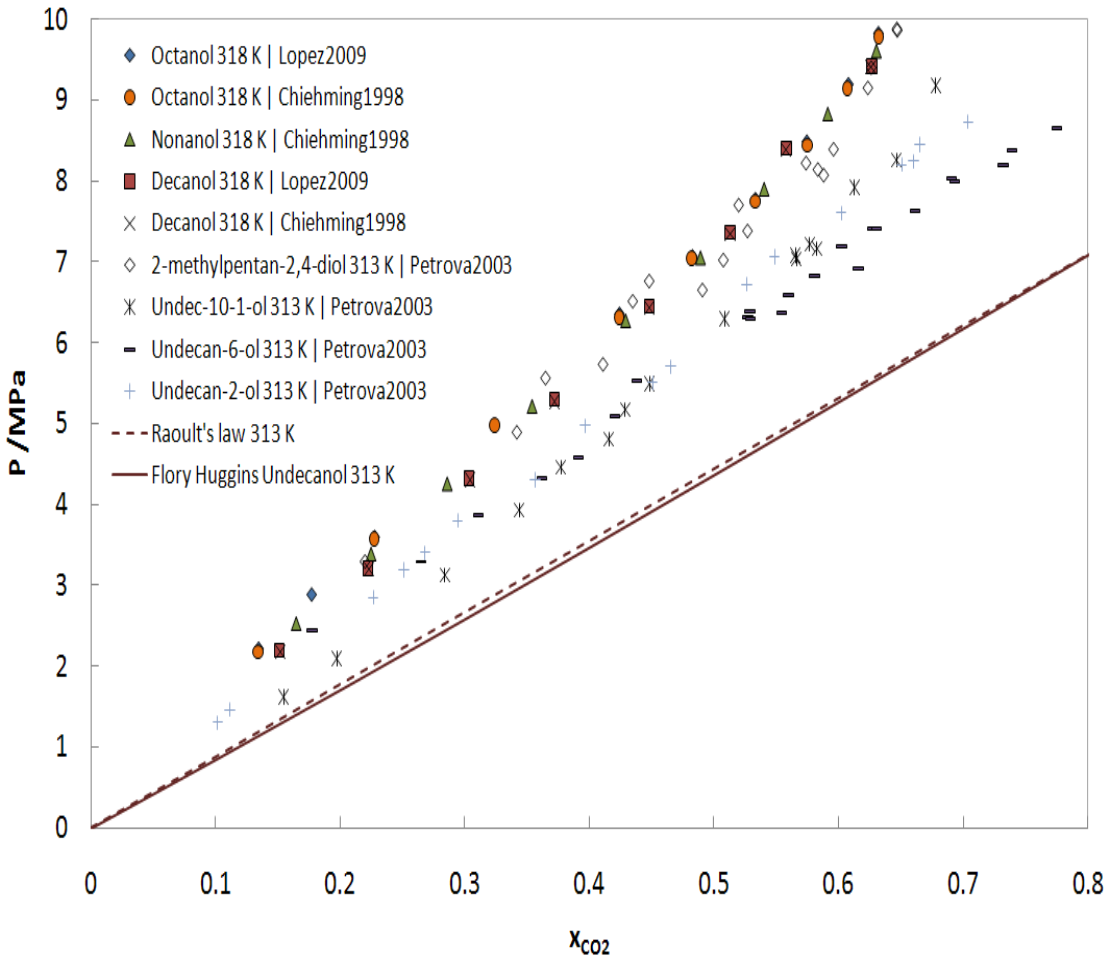

Figure D.2. Pressure - CO_2 molar composition diagram for the systems CO_2 + Alcohols at 313 K.[161, 166, 283]

In spite of the stability of the CO_2-OH EDA complexes observed spectroscopically[104, 284] the alcohol containing systems are the only with positive deviations to ideality as sketched in Figure D.1 and depicted in Figure D.2.

The pressure *vs*. mol fraction plot of the CO_2 solubility in alkanes sketched in Figure **D.3** shows a behavior very close to the ideal behavior described by Raoult's law. Given the negative deviations to ideality predicted by the Flory-Huggins model for these systems the near ideal behavior must result from positive deviations in the residual (enthalpic) term. These arise from CO_2-alkane interactions that must be weaker than the CO_2-CO_2 or alkane-alkane interactions.

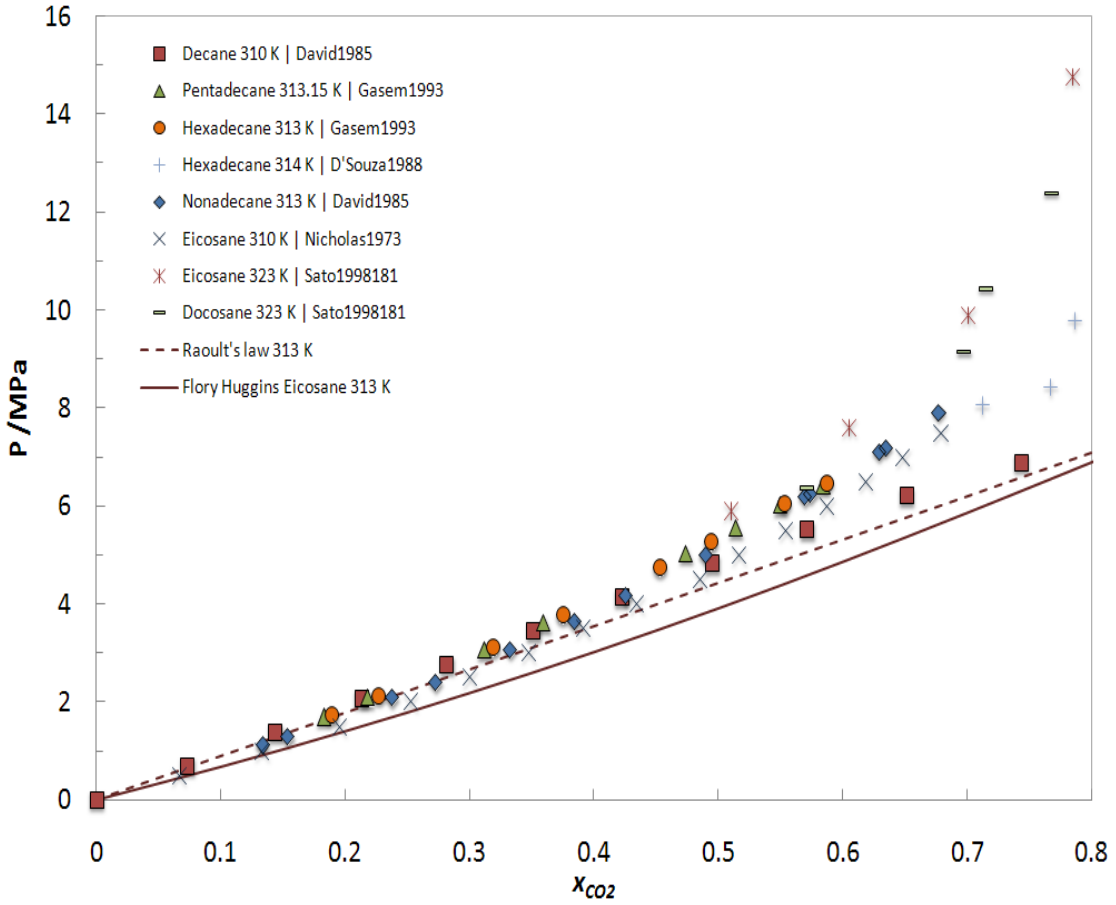

Figure D.3. Pressure - CO_2 molar composition diagram for the systems CO_2 + Akanes at 313 K.[186, 285-288]

Both fatty acids and PEGs show a non-ideal behavior than can be well described by the Flory-Huggins equation while the esters display the largest deviations to the ideal behavior observed for all the systems studied as shown in Figures D.1, D.4 and D.5. For these systems the Electron Donor-Acceptor complexes formed between CO_2 and the carbonyl group, though not stronger than those formed with the hydroxyl groups of alcohols are favored as the CO_2-carbonyl interactions seem to be energetically favorable when compared with the CO_2-CO_2 interactions and the carbonyl-carbonyl interactions established between the ester molecules.

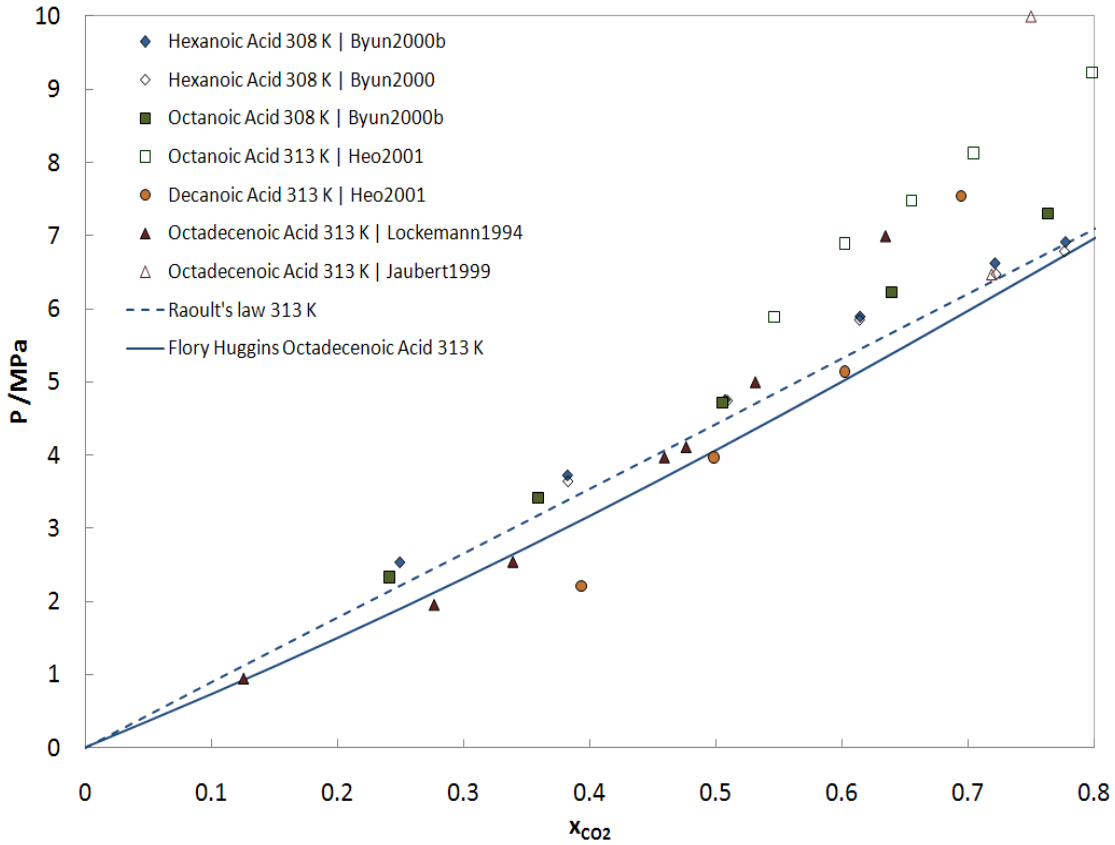

Figure D.4. Pressure - CO_2 molar composition diagram for the systems CO_2 + Fatty acids at 313 K.[159, 160, 164, 289-291]

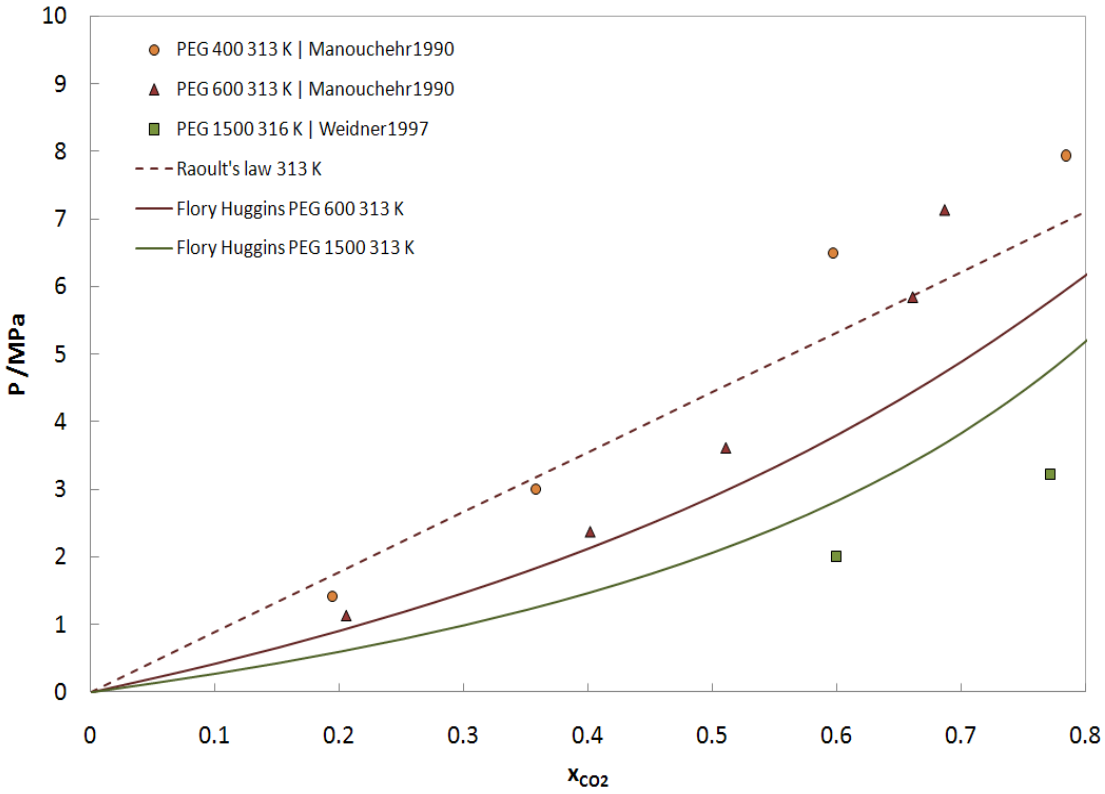

Figure D.5. Pressure - CO_2 molar composition diagram for the systems CO_2 +PEGs at 313 K.[292, 293]

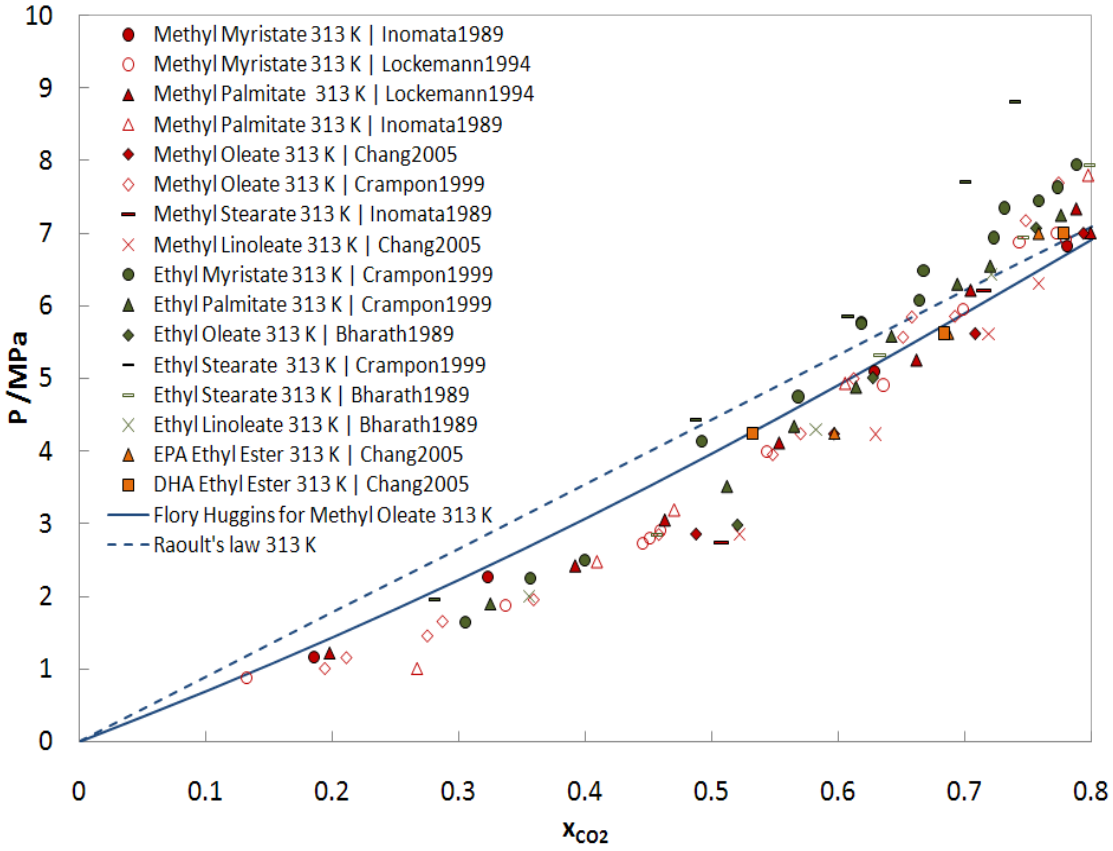

Figure D.6. Pressure - CO_2 molar composition diagram for the systems CO_2 + Fatty acid esters at 313 K.[159, 162, 165, 188, 289]

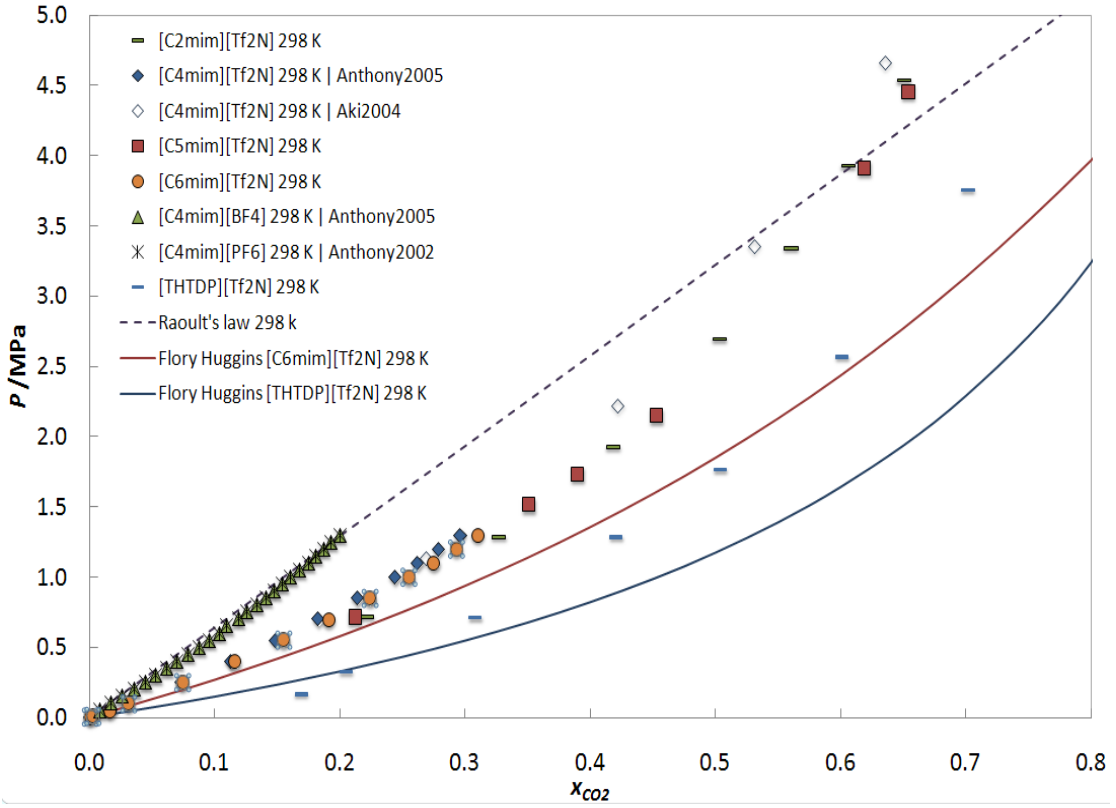

Figure D.7. Pressure - CO_2 molar composition diagram for the systems CO_2 + Ionic Liquids at 313 K.[36, 46, 47, 49, 50, 119]

[THTDP][Cl] Experimental measurements:

The results obtained are reported in Table D.1.

Table D.1. Bubble point data of the system CO_2 (1) + [THTDP][Cl] (2).

x_1	P /MPa	x_1	P /MPa	x_1	P /MPa	x_1	P /MPa
	313 K				363 K		
0.119	0.168	0.503	2.850	0.119	0.770	0.503	5.692
0.164	0.371	0.603	4.135	0.164	1.089	0.603	8.330
0.200	0.517	0.701	6.130	0.200	1.397	0.701	12.821
0.305	1.120	0.752	7.503	0.305	2.440	0.752	16.927
0.400	1.824	0.800	16.31	0.400	3.679	-	-

Chapter 9 Figure 9.2:

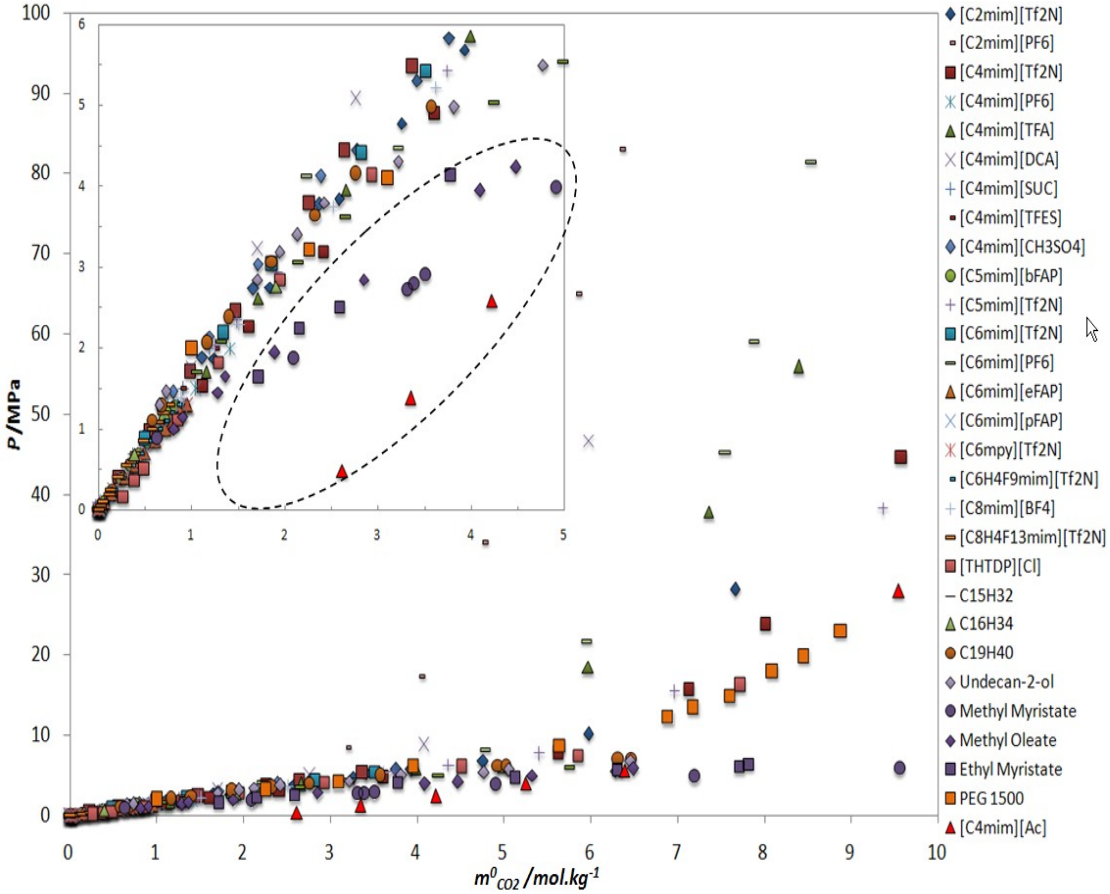

Figure D.8. *(Chapter 9 Figure 9.2)* Pressure - molality diagram of CO_2 + non volatile solvents at 313 K.[28, 30, 34, 36, 50, 52, 53, 59, 62, 131, 166, 185-188]

Figure D.8 represents, on a p-m diagram at 298 K, the solubility of CO_2 in a large number of ionic liquids, listed in Table D.2, along with the solubility of CO_2 in various other solvents.[28, 30, 34, 36, 50, 52, 53, 59, 62, 131, 166, 185-188]

Table D.2. List of ionic liquids depicted in Figure 9.3.

[C_2mim][NTf2]	1-ethyl-3-methylimidazolium bis(trifluoromethylsulfonyl)imide[36][59]
[C_4mim][NTf2]	1-butyl-3-methylimidazolium bis(trifluoromethylsulfonyl)imide[50]
[C_5mim][NTf2]	1-methyl-3-pentylimidazolium bis(trifluoromethylsulfonyl)imide[36]
[C_6mim][NTf2]	1-hexyl-3-methylimidazolium bis(trifluoromethylsulfonyl)imide[52]
[C_4mim][BF_4]	1-butyl-3-methylimidazolium tetrafluoroburate[34]
[C_8mim][BF_4]	1-octyl-3-methylimidazolium tetrafluoroburate[131]
[C_2mim][PF_6]	1-ethyl-3-methylimidazolium hexafluorophosphate[62]
[C_4mim][PF_6]	1-butyl-3-methylimidazolium hexafluorophosphate[34][53]
[C_6mim][PF_6]	1-hexyl-3-methylimidazolium hexafluorophosphate[62]
[C_4mim][TFA]	1-butyl-3-methylimidazolium trifluoroacetate[30]
[C_4mim][DCA]	1-butyl-3-methylimidazolium dicyanamide[50]
[C_4mim][SUC]	1-butyl-3-methylimidazolium succinamate[34]
[C_4mim][TFES]	1-butyl-3-methylimidazolium tetrafluoroethanesulfonate[34]
[C_4mim]$_2$[IDA]	bis(1-butyl-3-methylimidazolium).iminodiacetate[34]
[C_5mim][NTf2]	1-methyl-3-pentylimidazolium bis(trifluoromethylsulfonyl)imide[36]
[C_5mim][bFAP]	1-methyl-3-pentylimidazolium tris(nonafluorobutyl)trifluorophosphate[28]
[C_6mim][NTf2]	1-hexyl-3-methylimidazolium bis(trifluoromethylsulfonyl)imide[34]
[C_6mim][eFAP]	1-hexyl-3-methylimidazolium tris(pentafluoroethyl)trifluorophosphate[28]
[C_6mim][pFAP]	1-hexyl-3-methylimidazolium tris(heptafluoropropyl)trifluorophosphate[28]
[C_6mpy][pFAP]	1-hexyl-3-methylpyridinium tris(heptafluoropropyl)trifluorophosphate[28]
[C_6mpy][NTf2]	1-hexyl-3-methylpyridinium bis(trifluoromethylsulfonyl)imide
[$C_6H_4F_9$mim][NTf2]	1-methyl-3-(nonafluorohexyl)imidazolium bis(trifluoromethylsulfonyl)imide[28]
[$C_8H_4F_{13}$mim][NTf2]	1-methyl-3-(tridecafluorooctyl)imidazolium bis(trifluoromethylsulfonyl)imide[28]
[TBP][FOR]	tetra-n-butylphosphonium formate[34]
[THTDP][Cl]	trihexyltetradecylphosphonium chloride[119]
[C_4mim][CH_3SO_4]	1-butyl-3-methylimidazolium methyl sulfate[53]
[C_4mim][Ac]	1-butyl-3-methylimidazolium acetate[71]

Chapter 9 Figure 9.3:

For pressures up to 10 MPa the fugacity of CO_2 is proportional to the system pressure and can be described by

$$p = H_i m_i^o \tag{D.6}$$

where H_i combines the Henry's constant, $k_{H,i}^{(m)}$, with the gas phase non ideality, proportional to pressure, and the liquid phase non ideality, proportional to concentration.

The best description of the Henry's constant temperature dependence is provided by Benson and Krause,[182, 184] and within a temperature range of 100 K can be expressed as

$$\ln H_i = \alpha + \frac{\beta}{T} \tag{D.7}$$

Combining Eqs. (D.1) and (D.2) it is possible to develop a general description for the solubility of CO_2 in non volatile solvents. For this purpose experimental data from various authors and various types of non volatile solvents was used. This data was retrieved from the literature.[30, 36, 50, 52, 59, 131] The result is shown in Figure where the value of H_i at each temperature is reported.

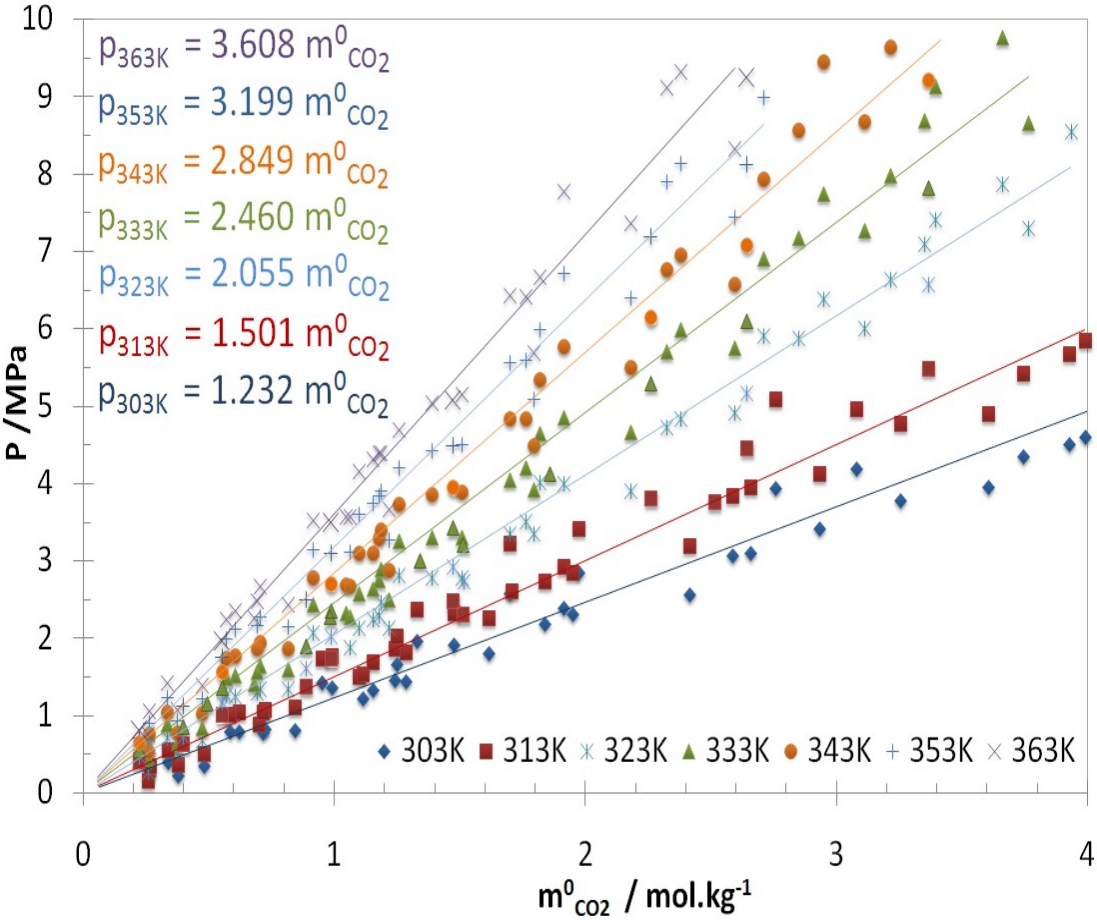

Figure *D.9.* Pressure - molality diagram of CO_2 + non volatile solvents. Data from the literature.[30, 36, 50, 52, 59, 131]

The correlation of Eq. (D.2) to the Henry's constants reported in Figure D.9 is depicted in Figure D.10

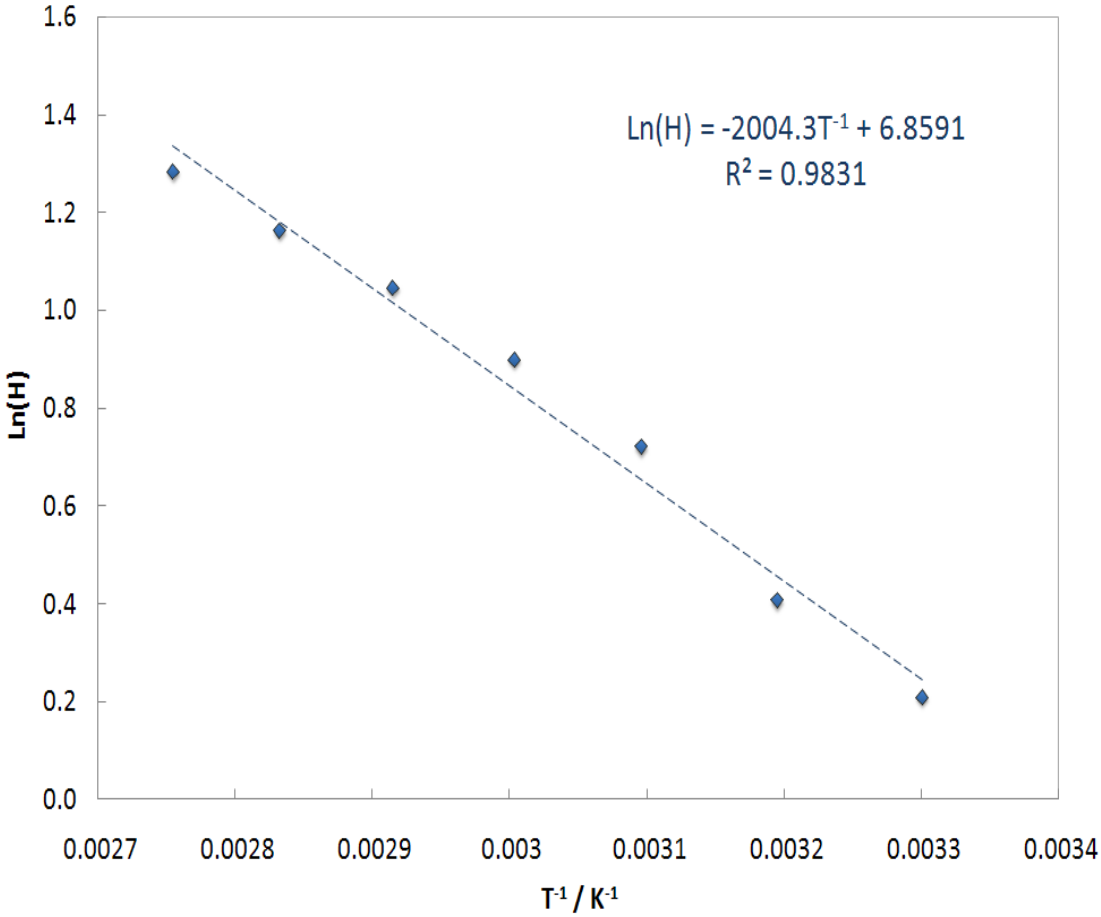

Figure *D.10.* Ln(*H*) *versus* T^{-1} of CO_2 + non volatile systems depicted in Figure D.9.

E. Appendix E

Supplementary data for the "High Pressure Phase Behavior of Carbon Dioxide in 1-Butyl-3-methylimidazolium Bis(trifluoromethylsulfonyl)imide and 1-Butyl-3-methylimidazolium Dicyanamide Ionic Liquids" chapter

Table E.1. Bubble point data of the system CO_2 (1) + $[C_4mim][NTf_2]$ (2).

x_1	T /K	p /MPa	x_1	T /K	p /MPa	x_1	T /K	p /MPa	x_1	T /K	p /MPa	x_1	T /K	p /MPa
0.231	292.65	0.629	0.319	293.21	0.915	0.404	293.53	1.410	0.503	293.22	1.997	0.602	293.27	3.052
0.231	303.18	0.786	0.319	303.05	1.223	0.404	303.10	1.812	0.503	303.12	2.568	0.602	303.31	3.962
0.231	313.32	1.050	0.319	313.19	1.540	0.404	313.17	2.273	0.503	313.10	3.196	0.602	313.13	4.912
0.231	323.22	1.303	0.319	323.27	1.892	0.404	323.26	2.787	0.503	323.20	3.909	0.602	323.13	6.015
0.231	333.19	1.574	0.319	333.17	2.283	0.404	333.23	3.316	0.503	333.12	4.670	0.602	333.20	7.269
0.231	343.00	1.874	0.319	342.87	2.682	0.404	343.11	3.897	0.503	343.24	5.499	0.602	343.02	8.675
0.231	353.20	2.179	0.319	353.09	3.121	0.404	353.12	4.512	0.503	353.17	6.412	0.602	353.20	10.196
0.231	363.26	2.485	0.319	363.19	3.579	0.404	363.17	5.156	0.503	363.18	7.372	0.602	363.23	11.776

x_1	T /K	p /MPa	x_1	T /K	p /MPa	x_1	T /K	p /MPa	x_1	T /K	p /MPa
0.701	293.37	4.433	0.749	293.32	5.907	0.771	293.42	12.829	0.801	293.26	33.263
0.701	303.19	5.880	0.749	303.19	10.812	0.771	303.31	18.726	0.801	303.19	39.373
0.701	313.11	7.860	0.749	313.12	15.810	0.771	313.23	23.943	0.801	313.25	44.740
0.701	323.09	10.215	0.749	323.11	20.543	0.771	323.13	28.960	0.801	323.30	49.990
0.701	333.10	13.150	0.749	333.17	25.124	0.771	333.28	33.693			
0.701	343.25	16.144	0.749	343.20	29.205	0.771	343.08	38.081			
0.701	353.14	19.437	0.749	353.09	33.219	0.771	353.22	42.030			
0.701	362.99	22.468	0.749	363.18	36.365	0.771	363.25	46.010			

Table E.2. Bubble point data of the system CO_2 (1) + [C_4mim][DCA] (2).

x_1	T /K	p /MPa	x_1	T /K	p /MPa	x_1	T /K	p /MPa	x_1	T /K	p /MPa	x_1	T /K	p /MPa
0.200	293.36	1.018	0.300	293.50	1.980	0.410	293.38	3.015	0.507	293.44	4.496	0.601	293.41	32.606
0.200	303.45	1.360	0.300	303.40	2.590	0.410	303.45	3.950	0.507	302.91	6.056	0.601	303.14	39.866
0.200	313.36	1.771	0.300	313.06	3.230	0.410	313.32	5.088	0.507	313.03	8.856	0.601	313.17	46.749
0.200	322.94	2.260	0.300	323.04	4.005	0.410	323.47	6.395	0.507	322.93	13.184	0.601	323.07	53.174
0.200	332.72	2.644	0.300	333.28	4.860	0.410	333.13	7.743	0.507	333.21	17.566	0.601	333.15	59.007
0.200	343.12	3.108	0.300	343.34	5.776	0.410	343.01	9.452	0.507	343.12	21.750	0.601	343.17	64.217
0.200	353.09	3.745	0.300	353.10	6.722	0.410	353.13	11.166	0.507	353.01	25.759	0.601	353.19	69.002
0.200	363.25	4.328	0.300	363.11	7.776	0.410	363.18	13.106	0.507	363.20	29.583	0.601	363.21	73.64

Table E.3. Interaction parameters for the studied systems and predicted Henry's constants.

NP	*T* K	k_{ij}	A_{12} J.mol^{-1}	A_{21} J.mol^{-1}	$\|\Delta P\|$ %	H_{12} MPa
CO_2 + [C_4mim][DCA]						
5	294	0.0011	9408.3848	-1495.9484	2.9	4.50
5	298	0.0347	8918.0020	-1494.1405	2.7	4.94
5	303	0.0781	8192.4209	-1472.2108	1.9	5.58
5	313	0.1076	5423.5389	-1224.9851	1.9	7.28
5	323	0.0939	3965.2209	-924.8767	1.7	8.37
5	333	0.1719	10870.9717	-1625.9764	4.1	10.03
5	343	0.1836	9065.5234	-1582.2672	4.2	11.26
5	348	0.1061	3379.2601	-701.4223	2.7	11.93
5	353	0.1944	9170.4082	-1608.2632	4.3	12.88
5	363	0.1837	6682.6597	-1416.1205	4.1	15.22
CO_2 + [C_4mim][NTf_2]						
10	294	0.1192	6953.1221	-1773.8668	2.9	1.95
10	298	0.1483	10107.4219	-1956.5963	4.1	2.22
10	303	0.1131	5185.5443	-1577.0179	1.7	2.65
10	313	0.1094	4510.4612	-1455.0227	1.5	3.30
10	323	0.0956	4145.6373	-1369.7626	2.3	3.84
9	333	0.0460	3817.1826	-1254.1760	2.7	4.62
9	343	0.0437	3499.4506	-1153.3373	3.4	5.23
8	348	0.0222	3265.4848	-1061.9391	3.2	5.98
8	353	0.0234	3180.8903	-1030.9774	3.2	6.13
8	363	0.0312	3060.1939	-984.8977	3.1	7.77

Table E.4. Properties of the substances used in the modeling.

Compound	T_c /K	P_c /MPa	ω	r	q
CO_2	304.21[a]	7.38[a]	0.2236[a]	3.26[c]	2.38[c]
[C_4mim][DCA]	782.96[b]	2.44[b]	0.8419[b]	22.63[c]	14.86[c]
[C_4mim][NTf2]	826.30[b]	2.76[b]	0.3004[b]	32.67[c]	20.68[c]

[a][282]

[b]Calculated with [281]

[c]Calculated with [82]

Table E.5. Coefficients A and B in equation (4) and partial molar enthalpy and partial molar entropy of solvation obtained for CO_2 (1) + ILs (2) systems.

Ionic Liquid	A	B	$\lvert\Delta H_{12}\rvert$ %	$\Delta_{solv}H$ kJ.mol^{-1}	$\Delta_{solv}S$ J.mol^{-1}.K^{-1}	$-T\cdot\Delta_{solv}S\rvert_{T=298\ K}$ kJ.mol^{-1}
[C_4mim][DCA]	-1833.219	10.077	0.05	-15.24	-83.79	24.98
[C_4mim][NTf_2]	-2000.530	9.831	0.07	-16.63	-81.74	24.37

F. Appendix F

Supplementary data for the "High Carbon Dioxide Solubilities in Trihexyltetradecylphosphonium-based Ionic Liquids" chapter

Table F.1. Bubble point data of the system CO_2 (1) + [THTDP][NTf_2] (2).

x1	*T* /K	*p* /MPa	*x1*	*T* /K	*p* /MPa	*x1*	*T* /K	*p* /MPa	*x1*	*T* /K	*p* /MPa	*x1*	*T* /K	*p* /MPa
0.169	293.26	0.106	0.205	293.34	0.252	0.308	293.20	0.612	0.421	293.30	1.145	0.504	293.37	1.584
0.169	303.25	0.226	0.205	303.22	0.399	0.308	303.15	0.806	0.421	303.22	1.425	0.504	303.58	1.966
0.169	313.20	0.355	0.205	313.10	0.555	0.308	313.16	1.023	0.421	313.24	1.748	0.504	313.05	2.378
0.169	323.26	0.471	0.205	323.11	0.716	0.308	323.25	1.266	0.421	323.22	2.079	0.504	323.24	2.823
0.169	333.25	0.609	0.205	333.15	0.887	0.308	333.13	1.492	0.421	333.38	2.439	0.504	333.21	3.267
0.169	343.22	0.760	0.205	343.20	1.055	0.308	343.13	1.739	0.421	343.19	2.786	0.504	343.27	3.737
0.169	353.21	0.909	0.205	353.21	1.235	0.308	353.11	1.993	0.421	353.21	3.154	0.504	353.26	4.216
0.169	363.24	1.066	0.205	363.40	1.425	0.308	363.29	2.246	0.421	363.34	3.535	0.504	363.45	4.702
x1	*T* /K	*p* /MPa	*x1*	*T* /K	*p* /MPa	*x1*	*T* /K	*p* /MPa	*x1*	*T* /K	*p* /MPa	*x1*	*T* /K	*p* /MPa
0.601	292.88	2.275	0.702	293.14	3.305	0.806	293.17	4.817	0.822	293.15	5.510	0.830	293.20	7.546
0.601	303.27	2.845	0.702	303.11	4.197	0.806	303.31	6.208	0.822	303.20	7.450	0.830	303.20	9.480
0.601	313.10	3.427	0.702	313.11	4.975	0.806	313.39	7.948	0.822	313.19	9.634	0.830	313.23	11.584
0.601	323.24	4.020	0.702	323.15	5.921	0.806	323.28	10.007	0.822	323.31	12.009	0.830	323.23	13.838
0.601	333.22	4.657	0.702	333.27	6.912	0.806	333.29	12.119	0.822	333.24	14.307	0.830	333.28	16.063
0.601	343.20	5.342	0.702	343.38	7.946	0.806	343.40	14.180	0.822	343.10	16.481	0.830	343.28	18.182
0.601	353.23	5.995	0.702	353.33	8.996	0.806	353.23	16.095	0.822	353.20	18.493	0.830	353.41	20.290
0.601	363.31	6.675	0.702	363.53	10.078	0.806	363.28	17.975	0.822	363.21	20.420	0.830	363.45	22.264
x1	*T* /K	*p* /MPa	*x1*	*T* /K	*p* /MPa	*x1*	*T* /K	*p* /MPa	*x1*	*T* /K	*p* /MPa	*x1*	*T* /K	*p* /MPa
0.840	293.20	12.025	0.850	293.33	18.870	0.860	293.30	26.885	0.870	293.26	44.564	0.879	296.58	72.185
0.840	303.18	12.808	0.850	303.10	18.188	0.860	303.02	24.711	0.870	302.95	34.630	0.879	303.08	49.350
0.840	313.29	14.587	0.850	313.21	18.747	0.860	313.18	23.840	0.870	313.10	30.585	0.879	313.35	39.536
0.840	323.19	16.420	0.850	323.22	20.190	0.860	323.34	24.304	0.870	323.24	29.743	0.879	323.35	36.280
0.840	333.23	18.457	0.850	333.26	21.719	0.860	333.19	25.423	0.870	333.20	30.253	0.879	333.38	35.408
0.840	343.18	20.490	0.850	343.12	23.608	0.860	343.19	26.972	0.870	343.12	31.183	0.879	343.23	35.732
0.840	353.26	22.557	0.850	353.01	25.482	0.860	353.26	28.426	0.870	353.25	32.463	0.879	353.06	36.563
0.840	363.14	24.401	0.850	363.14	27.163	0.860	363.28	30.227	0.870	363.35	33.815	0.879	361.67	37.445

Table F.2. Bubble point data of the system CO_2 (1) + [THTDP][Cl] (2).

x_1	T /K	p /MPa	x_1	T /K	p /MPa	x_1	T /K	p /MPa	x_1	T /K	p /MPa	x_1	T /K	p /MPa
0.119	313.16	0.168	0.164	303.35	0.225	0.200	303.42	0.357	0.305	303.40	0.820	0.400	303.27	2.311
0.119	323.16	0.274	0.164	313.03	0.371	0.200	313.27	0.517	0.305	313.54	1.120	0.400	313.56	2.850
0.119	333.46	0.453	0.164	323.30	0.523	0.200	323.40	0.682	0.305	323.66	1.355	0.400	323.57	3.357
0.119	343.37	0.546	0.164	333.30	0.641	0.200	333.50	0.849	0.305	333.59	1.605	0.400	333.63	3.924
0.119	353.30	0.690	0.164	343.00	0.784	0.200	343.68	1.033	0.305	343.52	1.873	0.400	343.55	4.495
0.119	363.22	0.770	0.164	353.16	0.943	0.200	353.75	1.220	0.305	353.66	2.160	0.400	353.46	5.092
			0.164	363.20	1.089	0.200	363.66	1.397	0.305	363.54	2.440	0.400	363.58	5.692
x_1	T /K	p /MPa	x_1	T /K	p /MPa	x_1	T /K	p /MPa	x_1	T /K	p /MPa	x_1	T /K	p /MPa
0.503	303.32	2.311	0.603	303.33	3.417	0.701	303.36	4.987	0.752	303.42	5.998	0.800	302.55	14.995
0.503	313.47	2.850	0.603	313.28	4.135	0.701	313.70	6.130	0.752	313.38	7.503	0.800	313.44	16.310
0.503	323.43	3.357	0.603	323.47	4.924	0.701	323.56	7.314	0.752	323.45	9.328	0.800	323.83	17.595
0.503	333.47	3.924	0.603	333.69	5.760	0.701	333.54	8.658	0.752	333.58	11.307	0.800	333.78	19.295
0.503	343.55	4.495	0.603	343.64	6.586	0.701	343.48	10.018	0.752	343.46	13.226	0.800	343.72	21.108
0.503	353.64	5.092	0.603	353.69	7.457	0.701	353.77	11.461	0.752	353.58	15.138	0.800	353.66	22.815
0.503	363.67	5.692	0.603	363.53	8.330	0.701	363.68	12.821	0.752	363.67	16.927	0.800	363.65	24.570

Table F.3. Temperature-independent interaction parameters and predicted Henry's constant for the studied systems.

T /K	H_{12} /MPa	T /K	H_{12} /MPa
[THTDP][NTf_2] + CO_2		[THTDP][Cl] + CO_2	
K_{ij}=0.001116T-0.2307 A_{12}=-2.534·T+1867.153 A_{21}=2.490·T+351.268 |Δp| (%) = 9.2		K_{ij}=0.00574T-3.0269 A_{12}=14.331·T-3908.572 A_{21}=2.298·T+570.848 |Δp| (%) = 9.4	
293.44	1.98	-	-
303.18	2.30	303.27	1.89
313.19	2.64	313.36	2.40
323.24	3.00	323.48	2.99
333.25	3.38	333.55	3.67
343.21	3.76	343.50	4.41
353.22	4.14	353.57	5.21
363.21	4.54	363.54	6.08

Table F.4. Properties of the substances used in the modeling.

Compound	T_c /K	P_c /MPa	ω	r	q
CO_2	304.21[a]	7.38[a]	0.2236[a]	3.26[c]	2.38[c]
[THTDP][NTf_2]	1588.22[b]	8.51[b]	0.8801[b]	82.08[c]	52.97[c]
[THTDP][Cl]	1225.80[b]	7.95[b]	0.7698[b]	69.29[c]	44.07[c]

[a]ref, [282]; [b]Calculated with [281]; [c]Calculated with [82]

Table F.5. Coefficients A and B in Eq. 5.4 and partial molar enthalpy and partial molar entropy of solvation obtained for CO_2 + ILs systems.

Ionic Liquid	A	B	$\|\Delta H_{12}\|$ %	$\Delta_{solv}H$ kJ.mol^{-1}	$\Delta_{solv}S$ J.mol^{-1}.K^{-1}	$-T\cdot\Delta_{solv}S\|_{T=298\ K}$ kJ.mol^{-1}
[THTDP][NTf_2]	-1268.272	5.015	0.65	-10.54	-32.31	9.63
[THTDP][Cl]	-2147.851	7.737	0.84	-17.86	-53.86	16.06

G. Appendix G

Supplementary data for the "High pressure CO2 solubility in N-methyl-2-hydroxyethylammonium protic ionic liquids" chapter

Table G.1. Bubble point data of the system CO_2 (1) + m-2-HEAF (2).

x_1	T /K	p /MPa	x_1	T /K	p /MPa	x_1	T /K	p /MPa	x_1	T /K	p /MPa	x_1	T /K	p /MPa
0.057	293.22	0.494	0.119	293.21	1.194	0.172	293.30	1.835	0.231	293.26	2.482	0.281	293.37	3.108
0.057	303.07	0.666	0.119	303.12	1.563	0.172	303.22	2.317	0.231	303.15	3.155	0.281	303.27	3.959
0.057	313.25	0.889	0.119	313.16	1.912	0.172	313.16	2.843	0.231	313.26	3.895	0.281	313.33	4.940
0.057	323.28	1.105	0.119	323.28	2.284	0.172	323.18	3.435	0.231	323.22	4.746	0.281	323.13	5.985
0.057	333.31	1.354	0.119	333.30	2.710	0.172	333.25	4.078	0.231	333.21	5.622	0.281	333.15	7.176
0.057	343.42	1.662	0.119	343.18	3.133	0.172	343.27	4.742	0.231	343.29	6.576	0.281	343.19	8.456
0.057	353.26	1.950	0.119	353.19	3.612	0.172	353.18	5.414	0.231	353.20	7.572	0.281	353.24	9.764
0.057	363.21	2.280	0.119	363.27	4.071	0.172	363.23	6.112	0.231	363.31	8.549	0.281	363.42	11.138
x_1	T /K	p /MPa	x_1	T /K	p /MPa	x_1	T /K	p /MPa	x_1	T /K	p /MPa	x_1	T /K	p /MPa
0.336	293.27	3.808	0.381	293.30	4.417	0.429	293.32	5.116	0.483	293.29	12.094	0.534	293.32	26.849
0.336	303.18	4.885	0.381	303.23	5.746	0.429	303.14	6.950	0.483	303.20	17.625	0.534	303.37	32.578
0.336	313.12	6.150	0.381	313.10	7.366	0.429	313.31	11.215	0.483	313.30	22.384	0.534	313.32	37.662
0.336	323.23	7.632	0.381	323.11	9.467	0.429	323.28	15.098	0.483	323.29	26.654	0.534	323.17	42.016
0.336	333.17	9.293	0.381	333.25	12.078	0.429	333.33	18.618	0.483	333.25	30.414	0.534	333.27	45.617
0.336	343.23	11.098	0.381	343.23	14.687	0.429	343.21	21.819	0.483	343.23	33.635	0.534	343.28	48.511
0.336	353.28	12.966	0.381	353.50	17.347	0.429	353.23	24.718	0.483	353.21	36.359	0.534	353.22	50.852
0.336	363.17	14.818	0.381	363.31	19.623	0.429	363.15	27.090	0.483	363.25	38.678	0.534	363.28	52.910

Table G.2. Bubble point data of the system CO_2 (1) + m-2-HEAA (2).

x_1	T /K	p /MPa	x_1	T /K	p /MPa	x_1	T /K	p /MPa	x_1	T /K	p /MPa
0.157	313.27	0.840	0.208	313.12	1.732	0.249	312.93	2.790	0.299	313.28	3.903
0.157	323.40	1.230	0.208	323.33	2.194	0.249	323.22	3.571	0.299	323.37	4.865
0.157	333.60	1.680	0.208	333.36	2.774	0.249	333.16	4.225	0.299	333.59	6.070
0.157	343.42	2.151	0.208	343.37	3.438	0.249	343.06	5.027	0.299	343.37	7.421
0.157	353.25	2.682	0.208	353.28	4.187	0.249	353.31	6.235	0.299	353.44	8.923
0.157	363.20	3.357	0.208	362.62	4.910	0.249	363.48	7.794	0.299	363.27	10.516
x_1	T /K	p /MPa	x_1	T /K	p /MPa	x_1	T /K	p /MPa			
0.402	313.26	7.498	0.452	313.02	19.475	0.500	313.09	46.587			
0.402	323.21	10.590	0.452	323.16	26.393	0.500	323.23	55.198			
0.402	333.23	14.872	0.452	333.33	33.002	0.500	333.33	62.754			
0.402	343.25	19.405	0.452	343.31	38.887	0.500	343.36	69.597			
0.402	353.19	24.254	0.452	353.48	44.317	0.500	353.38	75.591			
0.402	363.25	28.545	0.452	363.61	49.244	0.500	363.35	80.500			

Table G.3. Bubble point data of the system CO_2 (1) + CH_4 (2) + 2mHEAA (3).

x_1	x_2	T /K	p /MPa
0.236	0.052	313.13	32.85
0.236	0.052	323.30	33.29
0.236	0.052	333.11	34.02
0.236	0.052	343.23	34.96
0.236	0.052	353.25	35.95
0.236	0.052	363.37	36.92

Table G.4. Results of the consistency test using PR+WS/NRTL, with estimated k_{ij}, α, A_{12} and A_{21} parameters, and Henry constant predicted.

NP	*T* /K	k_{ij}	α	A_{12} kJ/Kmol	A_{21} kJ/Kmol	|ΔP| /%	Result	H_{12} /MPa
CO_2 + m-2-HEAF, ln H_{12} = -2163.8783/T + 9.7305, %|ΔH_{12}| = 2.2								
6	293.15	-1.0000	0.5500	-47447.8438	-582.2807	2.1	TC	9.91
6	303.15	-0.0852	0.4706	7901.9165	56426.9609	1.9	TC	13.95
6	313.15	-0.2812	0.3850	9843.7500	-65.5746	0.3	TC	17.06
6	323.15	-0.1106	0.4493	7648.2334	33752.0586	0.2	TC	20.96
6	333.15	0.4536	0.3253	1926.8668	46596.8359	0.3	TC	25.55
6	343.15	0.4073	0.5391	2646.3318	24960.9375	0.4	TC	31.17
6	353.15	0.5625	0.3613	1859.4362	39505.7617	0.4	TC	36.42
6	363.15	0.6750	0.4489	1569.2855	30238.8379	0.4	TC	42.42
CO_2 + m-2-HEAA, ln H_{12} = -3304.5677/T + 12.2156, %|ΔH_{12}| = 2.6								
7	313.15	-0.9980	0.2527	-71728.2344	-3126.9836	9.6	NFC/TC	5.12
7	323.15	0.1860	0.3805	-49838.1055	-3911.3367	11.1	NFC/TC	7.52
7	333.15	-0.9780	0.2724	-78574.2422	-3889.1602	1.9	NFC/TC	10.15
7	343.15	1.0000	0.3721	-89949.1953	-8085.9268	7.6	NFC/TC	12.85
7	353.15	0.1937	0.2000	31291.0371	-3864.1941	6.6	NFC/TC	18.21
7	363.15	0.2360	0.2000	29020.3438	-4191.6221	5.4	NFC/TC	21.86

Table G.5. Properties of the substances used in the modeling.

Compound	T_b /K	T_c /K	P_c /MPa	ω
CO_2		304.21[a]	7.38[a]	0.2236[a]
m-2-HEAF	514.55[c]	698.95[b]	4.14[b]	0.9359[d]
m-2-HEAA	538.13[c]	715.66[b]	3.33[b]	0.9836[d]

[a]ref, [282]; [b]Calculated with [67]; [c]Calculated with [294]; [d]Calculated with [281]

H. Appendix H

Supplementary data for the "Non-ideality of Solutions of NH3, SO2, and H2S in Ionic Liquids and the Prediction of their Solubilities using the Flory-Huggins Model" chapter

Table H.1. SO_2, NH_3 and H_2S properties needed for the PR EoS.[122]

Gas	*Tc* /K	*Pc* /MPa	ω
SO_2	430.75	7.88	0.245
NH_3	405.65	11.28	0.253
H_2S	373.53	8.96	0.094

Table H.2. Average pressure deviations, $AD_{\Delta p}$, between the available VLE[138, 226, 227, 233, 234, 295] and the equilibrium pressure predicted by the Flory-Huggins model, as function of the temperature, for the IL + SO_2, IL + NH_3 and IL + H_2S systems.

T /K	$AD_{\Delta p}$	T /K	$AD_{\Delta p}$	T /K	$AD_{\Delta p}$	T /K	$AD_{\Delta p}$	T /K	$AD_{\Delta p}$
SO_2 + [C_6mim][NTf_2] [138]		***NH_3 + [C_8mim][BF_4]*** [226]		**NH_3 + [C_2mim][$EtSO_4$]** [295]		**NH_3 + [C_2mim][Ac]** [295]		***NH_3 + [C_4mim][BF_4]*** [295]	
298	-0.032	293	0.03	283	-0.1	283	-0.1	282	-0.06
313	-0.042	298	0.0004	298	-0.1	298	-0.1	298	-0.08
333	0.038	313	0.05	***NH_3 + [C_4mim][PF_6]*** [295]		***NH_3 + [C_4mim][BF_4]*** [226]		324	-0.15
SO_2 + [C_6mpy][NTf_2] [138]		323	0.12	283	-0.05	293	-0.04	***NH_3 + [C_2mim][BF_4]*** [226]	
298	0.002	333	0.09	298	-0.05	298	-0.11	293	-0.11
SO_2 + [C_6mim][NTf_2] [227]		***NH_3 + [C_2mim][NTf_2]*** [295]		325	-0.05	313	-0.06	298	-0.13
283	0.009	283	-0.09	***NH_3 + [C_6mim][BF_4]*** [226]		323	-0.15	313	-0.13
298	0.026	299	-0.13	293	-0.06	333	-0.06	323	-0.15
323	0.038	323	-0.08	298	-0.07	***NH_3 + [C_6mim][Cl]*** [295]		333	-0.17
348	0.059	***H_2S + [C_4mim][BF_4]*** [233]		313	-0.06	283	-0.05	***H_2S + [C_4mim][NTf_2]*** [233]	
H_2S + [C_6mim][BF_4] [234]		303	-0.09	323	-0.006	298	-0.07	303	-0.13
303	-0.07	313	-0.08	333	0.03	324	-0.11	313	-0.11
313	-0.06	323	-0.06	***H_2S + [C_6mim][PF_6]*** [234]					
				303	-0.20				
				313	-0.20				

Table H.3. Deviations, Δp, between the available VLE[138, 227] and the equilibrium pressure predicted by the Flory-Huggins model, as function of SO_2 mole fractions and temperature, for the IL + SO_2 systems.

x_{SO2}	Δp /MPa	x_{SO2}	Δp /MPa	x_{SO2}	Δp /MPa	x_{SO2}	Δp /MPa	x_{SO2}	Δp /MPa
SO_2 + [C_6mim][NTf_2][138]						**SO_2 + [C_6mim][NTf_2][227]**			
298 K		**313 K**		**333 K**		**283 K**		**298 K**	
0.310	-0.005	0.103	-0.005	0.0676	-0.004	0.171	0.005	0.124	0.008
0.478	0.001	0.228	0.004	0.136	0.004	0.512	0.01	0.377	0.02
0.616	0.005	0.367	-0.03	0.248	0.02	0.616	0.01	0.477	0.03
0.711	0.005	0.533	-0.05	0.374	0.04	0.706	0.01	0.553	0.03
0.781	0.003	0.655	-0.07	0.488	0.07	0.767	0.01	0.667	0.03
0.844	-0.2	0.719	-0.1	0.58	0.1	0.825	0.01	0.752	0.03
						0.875	0.005	0.82	0.03
								0.881	0.03
x_{SO2}	Δp /MPa	x_{SO2}	Δp /MPa	x_{SO2}	Δp /MPa				
SO_2 + [C_6mim][NTf_2][227]				**x_{SO2} + [C_6mpy][NTf_2][138]**					
323 K		**348 K**		**298 K**					
0.049	0.005	0.037	0.01	0.138	-0.01				
0.192	0.02	0.124	0.03	0.343	-0.001				
0.266	0.03	0.169	0.04	0.522	0.003				
0.329	0.03	0.21	0.05	0.660	0.005				
0.431	0.04	0.28	0.06	0.775	0.003				
0.513	0.05	0.343	0.08	0.854	0.01				
0.581	0.06	0.401	0.1						
0.639	0.07	0.457	0.1						

Table H.4. Deviations, Δp, between the available VLE[226, 295] and the equilibrium pressure predicted by the Flory-Huggins model, as function of NH_3 mole fractions and temperature, for the IL + NH_3 systems.

x_{NH3}	Δp /MPa	x_{NH3}	Δp /MPa	x_{NH3}	Δp / MPa	x_{NH3}	Δp /MPa	x_{NH3}	Δp /MPa	x_{NH3}	Δp /MPa	x_{NH3}	Δp /MPa
NH_3 + $[C_2mim][EtSO_4]$[295]				**NH_3 + $[C_2mim][Ac]$[295]**				***NH_3 + $[C_4mim][PF_6]$[295]***					
283 K		**298 K**		**283 K**		**298 K**		**283 K**		***298 K***		***325 K***	
0.536	-0.1	0.518	-0.1	0.624	-0.1	0.599	-0.1	0.371	-0.04	0.351	*-0.02*	0.292	-0.02
0.707	-0.1	0.694	-0.2	0.749	-0.1	0.730	-0.1	0.471	-0.05	0.435	*-0.06*	0.389	-0.04
0.805	-0.1	0.798	-0.1	0.802	-0.1	0.788	-0.1	0.584	-0.06	0.557	*-0.05*	0.492	-0.04
0.839	-0.1	0.833	-0.1	0.834	-0.1	0.825	-0.1	0.862	-0.05	0.740	*-0.07*	0.681	-0.1
0.875	-0.1	0.871	-0.1	0.847	-0.1	0.839	-0.1			0.854	*-0.04*	0.828	-0.06
				0.877	-0.1	0.871	-0.1						
x_{NH3}	Δp /MPa	x_{NH3}	Δp /MPa	x_{NH3}	Δp /MPa	x_{NH3}	Δp /MPa	x_{NH3}	Δp /MPa	x_{NH3}	Δp /MPa	x_{NH3}	Δp /MPa
NH_3 + $[C_4mim][BF_4]$[295]						***NH_3 + $[C_4mim][BF_4]$[226]***							
282 K		**298 K**		**324 K**		**293 K**		**298 K**		***313 K***		**323 K**	
0.201	-0.04	0.173	-0.06	0.122	-0.1	0.2645	-0.03	0.3175	-0.07	0.0989	-0.02	0.1296	-0.04
0.303	-0.05	0.266	-0.08	0.199	-0.1	0.3818	-0.02	0.4654	-0.08	0.2001	-0.05	0.2798	-0.1
0.404	-0.07	0.367	-0.09	0.292	-0.2	0.5087	-0.05	0.5555	-0.08	0.3368	-0.08	0.3799	-0.2
0.582	-0.08	0.548	-0.1	0.473	-0.2	0.691	-0.06	0.595	-0.1	0.4431	-0.08	0.4697	-0.2
0.709	-0.09	0.683	-0.1	0.622	-0.2	0.7531	-0.05	0.6635	-0.2	0.5615	-0.07	0.5087	-0.2
0.844	-0.04	0.833	-0.08	0.805	-0.07								
x_{NH3}	Δp /MPa	x_{NH3}	Δp /MPa	x_{NH3}	Δp /MPa	x_{NH3}	Δp /MPa	x_{NH3}	Δp /MPa	x_{NH3}	Δp /MPa	x_{NH3}	Δp /MPa
NH_3 + $[C_4mim]$ $[BF_4]$[226]		***NH_3 + $[C_2mim][BF_4]$[226]***										***NH_3 + $[C_6mim]$ $[BF_4]$[226]***	
333 K		**293 K**		**298 K**		**313 K**		**323 K**		***333 K***		**293 K**	
0.0608	-0.01	0.2153	-0.06	0.1474	-0.05	0.1255	-0.06	0.0838	-0.05	0.1185	-0.07	0.3815	-0.01
0.1103	-0.05	0.3392	-0.1	0.4169	-0.1	0.2546	-0.1	0.2043	-0.1	0.175	-0.1	0.4933	-0.07
0.1689	-0.06	0.4976	-0.1	0.4669	-0.1	0.3238	-0.1	0.2853	-0.2	0.2284	-0.2	0.6032	-0.08
0.2519	-0.09	0.578	-0.2	0.5386	-0.2	0.4466	-0.2	0.3304	-0.2	0.2538	-0.2	0.724	-0.06
0.3397	-0.1	0.6921	-0.1	0.6176	-0.2	0.5257	-0.1	0.3896	-0.2	0.2549	-0.3	0.7543	-0.08
x_{NH3}	Δp /MPa	x_{NH3}	Δp /MPa	x_{NH3}	Δp /MPa	x_{NH3}	Δp /MPa	x_{NH3}	Δp /MPa	x_{NH3}	Δp /MPa	x_{NH3}	Δp /MPa

$NH_3 + [C_6mim][BF_4]$[226]								$NH_3 + [C_8mim][BF_4]$[226]					
298 K		**313 K**		**323 K**		***333 K***		**293 K**		**298 K**		**313 K**	
0.3673	-0.04	0.2722	-0.04	0.1898	-0.01	0.128	-0.001	0.4202	0.05	0.2788	0.004	0.2832	0.02
0.4977	-0.06	0.3861	-0.06	0.3548	-0.03	0.1983	-0.001	0.5409	-0.002	0.438	-0.002	0.3982	0.02
0.5756	-0.08	0.4829	-0.09	0.4106	-0.02	0.2949	0.03	0.6402	0.001	0.7028	0.04	0.5051	0.06
0.6992	-0.06	0.5769	-0.03	0.455	-0.02	0.3703	0.04	0.7596	0.06	0.5868	-0.01	0.5741	0.06
0.6974	-0.1	0.6236	-0.06	0.5779	0.05	0.5106	0.1	0.8081	0.04	0.7476	-0.03	0.6438	0.09
x_{NH3}	**Δ*p* /MPa**	x_{NH3}	**Δ*p* /MPa**	x_{NH3}	**Δ*p* /MPa**	x_{NH3}	**Δ*p* /MPa**	x_{NH3}	**Δ*p* /MPa**	x_{NH3}	**Δ*p* /MPa**	x_{NH3}	**Δ*p* /MPa**
$NH_3 + [C_8mim][BF_4]$[226]				$NH_3 + [C_2mim][NTf_2]$[295]						$NH_3 + [C_6mim][Cl]$[295]			
323 K		**333 K**		**283 K**		**299 K**		**323 K**		**283 K**		**298 K**	
0.1564	0.03	0.1321	0.02	0.220	-0.1	0.171	-0.1	0.089	-0.1	0.095	-0.02	0.086	-0.03
0.3471	0.07	0.2555	0.05	0.504	-0.1	0.430	-0.1	0.305	-0.1	0.254	-0.03	0.231	-0.04
0.4525	0.1	0.3798	0.1	0.634	-0.1	0.568	-0.2	0.444	-0.2	0.363	-0.05	0.337	-0.07
0.5485	0.2	0.4447	0.1	0.811	-0.1	0.768	-0.2	0.673	-0.2	0.562	-0.06	0.537	-0.08
0.6002	0.2	0.5022	0.2	0.931	-0.1	0.921	-0.1	0.888	-0.003	0.745	-0.09	0.728	-0.1
				0.948	-0.04	0.943	-0.05	0.926	0.10	0.837	-0.08	0.828	-0.1

x_{NH3}	**Δ*p* /MPa**
$NH_3 + [C_6mim][Cl]$[295]	
324 K	
0.060	-0.06
0.194	-0.04
0.294	-0.06
0.479	-0.1
0.681	-0.2
0.799	-0.2

Table H.5. Deviations, Δp, between the available VLE[233, 234] and the equilibrium pressure predicted by the Flory-Huggins model, as function of H_2S mole fractions and temperature, for the IL + H_2S systems.

x_{H2S}	Δp /MPa	x_{H2S}	Δp /MPa	x_{H2S}	Δp /MPa	x_{H2S}	Δp /MPa	x_{H2S}	Δp /MPa
$H_2S + [C_4mim][BF_4]$[233]						$H_2S + [C_6mim][BF_4]$[234]			
303 K		313 K		323 K		303 K		313 K	
0.039	-0.01	0.038	-0.01	0.035	-0.01	0.072	-0.03	0.07	-0.03
0.081	-0.02	0.076	-0.03	0.074	-0.02	0.144	-0.03	0.139	-0.03
0.120	-0.04	0.111	-0.04	0.11	-0.03	0.233	-0.05	0.226	-0.04
0.163	-0.08	0.166	-0.07	0.168	-0.04	0.303	-0.05	0.295	-0.03
0.183	-0.09	0.180	-0.08	0.187	-0.05	0.38	-0.09	0.371	-0.07
0.228	-0.1	0.220	-0.1	0.225	-0.1	0.441	-0.1	0.433	-0.09
0.270	-0.1	0.250	-0.1	0.24	-0.1	0.469	-0.1	0.46	-0.09
0.310	-0.2	0.280	-0.1	0.28	-0.1	0.499	-0.1	0.491	-0.1
0.354	-0.2	0.32	-0.2	0.303	-0.1				
x_{H2S}	Δp /MPa	x_{H2S}	Δp /MPa	x_{H2S}	Δp /MPa	x_{H2S}	Δp /MPa		
$H_2S + [C_4mim][NTf_2]$[233]				$H_2S + [C_6mim][PF_6]$[234]					
303 K		313 K		303 K		313 K			
0.07	-0.03	0.065	-0.03	0.067	-0.07	0.063	-0.07		
0.128	-0.06	0.120	-0.06	0.113	-0.1	0.108	-0.1		
0.174	-0.08	0.163	-0.08	0.166	-0.1	0.159	-0.1		
0.209	-0.1	0.196	-0.1	0.244	-0.2	0.233	-0.2		
0.241	-0.1	0.227	-0.1	0.296	-0.2	0.284	-0.2		
0.273	-0.1	0.258	-0.1	0.345	-0.3	0.333	-0.3		
0.307	-0.2	0.291	-0.2	0.396	-0.3	0.383	-0.3		
0.364	-0.2	0.347	-0.2	0.441	-0.3	0.428	-0.3		
0.444	-0.2	0.434	-0.2						
0.51	-0.2	0.065	-0.03						

I. Appendix I

Supplementary data for the "The Polarity Effect upon the Methane Solubility in Ionic Liquids: A Contribution for the Design of Ionic Liquids for Enhanced CO2/CH4 and H2S/CH4 Selectivities" chapter

Table I.1. Bubble point data of the system CH_4 (1) + [THTDP][NTf_2] (2).

x_1	T /K	p /MPa	x_1	T /K	p /MPa	x_1	T /K	p /MPa	x_1	T /K	p /MPa	x_1	T /K	p /MPa
0.123	293.00	1.264	0.209	293.09	2.384	0.297	293.12	4.229	0.398	293.23	7.428	0.503	293.28	12.005
0.123	303.15	1.426	0.209	303.23	2.632	0.297	303.39	4.564	0.398	303.07	7.978	0.503	303.21	12.742
0.123	313.43	1.640	0.209	313.42	2.879	0.297	313.44	4.905	0.398	313.24	8.436	0.503	313.06	13.421
0.123	323.56	1.781	0.209	323.18	3.127	0.297	323.29	5.225	0.398	323.24	8.927	0.503	323.32	14.052
0.123	333.31	1.943	0.209	333.26	3.345	0.297	333.24	5.550	0.398	333.26	9.357	0.503	333.29	14.625
0.123	343.11	2.115	0.209	343.08	3.557	0.297	343.10	5.870	0.398	343.39	9.787	0.503	343.22	15.205
0.123	353.11	2.261	0.209	353.14	3.777	0.297	353.17	6.185	0.398	353.26	10.165	0.503	353.09	15.735
0.123	363.30	2.417	0.209	363.09	4.032	0.297	363.20	6.390	0.398	363.43	10.536	0.503	363.23	16.263
x_1	T /K	p /MPa	x_1	T /K	p /MPa	x_1	T /K	p /MPa	x_1	T /K	p /MPa	x_1	T /K	p /MPa
0.606	293.33	21.051	0.664	293.07	29.481	0.712	293.29	40.393	0.755	293.06	54.028	0.786	293.13	64.054
0.606	303.12	21.795	0.664	303.37	30.205	0.712	303.21	40.498	0.755	303.21	53.467	0.786	303.26	63.608
0.606	313.08	22.407	0.664	313.42	30.778	0.712	313.22	40.732	0.755	313.14	53.286	0.786	313.42	62.834
0.606	323.30	23.085	0.664	323.46	31.328	0.712	323.10	40.905	0.755	323.25	53.110	0.786	323.44	61.974
0.606	333.20	23.696	0.664	333.46	31.843	0.712	333.17	41.175	0.755	333.24	52.783	0.786	333.28	61.285
0.606	343.13	24.275	0.664	343.25	32.266	0.712	343.28	41.270	0.755	343.18	52.558	0.786	343.20	60.375
0.606	353.34	24.835	0.664	353.30	32.934	0.712	353.23	41.545	0.755	353.24	52.664	0.786	353.44	59.839
0.606	363.26	25.245	0.664	363.26	33.429	0.712	363.52	41.762	0.755	363.34	52.485	0.786	363.22	59.473
												0.853	363.73	99.379

Table I.2. Bubble point data of the system CH_4 (1) + [C_4mim][NTf_2] (2).

x_1	T /K	p /MPa	x_1	T /K	p /MPa	x_1	T /K	p /MPa	x_1	T /K	p /MPa
0.041	293.48	1.165	0.114	293.62	4.967	0.167	292.97	8.955	0.213	292.86	13.312
0.041	313.73	1.567	0.114	313.71	5.586	0.167	313.55	9.904	0.213	313.62	14.601
0.041	332.65	1.722	0.114	333.47	6.092	0.167	333.36	10.759	0.213	333.70	15.663
0.041	353.43	2.067	0.114	353.15	6.658	0.167	353.38	11.310	0.213	353.38	16.597
x_1	T /K	p /MPa	x_1	T /K	p /MPa	x_1	T /K	p /MPa	x_1	T /K	p /MPa
0.263	293.36	20.565	0.302	293.31	29.327	0.362	293.31	51.267	0.400	293.31	71.340
0.263	313.51	21.520	0.302	313.38	29.610	0.362	313.43	49.180	0.400	313.38	66.847
0.263	333.64	22.480	0.302	333.40	29.897	0.362	333.50	46.879	0.400	333.06	63.275
0.263	353.81	23.160	0.302	352.76	30.720	0.362	353.41	45.183	0.400	353.30	60.550

Table I.3. Bubble point data of the system CH_4 (1) + m-2-HEAPr (2).

x_1	T /K	p /MPa	x_1	T /K	p /MPa	x_1	T /K	p /MPa
0.030	293.00	3.963	0.047	293.46	7.087	0.074	293.20	13.525
0.030	303.47	4.166	0.047	303.60	7.290	0.074	303.21	13.562
0.030	313.33	4.316	0.047	313.24	7.450	0.074	313.26	13.630
0.030	323.30	4.484	0.047	323.23	7.619	0.074	323.34	13.664
0.030	333.18	4.650	0.047	333.18	7.790	0.074	333.25	13.717
0.030	343.26	4.783	0.047	343.19	7.920	0.074	343.34	13.728
0.030	353.22	4.941	0.047	353.40	8.075	0.074	353.43	13.745
0.030	363.17	5.037	0.047	363.17	8.176	0.074	363.41	13.782
x_1	T /K	p /MPa	x_1	T /K	p /MPa			
0.101	293.39	29.090	0.132	323.15	46.675			
0.101	303.06	27.110	0.132	333.38	44.588			
0.101	313.26	26.545	0.132	343.17	41.999			
0.101	323.11	26.006	0.132	353.30	39.817			
0.101	333.20	25.174	0.132	363.37	37.821			
0.101	343.32	24.494						
0.101	353.43	23.998						
0.101	363.48	23.465						

Table I.4. Bubble point data of the system CH_4 (1) + [C_4mim][[CH_3SO_3] (2).

x_1	T /K	p /MPa	x_1	T /K	p /MPa	x_1	T /K	p /MPa
0.062	353.30	14.358	0.097	353.75	29.520	0.141	353.65	49.850
0.062	363.40	14.480	0.097	363.95	29.656	0.141	363.27	48.180

Table I.5. Carbon dioxide / methane selectivities as function of temperature for the studied ILs.

T /K	CO_2/CH_4 Selectivities						
	[THTDP][NTf_2]	**[C_4mim][NTf_2]**	**m-2-HEAPr**	**[C_4mim][CH_3SO_3]**	**[C_6mim][NTf_2]** [23]	**[C_4mim][CH_3SO_4]** [296]	**[C1mim][CH_3SO_4]** [23]
293.15	6.36	20.98	91.37				
303.15	6.17	19.34[a]	81.50		9.51	35.00[a]	67.30a
313.15	6.16	18.50	70.88		8.14	20.83	
323.15	5.72		62.84				
333.15	5.30	13.96	55.93			19.54	
343.15	4.93		49.58		5.31		
353.15	4.54	12.75	44.67	46.74	4.84		
363.15	4.40		39.53	45.17			

[a] Interpolated